Properties of hemp fibre polymer composites - An optimisation of fibre properties using novel defibration methods and fibre characterisation

Thygesen, Anders

Publication date:
2006

Document Version
Publisher's PDF, also known as Version of record

Risø-PhD-11(EN)

Properties of hemp fibre polymer composites

-An optimisation of fibre properties using novel defibration methods and fibre characterisation

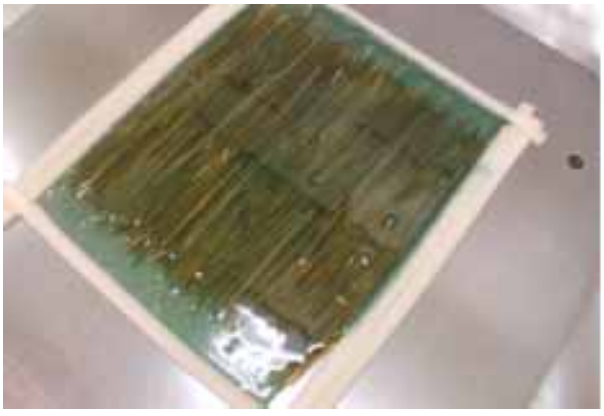

Anders Thygesen

Risø National Laboratory
Roskilde
Denmark
April 2006

Author: Anders Thygesen
Title: Properties of hemp fibre polymer composites -An optimisation of fibre properties using novel defibration methods and fibre characterisation
Department: BIO & AFM

This thesis is submitted in partial fulfilment of the requirements for the Ph.D. degree at The Royal Agricultural and Veterinary University of Denmark

Abstract:
Characterization of hemp fibres was carried out with fibres obtained with low handling damage and defibration damage to get an indication of how strong cellulose based fibres that can be produced from hemp. Comparison was made with hemp yarn produced under traditional conditions where damage is unavoidable. The mild defibration was performed by degradation of the pectin and lignin rich middle lamellae around the fibres by cultivation of the mutated white rot fungus *Phlebia radiata* Cel 26. Fibres with a cellulose content of 78% w/w could thereby be produced which is similar to the cellulose content obtained by steam explosion of hemp fibres prior defibrated with pectin degrading enzymes. The S2 layer in the fibre wall of the hemp fibres consisted of 1-4 cellulose rich and lignin poor concentric layers constructed of ca. 100 nm thick lamellae. The microfibril angle showed values in the range 0-10° for the main part of the S2-layer and 70-90° for the S1-layer. The microfibrils that are mainly parallel with the fibre axis explain the high fibre stiffness, which in defibrated hemp fibres reached 94 GPa. The defibrated hemp fibres had higher fibre stiffness (88-94 GPa) than hemp yarn (60 GPa), which the fibre twisting in hemp yarn explains. The hemp fibre stiffness appeared to increase linearly with cellulose content and crystallinity and to decrease with cellulose twisting angle. Pure crystalline cellulose had an estimated stiffness of 125 GPa. The defibration with P. radiata Cel 26 resulted in fibre strength of 643 MPa, which is similar to the strength of traditionally produced hemp yarn (677 MPa) even though mild processing was applied. The plant fibre strength seemed therefore to be linearly dependent on the cellulose content and not clearly dependent on the introduced physical damage during handling and defibration. Pure cellulose appeared to have effective strength of 850 MPa that is about 10% of the strength on the molecular level.

Risø-PhD-11(EN)
April 2006

ISBN 87-550-3440-3

Contract no.:
+45 46774279

Group's own reg. no.: 1620034

Sponsorship:

The Danish Research Agency of the Ministry of Science

Cover :
Upper picture:
Hemp field at Danish Institute of Agricultural Sciences.

Lower picture:
Mat of aligned hemp fibres that has been impregnated with epoxy resin.

Pages:
Tables:
References:

Risø National Laboratory
Information Service Department
P.O.Box 49
DK-4000 Roskilde
Denmark
Telephone +45 46774004
bibl@risoe.dk
Fax +45 46774013
www.risoe.dk

Contents

PhD thesis:

Properties of hemp fibre polymer composites

An optimisation of fibre properties using novel defibration methods and detailed fibre characterisation

Ph.D. student:
Anders Thygesen

Supervisors:
Hans Lilholt [a]
Anne Belinda Thomsen [b]
Claus Felby [c]

Affiliations:
a: Materials Research Department, Risø National Laboratory
b: Biosystems Department, Risø National Laboratory
c: Danish Centre for Forest, Landscape and Planning, Royal Veterinary and Agricultural University, Denmark

Thesis submitted 2. May 2005 to:
Danish Centre for Forest, Landscape and Planning,
Royal Veterinary and Agricultural University, Denmark

Preface

This thesis is submitted as a partial fulfilment of the requirements for the Danish Ph.D. degree. The study was carried out from September 2001 to April 2005 at the Danish centre for Forest, Landscape and Planning, The Royal Veterinary and Agricultural University (KVL). Part of the experimental research has been carried out at Materials Research Department (AFM), Risø National Laboratory, at the Biosystems Department (BIO), Risø National Laboratory, at the Wood Ultra Structure Research Centre, Swedish University of Agricultural Sciences (SLU) and at Department of Chemistry, Technical University of Denmark. It was defended 23rd September 2005.

During the three years of work that has resulted in this thesis, many people have contributed in one way or another. I am very grateful of all of you; but there are some who deserve special thanks. First of all I will thank Dr. Anne Belinda Thomsen for introducing me to the project and for the 8 month I was involved in bioethanol research. I wish to acknowledge all my supervisors for their encouraging support and inspiration and for giving me the freedom to choose the subjects of my interest. Especially, I am thankful for the many fruitful discussions of the applied experimental procedures and the obtained results.

Furthermore I express my gratitude to Mrs. Ann-Sofie Hansen, Mr. Henning K. Frederiksen, Mr. Tomas Fernqvist, Mrs. Ingelis Larsen, Dr. Bo Madsen, Engineer Tom L. Andersen, Lecturer Kenny Ståhl and Dr. Geoffrey Daniel.

This work was part of the project "High performance hemp fibres and improved fibre networks for composites" supported by the Danish Research Agency of the Ministry of Science. Their support is gratefully acknowledged.

This work was supervised by:

Professor Claus Felby (SL-KVL)	Main supervisor
Senior Scientist Hans Lilholt (AFM)	Co-supervisor
Senior Scientist Anne Belinda Thomsen (BIO)	Co-supervisor

Risø National Laboratory: 5th April-2006

1 Resumé

Karakterisering af hampefibre blev udført med fibre fremstillet ved skånsomme metoder for at få en indikation af hvor stærke fibre der kan produceres fra hampeplanten. Sammenligning blev lavet med hampegarn produceret under traditionelle betingelser, hvor skader ikke kan undgås. Den skånsomme defibrering af hampestænglerne blev udført ved nedbrydning af den pektin- og ligninholdige midtlamel omkring fibrene ved kultivering af den muterede svamp *Phlebia radiata* Cel 26. De fremstillede fibre havde et celluloseindhold på 78 %, hvilket også kan opnås ved enzymbehandling med pektinnedbrydende enzymer efterfulgt af steam explosion behandling. S2-laget i fibrenes cellevæg bestod af 1-4 lag med højt celluloseindhold og lavt ligninindhold. Disse lag bestod endvidere af ca. 100 nm tykke lameller. Mikrofibrilvinklen var 0-10° i hovedparten af S2-laget og 70-90° i S1-laget. Siden mikrofibrilorienteringen næsten var parallel med fiberretningen havde fibrene høj stivhed der kunne blive 94 GPa efter defibreringen. De defibrerede hampefibre var dermed stivere end hampegarn (60 GPa), hvilket kan skyldes snoningsvinklen der introduceres under spindingsprocessen. Hampefibrenes stivhed var også lineært voksende som funktion af celluloseindholdet og cellulosekrystalliniteten og aftagende som funktion af snoningsvinklen eller mikrofibrilvinklen. Krystallinsk cellulose havde en estimeret stivhed på 125 GPa. Defibreringen med *P. radiata* Cel 26 resulterede i fibre med en styrke beregnet på basis af kompositstyrken a 643 MPa, der er tilsvarende styrken af hampegarnet (677 MPa) selvom skånsomme behandlingsmetoder blev anvendt. Plantefiberstyrken så også ud til at stige lineært med celluloseindholdet og var ikke mærkbart afhængig af defibreringsmetoden. Ren cellulose havde dermed en styrke a 850 MPa hvilket er ca. 10 % af styrken på molekylært niveau.

2 List of publications

2.1 Published papers

Paper I. Anders Thygesen, Frants Torp Madsen, Hans Lilholt, Claus Felby and Anne Belinda Thomsen (2002). Changes in chemical composition, degree of crystallisation and polymerisation of cellulose in hemp fibres caused by pre-treatment. In: Lilholt, H., Madsen, B., Toftegaard, H., Cendre, E., Megnis, M., Mikkelsen, L.P., Sørensen, B.F. (Ed.), Sustainable natural and polymeric composites - science and technology. *Proceedings of the 23th Risø International Symposium on Materials Science*, Risø National Laboratory, Denmark, pp. 315-323.

Paper II. Anders Thygesen, Geoffrey Daniel, Hans Lilholt, Anne Belinda Thomsen (2005). Hemp fiber microstructure and use of fungal defibration to obtain fibers for composite materials. *Journal of Natural fibers* 2(4) pp. 19-37.

Paper III. Anders Thygesen, Jette Oddershede, Hans Lilholt, Anne Belinda Thomsen, and Kenny Ståhl (2005). On the determination of crystallinity and cellulose content in plant fibres *Cellulose* 12 pp. 563-576.

Paper IV. Anders Thygesen, Anne Belinda Thomsen, Geoffrey Daniel and Hans Lilholt (2005). Comparison of composites made from fungal defibrated hemp with composites of traditional hemp yarn. *In press in Industrial Crops and Products*.

2.2 Submitted papers

Minna Nykter, Hanna-Riitta Kymäläinen, Anne Belinda Thomsen, Anna-Maija Sjöberg, Anders Thygesen. Effects of thermal and enzymatic treatments on the microbiological quality and chemical composition of fibre hemp (*Cannabis sativa* L.) fibres. *Submitted to Biomass & Bioenergy*.

2.3 Posters

Anders Thygesen, Sokol Ndoni, Hans Lilholt, Frants Torp Madsen, Claus Felby and Anne Belinda Thomsen (2002). Evaluation of method for the determination of degree of polymerisation in cellulose from hemp. *H. C. Ørstedsinstittet, 7th Symposium in Analytical Chemistry, 20-21st August- 2002.*

Anders Thygesen, Jette Oddershede, Hans Lilholt, Anne Belinda Thomsen, Geoffrey Daniel and Kenny Ståhl (2003). Cellulose crystallinity in plant materials. *The Danish University of Pharmaceutical Sciences, 5th DANSYNC meeting, 27-28th May-2003*.

Anders Thygesen, Anne Belinda Thomsen, Hans Lilholt, Geoffrey Daniel (2003). Microscopical and cytochemical observation on hemp stems with emphasis on fibres. *Cost Action E20 meeting, Helsinki, 4-6th September-2003*.

2.4 Oral presentations

Anders Thygesen, Frants Torp Madsen, Hans Lilholt, Claus Felby and Anne Belinda Thomsen (2002). High performance hemp fibres and improved fibre network for composites. *Cost Action E20 meeting, Reims, 30th May – 1st June- 2002*.

2.5 Supplementary publications

Anders Thygesen, Anne Belinda Thomsen, Anette Skammelsen Schmidt, Henning Jørgensen, Birgitte K. Ahring, Lisbeth Olsson (2003). Production of cellulose and hemicellulose-degrading enzymes by filamentous fungi cultivated on wet-oxidised wheat straw. *Enzyme Microbial Technology*: 32 (5) p. 606-615.

Anders Thygesen, Mette Hedegaard Thomsen, Henning Jørgensen, Børge Holm Christensen, Anne Belinda Thomsen (2004). Hydrothermal treatment of wheat straw on pilot plant scale, *2nd World Conference and Technology Exhibition on Biomass for Energy, Industry and Climate Protection*, Rome, Italy, 10-15th May 2004.

Anne Belinda Thomsen, Søren K. Rasmussen, Vibeke Bohn, Kristina Vad Nielsen, Anders Thygesen (2005). Hemp raw materials: The effect of cultivar, growth conditions and pretreatment on the chemical composition of the fibres. *Risø National Laboratory. Report No.: R-1507*.

Anne Belinda Thomsen, Anders Thygesen, Vibeke Bohn, Kristina Vad Nielsen, Bodil Pallesen, Michael Søgaard Jørgensen (2005). Effects of chemical-physical pre-treatment processes on hemp fibres for reinforcement of composites and for textiles. *Industrial Crops and Products - accepted.*

Mette Hedegaard Thomsen, Anders Thygesen, Børge Holm Christensen, Jan Larsen, Anne Belinda Thomsen (2006). Preliminary results on optimising hydrothermal treatment used in co-production of biofuels. *Applied Biochemistry and Biotechnology (In press)*.

3 My contribution to the papers

Paper I. Anne Belinda Thomsen had the idea and I contributed in planning the study. I did the pre-treatment experiments and determined the crystallinities and degree of polymerisation in cellulose. I analysed the methods and wrote up 80-90% of the paper.

Paper II. I had the idea of using microscopy and fungal treatment for investigation of the structure in hemp fibres. I planned the experiments with Geoffrey Daniel. I did the rest of the study and wrote the paper with minor contribution from Geoffrey Daniel.

Paper III. Kenny Ståhl, Jette Oddershede and Anders Thygesen had the idea of using the Rietveld and Debye methods for determination of cellulose crystallinity. I selected the samples and planned the chemical analysis. I did the chemical analysis and I analysed the results obtained by the X-ray measurement. I analysed the determined crystallinities and chemical composition based on plant species.

Paper IV. I had the idea of using fungal treatment to obtain fibres for reinforcement in composite materials and I planned the experimental setup and progress. I did the main part of the experimental work and I wrote the paper.

4 Introduction

Hemp (*Cannabis sativa* L.) has been cultivated for at least 6000 years and it may be one of the oldest non-food crops. The most usual purpose of hemp cultivation is to isolate the fibres present in the bark on the hemp stem surface (Garcia-Jaldon et al., 1998), for production of ropes, textiles and paper. Other useful materials from hemp are the seed, which can be used for oil production (Deferne and Pate, 1996) and cannabinoids for medical, spiritual and recreational purposes.

Hemp originates from Central Asia (van der Werf et al., 1996) but has been cultivated from Equator to the polar circle (Vavilov, 1926). Plant breeding of hemp has been performed in eastern and central Europe (de Meijer, 1995) to increase the fibre yield (Bócsa, 1971) and get very low contents of psychoactive substances (Fournier et al., 1987). Legal cultivars for fibre production have thereby been obtained. The biomass yield in hemp is high, and hemp improves the soil structure (du Bois, 1982). The tall plant stems of hemp suppress weeds effectively and diseases and pests are rarely recorded. Thereby addition of pesticides is not needed (Robinson, 1996). It has also been reported that hemp produces several times more of the important fibre component, cellulose, than crops such as corn, kenaf (van der Werf et al., 1996) and sugar cane (Herer, 1985).

Cellulose is of interest, since it has very high theoretical strength (15 GPa) and obtainable strength (8 GPa) (Lilholt and Lawther, 2000). However, the strength of single fibres of hemp is only 800-2000 MPa (Madsen et al., 2003). It is still a high strength compared to 500-700 MPa, which is a typical fibre strength obtained with plant fibre reinforced composites today (Madsen and Lilholt, 2003). It is suspected that fibre damage introduced during processing of hemp for making yarn and finally composite processing decreases the fibre strength. Therefore it is of interest to determine the potential for hemp fibres in composites using as mild pre-treatment conditions as possible to keep the fibres intact. Thorough characterization of the fibres is needed to explain how fibre damages affect the fibre strength.

Hemp fibres have also gained interest for use in composite materials due to concern about how the high production and disposal of synthetic fibres affects the environment (Cromack, 1998). In the last 20-30 years, glass fibres have been used for reinforcement of composite materials in for example wind turbine blades and boats since glass fibres have lower density than steel and high strength. Glass fibre production requires high temperatures and thereby energy consumption. Hemp fibres are produced by the photosynthesis with solar energy and uptake of CO_2 and H_2O (Figure 1). A similar emission of CO_2 occurs when the fibres are burned after usage making the fibres CO_2-neutral resulting in a slight reduction of the global CO_2-emission.

Hemp fibres have also lower density than glass fibres and similar stiffness (Madsen, 2004). Lighter materials can thereby potentially be made with hemp fibres as reinforcement. By replacing some of the steel panels in cars with hemp fibre composites, a weight reduction might be obtainable. That will result in lower consumption of steel and gasoline and thereby reduction of the transport based CO_2-emission. The other main component formed by the plant is the woody core (*shives*) that can be used for bioethanol production like wheat straw (Felby et al., 2003) and softwood (Söderström, 2004), resulting in further reduction of the transport based CO_2-emission by replacement of fossil fuel.

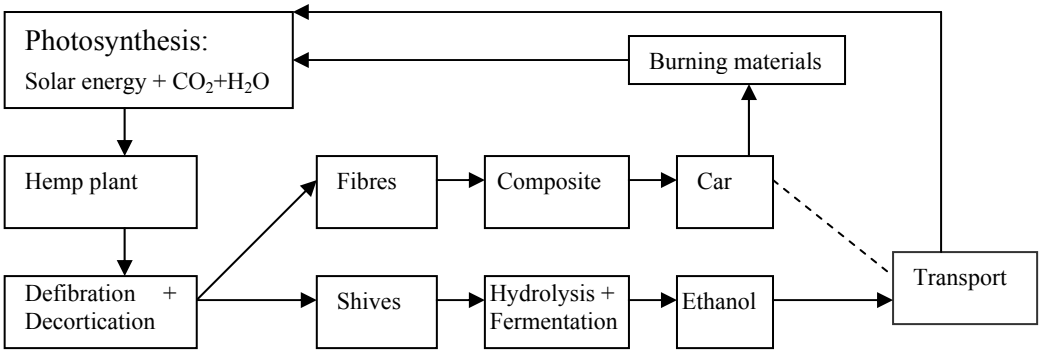

Figure 1. The carbon cycle of the application of the hemp plant for both material- and ethanol production.

The current application of plant fibres in composites is for non-structural components with random fibre orientation. These components are used by the automotive industry and the building industry (Broge, 2000; Clemons, 2000; Karus et al., 2002; Parikh et al., 2002). For example, flax fibres are used instead of synthetic fibres as reinforcement of polypropylene in inner panels for cars. This type of usage is primarily driven by price and demand of ecological awareness, and to a lower extent by the reinforcing effect of the fibres (Bledzki et al. 2002; Kandachar, 2002). The next step is to attract industrial interest to use plant fibres in load bearing materials in for example cars.

Bast fibres from hemp possess by nature a high variability in structure. Fundamental structural characterization is therefore needed before hemp fibres can be used as reinforcement in composite materials. The steps the hemp stems have to go through to get fibres for reinforcement of composites have to be improved too. Traditionally field retting is used for defibration to degrade the binding between the bast fibres on the stem surface and the shives (Meijer et al., 1995), resulting in fibres of variable quality dependent on weather conditions and the attacking microorganisms. The retted stems are mechanically decorticated to isolate the fibres. The decortication equipment has not been developed sufficiently, so the production rate and fibre quality are not as good as required for production of fibres for advanced purposes. Thus, milder and more effective defibration and decortication processes must be developed before hemp fibres can compete with synthetic fibres.

4.1 The aim of the thesis

The aim of the thesis was to study the morphology and the chemical composition of hemp fibres and relate these properties to the composite properties obtained with hemp fibres as reinforcement. The developed methods for determination of the fibre properties were used to investigate the tested pre-treatment methods. For the fibre production to be feasible it is essential to use pre-treatment conditions, which maximise the yield of fibres and introduce as low damage as possible to the fibres. Biological pre-treatment was used since it has the advantage of being performed at low temperature and thereby cause low thermal and physical damage to the fibres. The traditional bio-treatment of the hemp stems, water retting (Meijer et al., 1995; Rosember, 1965) was compared with cultivation of the mutated white rot fungus *P. radiata* Cel 26, which does not degrade cellulose to a significant degree. The treated and untreated hemp stems were hand peeled, since it is a mild decortication procedure for production of fibres compared to mechanical methods.

4.2 The outline of the thesis

The first six chapters of this thesis provide background information and put this work into perspective using the fibre and cellulose characterization papers (Paper II and III). The fibres were characterized by histochemistry and microscopy in Paper II to determine their ultra structure and cellulose microfibril angle. Since cellulose is the reinforcing polymer in hemp fibres, this component was analyzed for crystallinity by X-ray diffraction (Paper III). Finally, this chemical and structural information was used to explain the mechanical properties of the fibres that are relevant in composite materials.

The procedure, for getting from the hemp plant to fibre-reinforced composites is discussed in chapter 6. In addition, problems like fibre decay and mechanical damage during the process steps are discussed.

Chapter 7 summarizes the pre-treatment results mainly presented in paper I and IV. Steam explosion, wet oxidation and enzyme treatment are compared as defibration methods with determination of chemical composition, cellulose crystallinity and cellulose chain length (Paper I). These defibration methods are compared with fungal treatment and water retting of hemp stems in Paper II and Paper IV.

In chapter 8 and 9, composites reinforced with the defibrated hemp fibres are compared with composites with raw hemp fibres. By making composite tests and fibre bundle tests, it could be investigated how the fibre structure and composition affects the mechanical fibre properties. Finally, chapter 10 gives some concluding remarks.

5 The hemp plant

The experimental study of hemp fibre structure (Part 5.2) and chemical composition including cellulose crystallinity (Part 5.3) are based on investigation of the middle section of hemp stems from the Felina cultivar cultivated at Danish Institute of Agricultural Sciences in 2001 as described in Part 5.1.

5.1 Hemp cultivars and growth

Hemp (*Cannabis sativa* L., Figure 2) belongs to the Angiosperm phylum since it has vessel elements in the woody core (xylem) like hardwood. It belongs to the eudicotyledons like hardwoods, numerous bushes and herbs, since it has two cotyledons (i.e. seed leaves). The long and flexible hemp fibres are embedded in the bark (cortex) on the surface of the stem.

In Northern Europe, hemp plants get 1.9-2.5 m tall dependent on cultivar, sunlight and weather conditions (Cromack, 1998). In the cultivation experiments at Danish Institute of Agricultural Sciences in 2001, the stems diameter was highest for the cultivars, Felina and Futura (7-12 mm) and lowest for Finola and Fedora (5-7 mm) (Table 1).

Figure 2. Hemp field with mature hemp plants (left). Hemp stem, leaf and plant top (right).

5.1.1 Cultivation including the experiments at Danish Institute of Agricultural Sciences

Hemp originates from Central Asia (van der Werf et al., 1996) but can be cultivated from the Equator to the polar circle (Vavilov, 1926). In Central Europe, the optimal stem yield is obtained when the plants are sowed in March. Then the period with maximum daylight (May-July) will be used fully.

The cultivation experiments at Danish Institute of Agricultural Sciences in 2001 were done at the research site Flakkebjerg of The Danish Institute of Agricultural Sciences. The location is 55°20'N, 11°10'E and 0-50 m above sea level. The hemp cultivars Fedora, Felina, Fenola and Futura, were sown May 7th due to the risk of frost in April (<-5°C; van der Werf et al., 1996). The harvest was done October 17th, but must be done later if seed production is preferred to obtain mature seed. The maturation is not obtainable in Scandinavia due to the short growth season (Sankari, 2000).

The only fertilizer used was 360/480 kg NH_4NO_3-fertilizer/ha equivalent to 90/120 kg N/ha. The plants were grown without addition of pesticides (Robinson, 1996) and with a seed dosage of 16-32 kg seed/ha.

It has been reported that the maximum stem yield is obtained by sowing 90 plants/m^2 (seed dosage = 15-17 kg seed/ha; Cromack, 1998). If the sowing density is too low branches will be formed at high extend (van der Werf et al., 1996) and make the fibre production difficult. If the plant density is too high, natural thinning will occur and intermediate plants will die resulting in fibre decay (van der Werf et al., 1995). Flowering should be as late as possible since the fibre production rate is lower when seed formation takes place (van der Werf et al., 1996).

5.1.2 Fibre and seed yield

The cultivation experiments at Danish Institute of Agricultural Sciences in 2001, showed that the hemp cultivars Futura and Felina produced few seeds (200-220 kg/ha) and high fibre yields of 2.6 and 2.9 ton/ha, respectively (Table 1). The yield was highest with high dosage of fertilizer and low dosage of seed (120 kg N/ha, 16 kg seed/ha, Table 1**,** Figure 3).

Since the fibre yield with Felina was 39 kg/100 kg stem without retting (Paper II; van der Werf et al., 1996) and 27 kg/100 kg stem with retting there was a loss of 25% fibres in the retting procedure. Finola produced less fibre mass (0.4 ton/ha) but much seed (2.1 ton/ha), while Fedora produced much stem material (9.8 ton/ha) and a low fibre yield (14 g/100 g stem; Table 1).

Table 1. Harvested hemp shown as stem size (m), produced seed, leaves, stems and fibres (kg/ha) by growth of four cultivars (Data from HeFiNaC meeting nr. 14).

Hemp cultivar	Seed kg/ha	Leaves kg/ha	Stems kg/ha	Fibres[1] kg/ha	Fibres[1] g/100 g stem	Stem diameter[2] (mm)	Stem length[3] (m)
Finola	2100	1300	2600	400	17	7	
Fedora 19	600	2300	9800	1400	14	7	2.2
Felina 34	200	1800	9600	2600	27	12	2.2
Futura 77	200	1600	10800	2900	27	11	2.2

1: The fibre yield is amount of fibres after water retting either pr. ha or pr. 100 g raw stem.
2: The stem diameter is measured in the lower part of the stem.
3: The stem length after growth in Southern England with 34-37 kg seed/ ha (Cromack, 1998).

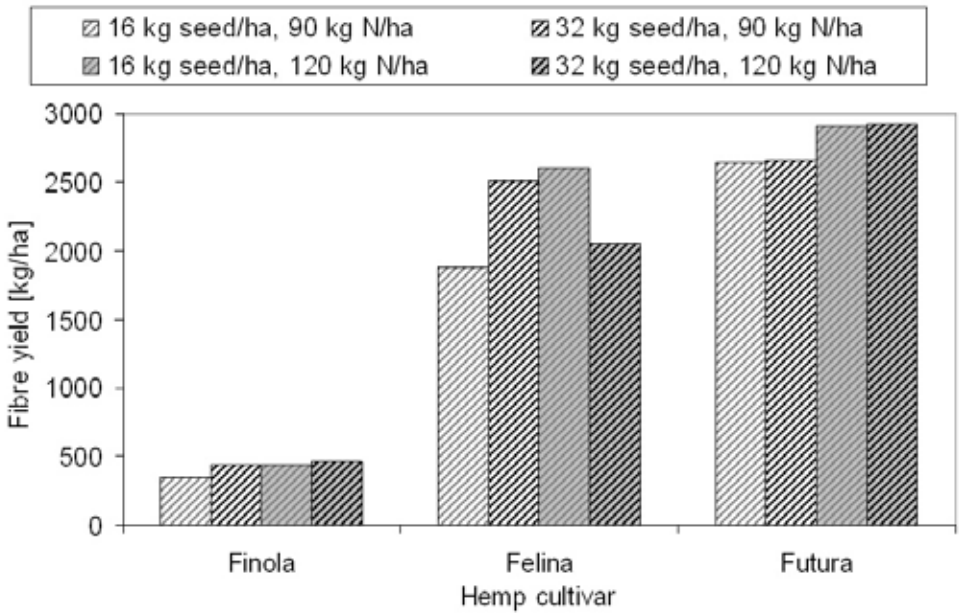

*Figure 3. Produced hemp fibres showed as the area based yield (*a*) (kg/ha) after growth of three cultivars at Danish Institute of Agricultural Sciences in Flakkebjerg in 2001 with varied seed and fertilizer (N) addition (Data from HeFiNaC meeting nr. 14).*

5.1.3 Climate in the growth period in 2001

Since there was not climate data for the Flakkebjerg site, Årslev was used which is a station at the same altitude and 20 km west of the Great belt on Fyn.10 km southwest of Odense. and 60 km west of Flakkebjerg.

The temperature was generally 7-20°C in the first 5 weeks and the last 7 weeks of the cultivation period. The rest of the time was summer with temperatures between 10 and 25°C. Frost and extreme heat (>35°C) was avoid during the entire growth period (Figure 4). The precipitation came at moderate rate of up to 60 mm/week. Until week 30, the amount of precipitation was in average 10 mm/week and thereafter 20 mm/week. It is usual with most precipitation during late summer and autumn in Denmark (Cappelsen & Jørgensen, 2002). The longest dry period lasted 2 weeks (week 29-30) so the plant growth was presumably not stopped due to lack of water. The total amount of precipitation in the period was 350 mm (Figure 5). The amount of sunshine was highest in the beginning of the period (75 hours/week). From week 27 to 42, the amount of sunshine decreased from 75 to 25 hours/week at an approximately linear trend (Figure 6) due to decreasing day length and slightly increasing cloud cover (Cappelsen & Jørgensen, 2002). The total amount of sunshine was 1300 hours in the period.

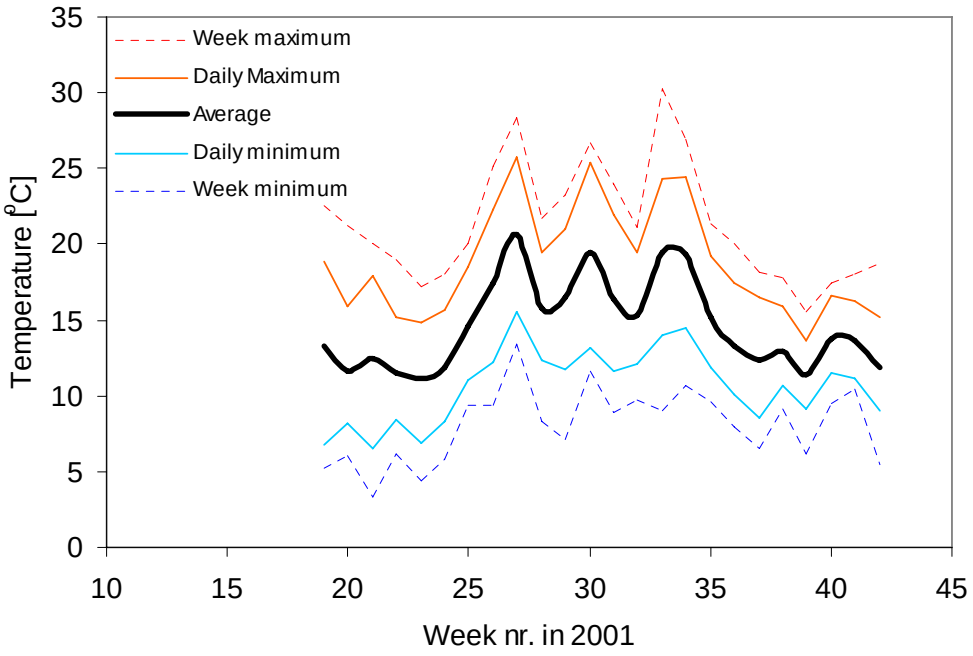

Figure 4. Temperature at the Årslev site in the growth period displayed as weekly average (thick line), maximum and minimum (dotted lines). Average of the daily minimum – and maximum temperature every week are included (full lines) (data from Cappelsen, 2004).

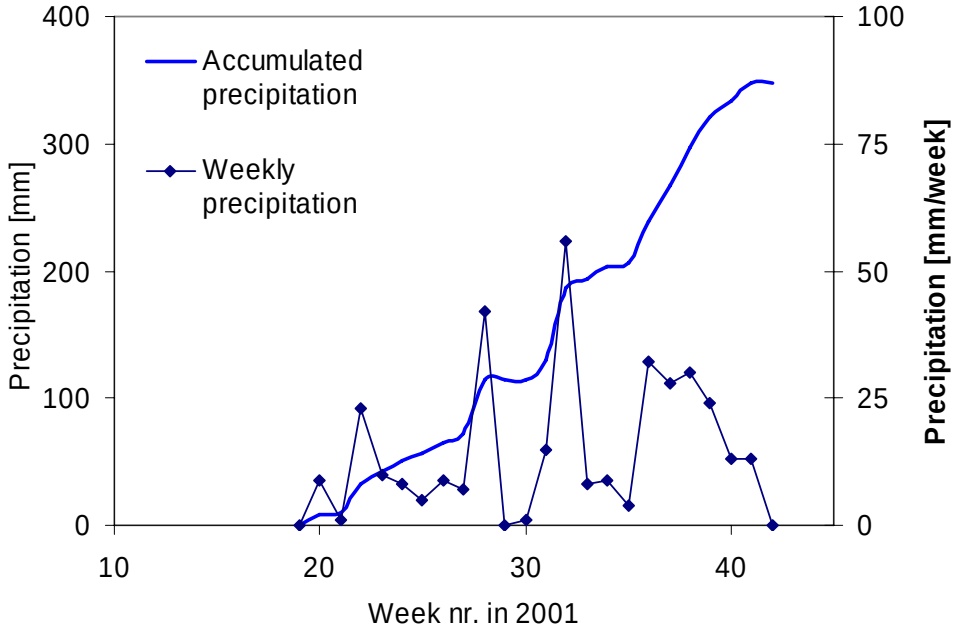

Figure 5. Precipitation at the Årslev site in the growth period displayed as weekly precipitation and the accumulated precipitation (data from Cappelsen, 2004).

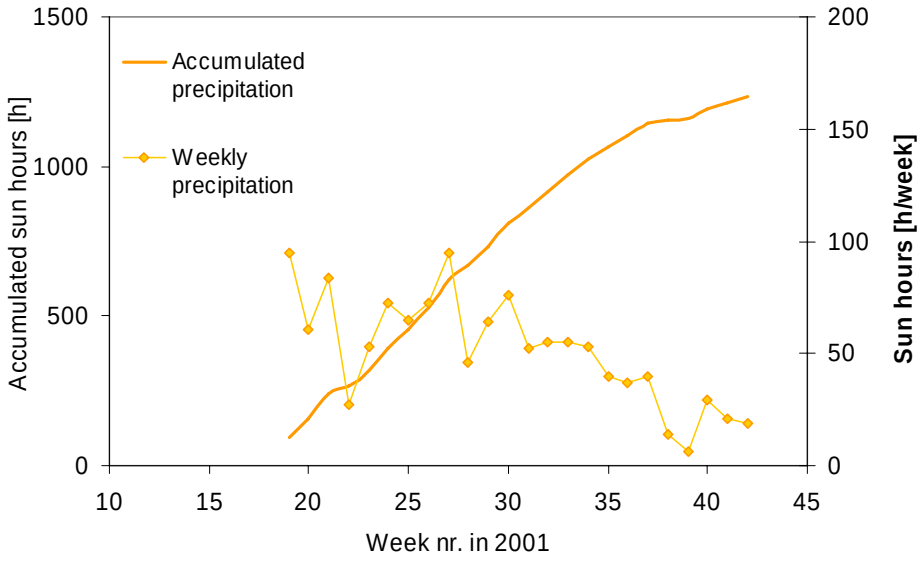

Figure 6. Sun hours at the Årslev site in the growth period displayed as weekly sunshine and accumulated sun shine (data from Cappelsen, 2004).

5.2 Structure of hemp fibres

The structural study is based on the middle section of hemp stems from the cultivar Felina that was cultivated at Danish Institute of Agricultural Sciences in 2001.

5.2.1 Structure on the plant stem level (0.002-10 mm)

The hemp fibres are present in bundles as long as the stems, which can easily be peeled off the xylem surface by hand or machine (Figure 7). The fresh stem consists of a hollow cylinder of 1-5 mm thick xylem covered by 10-50 µm cambium, 100-300 µm cortex, 20-100 µm epidermis and 2-5 µm cuticle (Garcia-Jaldon et al. 1998). The pith is empty space in dry stems.

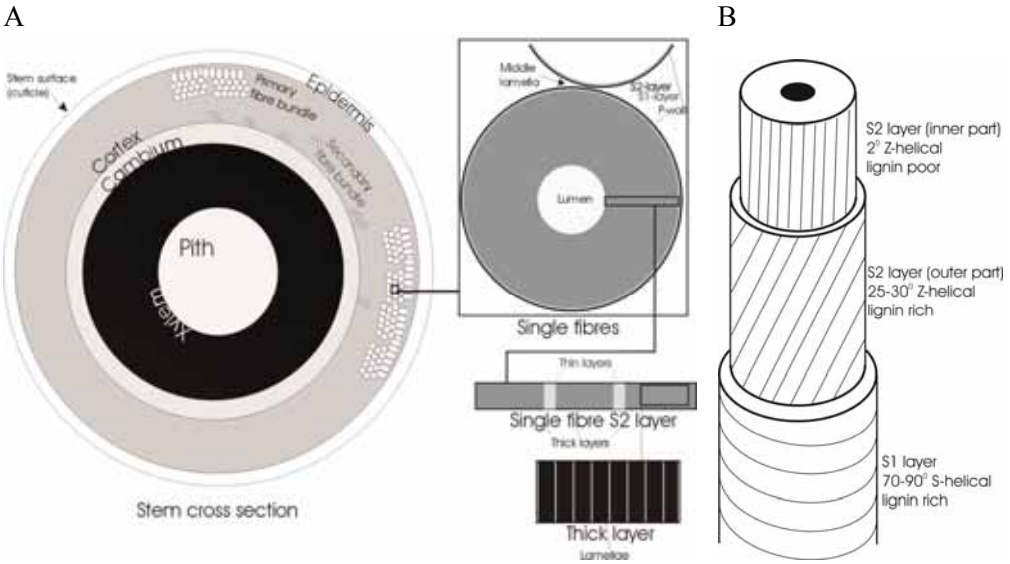

Figure 7. A: Model of transverse hemp stem section zooming to single fibres, secondary cell wall and finally the cell wall lamella. B: Model of the microfibril orientation throughout the secondary cell wall (Paper II).The S3 layer was not found in hemp fibres.

5.2.2 Structure on the fibre bundle level (1-100 μM)

The cortex part of the hemp stems in Felina contains bundles of 100-300 polygonal-shaped primary and secondary single fibres with 4 to 6 sides (Figure 7; Figure 9; Paper II). The single fibres are long (5-55 mm) compared with the fibres in the xylem (0.2-0.6 mm; Table 2; Vignon et al., 1995). The primary fibres nearest the stem surface are large (cell wall thickness = 7-13 μm; length = 20 mm; Sankari, 2000). These fibres are formed at the early growth stage during the phase of rapid stem elongation and contribute in Fedora, Felina and Futura to 92-95% of the bast fibres located in the cortex (Mcdougall et al., 1993; Sankari, 2000). The secondary fibres near the cambium layer are smaller (cell wall thickness = 3-6 μm; length = 2 mm; Sankari, 2000) and only present in the thick part of the stem (Mcdougall et al., 1993; Figure 9b).

The average area of the transverse fibre section including cell lumen was calculated to 780 $\mu m^2 \pm 300$ μm^2 and the lumen fraction in the fibres to 9% ± 7% (Paper II). The variation in area is due to actual variation in fibre size and not due to inaccurate measurement. Therefore the load carrying part of the single fibers is high (91%) compared with wood and straw fibres with larger lumens. Jute fibres and flax fibres have also small lumens (Cichocki and Thomason, 2002; Henriksson et al., 1997).

Table 2. Characteristics of different bast fibres (hemp, flax, jute and ramie), leaf fibres (sisal), seed fibres (cotton), wood fibres (Norway spruce) and straw fibres (wheat straw).

Plant	Fibre type [2]	Length (mm)	Diameter (μm)	L/D	Microfibril angle (degrees)
Hemp fibres	Bast fibres	5-60	20-40	100-2000	4
Hemp shives	Tracheid fibres	0.2-0.6	10-30	20	
Flax fibres		2-40	20-23	100-2000	10
Jute fibres	Bast fibres	2-3	16	160	8
Ramie fibres		40-150	30	40-150	8
Sisal fibres	Perivascular fibres	2-4	20	140	20
Cotton fibres	Epidermal hair on seed tubes	20-70	20-30	1250	n.a.[3]
Norway spruce[1]	Tracheid fibres	1-4	30-40	60-90	5-30
Wheat straw	Tracheid fibres + perivascular fibres	0.5-2	20-35	17-80	0° in epidermis Rest: random

1: The microfibril angle is 30° in earlywood decreasing to 5° in intermediate wood and latewood (Bergander et al., 2002).
2: Tracheids are the fibres in the xylem (woody structure); Bast fibres are arranged in bundles in the cortex (phloem). Perivascular fibres are located outside the xylem in straw fibres and leaves (Mcdougall et al., 1993).
3: n.a. = Not available
References: Fink et al., 1999; Liu et al., 2005; Mukherjee and Satyanarayana, 1986; Vignon et al., 1995.

5.2.3 Structure on the cell wall level (0.05-20 μm)

The distribution of lignin, pectin and wax was determined within the cell wall of hemp fibres by histochemistry. The inner part of the secondary wall in single fibres of Felina was found lignin poor by negative Wiesner reaction and negative Mäule reaction (Paper II; Figure 8a), while the outer part of the fibre wall was found lignin rich by positive reaction (red staining).

It seems likely, that the first lignification step occurs in the compound middle lamellae, which had the same high lignin content in thick- and thin-walled fibres (Paper II). The second lignification step occurred during synthesis of the outer part of the S2 layer. The lignin synthesis appeared reduced in later stages of fibres development due to the low lignin content in the inner part of the S2 layer.

Both the parenchyma cells and the single fibre compound middle lamellae contained pectin, while the secondary wall lacked pectin according to the staining reaction with Ruthenium Red (Figure 8b). Wax was found in the epidermis cells with highest content in the cuticle layer according to hydrophobic red staining with Sudan IV (Figure 8c). Apparently lignin was not stained with Sudan IV since the sites with lignin observed in Figure 8a were not stained.

According to the histochemical investigation, pectin degradation can provide separation of the fibre bundles from the xylem surface, while separation of the fibre bundles into single fibres requires both lignin and pectin degradation (Figure 8b and c; Paper II). Wax can inhibit binding between plant fibres and epoxy (Bos et al., 2004), so it must be extracted to obtain strong fibre-matrix interface in composite materials.

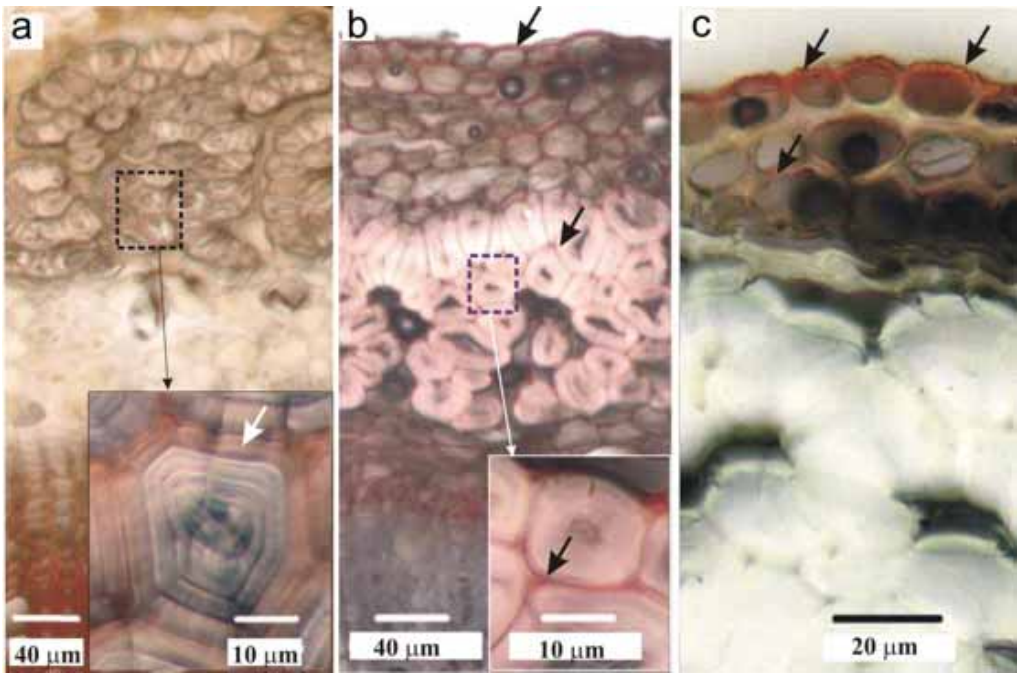

Figure 8. Lignin (a), pectin (b) and wax (c) stained in transverse sections of hemp stem. Lignin stained red by the Mäule reaction (a) (arrows = strongly lignified part of the cell wall). Pectin stained by Ruthenium Red (b) (arrows = pectin rich compound middle lamellae). Wax stained by Sudan IV (c) (arrows = wax rich cuticle layer).

The microstructure of the fibre wall in the hemp fibres and the decay patterns caused by fungal cultivation on hemp were investigated by transmission electron microscopy. The fibre middle lamellae (ML) and primary wall (P) were found to have thickness of 30-50 nm and 70-110 nm, respectively (Figure 10A, B). The secondary cell wall was composed of a 100-130 nm thick S1 layer and a 3-13 μm thick S2 layer (Paper II). Both SEM and TEM observations showed that the S2 layer had a laminate structure of 1 to 4 concentric layers of 1-5 μm in thickness (Figure 9C-D; Figure 10B-C). These layers were constructed of 100 nm thick lamellae. Thin layers of 200-240 nm in thickness were located in between the concentric layers (Figure 10A). These thin layers seems to lack cellulose, since they were selectively degraded by the mutated white rot fungus *P. radiata* Cel 26, which does not degrade cellulose at significant degree (Nyhlen and Nilsson, 1987; Figure 10C).

Inter-laminar cracks were also observed in the fibre wall after fibre bundle test showing that the interface between the wall-layers is weak (Paper II). The cracks might have a negative effect on the overall fibre strength due to lack of stress transfer through the cell wall.

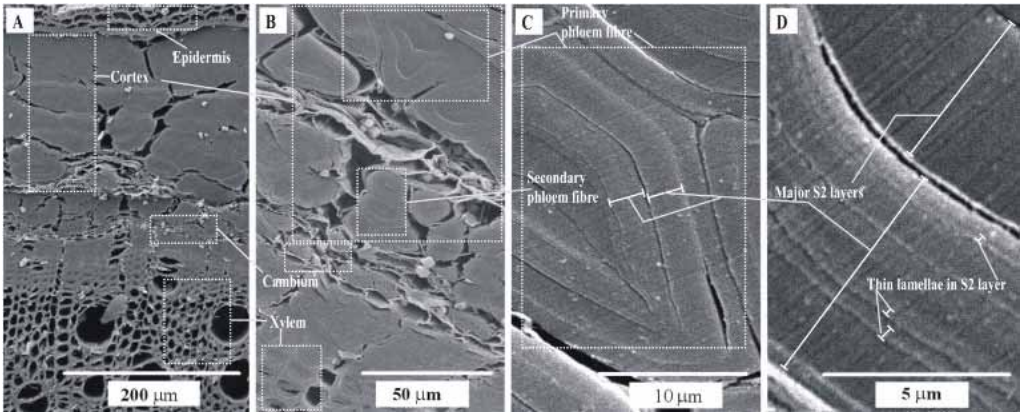

Figure 9. Hemp stem shown at increasing magnification using different transverse sections in SEM: A: Xylem + cambium + cortex + epidermis; B: Primary and secondary single fibres; C: Major layers in primary single fibre; D: Thin lamellae within the S2 layer (Paper II).

The microfibril angle through the fibre wall was investigated by polarised light microscopy and scanning electron microscopy. It was found that the microfibrils in fibres of Felina hemp had a main orientation of 0-5° in the S2-layer. The presence of Z-helical angles in the range 25-30° was observed (Figure 11A), but with variation between the fibres (Paper II). Difference in microfibril angle is also present between early wood and late wood (Table 2). Superficial attack of hemp fibres (Figure 11C) and polarization light microscopy showed the S1 layer with microfibril angles in the range of 70-90° (Paper II). The average MFA in hemp fibres of 4° that is measured by X-ray diffraction (Fink et al., 1999) is thereby confirmed with more detailed information. The low overall MFA in hemp fibres explains the high stiffness in the range 50-80 MPa compared with sisal (6-22 GPa) with similar cellulose content and higher MFA i.e. 10-25° (Table 2,Table 3).

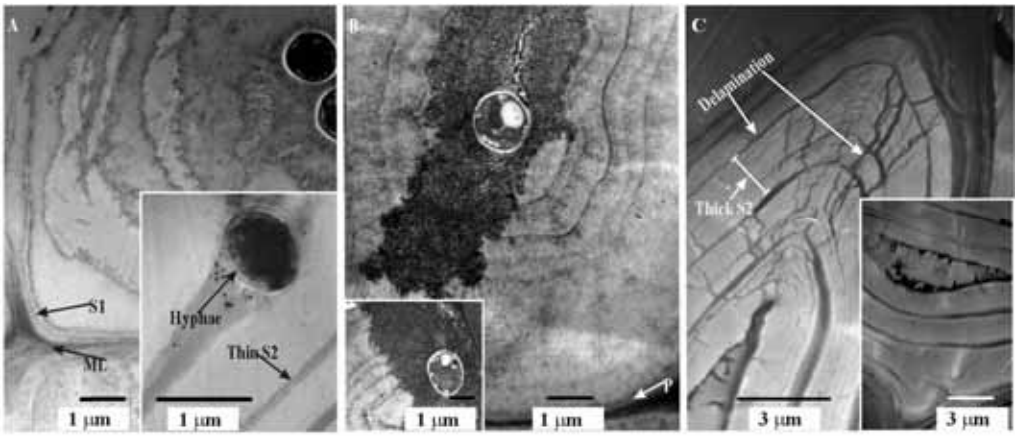

Figure 10. Single fibres partially decayed by fungi (transverse sections). A: P. mutabilis decay of the thick layers in S2. B: P. radiata *(wild) decay of the cell wall from the lumen side. C:* P. radiata *Cel 26 decay of the thin layers between the thick concentric S2 layers (Paper II).*

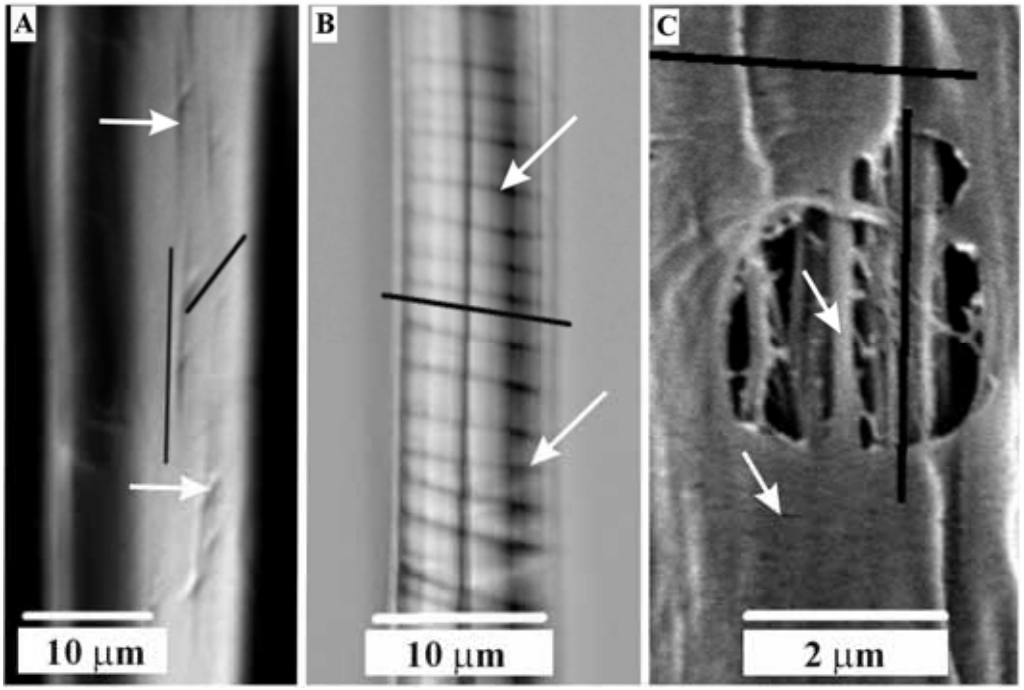

Figure 11. Microfibril angles (MFA) in fungal colonized and delignified single fibres shown with black lines and white arrows: A: Crossing cavities parallel with two different MFA in S2. B: A third MFA identified as dark and winding cavities in S1. C: P. radiata *Cel 26 treated fibre with the S1 layer partly stripped off revealing the underlying S2 layer (Paper II).*

5.3 Chemical composition of hemp fibres

Fibres from different plant species can appear quite different. However the chemical composition is fairly similar. Plant fibres consist mainly of cellulose, hemicellulose and lignin in different proportions. These components comprise 80-90% of the dry material (Table 3). The rest consists of mainly minerals, pectin, waxes and water-soluble components. Variation in the chemical composition can occur within the hemp species depending on environmental conditions and within the hemp plant between woody cores, bast fibres and leaves.

Plant fibres have in general been analysed by strong acid hydrolysis (Kaar et al., 1991), comprehensive fibre analysis (Browning, 1967) and agricultural fibre analysis (Goering and Van Soest, 1970). These methods were compared in Paper III. The comprehensive fibre analysis was found to cause a slight overestimation of the hemicellulose content and determine similar cellulose content compared with the strong acid hydrolysis. Anyway the comprehensive fibre analysis was in general applied (Figure 11), since it enables determination of pectin, wax and water-soluble components that are important in relation to defibration of hemp.

Table 3. Composition found in different bast fibres (hemp, flax, jute and ramie), leaf fibres (sisal), seed fibres (cotton), wood fibres (Norway spruce) and straw fibres (barley straw and corn stover) (Paper III and IV).

Fibre composition (g/100 g DM)	Cellulose	Hemi-cellulose	Lignin	Pectin	Wax	Water extractives	Minerals
Hemp fibres from different cultivars							
Felina 34	64	14	5	5	0	8	4
Uso	60	15	3	7	1	10	4
Futura 77 [1]	54	14	13		15[2]		4
Fedora 19 (stems) [1]	61	10	12		12[2]		4
Fedora 19 (shives) [1]	47-48	21-25	16-19		8-9[2]		1-2
Fibres from other plants							
Flax[3a]	64	16	2	2	n.a.[4]	n.a.[4]	n.a.[4]
Jute[3b]	58-60	14-16	12	0-2	n.a.[4]	n.a.[4]	8
Ramie[3b]	69	13	0-1	2	n.a.[4]	n.a.[4]	n.a.[4]
Sisal[3b]	53-66	12	10-14	1	n.a.[4]	n.a.[4]	7
Cotton	81	12	2	2	2	2	0
Norway spruce	49	20	29	1	0	1	0
Barley straw	43	38	9	0	0	5	5
Corn stover	33	33	14	1	3	10	7

1: Measured by the agricultural fibre analysis (Paper III; Thomsen et al., 2005).
2: Measured "non cell wall material" including pectin, wax and water extractives.
3: a: Mcdougall et al. (1993); b: Han and Rowell (1996); Mcdougall et al. (1993)
4: n.a. = Not available

Bast fibres from hemp, flax, jute and ramie contain 50-70% cellulose, 10-15% hemicellulose, 5-15% lignin and 5-10% pectin (Han and Rowell, 1996; Mcdougall et al., 1993; Table 3). Fibres from Felina hemp contained less lignin than fibres from the other hemp cultivars. The cellulose content in Felina hemp fibres and Fedora hemp fibres were on the same level as in flax fibres and jute fibres (60% w/w). The chemical composition of the hemp shives was similar to the composition of Norway spruce. Woody fibres like Norway spruce contain less cellulose (45-50%) and more lignin than hemp fibres. The straw fibres from barley and corn contained less cellulose (30-45%) and more hemicellulose (30-40%) than wood and almost no pectin (<1%). In barley straw, the lignin content (9%) seems underestimated, while the hemicellulose content (38%) seems overestimated by the comprehensive fibre analysis compared to previous findings of 15% lignin and 24-29% hemicellulose (Bledzki et al., 2002).

5.3.1 Cellulose and crystallinity

Cellulose is a linear polymer of D-glucose molecules (poly[β-1,4-D-anhydroglucopyranose], ($C_{6n}H_{10n+2}O_{5n+1}$). Two adjacent glucose units are linked by elimination of one water molecule between their hydroxyl groups at carbon atoms 1 and 4. The repeating unit in the cellulose chain is strictly speaking cellobiose, consisting of two glucose units as shown in Figure 12a. The degree of polymerisation (n or DP) is the number of glucose units in the chain. The degree of polymerisation has been found to 4400 in cotton and to 2100 in pine pulp (Evans et al., 1989). Preliminary investigations showed that DP was 7000 in cellulose purified from raw hemp fibres (Paper I).

The glucose monomers in cellulose form hydrogen bonds both within its own chain (intramolecular) forming fibrils and with neighbouring chains (intermolecular), forming microfibrils. These hydrogen bonds lead to formation of a linear crystalline structure with a high theoretical tensile strength of 15 GPa (Lilholt and Lawther, 2000).

Plant cells form cellulose just outside the cell membrane (Salisbury and Ross, 1992), which crystallises to form microfibrils of 6 × 6 chains in transverse section (Heiner and

Teleman, 1997). The crystal structure of the formed cellulose is called cellulose Iβ (Nishiyama et al., 2002; Sarko and Muggli, 1974). Cellulose Iβ has a monoclinic unit cell with space group $P2_1$ and the cellulose chains arranged along the unique *c*-axis shown in Figure 12b. Bacteria can also form cellulose Iα with a triclinic unit cell. By treatment with NaOH, the more chemically stable cellulose II is formed by rearrangement of the chains. Cellulose II is not formed in many plant fibres since the structure is determined by the enzyme complex in the plant cell were cellulose synthesis occurs. However, Cullulose II is formed in some algae and bacteria.

X-ray powder diffraction is a suitable method to study the cellulose crystallinity due to the separate able diffraction from peaks caused by cellulose crystals and diffraction from amorphous cellulose, hemicellulose, lignin, pectin and minerals (Paper III). The crystallite diameter can also be estimated with X-ray diffraction based on the width of peaks representing directions perpendicular to the fibre axis (Miller indices: 110, $1\,\bar{1}\,0$ and 200). The crystallite length can be estimated based on the width of peaks representing directions parallel with the fibre axis (Miller index: 004).

Both the X-ray measurement geometries reflection mode and transmission mode were investigated to get an accurate procedure for determination of cellulose crystallinity. Reflection mode was found suitable since air scattering thereby can be neglected, which in transmission mode contributed to the amorphous scattering.

The most common sample preparation procedure is plane loading by pressing on top of the sample. This was not suitable for cellulose fibres due to underestimation of the diffraction peaks representing the fibre direction, mentioned as preferred orientation. Therefore side loading of samples was used, which gives more random fibre orientation in the sample and reduced effect of preferred orientation (Figure 13).

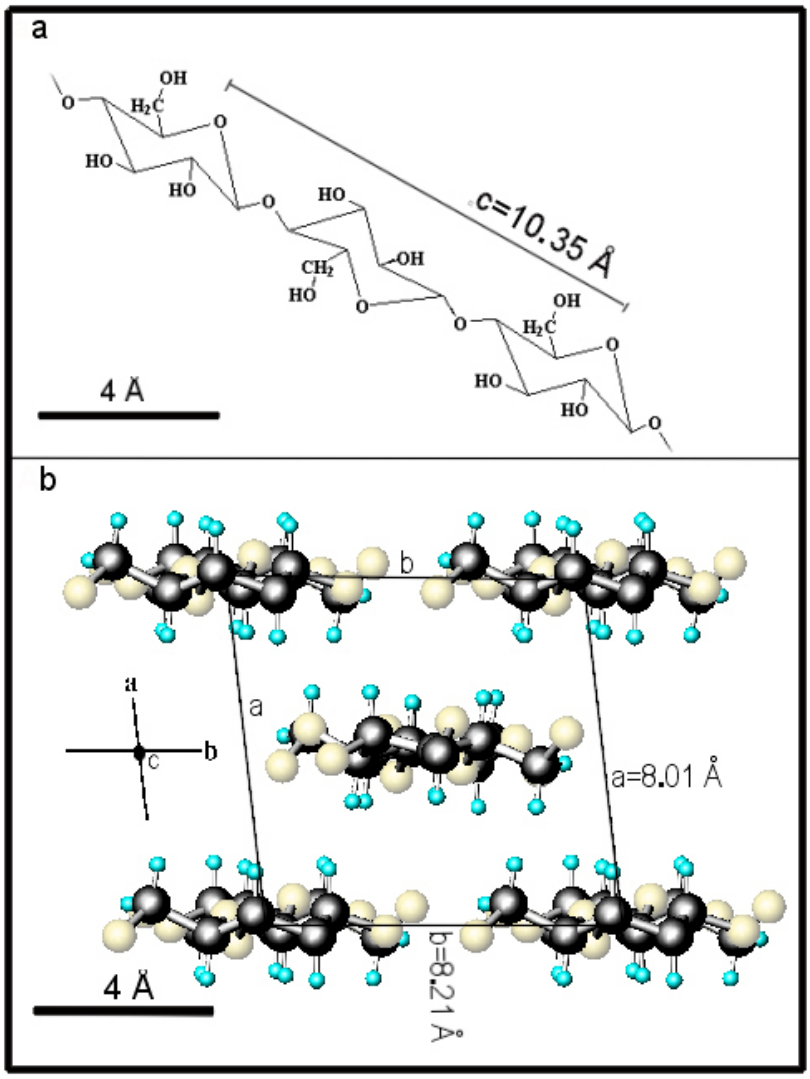

Figure 12. (a) The repeated cellobiose unit in cellulose as compared to the c*-axis length. (b) The cellulose Iβ structure viewed along the unique* c*-axis of the $P2_1$ unit cell with the* a- *and* b*-axis in the paper plane (five molecule chain ends are shown) (Paper III).*

Due to disagreement about how to separate the amorphous and crystalline diffraction in the obtained diffractograms, the cellulose crystallinity was calculated by four methods: the peak height ratio method (Segal et al., 1959), the amorphous standard method (Ruland, 1961; Vonk, 1973), the Rietveld refinement method (Rietveld, 1967, 1969) and the Debye calculation method (Debye, 1915). The peak height ratio method was found unreliable due to variation in crystallite size and resulting variation in peak overlapping. The amorphous standard method was better but not sufficiently reliable due to the poorly determined intensity for low diffraction angles ($2\theta < 15°$). The Rietveld method was more advanced and gave a more detailed result, since the known crystal lattice structure for cellulose Iβ was used (Nishiyama et al., 2002) and refined in combination with refinement of crystallite size. The peak shapes and sizes were thereby fitted to the measured diffraction peaks and the amorphous scattering was determined as the residual scattering (Figure 13). The Debye method also uses the cellulose Iβ structure for calculation of the shape and size of the diffraction peaks based on the crystallite size. Thereby, a more reliable determination of the crystalline part is obtained. However, due

to the computing effort and the subjective and manual fitting of crystallite size with the Debye method, the Rietveld method is more suited as a standard method.

The results for cellulose content and crystallinity are presented in Table 4 and compared in Figure 14. The highest cellulose crystallinity (90-100 g/100 g cellulose) was found in barley straw, corn stover and Felina hemp fibres (full drawn line in Figure 14).

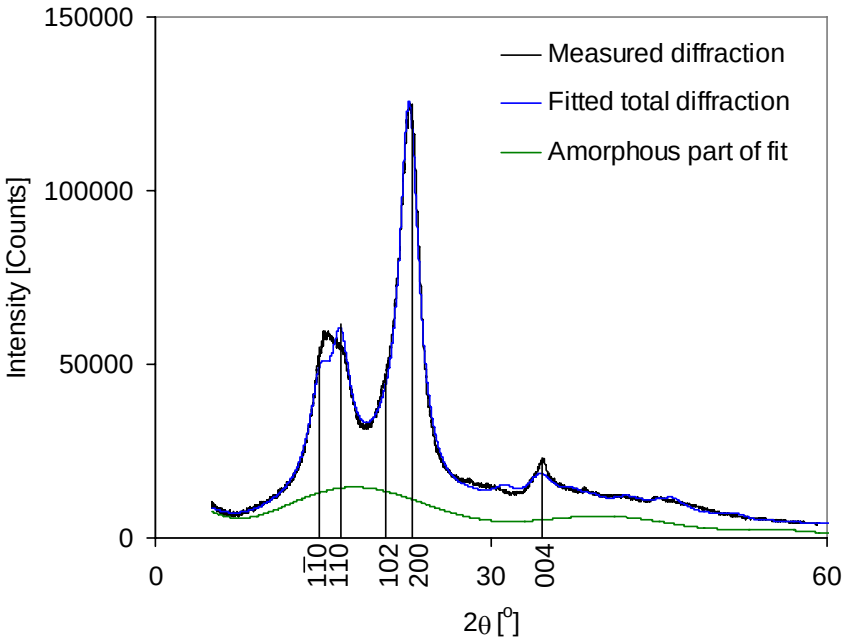

Figure 13. Diffractogram of water retted hemp fibres measured in reflection mode of a side-loaded fibre sample. Determination of the crystalline cellulose content was done by Rietveld refinement. The obtained fits for the amorphous and the crystalline diffraction are shown (further details in Paper III). The peak positions are marked with Miller indices.

Norway spruce had a cellulose crystallinity of 67 g/100 g cellulose, which is similar to previous findings of 51-71 g/100 g cellulose also determined with X-ray diffraction (Andersson et al., 2003). The cellulose crystallinity was on the same level in filter paper (65 g/100 g cellulose) and was also comparable to the crystallinity of 68 g/100 g cellulose that has been measured in pine kraft pulp by 13C-NMR (Liitia et al., 2003). The cellulose crystallinity of wood based materials was thereby found to be on the same level when determined by X-ray diffraction and by 13C-NMR, and the pulping process had only slight effect on the cellulose crystallinity. The present data as well as literature data are shown in Figure 14 and related by the dotted line, which represents the sample crystallinities at a cellulose crystallinity of 65-g/100 g cellulose.

Table 4. The plant fibres cellulose crystallinity, calculated by Rietveld refinement, (g/100 g cellulose) and chemical composition measured by comprehensive fibre analysis (g/100 g dry matter) (Paper III and IV).

Material	Cellulose crystallinity g/100 g cellu.	Cellulose g/100 g DM	Sample crystallity g/100 g DM	Amorphous cellulose g/100 g DM	Residual components g/100 g DM
Hemp fibres	94	64	60	4	36
Norway spruce	67	49	33	16	51
Barley straw	100	43	43	0	57
Corn stover	100	33	33	0	67

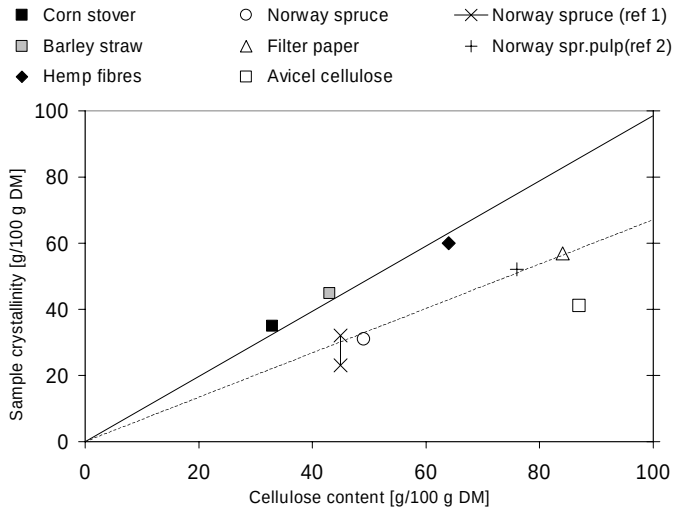

Figure 14. Sample crystallinity determined by Rietveld refinement compared to the cellulose content. The relationship for non-woody materials (full drawn line) and the relationship for wood based materials (dotted line) are shown (ref 1 = Andersson et al. (2003); ref 2 = Liitia et al,(2003); Paper III; Paper IV).

5.3.2 Hemicellulose

Hemicellulose in hemp and straw fibres are short and highly branched polymers of pentoses such as xylose and arabinose (Puls and Schuseil, 1993). Hemicellulose contains also substituents like acetyl groups and glucoronic acid (Figure 15). The degree of polymerisation is much lower than in cellulose ranging from 20 to 300. By attached ferulic acid and *p*-coumaric residues, hemicellulose can form covalent bonds to lignin (Bjerre and Schmidt, 1997). Hydrogen bonds are formed between xylan and cellulose. Due to this linking effect of hemicellulose, hemicellulose degradation leads to disintegration of the fibres into cellulose microfibrils resulting in lower fibre bundle strength (Morvan et al., 1990).

Mainly the acid residues attached to hemicellulose make it highly hydrophilic and increase the fibres water uptake, which increases the risk of microbiological fibre degradation. It has been found that hemicellulose is thermally degraded at lower temperature (150-180°C) than cellulose (200-230°C) by wet oxidation (Bjerre et al., 1996) and composite manufacturing (Madsen, 2004).

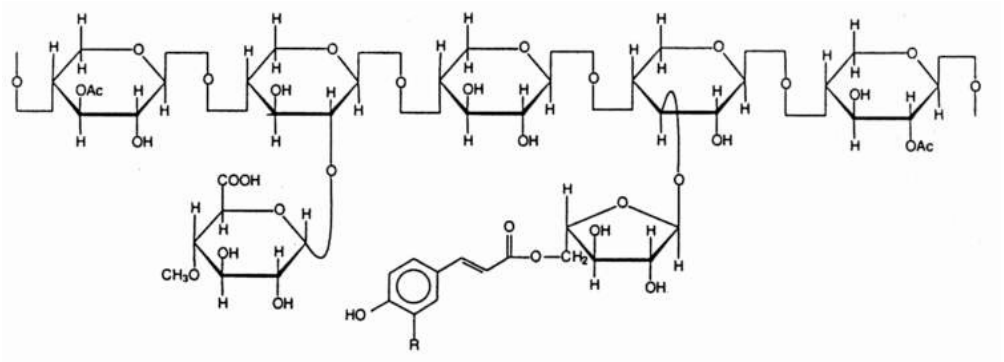

Figure 15. The structure of hemicellulose in non-woody fibres (grasses) showed as the acetylated xylan chain with α-1,2 bond to 4-O-methyl glucuronic acid (left side group) and with α-1,3 bond to L-arabinofuranose, which also is linked to phenolic acid (right side group) (Puls and Schuseil, 1993).

5.3.3 Lignin

Together with cellulose, lignin is the most abundant and important polymeric organic substance in the plant world. Lignin increases the compression strength of plant fibres by gluing the fibres together to form a stiff structure, making it possible for trees of 100 meters to remain upright. Lignin is a very complex three dimensional polymer, made of different phenylpropane units, which are bound together by ether and carbon-carbon bonds (Fan et al., 1982). Since hemp belongs to the Angiosperm phylum, it contains hardwood lignin of coniferyl alcohol, sinapyl alcohol and a minor content of *p*-coumaryl alcohol (Paper II). It was shown by treatment of hemp with *P. radiata* Cel 26, that degradation of lignin and pectin presumeably reduces the fibre bundle tensile strength slightly (Paper II). Therefore lignin seems to act like a matrix material within the fibres, making stress transfer on microfibril scale and single fibre scale possible.

5.3.4 Pectin

Pectin is a heterogeneous structure of acidic structural polysaccharides, found in fruits and bast fibres (Table 3). The majority of the structure consists of homopolymeric partially methylated poly-α-(1→4)-D-galacturonic acid residues but there are substantial 'hairy' non-gelling areas of alternating α-(1→2)-L-rhamnosyl-α-(1→4)-D-galacturonosyl sections containing branch-points with mostly neutral side chains (1-20 residues) of mainly L-arabinose and D-galactose (rhamnogalacturonan I). Pectin is the most hydrophilic compound in plant fibres due to the carboxylic acid groups and was easily degraded by defibration with fungi (Paper IV). Tests of hemp fibres as single fibres and fibre bundles showed that treatment with pectinase enzymes and thereby pectin degradation decreases the fibre strength slightly (Paper II; Madsen et al., 2003).

6 From hemp plant to composites

The traditional procedure for hemp processing is to grow the hemp plants for one growth season and cut the stems near the ground in the harvest (Figure 16a-c). The harvested hemp is either field retted or water retted to loosen the fibres from the stem surface (de Meijer, 1995). After retting, the fibres are extracted from the dry stems by decortification. Mats are formed of the fibres (g) and press consolidated with melted polypropylene (h) to form composite sheets (i) (Andersen and Lilholt, 1999).

Figure 16. Traditional procedure for going from the hemp plant to fibre reinforced composite materials. The process goes through field cultivation (a → c), retting and decortification (d → f) and addition of polypropylene, heat and press consolidation (g → i).

6.1 From plant stem to fibre assemblies

The traditional procedure for production of fibres from hemp is field retting, a natural process which results in fibres of variable quality due to differences in weather conditions (Figure 17; Meijer et al., 1995). During this process fungi and yeasts colonise the hemp and produce polysaccharide-degrading enzymes, which macerate and disrupt the parenchyma cells. This process can be replaced with the more controllable water retting procedure in which the plant stems are placed in tanks with 30-40°C hot water for 4 days (Meijer et al., 1995; Rosember, 1965).

After retting, the woody core is broken into small pieces that can be separated from the fibres by *decortification*. This is industrially done with pairs of rotating rollers (Hobson et al., 2001), which crush the shives. In lab-scale, the fibres are isolated with hand peeling. The extracted fibres are in the form of large fibre bundles useful in non-woven

fibre mats, which are made by air-drying and needle punching (Figure 17-left) (Dobel, 2002; Eriksen and Pallesen, 2002) with uncontrolled and thereby random fibre orientation. Production of aligned fibre assemblies can also be done at laboratory scale by combing the fibres in water, stretching them and air-drying them (Paper IV).

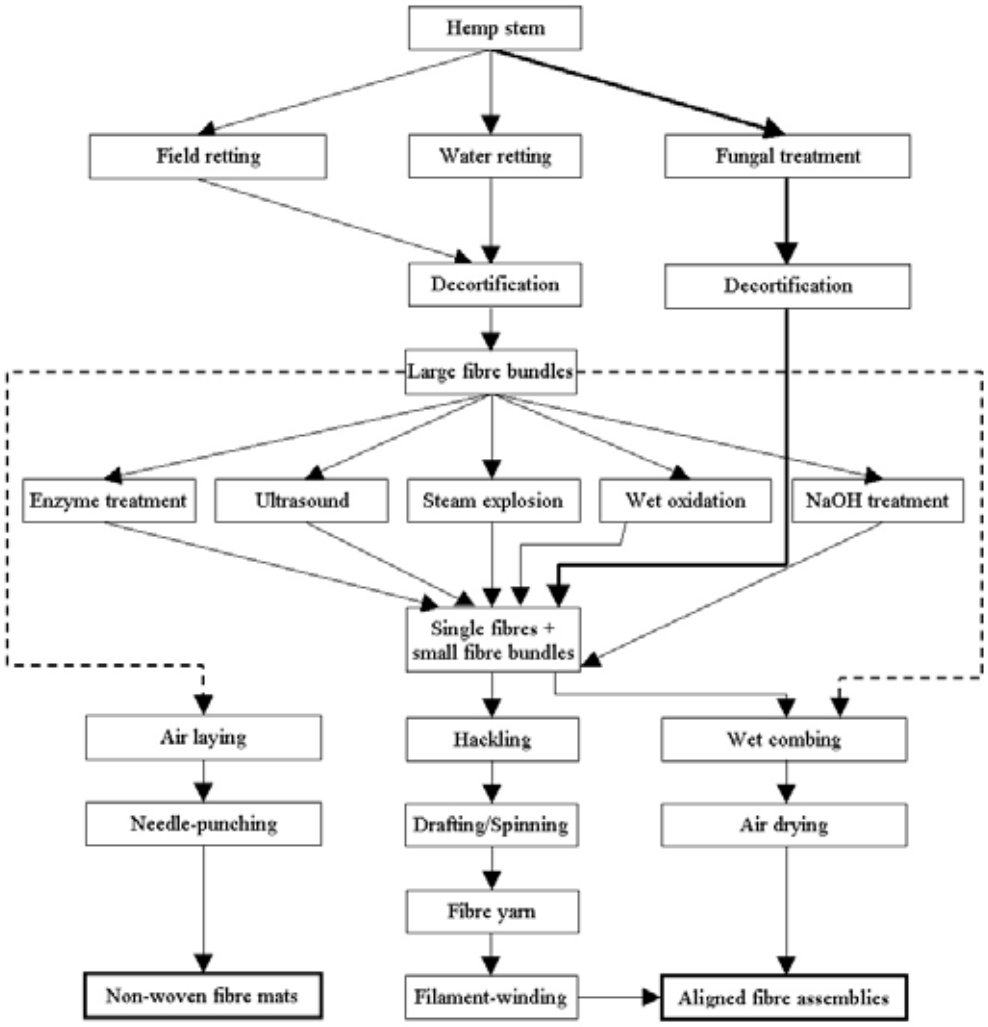

Figure 17. Retting and defibration processes, used to make fibre mats and aligned fibre assemblies of fibres from hemp stems.

6.1.1 Defibration

During water retting, the hemp bast is separated into large fibre bundles (Paper IV). Additional treatment is required to defibrate the fibre bundles into single fibres and small fibre bundles useful for production of hemp yarn. It is done by degradation or disruption of the middle lamellae between the single fibres. Enzyme treatment (Paper I; Brühlmann et al., 2000; Madsen et al., 2003), wet oxidation (Thomsen et al., 1999; Paper I) and NaOH treatment (Mwaikambo and Ansell, 1999; Wang et al., 2003) can degrade pectin and lignin in the middle lamellae between the single fibres.

Physical defibration methods include steam explosion (Paper I; Garcia-Jaldon et al., 1998; Madsen et al., 2003; Vignon et al., 1996) and ultrasound treatment (Zimmer and Kloss, 1995). It is suspected that these treatments introduce damage to the fibres. Fungal treatment of hemp stems has the advantage of degrading lignin, so single fibres can be obtained without a defibration step (Paper II). This procedure has been used for

defibration of flax fibres (Henriksson et al., 1997) and was used to obtain hemp fibres for composite materials in Paper IV.

6.1.2 Yarn production

The retted fibre bundles of 0.5-2 m length are traditionally used directly for production of yarn for rope production (Ole Magnus, Personal communication: telephone +45-86994515). First *hackling* is done in two steps to straighten the fibres and remove short disordered fibres with a metal-pinned brush; this results in a *sliver* of parallel fibres useful for spinning. At industrial scale, the *hackling* is performed using metal-pinned brushes and rotating rollers to pull the fibres forward. This technique is basically also used to make *sliver* of shorter fibres like flax fibres (15-200 mm; Grosberg and Iype, 1999).

By manual yarn *spinning*, some fibres from the sliver are mounted on a rotating hook. The fibres are stretched during the twisting process and more fibres are added, while the hand is moved backward to elongate the spun amount of yarn and keep a constant yarn thickness. At industrial scale, the stretching part of this process is called *drafting*. In drafting, the fibres become straightened by passing the *sliver* through a series of rollers with increasing rotational speed in the forward direction (Figure 18-left). The drafting process elongates the thick sections of the filament so they get the same thickness as the thinner sections, resulting in a uniform *sliver* ready for spinning (Figure 18-centre; Madsen, 2004).

The most common spinning method is ring spinning, in which *slivers* delivered from the *drafting* rollers become twisted by the *traveller* that is freely rotating on a ring (Madsen, 2004). The ring distributes the yarn onto a rotating bobbin. Each *traveller* rotation introduces one twist. Increased delivering speed from the *drafting* rollers decreases the number of twists per length. The twisting forces the fibres to take a helical structure and results in inherent sliding friction between the fibres (Madsen, 2004) and in axial strength in the yarn (Grosberg and Iype, 1999). The produced yarn can be wound on a metal frame (Figure 18-right) to get aligned fibre assemblies, ready for composite production (Madsen and Lilholt, 2003).

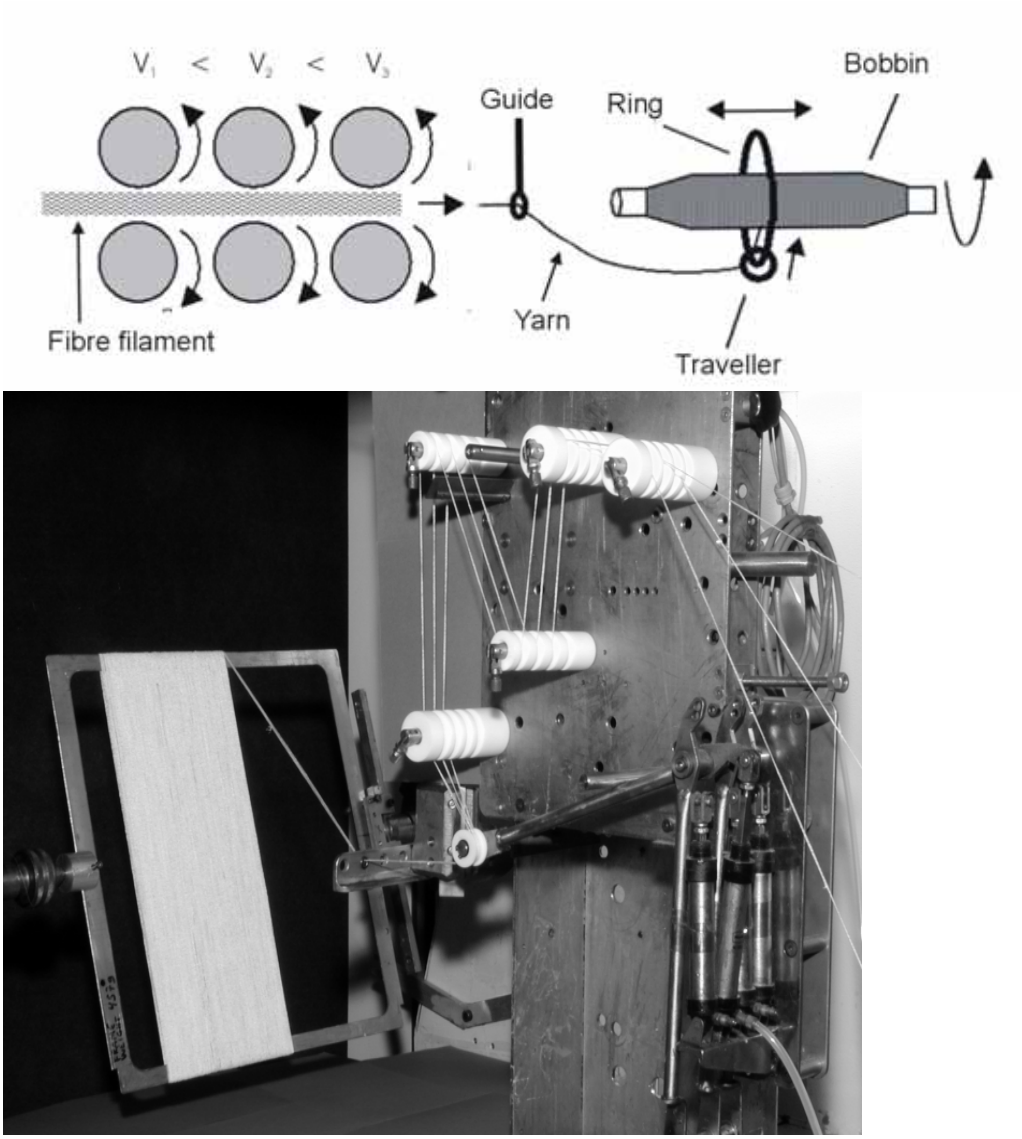

Figure 18. From fibre filament to aligned fibre assemblies: The drafting process with three pairs of rollers at different rotation speed (v; left), followed by ring spinning to get yarn (Grosberg and Iype, 1999; centre) and filament winding of yarn to get aligned fibre assemblies (Modified from Madsen, 2004; right).

6.2 From fibre assemblies to composite materials

6.2.1 Fibre part

Composite materials can be reinforced with non-woven fibre mats, with woven yarn and with wound yarn. Plant fibres from different origins are useful as reinforcement. These fibres originate from leaves (sisal, pineapple and henequen), from bast (flax, hemp, ramie, jute, kenaf), from seed (cotton) and from fruits (coconut husk) (Mohanty et al., 2000; Table 2; Table 3).

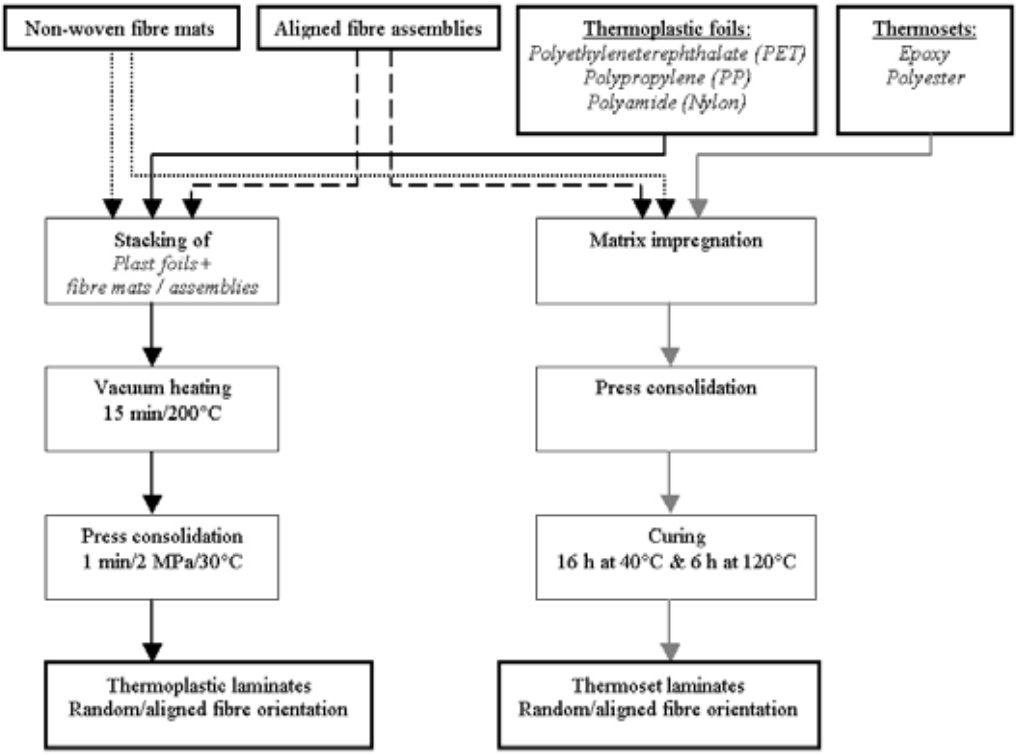

Figure 19. Pathway used to make composite materials of fibre mats and of aligned fibre assemblies with thermoplastics or with thermosets.

6.2.2 Matrix part

The matrix part of composite materials can both be thermoplastic like polyethyleneterephtalate (PET), polypropylene (PP) and polyamide (nylon) and thermoset, like epoxy and polyester (Figure 19; Figure 20). Thermoplastic has the advantage of giving greater fracture toughness, larger elongation at fracture, faster and more automatic processing, unlimited shelf life of raw material, recycling and a cleaner working environment (Lystrup, 1997).

Thermoset impregnated composite materials have the advantage of being processed at lower temperatures (40-120°C) compared with polypropylene at 200°C, since the thermal damage of the fibres is reduced at the lower temperature (Madsen, 2004; Figure 19-left; Figure 21-bottom). The polymer viscosity is low in thermosets (0.1-10 Pa·s; Lystrup, 1997) compared with thermoplastics (100-1000 Pa·s; Brüning and Disselbeck, 1992). However, the viscosity can be controlled during pressing within a wide range, since it decreases with increasing temperature.

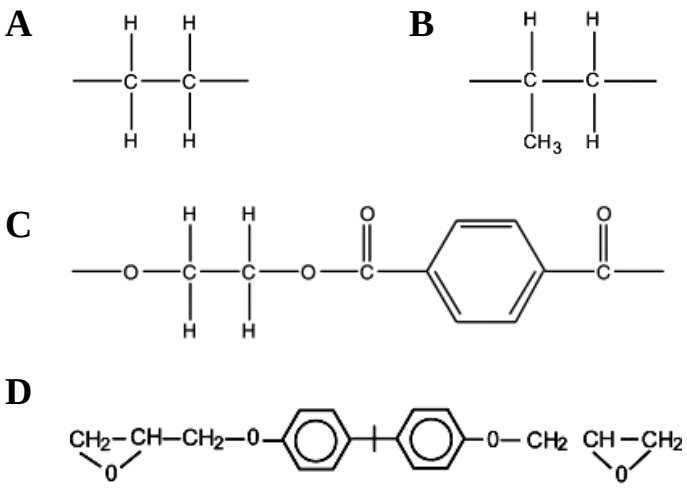

Figure 20. Chemical structure of (A) PE (polyethylene), (B) PP (polypropylene), (C) PET (polyethyleneterephtalate) and (D) epoxy (diglycidyl ether of bisphenol A) (Muzzy, 2000).

6.2.3 Composite processing

Composites can be made with fibres as mats and as aligned assemblies impregnated with matrix polymer (Figure 19-left and Figure 21-top). The processing techniques used are autoclave consolidation and mechanical press consolidation (Figure 22).

Autoclave consolidation is performed in vacuum to evaporate water and remove air from the fibres placed in vacuum backs (Figure 22a). The fibres and the fluid thermoset polymer are press consolidated during the curing process using pressurized air to compact the fibres.

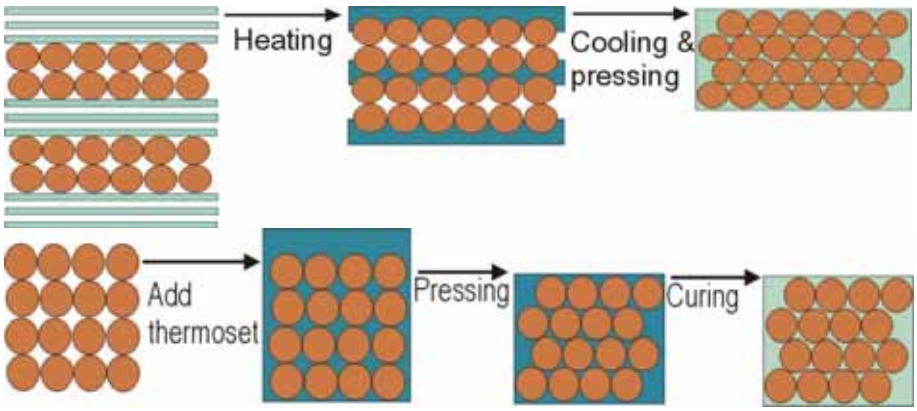

Figure 21. Above: Fabrication of thermoplastic composites of plastic foils and fibres by heating followed by cooling and pressing. Below: fabrication of thermoset composites by pressing and curing (brown=fibres, blue=liquid plastic, green=solid plastic).


a1: Lay up for autoclave consolidation


b1: Lay up for press consolidation


a2: Setup for the autoclave

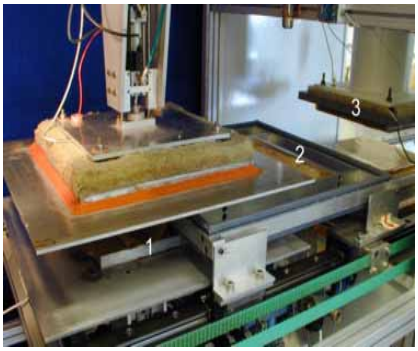

b2: Heat (1)→cooling (2)→pressing (3)

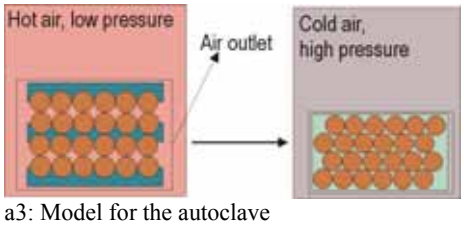

a3: Model for the autoclave

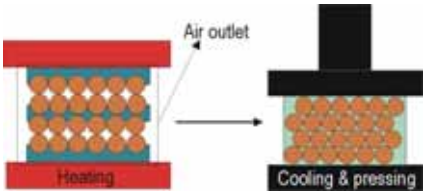

b3: Model for press consolidation

Figure 22a: Autoclave consolidation (a1) with air-pressure consolidation and with a tight vacuum bag containing the fibres and matrix polymer (a2) illustrated with a model (a3). b: Lay up with fibres and matrix polymer packed into slip foils (b1), heated to melt the polymer (b2-1) and press consolidated (b2-3) and illustrated with a model (b3).

In mechanical press consolidation, thermoplastic composites are made with heating (200°C for polypropylene, 10 min) under vacuum. The polymer is thereby melted and

water vapour and air are removed from the fibres so the molten polymer can impregnate them. Pressure consolidation (1 MPa) is used to improve the penetration of the fibre lay up and to increase the fibre compaction (Figure 22b; Andersen and Lilholt, 1999). Since the fibres will slide between each other during the compression, the obtainable fibre volume fraction in the final composite increases versus the consolidation pressure (Madsen and Lilholt, 2002).

6.2.4 Composite preparation in this study

The composites reinforced with aligned fibres that were made in this study were fabricated with epoxy as matrix material (Paper IV). Epoxy was used since this low viscosity polymer penetrates easily into the fibre assembly and forms covalent binding to the plant fibres resulting in strong interface (Obrien and Hartman, 1971). It was not suitable to make the composites in vacuum because of evaporation of chemicals from the fluid epoxy, which results in holes in the produced composites (Stephanie Feih, Personal communication: telephone +61-3-96769904). The composites were made with pressure consolidation using manually tightened clamps in a normal oven during pre-curing at 40°C and curing at 120°C (Figure 23; Figure 21-bottom).

a: Dried lay up

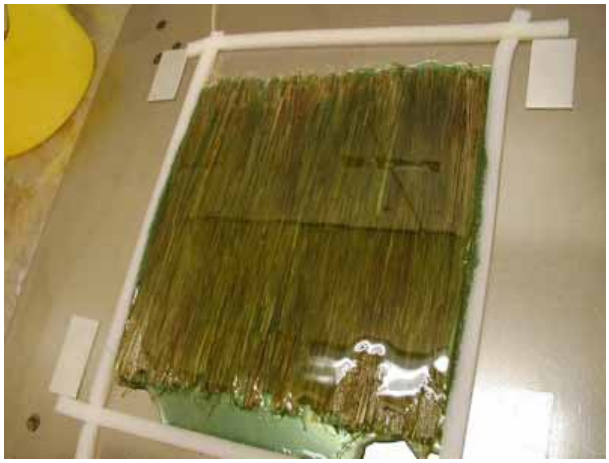

b: Epoxy added to the lay up

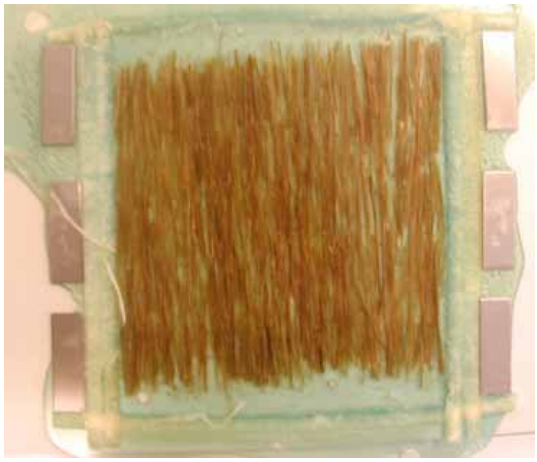

c: Cured laminate

Figure 23. Manual fibre lay up (a), addition of epoxy to the lay up (b) and curing of the epoxy to make a laminate (c).

7 Defibration methods

Defibration methods for production of fibres from the hemp plant can be divided into combined physical and chemical methods and biotechnological methods. The combined physical and chemical methods combine chemical reactions and physical disruption obtained at high pressure and high temperature. Procedures of this type include wet oxidation and steam explosion (Thomsen et al., 2005; Thygesen et al., 2002; Paper I). The biotechnological methods include water retting (Meijer et al., 1995; Paper IV), enzymatic defibration (Paper I) and fungal defibration (Henriksson et al., 1997; Paper IV).

7.1 Combined physical and chemical treatments

Both wet oxidation and steam explosion of hemp fibres increased the fraction of cellulose and decreased the fraction of lignin and non cell-wall materials like pectin and water extractives in the hemp samples (Figure 24). The amount of lost dry matter in a sample was an indication of the amount of lost cellulose, which in general was 12-17% w/w higher than the cellulose loss (Table 5).

In wet oxidation, the losses of dry matter were smaller (15-29 %) than in steam explosion (17-73 %). Correspondingly losses of cellulose were smaller (0-12 %) than in steam explosion experiments (0-69 %). Base addition resulted in large removal of cellulose so it might have a too strong effect on opening the structure of the plant constituents. The losses were in general higher when raw hemp fibres were treated (a) than when water-retted hemp fibres were treated, since some pectin and water extractives are extracted during the retting step (Paper IV).

The content of cellulose in the fibres increased by wet oxidation or steam explosion in retted hemp fibres from 73% to 85-90% and in raw hemp fibres from 60-64% to 73-75% (Figure 24). The most lignin was removed when oxidative conditions were applied since it is decomposed to low molecular phenolic compounds and oxidized to carboxylic acids (Klinke et al., 2002; Figure 25).

Impregnation with base before steam explosion reduced the hemicellulose extraction and increased the cellulose extraction (Thomsen et al., 2005). It has been shown that degradation of hemicellulose monomers to furans and carboxylic acids is reduced by base addition (Klinke et al., 2002).

a Wet oxidation conditions: 20-60 g Felina hemp fibres/l water; 10 bar O_2; 170°C; 10 min.
Steam explosion conditions: 50 g Felina hemp fibres/batch; 200°C; 10 min.

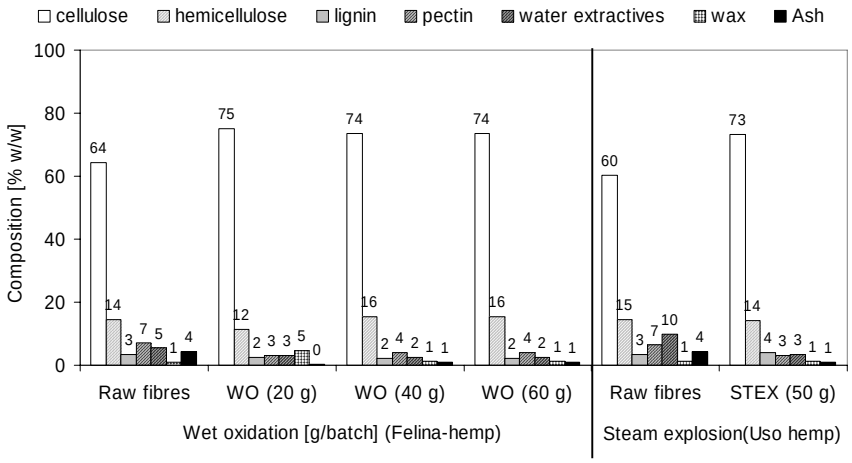

b Hydrothermal treatment: 10 g retted Fedora hemp fibres/l water; 170°C; 10 min.
Wet oxidation conditions: 10 g retted Fedora hemp fibres/l water; 10 bar O_2; 170°C; 10 min.
Steam explosion conditions: 50 g retted Fedora hemp fibres/batch; 200°C; 10 min.
Alkali: Wet oxidation: 5 g Na_2CO_3/l; Steam explosion: Impregnation: 50g Na_2CO_3/l for 1 hour.

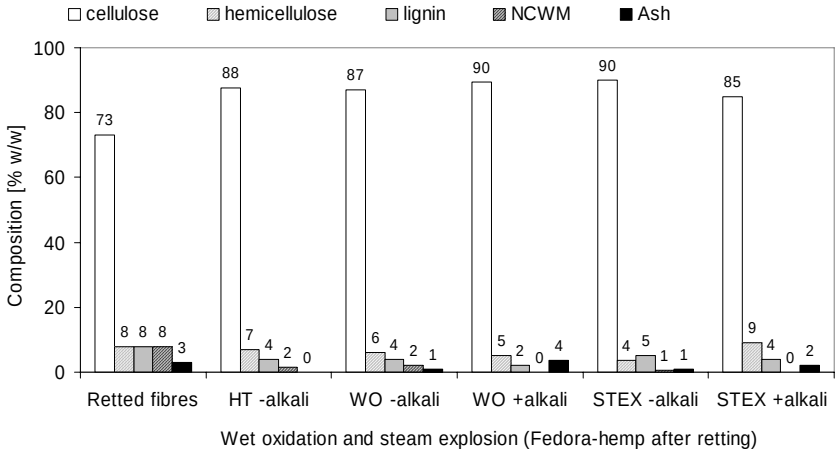

Figure 24. Chemical composition of the defibrated hemp fibres using wet oxidation and steam explosion. a: Wet oxidation and steam explosion on untreated hemp fibres with varied fibre addition (g fibres/batch) (Paper I). b: Effect of alkaline and oxidative conditions during the treatments applied on retted hemp (Thomsen et al., 2005).

Table 5. Fibre yield and cellulose recovery for the hemp fibres treated as presented in Figure 24 (Paper I; Thomsen et al., 2005).

	Fibre yield [% w/w]	Cellulose recovery [% w/w]
Use of raw hemp bast		
Wet oxidation (20 g batch)	78	90
Wet oxidation (40 g batch)	76	88
Wet oxidation (60 g batch)	83	97
Steam explosion (no alkali, 2 min)	74	90
Use of water retted hemp fibres		
Hydrothermal treatment (no alkali)	83	100
Wet oxidation (no alkali)	85	100
Wet oxidation (with alkali)	71	88
Steam explosion (no alkali)	83	100
Retted-STEX (with alkali)	27	31

Note: Conditions are shown in Figure 24.

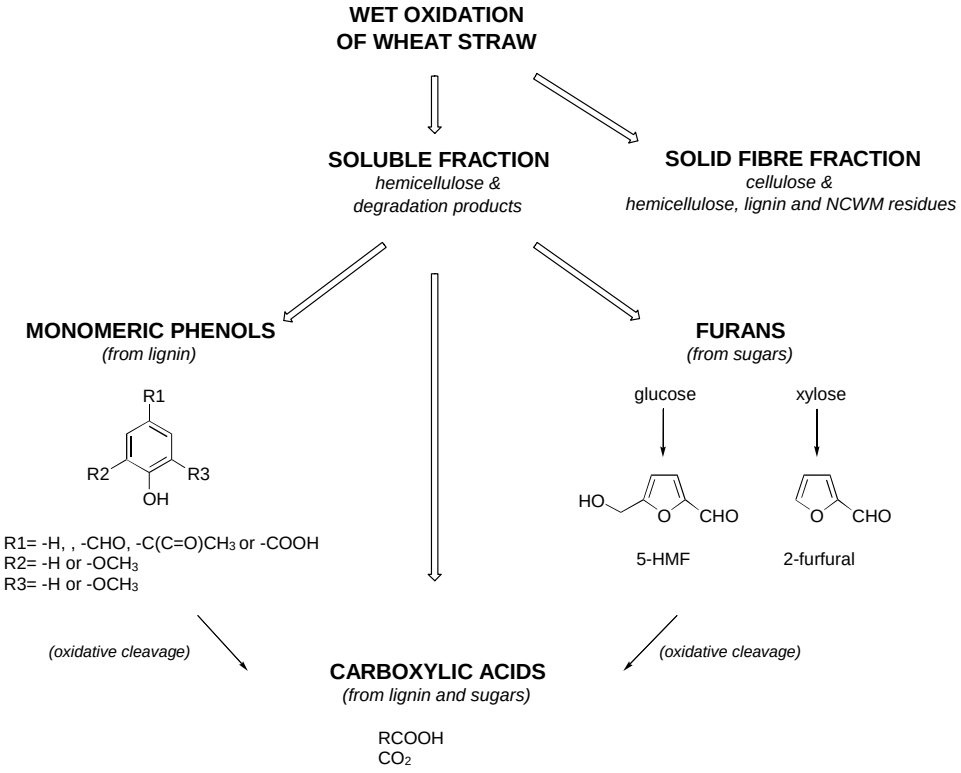

Figure 25. Principle of wet oxidation applied as pre-treatment of plant fibres. NCWM: water-soluble compounds like proteins and pectin; 5-HMF = 5-hydroxymethyl-2-furfural. The plant fibres are fractionated into a solid fraction of cellulose and a liquid fraction of hemicellulose and lignin. The intermediate phenols from lignin degradation and furans from sugar degradation are further oxidized to carboxylic acids and CO_2 (Klinke et al., 2002).

7.2 Biotechnological treatments

Treatment of Uso-hemp by combined field retting and exposure to frost during wintertime (Pasila, 2000) resulted in moderate increase in the cellulose content of the fibres (60→65% w/w) due to removal of water-soluble components and ash (unpublished data). The water retting process resulted in addition in pectin degradation

so higher cellulose content was obtained. Water retting is also a much faster process due to the higher microbial activity at the higher temperature (35°C; Paper IV).

Defibration of hemp with the fungus *P. radiata* Cel 26 resulted in addition to the fibre components degraded in water retting in hemicellulose and lignin degradation, so the cellulose content increased to 86% (Figure 26b). A similar chemical composition has been obtained by wet oxidation (Thomsen et al., 2005; Paper I), which is also an oxidative process. The cultivation resulted in slight cellulose decay, in the large-scale experiments, indicating the presence of cellulose degrading enzymes (Paper IV). However at the smaller scale the cellulose yield was high (96%) and the fibre wall remained intact as confirmed by TEM microscopy (Paper II; Figure 10).

The fungus *Ceriporiopsis subvermispora* degraded cellulose in the hemp fibres and formed much mycelium above the water surface, while stem pieces below the surface were not colonised by the fungus (Table 5, Figure 26b). The fungus grew well at low and medium scale cultivation with reduction of pH from 6 to 4.8 (Paper IV). At large scale, the sterilisation was insufficient resulting in lower fibre yield after 14 days cultivation (27 g/100 stem) and unchanged pH (Paper IV).

Lignin degradation was obtained by the treatment with *P. radiata* Cel 26 by peroxidase enzymes, confirmed as presence of H_2O_2 in the cultivation broth (Paper IV). Smaller fibre bundle transverse sections were therefore obtained by defibration with *P. radiata* Cel 26 ($3 \cdot 10^3$ μm^2) than by water retting and by *C. subvermispora* defibration (Paper IV), due to degradation of the lignin rich middle lamellae between the fibres.

Table 6. Fibre yield and cellulose recovery for the hemp fibres treated with the biotechnological methods presented in Figure 26 (Paper I; Paper IV).

Treatment	Fibre yield [% w/w]	Cellulose recovery [% w/w]
Water retting	68	79
Fungal defibration		
C.sub. treated 14 days	75	85
C.sub. treated 31 days	65	83
P.rad. treated 14 days	70	85
P.rad. treated 31 days	72	96
Enzymatic defibration using pectinex solution		
1 g/kg fibres	88	95
10 g/kg fibres	88	95
100 g/kg fibres	83	93
10 g/kg fibres followed by STEX	67	87

Note: Conditions are shown in Figure 26.

The treatment of hemp fibres with pectin degrading enzymes (Pectinex) resulted in moderate increase in the cellulose content of the fibres and in high cellulose recovery (93-95%, Table 6, Figure 26c). Neither pectin nor lignin was degraded during the treatment. Thereby it seems like that the enzyme mixture was insufficient for effective defibration. If the enzyme treatment was followed by steam explosion, pectin and hemicellulose degradation were also obtained resulting in more cellulose rich fibres (78% w/w).

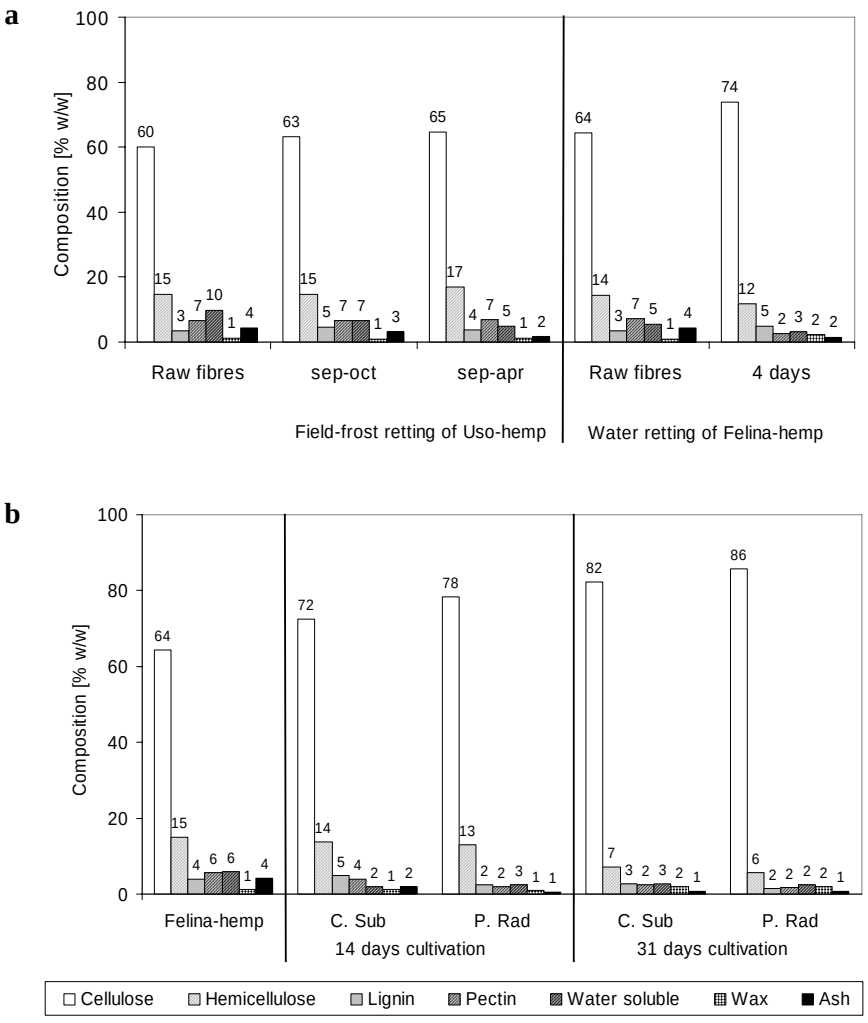

Figure 26. Chemical composition of hemp fibres treated with biotechnological methods. a: Frost treatment of Uso hemp and water retting of Felina hemp (Unpublished data; Paper IV). b: Fungal treatment of hemp (Paper IV). c: effect of pectin degrading enzymes (g pectinex solution/kg hemp bast, Paper I; Unpublished data).

7.3 The treatment procedures effect on cellulose crystallinity

Wet oxidation of corn stover resulted in increased content of crystalline cellulose in the fibres. The content of crystalline cellulose appeared to reach a level of 38-42% w/w for obtained cellulose contents of 50-60% w/w. Crystalline cellulose is thereby converted into its amorphous form at the high temperature applied during the treatment (190°C).

For the fungal defibrated hemp fibres, the cellulose crystallinity tended to decrease versus the obtained cellulose content showing that some crystalline cellulose was converted into amorphous form (Figure 27). Hemp yarn had even lower cellulose crystallinity and a sample crystallinity similar to water retted hemp fibres. The cellulose crystallinity remained constant during water retting of hemp, which was presumably due to the low lignin degradation, compared with the lignin degradation during defibration with *P. radiata* Cel 26 (Paper IV).

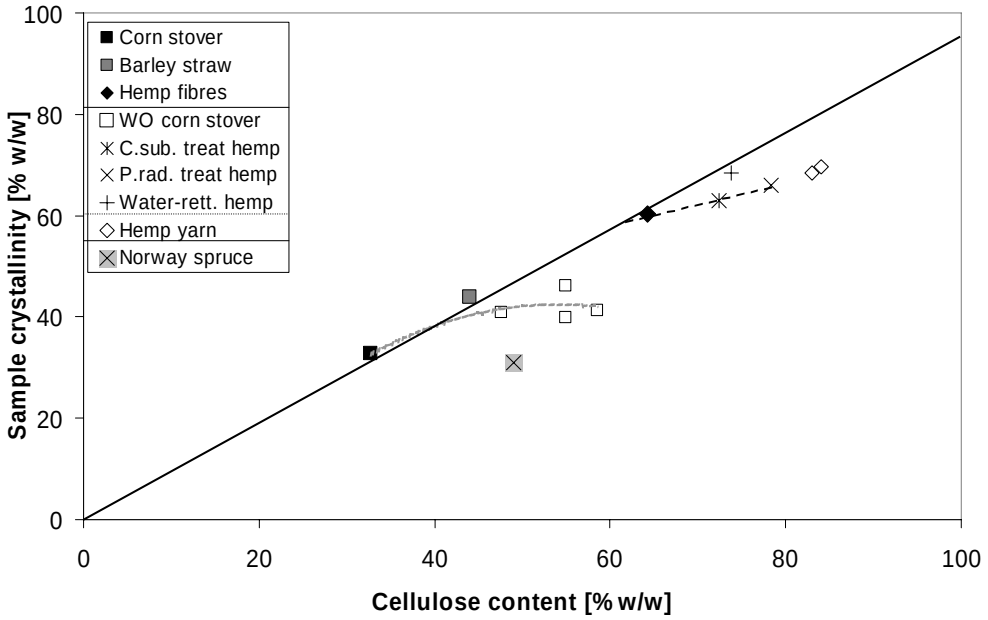

Figure 27. Sample crystallinity determined by Rietveld refinement versus the cellulose content determined by the comprehensive fibre analysis. The full drawn line shows the relationship for non-woody fibres. The grey line shows the effect of wet oxidation on corn stover. The effect of fungal treatment is shown by the dotted line (Paper III; Paper IV).

8 Fibre strength in hemp

The strength and the composition of hemp fibres depends on parameters like weather conditions, soil type, fertilization and defibration type (Hoffmann, 1961). Even the fibres within a single stem vary in strength with the weakest ones at the base of the stem presumably due to differences in chemical composition. The sensitivity to harvest year seems to vary between hemp cultivars with highest variation for *Uniko B* and lowest variation with *Uso 11* and *Felina 34* (Figure 28; Sankari, 2000). Low variation in the fibre strength indicates low sensitivity to weather conditions resulting in similar fibre properties each year.

8.1 Effect of hemp cultivar and the Weibull distribution

Hemp cultivars have bast fibres with different mechanical properties due to differences in the chemical composition of the fibres (Table 3). Based on cultivation experiments in Finland, the fibre strength with lowest standard deviation (100-200 MPa) was obtained with the cultivars *Futura*, *Fedora* and *Felina* with fibre bundle strength varying between 650 MPa and 1050 MPa (Sankari, 2000). Fibres from the cultivars *Uniko B* and *Secuieni* had higher fibre strength (550-1400 MPa) and higher standard deviation. Thereby lower effective strength will be obtained as explained by the Weibull distribution (Lilholt, 2002; Figure 28).

The Weibull effect is determined by a statistical procedure for calculation of the overall tensile strength of many fibres from the terms σ_0 and m, which depend on the average single fibre strength and the standard deviation. Increasing standard deviation (decreasing m) results in decreasing fibre bundle strength at constant average single fibre strength. Thus, raw Felina hemp fibres had a single fibre strength of 1200±400 MPa (Figure 29) and a fibre bundle strength of 950±230 MPa (Figure 30) which is 20% lower than the single fibre strength. According to the Weibull distribution the average fibre bundle strength is calculated as

$$\sigma_{av} = \sigma_0 \cdot V^{-\frac{1}{m}} \cdot \Gamma\left(1+\tfrac{1}{m}\right) \text{ and } V = e \times m$$

where σ_0 is a normalized stress term and Γ is the gamma function. The fibre bundle efficiency is the ratio between the overall fibre bundle strength and the average single fibre strength:

$$\sigma_{av} \Big/ \sigma_b = (e \times m)^{-\frac{1}{m}} \times \left(\Gamma\left(1+\tfrac{1}{m}\right)\right)$$

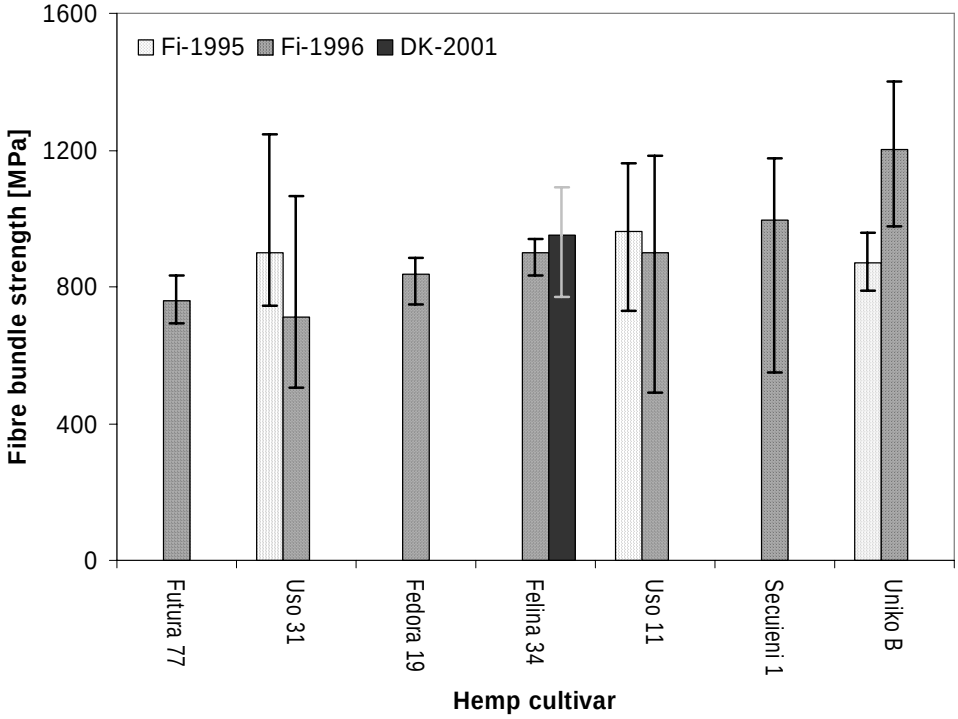

Figure 28. Fibre bundle strength of fibres from the hemp cultivars grown by Sankari (2000) in Finland. For the Finish samples, the test span length was 20 mm. For the fibres from Felina 34 that was grown at Danish Institute of Agricultural Sciences in 2001(DK-sample), the test span length was 3 mm. The cultivars are sorted according to increasing average strength.

8.2 Effect of pre-treatment of hemp

Steam explosion used for pre-treatment of hemp fibres resulted in single fibre strength reduced with 30% and lower standard deviation. That indicates that mainly the strong single fibres are weakened or degraded so the fraction of weak fibres increases (Madsen et al., 2003).

The effect of temperature during the treatment was only significant when defibration with pectin degrading enzymes was used for defibration before the steam explosion experiments. Thereby it was not critical if the treatment was performed at 185°C or 200°C, presumably due to low cellulose degradation at this temperature level. This combination of defibration procedures resulted in reduced variation on the single fibre strength (950±230 MPa; Figure 29) and more cellulose rich fibres (78%; Figure 26).

Enzyme treatment of hemp fibres resulted in increased standard deviation of the single fibre strength but with no significant reduction in strength (1150±550 MPa). The larger standard deviation will presumably have a negative effect on the effective fibre strength in composites due to the bundle effect explained with the Weibull distribution. Defibration of hemp by cultivation of *P. radiata* Cel 26 resulted in decrease in fibre bundle strength from 960 MPa to 850 MPa (Figure 30) due to extraction of most of the non-cellulosic binding materials (Figure 26b).

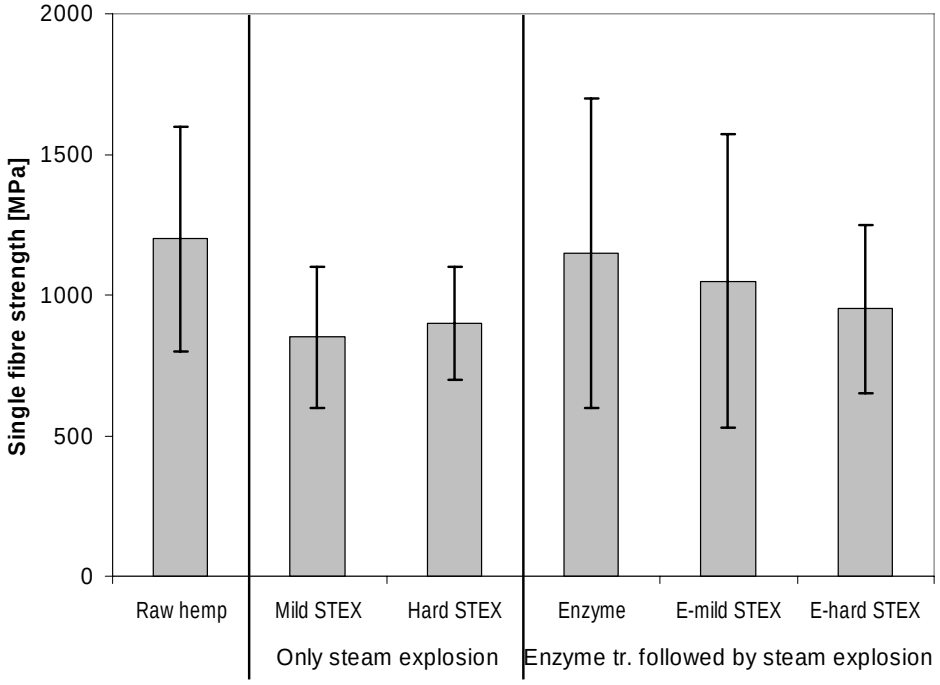

Figure 29. Single fibre strength of enzyme treated and steam exploded hemp fibres (mild STEX = 2 min at 185°C; hard STEX = 2 min at 200°C (Madsen et al., 2003).

Defibration of hemp by cultivation of *C. subvermispora* resulted in weaker fibres (780 MPa; Paper IV) presumably due to cellulose decay. The hemp yarn had a lower strength (Madsen, 2004) but with lower standard deviation. Barley straw had roughly the half strength (280 MPa) of hemp fibres presumably due to the lower cellulose content (45%) and the different fibre structure (Table 2; Liu et al., 2005).

Roughly 20% lower fibre strength was determined by fibre bundle test than by single fibre test of the raw felina hemp fibres combined with 60% lower standard deviation. The lower strength and standard deviation in the fibre bundle tests are presumably due to the bundle effect as explained with the Weibull distribution (Sankari, 2000).

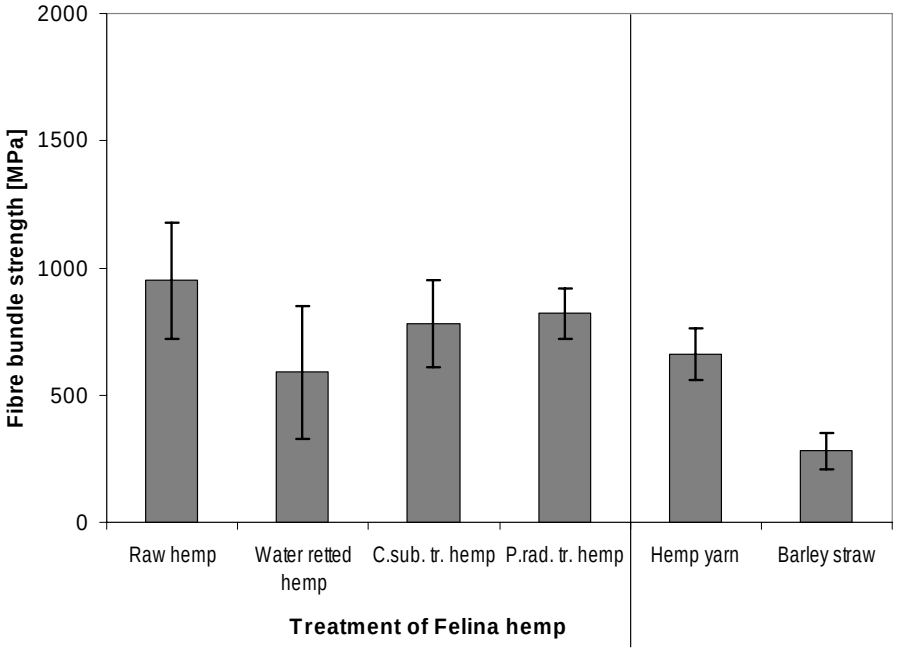

Figure 30. Fibre bundle strength of retted and fungal defibrated hemp fibres, compared with traditionally produced hemp yarn and barley straw (Paper IV).

8.3 Effect of microfibril angle and twisting angle

Studies of stiffness in wood fibres with different microfibril angles (Page et al., 1977) and studies of stiffness in composites with varied fibre angle to the test direction (Madsen, 2004) have shown decreasing stiffness versus the angle. This decreasing trend is illustrated in Figure 31.

Based on the microfibril angle throughout the fibre wall in hemp fibres, which varies concentrically, the cell wall stiffness when pulling in fibre axis direction is lowest in the S1 layer with microfibrils running perpendicular to the fibre axis. The microfibrils are almost parallel with the fibre axis in the inner 70-90% of the S2 layer (Davies and Bruce, 1997), which results in high stiffness. The difference in stiffness throughout the fibre wall will result in different stress concentrations during tensile test. That might explain the cracks that were observed between the concentric layers in the fractured fibres after fibre bundle tests (Paper II).

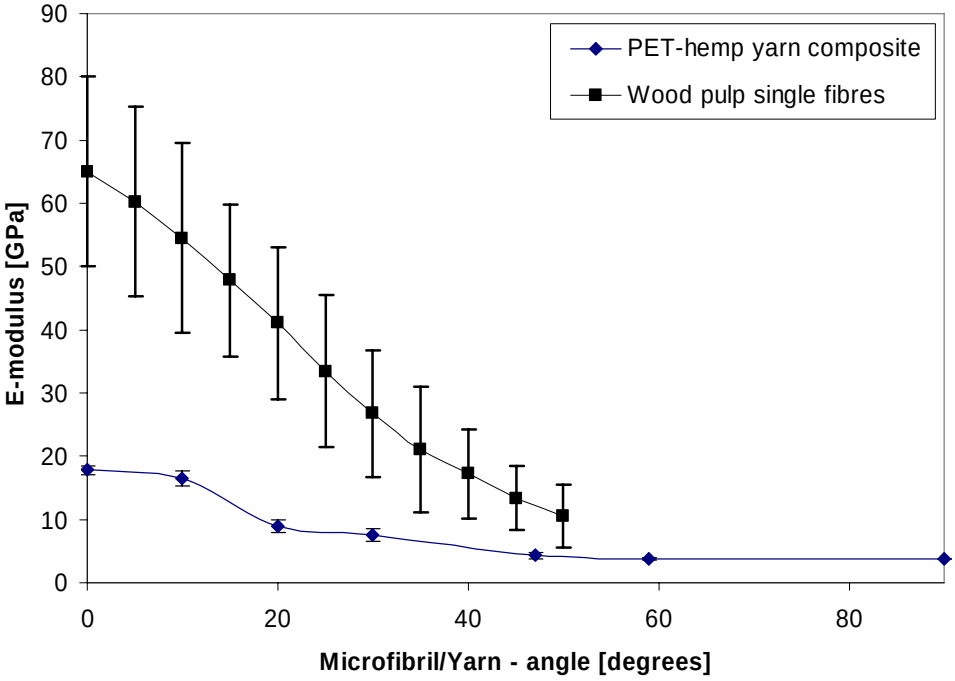

Figure 31. Comparison of reinforcing orientation on the single fibre level and the composite level: Relationship between wood fibre stiffness and microfibril angle in the S2 layer (Page et al., 1977). Stiffness of PET-hemp yarn composites with the yarn axis inclined at different angles to the test direction (Madsen, 2004). The uncertainty is determined as standard deviation on the calculated E-modulus shown as bars.

9 Composites reinforced with hemp fibres

9.1 Effect of fibre orientation on mechanical properties

Plant fibre reinforced composites are generally made with randomly orientated fibres or aligned fibres. Composites with aligned fibres are generally stronger and stiffer in the fibre direction than composites with randomly orientated fibres.

Both the strain and stress at which a composite fractures decrease when the fibre axis is inclined to increasing angles to the test direction. The composite tensile strength decreases by four times when the inclination angle to the fibre orientation is increased to 26° (Figure 32; Madsen, 2004) while the composite stiffness only decreases by two times.

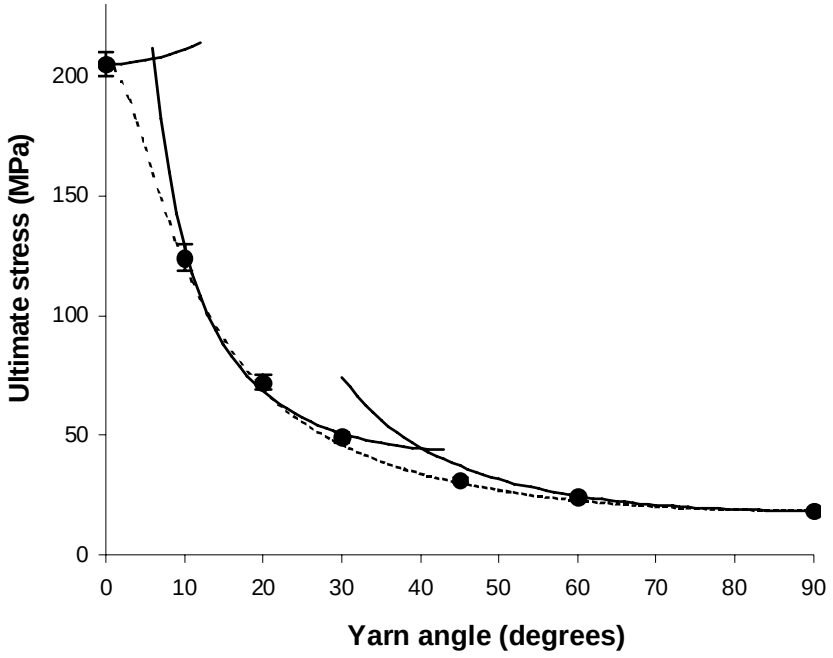

Figure 32. Ultimate stress of hemp yarn-PET composites with the yarn axis inclined at different angles to the test direction. The full lines are ultimate stress predicted from the maximum stress theory with a shear stress of 22 MPa. The dotted line is ultimate stress predicted from the Tsai-Hill criterion with a shear stress of 26 MPa (Madsen, 2004).

The prediction of ultimate stress for composites at a given fibre angle to the test orientation (sq) is made with two models: the maximum stress theory and the Tsai-Hill criterion. The maximum stress theory characterises three modes of failure, which are defined by the three following equations developed by Stowell and Liu (1961):

First mode: Failure is caused by tensile fracture of the fibres, when the fibre angle is inclined with 0°-15°.

$$\sigma_\theta = \frac{\sigma_x}{\cos^2\theta}$$

Second mode: Failure is controlled of shear forces between the fibres and not the fibre strength when the fibre angle is inclined with 15°-40°.

$$\sigma_\theta = \frac{\tau_{xy}}{\sin\theta \cos\theta}$$

where τ is shear stress in hemp yarn (26 MPa; Madsen, 2004).

Third mode: Tensile failure normal to fibres.

$$\sigma_\theta = \frac{\sigma_y}{\sin^2\theta}$$

The maximum stress theory is in agreement with results for composites with carbon fibres and epoxy resin. The Tsai-Hill criterion takes these three failure mechanisms into account in a more complex expression based on the composite strength in the fibre direction, perpendicular to the fibre direction and the shear stress between fibres and matrix. This expression is based on the maximum distortion energy and is defined by the equation below (Tsai, 1968).

$$\frac{1}{\sigma_\theta^{\,2}} = \frac{\cos^2\theta\left(\cos^2\theta - \sin^2\theta\right)}{\sigma_x^{\,2}} + \frac{\sin^4\theta}{\sigma_y^{\,2}} + \frac{\cos^2\theta \sin^2\theta}{\tau_{xy}^{\,2}}$$

in which the ultimate composite strength has been found to fit well with the three failure modes described above and with data for hemp yarn reinforced composites (Figure 32; Madsen, 2004).

9.2 Composition of the formed composites

The hemp fibre reinforced composites were observed using scanning electron microscopy in order to see the fibres shape, size and impregnation with the epoxy-matrix (Figure 33). This figure shows the fibres (light grey area), the matrix (dark grey area) and the air filled voids mentioned as porosity (black area).

There appeared to be porosity inside the fibre bundles and inside the epidermis on the fibre bundle surfaces of raw hemp bast and water retted hemp fibres when these were used as reinforcement of composites. Debonding between fibres and matrix had therefore occurred which generally results in reduced mechanical properties. The hemp fibres that were defibrated by cultivation of *P. radiata* Cel 26 appeared well impregnated with epoxy and no porosity could be observed on the fibre bundle surfaces. The same appearance was observed on the composites with hemp fibres defibrated by cultivation of *C. subvermispora* (Paper IV), showing that the fungal defibration resulted in good impregnation of the fibres.

The composites with barley straw contained much larger fibre lumens resulting in higher porosity content than in the hemp fibre composites. Large areas with no contact between matrix and fibres were observed, which resulted in very low composite strength perpendicular to the fibre axis (unpublished data).

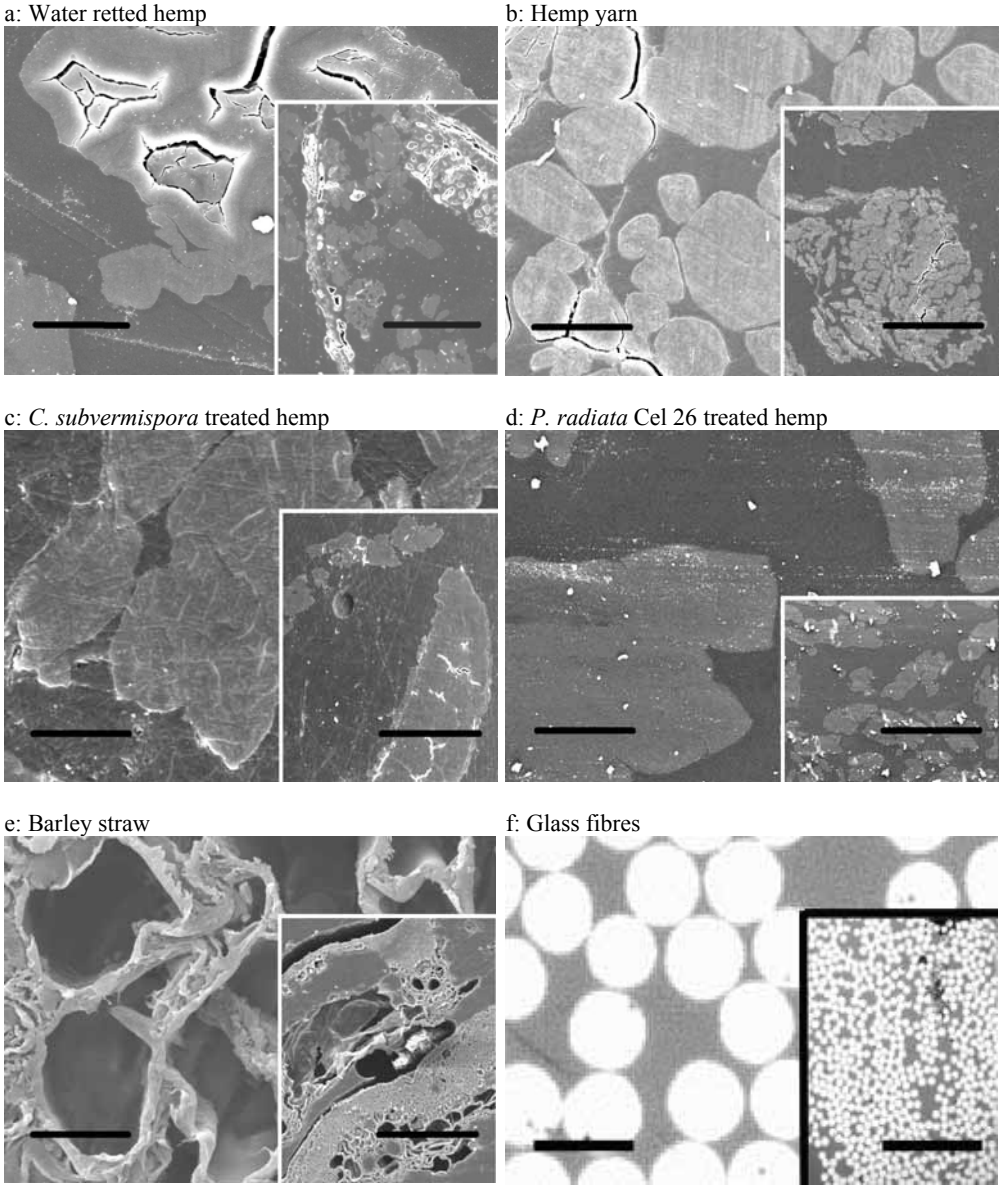

Figure 33. SEM microscopy photos of transverse composite sections recorded at low and high magnification with the applied fibres. The small inset pictures have a scale bar length of 200 μm and the background pictures 20 μm (Paper IV; unpublished data).

9.2.1 Fibre content in relation to fibre size and fibre type

The obtainable fibre content in the composites decreased versus the fibre bundles transverse section area from 35% v/v with hemp yarn of $1\times10^3\mu m^2$ to 26% v/v with raw hemp bast of $160\times10^3\mu m^2$. The obtainable fibre content appeared to decrease linearly versus the logarithm to the fibre transverse section area (Figure 34). This area was determined by image analysis on SEM photos as described in Paper II.

The compaction level increased due to the more uniform fibres of small size, which were easier to compact. The large fibres were very irregular in structure and therefore difficult to compact (Paper IV). In the composites reinforced with barley straw, a fibre content of only 10% v/v could be obtained since the fibres had large fibre lumens and surface porosities (Figure 33e). The glass fibres have smooth surfaces, no lumens and uniform

structure, which made much higher fibre contents possible (>55% v/v; Figure 33f; Unpublished data).

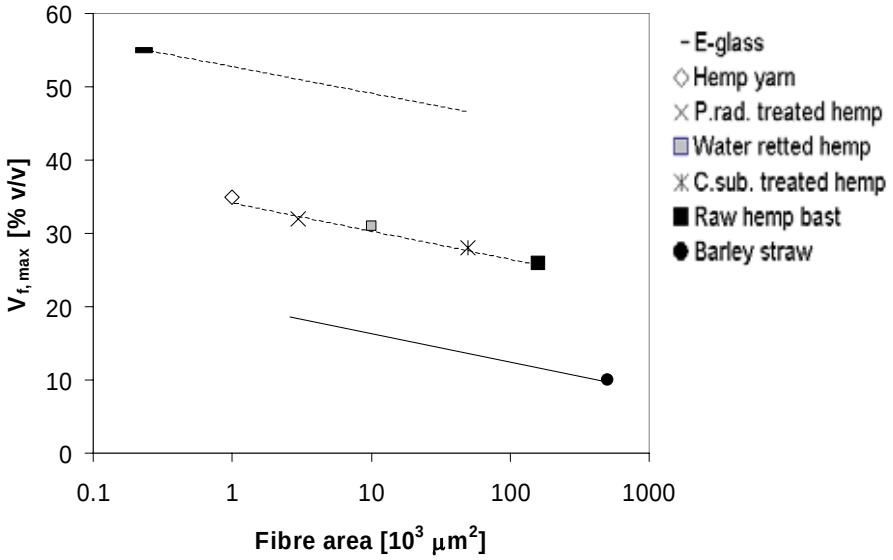

Figure 34. Obtainable fibre content with the applied fibre types versus the fibres transverse section area.

9.2.2 Modelling of porosity content and fibre content

The porosity content in the composites is presented in Paper IV and modelled versus volume fraction of fibres in Appendix B. The porosity content increased with increasing fibre content, due to fibre lumens and to voids at the fibre-matrix interface (Figure 35). It seemed reasonable to assume a linear relationship between the porosity content and V_f and V_m. The porosity constant α_f could be determined by linear regression of V_p versus V_f.

$$V_f = \frac{W_f \rho_m}{W_f \rho_m (1+\alpha_f) + (1-W_f)\rho_f (1+\alpha_m)}$$

$$V_m = V_f \frac{(1-W_f)\rho_f}{W_f \rho_m} = \frac{(1-W_f)\rho_f}{W_f \rho_m (1+\alpha_f) + (1-W_f)\rho_f (1+\alpha_m)}$$

$$V_p = \alpha_f V_f + \alpha_m V_m$$

Expression for the regression line for determination of α_f:

$$V_p = a \cdot V_f + b$$

The hemp fibres produced by fungal treatment were found to fit with α_f similar to α_f for hemp yarn (0.12-0.16 v/v), and the raw hemp bast with α_f similar to α_f for water retted hemp (0.26-0.28 v/v; Table 7; unpublished data). For hemp yarn and fungal defibrated hemp fibres, α_f was larger than for the glass fibres (0.03 v/v) due to fibre lumens in hemp fibres. In water retted hemp and raw hemp bast, α_f was even larger due to epidermis cells with large lumens and poor impregnation of these very large fibre bundles. It seemed reasonable to use $\alpha_m = 0.005$ v/v since there is high uncertainty on V_p for fibre volume fractions below 10% and since small air bubbles were observed in the epoxy matrix (Figure 35; unpublished data).

a: porosity versus volume fraction of fibres

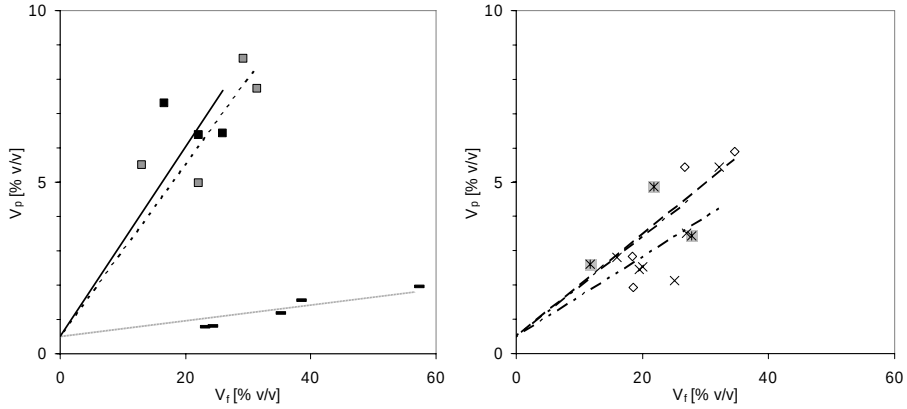

b: Volumetric distribution of fibres, matrix and porosity

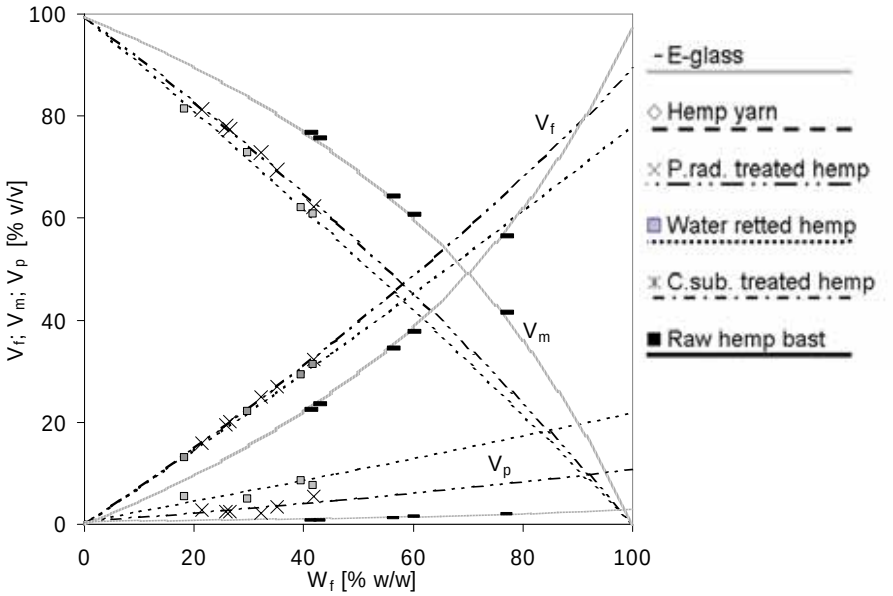

Figure 35. (a) Volume fractions of porosity showed versus fibre volume fraction in the composites. (b) Volume fractions of fibres, matrix and porosity versus weight fraction of fibres to show the distribution between the three components versus the amount of fibres. The lines in a *are drawn using linear regression and the lines in* b *are drawn using* α_m *fixed to 0.005 and* α_f *as shown in Table 7 (unpublished data).*

The fibre content V_f increased with W_f in all the laminates, so the attainable fibre volume fraction $V_{f,max}$ was not reached experimentally (Figure 35b). The slope of the curve for porosity versus V_f tended to bend upward, which indicates that the attainable fibre volume fraction was close to being reached, as it has been reported with flax yarn composites by Madsen and Lilholt (2003) and explained as structural porosity. However more data is needed to explain exactly how the fibre content in composites affects the porosity content.

Table 7. Porosity factors determined for matrix α_m and fibres α_f assuming a linear relationship as shown in Figure 35. Factors for consideration of porosity on composite strength n_σ and stiffness n_E are also presented (unpublished data).

	$b_{(\text{fixed value})}$	a	α_m	α_f	n_σ	n_E	ρ_f (g/cm^3)
Raw hemp bast	0.005	0.28	0.005	0.28	2.1	1	1.58
Water retted hemp	0.005	0.25	0.005	0.26	2.1	1	1.58
C. sub. treated hemp	0.005	0.15	0.005	0.16	2.1	1	1.58
P. rad. treated hemp	0.005	0.12	0.005	0.12	2.1	1	1.58
Hemp yarn	0.005	0.15	0.005	0.16	2.1	1	1.58
Barley straw	0.005	4.58	0.005	4.61	1	0	1.50
E-glass	0.005	0.023	0.005	0.028	2.1	1	2.65

Matrix density: $\rho_m = 1.136$ g/cm^3

9.3 Mechanical properties of the composites

The influence of porosity in the composites was determined to consider porosity in the calculation of fibre strength and fibre stiffness from the composite strength and stiffness and the composite composition.

9.3.1 Influence of porosity

The calculated fibre strength decreased versus the porosity content when porosity was not considered using the factor $(1\text{-}V_p)^n$ as outlined in Appendix B and by Toftegaard and Lilholt (2002).

$$\sigma_{cu} = \left(V_f \sigma_{fu} + V_m \sigma_m\left(\varepsilon_u\right)\right)\left(1 - V_p\right)^{n_\sigma}$$

$$E_c = \left(V_f E_f + V_m E_m\right)\left(1 - V_p\right)^{n_E}$$

Thereby, there seems to be inhomogeneous stress concentrations caused by porosity reducing the composite strength (Figure 36a). The correction factor (n_σ = 2.1) was reasonable, since the calculated fibre strength became generally independent of V_p, as required when the composite strength is corrected for porosity. The main reasons for the different slopes of the trend lines for σ_{fu} versus V_p are the high standard deviation on V_p of 2% v/v and on σ_{fu} of 100 MPa. The calculated fibre stiffness also decreased slightly versus V_p (Figure 36b). The correction factor for the flax fibre composite stiffness (n_E = 1.2; Toftegaard and Lilholt, 2002) appeared slightly too high, since E_f became increased versus V_p. Therefore n_E = 1 was used resulting in general independence of V_p on the calculated fibre stiffness (unpublished data).

a: Tensile strength (σ_{uf}) for n=2.1

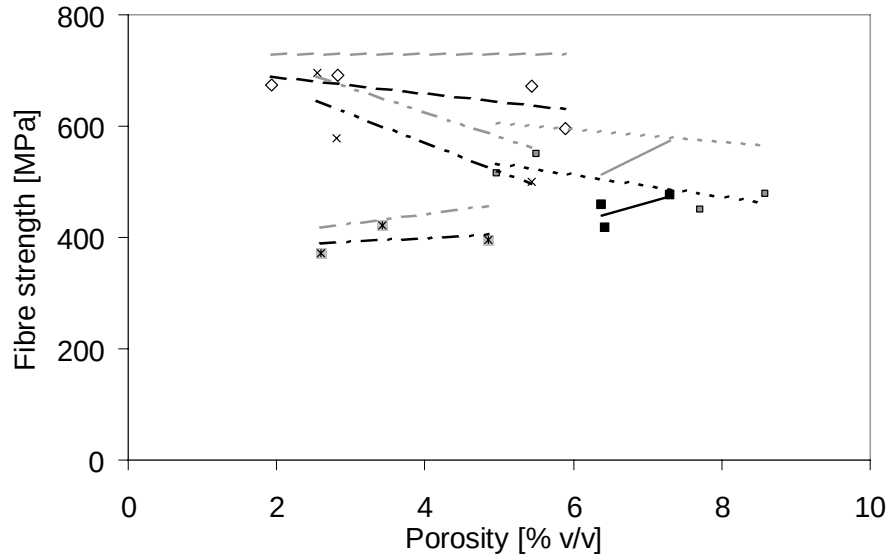

b: Stiffness (E_f) for n=1

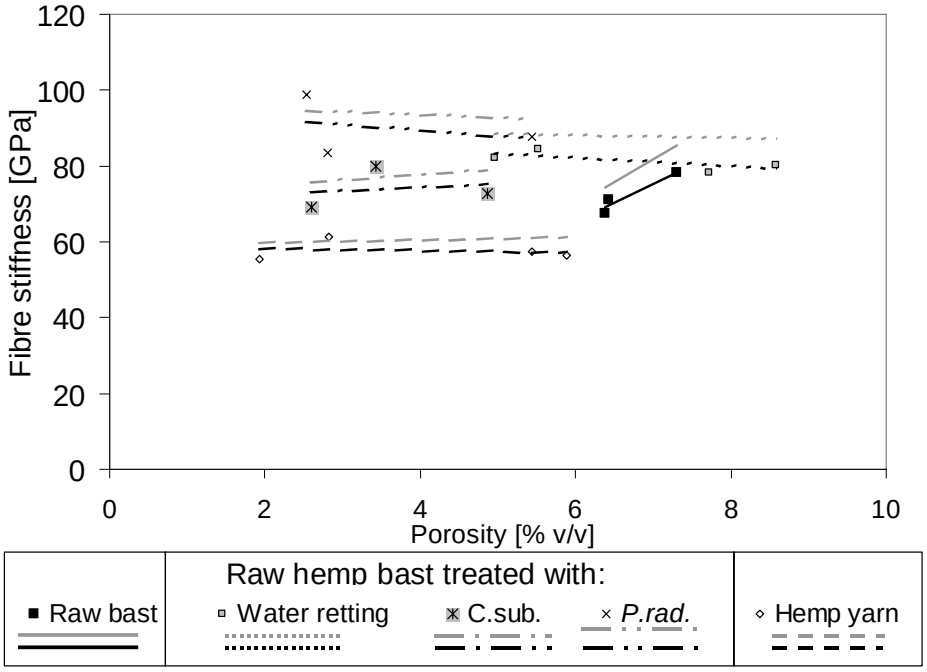

Figure 36. Tensile strength (a) and stiffness (b) calculated for the fibres versus composite porosity with n_σ = 2.1 and n_E=1. The markers and black regression lines represent results not corrected for porosity and the grey regression lines represent the results with correction of the composite properties for porosity (unpublished data).

Based on the determined factors for consideration of porosity, the effect of porosity on composite strength and fibre strength could be determined with a model. The result of the model shows a decrease in effective fibre strength from 700 to 560 MPa by an increase in porosity from 0 to 10% v/v (Figure 37a). The decrease in effective fibre strength and composite strength were thereby both 20%. The effective fibre stiffness decreased from 100 to 90 GPa by the increase in porosity from 0 to 10% v/v (Figure 37a). The decrease in effective fibre stiffness and composite stiffness were both 10%.

Thereby, the effective fibre strength is most affected by the porosity due to the higher n – value.

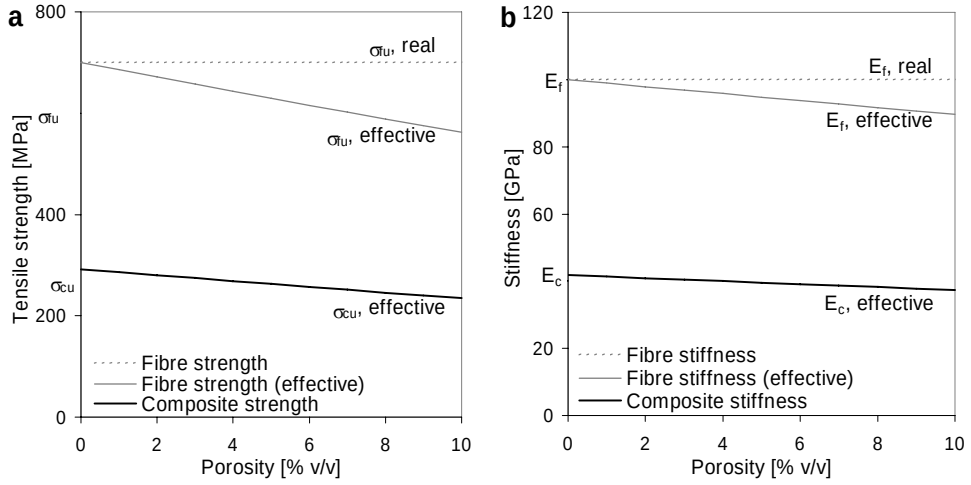

Figure 37. Model for composite strength (a) σ_{cu} *and composite stiffness (b)* E_c*, for* σ_{fu} *= 700 MPa and* E_f *= 100 GPa. For this model, the constant parameters are* V_f *= 40% v/v,* E_m *= 3 GPa and* $\sigma_m(\varepsilon_{fu})$ *= 20 MPa. The effect of porosity on composite strength is* n_σ *= 2 and on composite stiffness* n_E*=1. Finally, the effective fibre strength and fibre stiffness were calculated from* V_f *based on* σ_{cu} *and* E_c *using* $n_\sigma=n_E=0$ *resulting in negative slope of the resulting curves (unpublished data).*

9.3.2 Influence of fibre content on mechanical properties

The tensile strength and stiffness of the fabricated composites, taking porosity into account are presented in Figure 38. These terms (σ_{cup} and E_{cp}) are calculated from the measured strength and stiffness (σ_{cu} and E_c) using n_σ=2.1 and n_E=1. Finally, the fibre strength and stiffness determined from σ_{cup} and E_{cp} are calculated and presented in Table 8 (Paper IV).

For raw hemp bast and water-retted hemp, the curves for composite strength versus V_f were less steep than for the hemp fibres defibrated by cultivation of *P. radiata* Cel 26 and for hemp yarn. The raw hemp bast and the water-retted hemp fibres had therefore lower tensile strength of 535 MPa and 586 MPa, respectively than the *P. radiata* Cel 26 defibrated hemp (643 MPa). The failure strain of hemp fibre composites except the hemp yarn composites was 0.7 – 0.9% l/l. Based on this failure strain, the stress in the epoxy matrix was 18 – 25 MPa when the reinforcing fibres broke. The highest composite strength obtained using raw hemp bast, water retted hemp or *P. radiata* Cel 26 defibrated hemp, as reinforcement was 122 MPa, 153 MPa and 174 MPa, respectively. The composites with hemp fibres produced by cultivation of *P. radiata* Cel 26 were strongest due to the low porosity content, the high fibre strength and the high obtainable fibre content (Paper IV).

The curve for composite stiffness versus V_f was also steeper for the hemp fibres produced by cultivation of *P. radiata* Cel 26 than the curves for raw hemp bast and water retted hemp. The raw hemp bast and the water-retted hemp fibres had therefore lower stiffness of 78 GPa and 88 GPa, respectively than the hemp fibres defibrated by cultivation of *P. radiata* Cel 26 (94 GPa). The highest composite stiffness obtained using

raw hemp bast, water retted hemp or *P. radiata* Cel 26 defibrated hemp, as reinforcement was 20 GPa, 26 GPa and 30 GPa, respectively without consideration of porosity (E_c). Cultivation of *P. radiata* Cel 26 for defibration of hemp fibres resulted thereby both in the highest composite strength and highest composite stiffness.

Based on obtainable composite strength and stiffness, the best defibration method was cultivation of *P. radiata* Cel 26 followed by water retting and at last by cultivation of *C. subvermispora*. It was determined that the hemp fibres tensile strength and stiffness were affected by the investigated defibration methods at 90% probability using analysis of variance (F-test with number of samples = 4 and number of repetitions = 23 for $F_{0.1}$) (Paper IV).

The curve for composite strength for E-glass fibres had about twice the slope of the curves for hemp yarn and defibrated hemp fibres. That is due to the high strength of glass fibres (1200 – 1500 MPa) compared with hemp fibres (535 – 677 MPa). The composites reinforced with glass fibres with a maximum strength of 770 MPa could get much stronger than the hemp fibre reinforced composites (230 MPa) due to the higher obtainable fibre content. The curve for composite stiffness for E-glass fibres had similar slope to the curve for raw hemp bast. That is due to the moderate stiffness of glass fibres (71 – 77 GPa) compared with the defibrated hemp fibres (88 – 94 GPa). The composites reinforced with glass fibres had a maximum stiffness of 40 GPa, which is not much higher than obtained with hemp fibres (30 GPa).

The curve for composite strength for barley straw had about four times lower slope than the curves for defibrated hemp fibres. That is due to the low strength of barley straw (240 MPa) compared with the hemp fibres (535-677 MPa) and the higher porosity content. The composites reinforced with barley straw with a maximum strength of 19 MPa were up to 10 times weaker than the hemp fibre reinforced composites (230 MPa) due to the low obtainable fibre content and the very high porosity content (up to 44% v/v). The curve for composite stiffness had 15 times lower slope than the curves for the hemp based fibres. That is due to the low fibre stiffness (22 GPa) and high porosity content. The composites were therefore not much stiffer than the epoxy matrix (3 GPa).

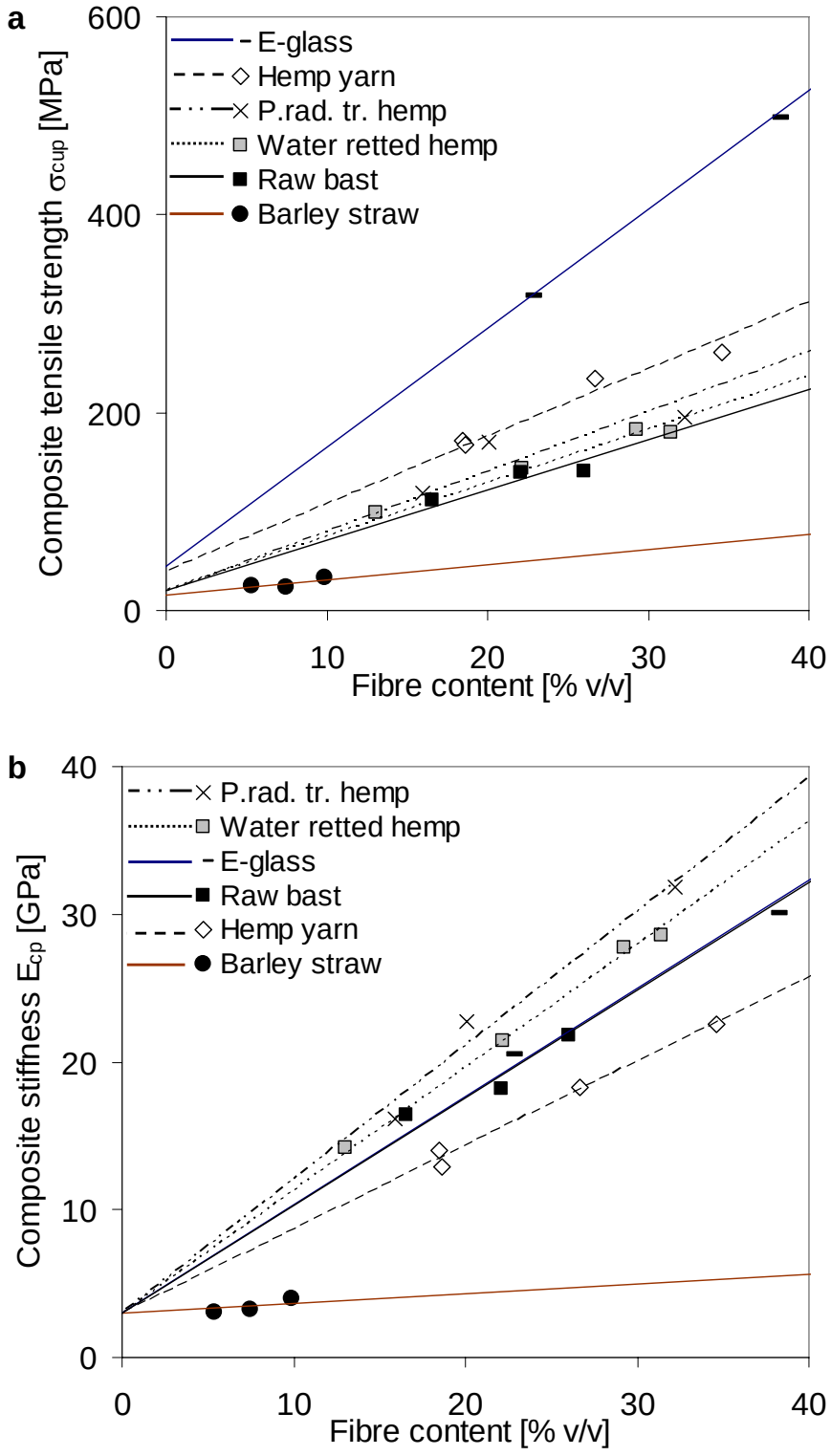

Figure 38. Tensile strength and stiffness for the composites corrected for porosity versus fibre content (Paper IV+unpublished data).

Table 8. Physical and mechanical properties of the laminates reinforced with the defibrated hemp fibres and hemp yarn. Consideration of porosity was done with n_σ*=2.1 for the composite tensile strength* σ_{cu} *and* n_E*=1.0 for the composite stiffness* E_c *(Paper IV).*

Fibre type and defibration	V_f-obt % v/v	V_p-range % v/v	ε_{cu} %	$\sigma_m(\varepsilon_{cu})$ MPa	σ_{fu} MPa	E_f GPa
Epoxy matrix	0	0.5	4	64	E_m = 2.93 GPa	
Raw hemp bast	26	6 – 7	0.9	23	535	78
Water retted hemp	31	5 – 9	0.7	19	586	88
C. sub. tr. hemp[1]	28	3 – 5	0.7	18	536	88
P. rad. tr. hemp	32	3 – 5	0.9	25	643	94
Hemp yarn	35	2 – 6	1.6	39	677	61
Barley straw[2]	10	25 – 44	0.6	17	240	22
E-glass	55	0.8 – 2	1.7	40	1350	78
Norway spruce[3]	26	74			340	41

1: Multiplied by 1.234 for strength and multiplied by 1.144 for stiffness to consider the effect of short fibre length.
2: For barley straw, n_σ=2.1 overestimated σ_{fup} (440 MPa) compared to the fibre bundle test (280 MPa). n_σ=1 gave a more reasonable result and was used.
3: Mechanical properties for dry Norway spruce (*Picea abies*), with a bulk density of 0.40 g/cm^3 and a cell wall density of 1.50 g/cm^3 after correction of the bulk tensile strength (88 MPa) and stiffness (11 GPa) for porosity (Boutelje and Rydell, 1986; Klinke et al., 2001).

9.3.3 Composites investigated in previous studies

Results of previous investigations of composite materials are usually given as fibre content and composite tensile strength and composite stiffness. The fibre strength and stiffness could thereby be calculated and is presented in Table 9.

The fibre strength determined for the hemp yarn composites was similar to previous results with flax yarn (575 Mpa; Madsen and Lilholt, 2003). The determined fibre stiffness of 58 GPa was also close to the stiffness (60 GPa) for hemp yarn in this study. The similar results are expected since hemp fibres and flax fibres have similar chemical composition (Table 3).

Investigations reported by Hepworth et al. (2000) with raw hemp bast and water retted hemp fibres in epoxy-composites have shown much lower composite strength (80-90 MPa) using 20% v/v fibres corresponding to a fibre strength of 290-340 MPa than obtained in this study. The lower strength can be due to incomplete fibre alignment and high porosity content, which were not presented in the paper. Flax fibres were reported to have high fibre stiffness that was comparable with the stiffness of the defibrated hemp fibres in this study (94 GPa). The sisal fibres had lower stiffness (38 GPa) presumable due to the high microfibril angle (20°) compared with flax fibres and hemp fibres (4°;Table 8).

Table 9. Mechanical properties in aligned plant fibre composites reported in the literature. Comparison is based on the calculated stiffness and tensile strength of the fibres.

Fibre	Matrix	V_f % v/v	σ_{cu} MPa	E_c GPa	[1] σ_{fu} MPa	[2] E_f GPa
Raw hemp fibres	Epoxy	20	91	8	340	28
Retted hemp fibres	Epoxy	20	82	7	290	23
Flax fibres	Epoxy	21	195	22	822	94
Flax yarn	Polypropylene	43	250	27	575	62
Jute yarn	Polyester	31	170	20	487	58
Sisal fibres	Epoxy	35	180	15	463	38
E-Glass fibres	Epoxy	55	1020	45	1831	79

1: Calculated tensile strength for the fibres, assuming that the stress in the matrix at the fracture strain (σ_m for $\varepsilon \approx 1\%$) is σ_m = 12 MPa for polypropylene and σ_m = 29 MPa for epoxy.
2: Calculated stiffness for the fibres, assuming that E = 1.18 GPa for polypropylene and E = 2.91 GPa for epoxy.
Note: Gamstedt et al., 1999; Hepworth et al., 2000; Madsen and Lilholt, 2003; Oksman, 2001; Roe and Ansell, 1985.

9.3.4 Composite strength relative to composite density

The ratio between composite strength and composite density and the ratio between fibre strength and fibre density is of interest for construction since it shows the properties based on the material weight instead of volume. The ratio was calculated by including the effect of porosity in calculation of volume fractions and composite strength. In the case of no stress concentrations ($n_E=n_\sigma=0$), E_c/ρ_c and σ_c/ρ_c were linear dependent on the weight fraction of fibres and independent on the porosity content (Figure 39). For the present case with stress concentrations ($n_E=1$; $n_\sigma=2.1$) the relation was not linear as shown with the dotted line in Figure 39.

$$\frac{E_c}{\rho_c}=\left(\frac{W_f E_f}{\rho_f}+\frac{\left(1-W_f\right)E_m}{\rho_m}\right)\times\left(\frac{W_f\left(\rho_m-\rho_f\right)+\rho_f}{W_f\rho_m\left(1+\alpha_f\right)+\left(1-W_f\right)\rho_f\left(1+\alpha_m\right)}\right)^{n_E}$$

$$\frac{\sigma_{cu}}{\rho_c}=\left(\frac{W_f\sigma_{fu}}{\rho_f}+\frac{\left(1-W_f\right)\sigma_m\left(\varepsilon_u\right)}{\rho_m}\right)\times\left(\frac{W_f\left(\rho_m-\rho_f\right)+\rho_f}{W_f\rho_m\left(1+\alpha_f\right)+\left(1-W_f\right)\rho_f\left(1+\alpha_m\right)}\right)^{n_\sigma}$$

The ratio for composite strength increased fastest for the glass fibre composites to 392 MPa/(g/cm^3) for composites with 55% v/v fibres and to 509 MPa/(g/cm^3) for pure glass fibres (Figure 39; Table 10). The curves for n_σ=2.1 had in general lower slope than the linear full drawn curves due to the effect of porosity. The data points for hemp yarn, water retted hemp and *P. radiata* Cel 26 defibrated hemp followed the dotted lines well due to the reduction of composite strength caused by porosity. The ratio σ_c/ρ_c reached 143 MPa/(g/cm^3) with *P. radiata* Cel 26 defibrated hemp and 104 with raw hemp bast due to the higher obtainable fibre content and the higher fibre strength with *P. radiata* Cel 26 defibrated hemp. For barley straw, the optimal fit was obtained using n_σ=1 resulting in composite strength nearly independent on W_f (28 MPa/(g/cm^3)). The Norway spruce had higher σ_c/ρ_c value (220 MPa/(g/cm^3)) than the hemp fibre composites (104-187 MPa/(g/cm^3)) due to the very low density of wood (0.4 g/cm^3) compared with hemp fibres (1.58 g/cm^3).

The ratio for composite stiffness increased for the glass fibre composites to 21.1 GPa/(g/cm^3) for composites with 55% v/v fibres and to 29.4 MPa/(g/cm^3) for pure glass fibres (Figure 39; Table 10). The curves for n_E=1 had in general lower slope than the

linear full drawn curves due to the effect of porosity explained with α_f. The data points for hemp yarn, water retted hemp and *P. radiata* Cel 26 defibrated hemp followed the dotted lines well due to the reduction of composite stiffness caused by porosity. The ratio E_c/ρ_c reached 24.7 GPa/(g/cm^3) with *P. radiata* Cel 26 defibrated hemp and 17.4 GPa/(g/cm^3) with raw hemp bast due to the higher obtainable fibre content and the higher fibre strength with *P. radiata* Cel 26 defibrated hemp. For barley straw, the optimal fit was obtained using n_E=0. The Norway spruce had the highest E_c/ρ_c value (27.5 GPa/(g/cm^3)) due to the very low density of wood (0.4 g/cm^3) compared with hemp fibres and glass fibres.

Table 10. Composite and fibre strength and stiffness compared to the density. Data are based on the highest obtained fibre content $V_{f,obt}$ for composites and on fibres.

Fibre type and defibration	ρ_c g/cm^3	σ_{cu} MPa	E_c GPa	σ_{cu}/ρ_c 10^3m^2/s^2	E_c/ρ_c 10^6m^2/s^2	σ_{fu}/ρ_f 10^3m^2/s^2	E_f/ρ_f 10^6m^2/s^2
Epoxy matrix	1.136	64	2.93	56	2.6	-	-
Raw hemp bast	1.18	122	20.4	104	17.4	339	49.4
Water retted hemp	1.19	153	26.4	129	22.2	370	55.7
C. sub. tr. hemp	1.22	130	24.3	107	19.9	340	55.7
P. rad. tr. hemp	1.22	174	30.1	143	24.7	407	59.5
Hemp yarn	1.23	230	21.3	187	17.3	428	38.6
Barley straw[3]	0.67	19	4.0	28	6.0	160	14.7
E-glass	1.96	769	41.5	392	21.1	509	29.4
Norway spruce[1]	0.40	88	11	220	27.5	220	27.5

1: Mechanical properties for dry Norway spruce (*Picea abies*), with a bulk density of 0.40 g/cm^3 and a cell wall density of 1.50 g/cm^3 after correction of the bulk tensile strength (88 MPa) and stiffness (11 GPa) for porosity (Boutelje and Rydell, 1986; Klinke et al., 2001).

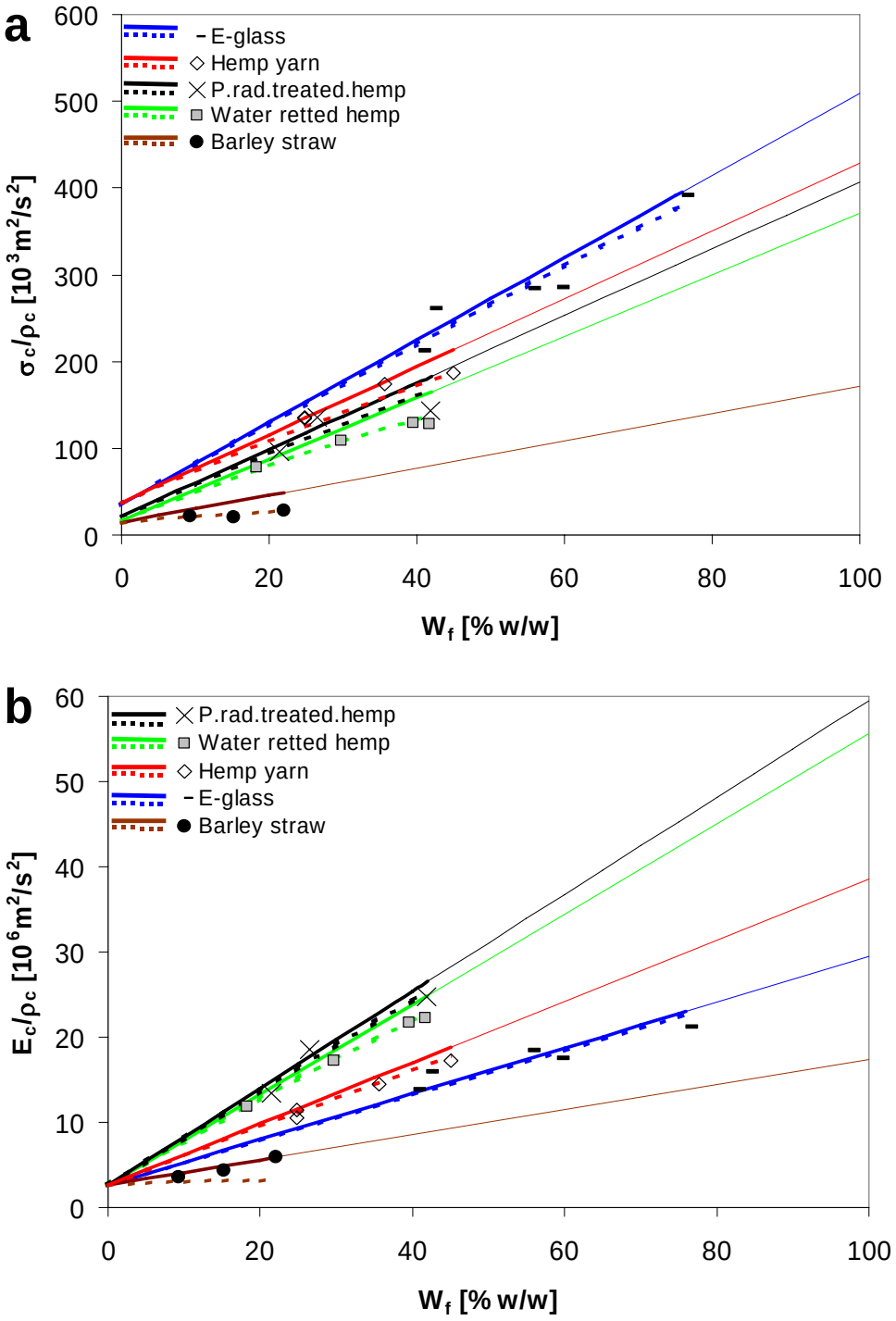

Figure 39. Composite stiffness (a) and composite strength (b) divided with composite density. Measured values of σ_c, E_c, ρ_c and W_f are used as data points. The lines are based on the model derived in Appendix D using ρ_f, ρ_m, α_f, α_m, n_E and n_σ from Table 7 and σ_f, $\sigma_m(\varepsilon_{cu})$, E_m, and E_f from Table 8.Full lines for $n_E=n_\sigma=0$ and dotted lines for $n_E=1$ and $n_\sigma=2.1$ except for barley straw with $n_\sigma=1$.

9.4 Effect of cellulose structure on fibre mechanical properties

Even though the hemp fibres were handled with mild methods like hand peeling and fungal defibration, higher fibre strength than 643 MPa was not obtained, which is similar to the strength of traditionally produced hemp yarn (677 MPa). The similar results are surprising and indicate that the final fibre strength is not very dependent on the defibration method applied (Table 8).

The hemp fibres and Norway spruce had tensile strength approximately linear increasing versus the cellulose content showing that pure cellulose has 850 MPa in tensile strength (Figure 40a). The determined cellulose strength was about 10% of the obtainable strength in agreement with Lilholt (2002). Therefore, strength reduction seems to occur from the molecular level to the single fibre level (8000→1200±400 MPa; Madsen et al., 2003) and from the single fibre level to the fibre assembly level (1200±400 → 643±111 MPa).

Single fibres are presumably weakened due to flaws like kinks inside the fibres (Bos et al., 2002), weak interface between the fibre wall concentric lamellae (Paper II) and insufficient binding strength between the reinforcing cellulose, hemicellulose, lignin and pectin (Morvan et al., 1990). Fibre assemblies are weakened due to variations in single fibre strength as explained by Weibull analysis (Lilholt, 2002) describing the fact that the fibre bundle strength is always lower than the average strength of the same fibres (Coleman, 1958). For flax fibres and cotton fibres, the bundle efficiency has been found as 0.46 – 0.60 indicating that the effective strength of many fibres in for example a composite is roughly half the single fibre strength (Bos et al., 2002; Kompella and Lambros, 2002). It has also been suggested that mild handling and defibration result in high single fibre strength but with larger scattering counteracting the higher fibre strength. These facts explain the similar strength in the composites with traditionally produced hemp yarn and mildly defibrated hemp fibres.

The fibre stiffness increased with the cellulose content in the fibres obtained by the fungal defibration and water retting. A linear dependence on the crystalline cellulose content could be established (Figure 40b). The hemp yarn had lower stiffness than implied from the cellulose content, which may be due to the high twisting angle introduced during the spinning process. It has been stated, that increasing twisting angles decrease fibre stiffness (Page et al., 1977).

The wood fibres had lower stiffness, which can be explained by the low cellulose crystallinity (60 – 70%) compared with the hemp fibres (90 – 100%; Figure 14). Amorphous cellulose, hemicellulose, lignin and pectin are expected to have lower stiffness than crystalline cellulose, which are linear molecules orientated in the test direction resulting in high stiffness. In contrast, the plant fibre stiffness appeared to increase linearly versus the cellulose content to 125 GPa for pure crystalline cellulose.

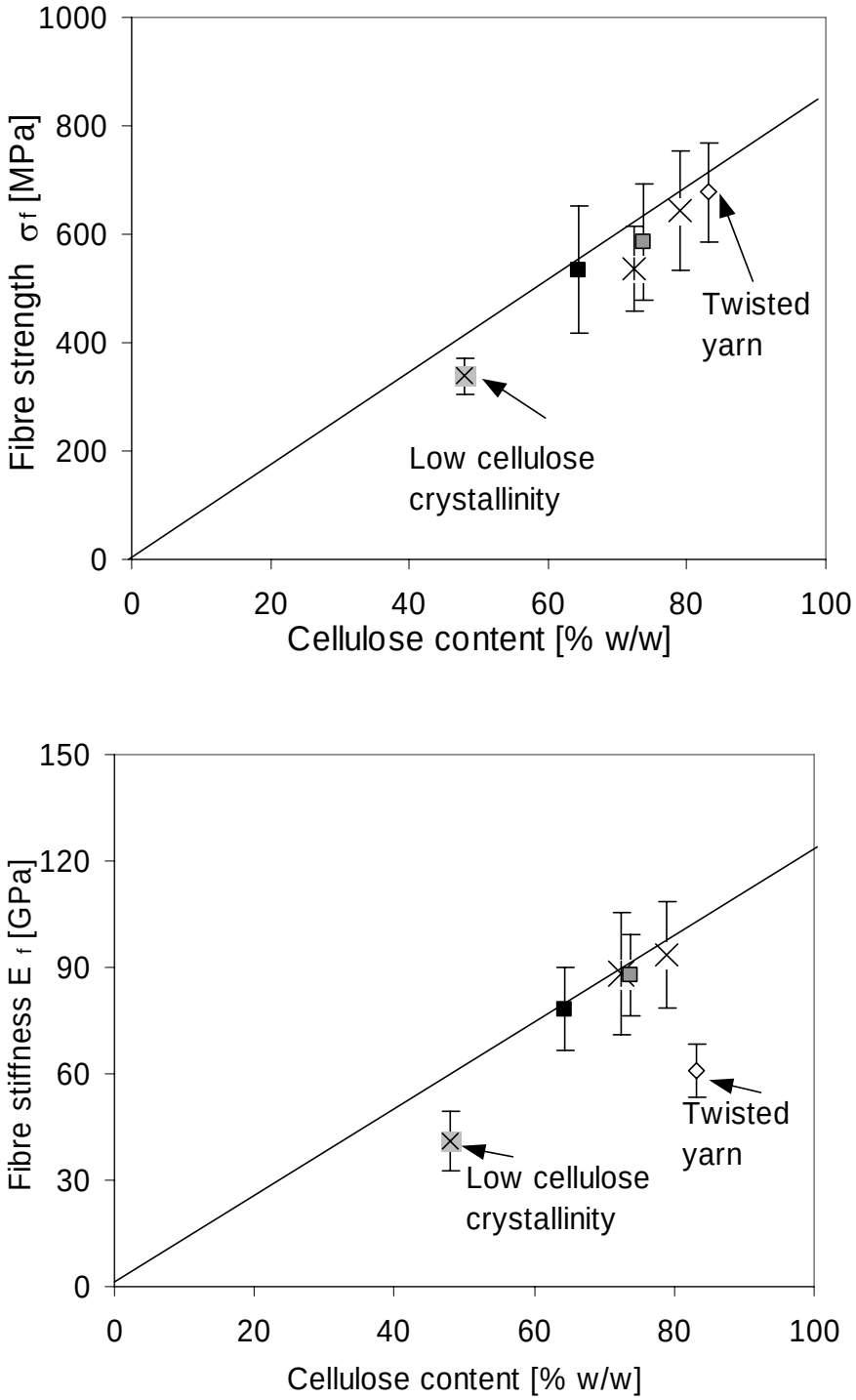

Figure 40. Fibre tensile strength (a) and stiffness (b) determined on porosity corrected composite data versus cellulose content for treated hemp fibres, hemp yarn, barley straw and Norway spruce. The effects of cellulose crystallinity and twisting angle are indicated.

10 Conclusions and future work

Hemp stems could be defibrated with the white rot fungus *Phlebia radiata* Cel 26 on at least the 100 g scale to make fibres for reinforcement of composites, since the pectin and wax rich epidermis was degraded. The fibres retained parallel orientation during the fungal defibration and water retting and are thereby useful for composites with aligned fibres. Lignin located in the middle lamellae between the single fibers made pectinase defibration difficult. Lignin degradation in the hemp fibres by cultivation of *P. radiata* Cel 26 resulted in more cellulose rich fibres (78%) than treatment with pectin degrading enzymes. Even though the hemp fibres were handled with mild methods like hand peeling and fungal defibration, fibre strength higher than 643 MPa was not obtained, which is similar to the strength of traditionally produced hemp yarn (677 MPa). Furthermore the fibre strength appeared to be linearly dependent on cellulose content and independent on cellulose crystallinity and microfibril angle. Pure cellulose had the estimated effective strength of 850 MPa that is about 10% of the strength on the molecular level. The plant fibre stiffness appeared to increase linearly with cellulose content, decrease with microfibril angle and increase with cellulose crystallinity. Pure crystalline cellulose had an estimated stiffness of 125 GPa.

Future investigations could be to investigate the fracture mechanics in plant fibre reinforced composites. That will potentially explain if the obtained composite strength is lower than determined based on the fibre strength or if the reduction in strength is only due to the effect of the Weibull distribution. Such investigations should be performed at varied fibre content and will in addition reveal further information about the effect of fibre content on the resulting porosity content. Composites with various biodegradable matrix materials like starch or lignin could be tested to get a completely biodegradable material. This investigation should focus on the matrix properties and on how to get a good interface with the fibres. The fungal defibration method could be replaced with constructed enzyme mixtures by genetic engineering or a designed and stable bacterial strain could be applied in the retting procedure.

11 References

Andersen TL, Lilholt H, 1999. Natural fibre composites: compaction of mats, press consolidation and material quality. *Japanese Journal of Applied Physics Part 1-Regular Papers Short Notes & Review Papers, Presented at 7th Euro-Japanese Symposium, 1-2nd July 1999*.

Andersson S, Serimaa R, Paakkari T, Saranpaa P, Pesonen E, 2003. Crystallinity of wood and the size of cellulose crystallites in Norway spruce (*Picea abies*). *Journal of Wood Science*, 49: pp. 531-537.

Bergander A, Brandstrom J, Daniel G, Salmen L, 2002. Fibril angle variability in earlywood of Norway spruce using soft rot cavities and polarization confocal microscopy. *Journal of Wood Science*, 48: pp. 255-263.

Bjerre AB, Olesen AB, Fernqvist T, Plöger A, Schmidt AS, 1996. Pretreatment of wheat straw using combined wet oxidation and alkaline hydrolysis resulting in convertible cellulose and hemicellulose. *Biotechnol Bioeng*, 49: pp. 568-577.

Bjerre AB, Schmidt AS, 1997. Development of chemical and biological processes for production of bioethanol: Optimization of the wet oxidation process and characterization of products. *Risø-R-967(EN)*, Risø National Laboratory: pp 5-9.

Bledzki AK, Sperber VE, Faruk O, 2002. Natural and wood fibre reinforcement in polymers. *Rapra Review Reports*, 13.

Bócsa I, 1971. The realization of specific breeding goals in hemp breeding. *Rostnövények*: pp. 29-34.

du Bois WF, 1982. Hemp as a raw material for the paper industry. *Bedrijfsontwikkeling*, 13: pp. 851-856.

Bos HL, Molenveld K, Teunissen W, van Wingerde AM, van Delft DRV, 2004. Compressive behaviour of unidirectional flax fibre reinforced composites. *J Mater Sci*, 39: pp. 2159-2168.

Bos HL, Van den Oever MJA, Peters OCJJ, 2002. Tensile and compressive properties of flax fibres for natural fibre reinforced composites. *J Mater Sci*, 37: pp. 1683-1692.

Boutelje JB, Rydell RR, 1986. Träfakta, 44 träslag i ord och bild. *TräteknikCentrum* Stockholm pp 27-29.

Broge JL, 2000. Natural fibers in automotive components. *Automotive Engineering International*, 108: pp. 120.

Browning BL, 1967. Methods of wood chemistry. New York: *Interscience Publishers*, A division of John Wiley & Sons.

Brühlmann F, Leupin M, Erismann KH, Fiechter A, 2000. Enzymatic degumming of ramie bast fibers. *Journal of Biotechnology*, 76: pp. 43-50.

Brüning HJ, Disselbeck D, 1992. Thermoplastic high-performance filament yarns and their use in fibre composites. *International man-made fibres progress*; Österreishisches Chemiefaser-Institut; Paper no. 31.

Cappelsen J, 2004. Ugeberetning - klimadata på ugebasis: oktober 1998 - december 2003. *Technical report No 04-15, Danish Meteorological Institute.*

Cappelsen J, Jørgensen BV, 2002. The Climate of Denmark 2002. *Technical report No 03-02, Danish Meteorological Institute.*

Cichocki FR, Thomason JL, 2002. Thermoelastic anisotropy of a natural fiber. *Compos Sci Technol*, 62: pp. 669-678.

Clemons C, 2000. Woodfiber-plastic composites in the United States – History and current and future markets. In the P*roceedings of the 3rd International Wood and Natural Fibre Composites Symposium*; Kassel, Germany: pp. 1-7.

Coleman BD, 1958. On strength of classical fibres and fibre bundles. *J mech phys solids*, 7: pp. 60-70.

Cromack HTH, 1998. The effect of cultivar and seed density on the production and fibre content of Cannabis sativa in southern England. *Ind Crops Prod*, 7: pp. 205-210.

Davies GC, Bruce DM, 1997. A stress analysis model for composite coaxial cylinders. *J Mater Sci*, 32: pp. 5425-5437.

de Meijer EPM, 1995. Fibre hemp cultivars: A survey of origin, ancestry, availability and breif agronomic characteristics. *Journal of the International Hemp Association*, 2: pp. 66-73.

Debye P, 1915. Zerstreuung von röntgenstrahlen. *P Ann Phys*, 46: pp. 809-823.

Deferne J-L, Pate DW, 1996. Hemp seed oil: A source of valuable fatty acids. *Journal of the International Hemp Association*, 3: pp. 1-7.

Dobel J, 2002. The future of airlaid forming. *Nonwoven World*, June-Juli: pp. 53-56.

Eriksen M, Pallesen BE, 2002. New generation airforming for flax and hemp. *Nonwoven World*, June-July: pp. 80-84.

Evans R, Wearne RH, Wallis AFA, 1989. Molecular-weight distribution of cellulose as its tricarbanilate by high-performance size exclusion chromatography. *Journal of Applied Polymer Science*, 37: pp. 3291-3303.

Fan LT, Lee Y-H, Gharpuray MM, 1982. The nature of lignocellulosics and their pretreatments for enzymatic hydrolysis. *Advanced Biochemical Engineering*, 23: pp. 158-187.

Felby C, Klinke HB, Olsen HS, Thomsen AB, 2003. Ethanol from wheat straw cellulose by wet oxidation pretreatment and simultaneous saccharification and fermentation. *ACS Symposium Series* 855; pp. 157-174.

Fink HP, Walenta E, Kunze J, 1999. The structure of natural cellulosic fibres - Part 2. The supermolecular structure of bast fibres and their changes by mercerization as revealed by X-ray diffraction and C-13-NMR-spectroscopy. *Papier*, 53: pp. 534-542.

Fournier G, Richezdumanois C, Duvezin J, Mathieu JP, Paris M, 1987. Identification of A New Chemotype in Cannabis-Sativa - Cannabigerol-Dominant Plants, Biogenetic and Agronomic Prospects. *Planta Medica*: pp. 277-280.

Gamstedt EK, Berglund LA, Peijs T, 1999. Fatigue mechanisms in unidirectional glass-fibre-reinforced polypropylene. *Compos Sci Technol*, 59: pp. 759-768.

Garcia-Jaldon C, Dupeyre D, Vignon MR, 1998. Fibres from semi-retted hemp bundles by steam explosion treatment. *Biomass & Bioenergy*, 14: pp. 251-260.

Goering HK, Van Soest PJ, 1970. Forage fiber analyses (apparatus, reagents, procedures and some applications). Washington, DC: *Agricultural Research Service*, USDA.

Grosberg P, Iype C, 1999. Yarn production. Theoretical aspects. 2nd ed. Manchester: *The Textile Institute*.

Han JS, Rowell JS, 1996. Chemical composition of fibers in paper and composites from agrobased resources. *Lewis Publishers*.

Heiner AP, Teleman O, 1997. Interface between monoclinic crystalline cellulose and water: Breakdown of the odd/even duplicity. *Langmuir*, 13: pp. 511-518.

Henriksson G, Akin DE, Hanlin RT, Rodriguez C, Archibald DD, Rigsby LL, et al., 1997. Identification and retting efficiencies of fungi isolated from dew-retted flax in the United States and Europe. *Appl Environ Microbiol*, 63: pp. 3950-3956.

Hepworth DG, Hobson RN, Bruce DM, Farrent JW, 2000. The use of unretted hemp fibre in composite manufacture. *Composites Part A-Applied Science and Manufacturing*, 31: pp. 1279-1283.

Herer J, 1985. Hemp & the marijuana conspiracy: The emperor wears no clothes. Van Nuys: *Hemp Publishing*.

Hobson RN, Hepworth DG, Bruce DM, 2001. Quality of fibre separated from unretted hemp stems by decortication. *Journal of Agricultural Engineering Research*, 78: pp. 153-158.

Hoffmann W, 1961. Hanf, *Cannabis sativa* L. In: Kappert H, Rudorf W, editors. Handbuch der Pflanzenzüchtung. Berlin: Paul Parey. pp. 204-261.

Hull D, Clyne TW, 1996. An introduction to composite materials, 2 ed. *Cambridge University Press*.

Kaar WE, Cool LG, Merriman MM, Brink DL, 1991. The Complete Analysis of Wood Polysaccharides Using Hplc. *Journal of Wood Chemistry and Technology*, 11: pp. 447-463.

Kandachar P, 2002. Oppertunities for product development for industrial applications in polymers reinforced with natural fibres. In: Lilholt, H., Madsen, B., Toftegaard, H., Cendre, E., Megnis, M., Mikkelsen, L.P., Sørensen, B.F. (Ed.), Sustainable natural and polymeric composites - science and technology. *Proceedings of the 23th Risø International Symposium on Materials Science*, Risø National Laboratory, Denmark, pp. 15-33.

Karus M, Kaup M, Ortmann S, 2002. Use of natural fibres in the German and Austrian automotive industry. Hürth, Germany. *Nova-Institute GmbH*.

Klinke HB, Ahring BK, Schmidt AS, Thomsen AB, 2002. Characterization of degradation products from alkaline wet oxidation of wheat straw. *Bioresour Technol*, 82: pp. 15-26.

Klinke HB, Lilholt H, Toftegaard H, Andersen TL, Schmidt AS, Thomsen AB, 2001. Wood and plant fibre reinforced polypropylene composites. *1st world conference on biomass for energy and industry:* James & James (Science Publishers), pp. 1082-1085.

Kompella MK, Lambros J, 2002. Micromechanical characterisation of cellulose fibers. *Polymer Testing*, 21: pp. 523-530.

Liitia T, Maunu SL, Hortling B, Tamminen T, Pekkala O, Varhimo A, 2003. Cellulose crystallinity and ordering of hemicelluloses in pine and birch pulps as revealed by solid-state NMR spectroscopic methods. *Cellulose*, 10: pp. 307-316.

Lilholt H, 2002. Strength of cellulose and fibres. In: Lilholt H, Madsen B, Toftegaard H, Cendre E, Megnis M, Mikkelsen LP, Sørensen BF (Ed.), Sustainable natural and polymeric composites - science and technology. *Proceedings of the 23th Risø International Symposium on Materials Science*, Risø National Laboratory, Denmark, pp. 225-30.

Lilholt H, Lawther JM, 2000. Natural organic fibres. Elsevier. In: Kelly, A. and Zweben, C. (Ed.), Comprehensive composite materials, vol. 1, pp. 303-325.

Liu R, Yu H, Huang Y, 2005. Structure and morphology of cellulose in wheat straw. *Cellulose*, 12: pp. 25-34.

Lystrup Aa, 1997. Processing technology for advanced fibre composites with thermoplastic matrices. In: Andersen SI, Brøndsted P, Lilholt H., Lystrup Aa, Rheinländer JT, Sørensen BF, Toftegaard H. (Ed.), Polymeric composites – Expanding the limits. *Proceedings of the 18th Risø International Symposium on Materials Science*, Risø National Laboratory, Denmark, pp. 69-80.

Madsen B. Properties of plant fibre yarn polymer composites - An experimental study. *Report nr. 082, Department of Civil Engineering*, Technical University of Denmark; 2004.

Madsen B, Lilholt H, 2002. Compaction of plant fibre assemblies in relation to composite fabrication. In: Lilholt, H., Madsen, B., Toftegaard, H., Cendre, E., Megnis, M., Mikkelsen, L.P., Sørensen, B.F. (Ed.), Sustainable natural and polymeric composites - science and technology. *Proceedings of the 23th Risø International Symposium on Materials Science*, Risø National Laboratory, Denmark, pp. 239-250.

Madsen B, Lilholt H, 2005. Plant fibre composites - porosity and volumetric interaction. Unpublished.

Madsen B, Lilholt H, 2003. Physical and mechanical properties of unidirectional plant fibre composites - an evaluation of the influence of porosity. *Compos Sci Technol*, 63: pp. 1265-1272.

Madsen FT, Burgert I, Jungnikl K, Felby C, Thomsen AB, 2003. Effect of enzyme treatment and steam explosion on tensile properties of single hemp fiber. *12th International Symposium on Wood and Pulping Chemistry (ISWPC)*; Madison, P80.

Mcdougall GJ, Morrison IM, Stewart D, Weyers JDB, Hillman JR, 1993. Plant fibers - botany, chemistry and processing for industrial use. *J Sci Food Agric*, 62: pp. 1-20.

Meijer WJM, Vertregt N, Rutgers B, van de Waart M, 1995. The pectin content as a measure of the retting and rettability of flax. *Ind Crops Prod*, 4: pp. 273-284.

Mohanty AK, Misra M, Hinrichsen G, 2000. Biofibres, biodegradable polymers and biocomposites: An overview. *Macromolecular Materials and Engineering*, 276: pp. 1-24.

Morvan C, Jauneau A, Flaman A, Millet J, Demarty M, 1990. Degradation of flax polysaccharides with purified endo-polygalacturonase. *Carbohydrate Polymers*, 13: pp. 149-163.

Mukherjee PS, Satyanarayana KG, 1986. An empirical-evaluation of structure property relationships in natural fibers and their fracture-behavior. *J Mater Sci*, 21: pp. 4162-4168.

Muzzy JD, 2000. Thermoplastics – Properties. In: Kelly A, Zweben C, editors. *Comprehensive Composite Materials* vol 2, Elsevier Science, chap. 2.

Mwaikambo LY, Ansell MP, 1999. The effect of chemical treatment on the properties of hemp, sisal, jute and kapok for composite reinforcement. *Die Angewandte Makromolekylare Chemie*, 272: pp. 108-116.

Nishiyama Y, Langan P, Chanzy H, 2002. Crystal structure and hydrogen-bonding system in cellulose 1 beta from synchrotron X-ray and neutron fiber diffraction. *Journal of the American Chemical Society*, 124: pp. 9074-9082.

Nyhlen L, Nilsson T, 1987. Combined T.E.M. and UV-microscopy on delignification of pine wood by *Phlebia radiata* and four other white rotters. Versailles, France. *Proc. of Lignin enzymic and microbial degradation symposium*: INRA Publications; pp. 277-282.

Obrien RN, Hartman K, 1971. Air Infrared Spectroscopy Study of Epoxy-Cellulose Interface. *Journal of Polymer Science Part C-Polymer Symposium*: pp. 293.

Oksman K, 2001. High quality flax fibre composites manufactured by the resin transfer moulding process. *Journal of Reinforced Plastics and Composites*, 20: pp. 621-627.

Page DH, El-Hosseiny F, Winkler K, Lancaster APS, 1977. Elastic modulus of single wood pulp fibers. *Tappi*, 60: pp. 114-117.

Parikh DV, Calamari TA, Sawhney APS, Blanchard EJ, Screen FJ, Myatt JC, et al., 2002. Thermoformable automotive composites containing kenaf and other cellulosic fibers. *Textile Research Journal*, 72: pp. 668-672.

Pasila A, 2000. The effect of frost on fibre plants and their processing. *Mol Cryst and Liq Cryst,* 353: pp. 11-22.

Puls J, Schuseil J, 1993. Chemistry of hemicelluloses: Relationship between hemicellulose structure and enzymes required for hydrolysis. In: Coughlan MP, Hazlewood GP, editors. *Hemicellulose and Hemicellulases Portland Press Research Monograph,* pp. 1-27.

Rietveld HM, 1967. Line Profiles of Neutron Powder-Diffraction Peaks for Structure Refinement. *Acta Crystallographica*, 22: pp. 151.

Rietveld HM, 1969. A Profile Refinement Method for Nuclear and Magnetic Structures. *Journal of Applied Crystallography*, 2: pp. 65.

Robinson R, 1996. The great book of hemp. *Park Street Press*, Main.

Roe PJ, Ansell MP, 1985. Jute-reinforced polyester composites. *J Mater Sci*, 20: pp. 4015-4020.

Rosember JA, 1965. Bacteria Responsible for Retting of Brazilian Flax. *Applied Microbiology*, 13: pp. 991-992.

Ruland W, 1961. X-ray determination of crystallinity and diffuse disorder scattering. *Acta Crystallographica*, 14: pp. 1180-1185.

Salisbury FB, Ross CW, 1992. Plant physiology, 4 ed. *Wadsworth Inc*.

Sankari HS, 2000. Comparison of bast fibre yield and mechanical fibre properties of hemp (*Cannabis sativa* L.) cultivars. *Ind Crops Prod*, 11: pp. 73-84.

Sarko A, Muggli R, 1974. Packing analysis of carbohydrates and polysaccharides.III. Valonia cellulose and cellulose-II. *Macromolecules*, 7: pp. 486-494.

Segal L, Creely JJ, Martin AE, Conrad CM, 1959. An empirical method for estimating the degree of crystallinity of native cellulose using the X-ray diffractometer. *Textile Research Journal*: pp. 786-794.

Söderström J, 2004. Optimisation of two-step steam pretreatment of softwood for bioethanol production. *Ph.D. thesis, Department of Chemical Engineering, Lund University*; 2004.

Stowell EZ, Liu TS, 1961. On the Mechanical Behaviour of Fibre-Reinforced Crystalline Materials. *Journal of the Mechanics and Physics of Solids*, 9: pp. 242-260.

Thomsen AB, Rasmussen S, Bohn V, Nielsen KV, Thygesen A, 2005. Hemp raw materials: The effect of cultivar, growth conditions and pretreatment on the chemical composition of the fibres. *Risø National Laboratory. Report No.: R-1507*.

Thomsen AB, Schmidt AS, Toftegaard H, Pedersen WB, Woidemann A, Lilholt H, 1999. Natural plant fibre composites based on wet-oxidised wheat straw and polypropylene. *Proceedings of the 6th Symposium of Renewable Resources for the Chemical Industry*, Germany, pp. 762-771.

Toftegaard H, Lilholt H, 2002. Effective stiffness and strength of flax fibres derived from short fibre laminates. In: Lilholt, H., Madsen, B., Toftegaard, H., Cendre, E., Megnis, M., Mikkelsen, L.P., Sørensen, B.F. (Ed.), Sustainable natural and polymeric composites - science and technology. *Proceedings of the 23th Risø International Symposium on Materials Science*, Risø National Laboratory, Denmark, pp. 325-334.

Tsai SW, 1968. Strength theories of filamentary structures. In: Schwartz RT, Schwartz HS, editors. Fundamental aspects of fiber reinforced plastic composites. New York: *Interscience*.

van der Werf HMG, Mathijssen EWJM, Haverkort AJ, 1996. The potential of hemp (*Cannabis sativa* L.) for sustainable fibre production: a crop physiological appraisal. *Annals of Applied Biology*, 129: pp. 109-123.

van der Werf HMG, Wijlhuizen M, de Schutter JAA, 1995. Plant density and self-thinning affect yield and quality of the fibre hemp (*Cannabis sativa* L.). *Field Crop Research*, 40: pp. 153-164.

Vavilov NI, 1926. Centers of origin of cultivated plants. In: Dorofeyev VF, editor. Origin and geography of cultivated plants. *Cambridge University Press*. pp. 22-135.

Vignon MR, Dupeyre D, Garcia-Jaldon C, 1996. Morphological characterization of steam-exploded hemp fibers and their utilization in polypropylene-based composites. *Bioresour Technol*, 58: pp. 203-215.

Vignon MR, Garcia-Jaldon C, Dupeyre D, 1995. Steam explosion of the woody hemp chénevotte. *International Journal of Biological Macromolecules*, 17: pp. 395-404.

Vonk CG, 1973. Computerization of Rulands X-ray method for determination of crystallinity in polymers. *Journal of Applied Crystallography*, 6: pp. 148-152.

Wang HM, Postle R, Kessler RW, Kessler W, 2003. Removing pectin and lignin during chemical processing of hemp for textile applications. *Textile Research Journal*, 73: pp. 664-669.

Zimmer H, Kloss D, 1995. Ultraschallaufschluss von Hanf. Ziele-Technologie-Anwendung-Resultate-Qualitätsmanagement. *Proceedings of the Bioresource Hemp '95 Symposium; Frankfurt, Germany*. Nova-Institut.

12 Symbols and Abbreviations

α_f/α_m	Porosity constants for fibres and matrix (vol/vol)
ε	Strain
σ	Ultimate stress (MPa)
ρ	Density (g/cm^3)
θ	Angle
τ	Shear stress (MPa)
σ_m	Matrix stress at the point of composite failure (MPa)
a	Fitting parameter (-)
b	Fitting parameter (-)/Sample width (mm)
C.sub.	*Ceriporiopsis subvermispora*
E	Stiffness (GPa)
HT	Hydrothermal treatment
l	Sample length (mm)
n	Sample size (-)
n_σ/n_E	Porosity constants for composite strength and stiffness
PE	Polyethylene, filament yarn
Pec	Pectinex (Flaxzyme)
PET	Polyethyleneterephthalate, filament yarn
PP	Polypropylene, filament yarn
P. rad.	*Phlebia radiata* Cel 26
STEX	Steam explosion
t	Sample thickness (mm)
TEX	Linear density (g/1000 m)
v	Absolute volume (cm^3)
V	Volume fraction (vol/vol)
$V_{f,(max)}$	Maximum attainable fibre volume fraction (vol/vol)
$V_{f,(obt)}$	Maximum obtainable fibre volume fraction (vol/vol)
w	Absolute mass (g)
W	Weight fraction
WO	Wet oxidation
Indices	
c	Composite
f	Fibres
m	Matrix
p	Porosity
u	Ultimate
x	Direction along fibres, axial direction (0°)
y	Direction perpendicular to fibres, transverse direction (90°)

Appendix A: Comprehensive composite data

Physical and mechanical properties measured for the composites and the calculated fibre properties after correction of composite strength and stiffness for porosity. Long fibre bundles over the entire test length (18 cm) and short overlapping fibres of 6 cm length were used in the fibre lay-ups.

Fibre type	Technique / fibre length	W_f %w/w	V_f %v/v	V_m %v/v	V_p %v/v	ρ_c g/cm^3	σ_{cu} MPa	E_c GPa	ε_c %	σ_M MPa	σ_{cup} MPa	E_{cp} GPa	σ_{fu} MPa	E_f GPa
No fibres	No cover	0	0	98	2	1.136	64	2.974	3.6	k=32.7				
Raw bast	>18 cm	23	17	76	7	1.126	95	15.2	0.78	21	111	16.4	575	85.3
		30	22	72	6	1.161	122	17.1	1.11	29	140	18.2	541	72.9
		35	26	68	6	1.178	122	20.4	0.75	20	141	21.9	489	76.3
Fibres from hemp stems treated with: Water retting	>18 cm	18	13	81	6	1.131	88	13.4	0.72	20	99	14.2	636	90.5
		30	22	73	5	1.177	129	20.3	0.72	20	143	21.4	582	86.9
		40	29	62	9	1.168	151	25.3	0.66	18	182	27.7	584	88.4
		42	31	61	8	1.187	153	26.4	0.66	18	181	28.6	540	85.4
C. sub.	6 cm	16	12	86	3	1.158	59	10.7	0.63	17	62	10.9	400	71.6
		29	22	73	5	1.177	100	18.0	0.70	19	111	19.0	446	76.8
		36	28	69	3	1.220	130	24.3	0.69	19	140	25.1	457	83.0
P. radiata cel 26	6 cm	26	19	78	2	1.194	112	16.1	0.95	25	118	16.5	506	72.8
		32	25	73	2	1.228	137	25.0	0.66	18	143	25.6	518	93.6
		35	27	69	4	1.216	150	22.7	0.84	23	162	23.5	539	79.3
	>18 cm	21	16	81	3	1.174	112	15.7	0.92	25	119	16.2	622	86.2
		27	20	77	3	1.196	162	22.1	1.09	29	171	22.7	740	101.8
		42	32	62	5	1.217	174	30.1	0.75	21	196	31.8	567	93.0
Hemp yarn Tex 47	Wound	18	18	79	3	1.189	161	13.6	1.78	43	171	14.0	746	63.4
		30	19	79	2	1.200	160	12.7	1.87	44	167	12.9	709	56.8
		40	27	68	5	1.198	209	17.3	1.82	43	235	18.3	770	61.0
		42	35	60	6	1.229	230	21.3	1.64	40	261	22.6	686	60.1
	>18 cm	9	23	73	3	1.208	164	16.0	1.55	38	200	16.5	730	61.3
		15	24	73	4	1.207	187	16.0	1.63	40	177	16.6	625	60.4
Hemp yarn Tex 91	>18 cm	22	22	75	3	1.204	157	13.1	1.93	45	166	13.5	611	51.9
		18	24	74	2	1.230	153	13.5	1.91	45	158	13.7	516	47.7
Barley straw	>18 cm	9	5	70	25	0.870	19	3.0	0.63	18	26	3.0	251	18.2
		15	7	55	37	0.743	15	3.2	0.58	16	23	3.2	194	21.2
		22	10	46	44	0.671	19	4.0	0.52	16	33	4.0	263	26.7
E-Glass	Wound	42	24	76	1	1.484	387	23.7	1.70	41	393	23.9	1539	91.8
		55	35	64	1	1.648	467	30.3	1.57	39	479	30.7	1316	83.4
	>18 cm	40	22	77	1	1.470	313	20.4	1.60	39	318	20.5	1281	81.3
		59	38	61	2	1.686	482	29.6	1.68	41	498	30.1	1251	74.7
	Wound	76	57	41	2	1.963	769	41.5	1.68	41	802	42.3	1418	72.7

Appendix B: Modelling of porosity content

The porosity content in the composites was determined by assuming that a composite on a macroscopic scale can be divided into fibres, matrix and porosity. The volume fraction of porosity V_p can then be calculated as

$$V_p = 1 - V_m - V_f$$

where the subscripts p, m and f denotes porosity, matrix and fibres, respectively. Equations for calculation of volume fractions of porosity, matrix and fibres based on experimentally obtained composite data are outlined in Paper IV. The porosity content in the composites was modelled versus the fibre weight fraction based on techniques developed by Madsen and Lilholt (2003, 2005), in which it is assumed that the volume fraction of porosity is linear dependent on both volume fraction of fibres V_f and of matrix V_m using the porosity constants α_f and α_m.

$$V_f = \frac{W_f \rho_m}{W_f \rho_m (1+\alpha_f) + (1-W_f)\rho_f (1+\alpha_m)}$$

$$V_m = V_f \frac{(1-W_f)\rho_f}{W_f \rho_m} = \frac{(1-W_f)\rho_f}{W_f \rho_m (1+\alpha_f) + (1-W_f)\rho_f (1+\alpha_m)}$$

$$V_p = \alpha_f V_f + \alpha_m V_m$$

This expression for the volumetric distribution between fibres, matrix and porosity is valid when the fibre content is below the maximum attainable volume fraction $V_{f,max}$ found by Madsen and Lilholt (2002). $V_{f,max}$ increases versus the compaction pressure applied when the liquid matrix and fibres are compacted before curing. If the weight fraction of fibres corresponds to a higher V_f than $V_{f,max}$, matrix will be partly replaced with air in the composite so the porosity content will increase while the fibre content remains constant at $V_{f,max}$. The porosity constants α_f and α_m can be determined by linear regression of V_p versus V_f as shown in Figure 35 using the following formulas.

$$V_p = \alpha_f V_f + \alpha_m V_m = \alpha_f V_f + \alpha_m (1 - V_f - V_p)$$

$$\Updownarrow$$

$$V_p (1+\alpha_m) = (\alpha_f - \alpha_m) V_f + \alpha_m$$

$$\Updownarrow$$

$$V_p = \frac{\alpha_f - \alpha_m}{1+\alpha_m} V_f + \frac{\alpha_m}{1+\alpha_m}$$

Expression for the regression line:

$$V_p = a \cdot V_f + b$$

The porosity constants can now be determined based on the regression line as follows:

Determination of α_m :

$$b = \frac{\alpha_m}{1+\alpha_m} \Leftrightarrow b\left(1+\alpha_m\right) = \alpha_m \Leftrightarrow \alpha_m\left(1-b\right) = b$$

$$\Updownarrow$$

$$\alpha_m = \frac{b}{1-b}$$

Determination of α_f :

$$a = \frac{\alpha_f - \alpha_m}{1+\alpha_m} \Leftrightarrow a\left(1+\alpha_m\right) = \alpha_f - \alpha_m \Leftrightarrow \alpha_f = a\left(1+\alpha_m\right) + \alpha_m$$

$$\Updownarrow$$

$$\alpha_f = a\left(\frac{1-b}{1-b} + \frac{b}{1-b}\right) + \frac{b}{1-b}$$

$$\Updownarrow$$

$$\alpha_f = \frac{a+b}{1-b}$$

Appendix C: Porosity and mechanical properties

The fibre strength σ_{fu} was calculated using the matrix stress σ_m at the strain of composite failure ε_u and the volume fractions of fibres and matrix as shown in Paper IV. The fibre stiffness E_f was calculated using the matrix stiffness E_m with "The rule of mixtures" (Hull and Clyne, 1996).

$$\sigma_{cu} = V_f \sigma_{fu} + V_m \sigma_m\left(\varepsilon_u\right) \Leftrightarrow \sigma_{fu} = \frac{\sigma_{cu} - V_m \sigma_m\left(\varepsilon_u\right)}{V_f}$$

$$E_c = V_f E_f + V_m E_m \Leftrightarrow E_f = \frac{E_c - V_m E_m}{V_f}$$

The equations above require that porosity does not affect σ_c and E_c to a larger extent than the reduction of V_m and V_f caused by increased porosity content V_p. However, σ_c and E_c depend on distribution, orientation and shape of the porosity voids since these can create inhomogeneous stress concentrations in the material. The material will fracture at locations with high stress concentration even though the average stress is low. Investigation of whether consideration of porosity was necessary in this case was performed by the term $(1\text{-}V_p)^n$ (Toftegaard and Lilholt, 2002). In which n=0 requires homogeneous stress concentration, and n>0 is used when the stress-concentration pattern decreases the composite strength σ_{cu} (Paper IV).

Calculation for fibre strength:

$$\sigma_{cu} = \left(V_f \sigma_{fu} + V_m \sigma_m\left(\varepsilon_u\right)\right)\left(1 - V_p\right)^{n_\sigma} = \sigma_{cup}\left(1 - V_p\right)^{n_\sigma}$$

$$\Updownarrow$$

$$\sigma_{fu} = \frac{\sigma_{cup} - V_m \sigma_m\left(\varepsilon_u\right)}{V_f} = \frac{\sigma_{cu}\left(1 - V_p\right)^{-n_\sigma} - V_m \sigma_m\left(\varepsilon_u\right)}{V_f}$$

Calculation for fibre stiffness:

$$E_c = \left(V_f E_f + V_m E_m\right)\left(1 - V_p\right)^{n_E} = E_{cp}\left(1 - V_p\right)^{n_E}$$

$$\Updownarrow$$

$$E_f = \frac{E_{cp} - V_m E_m}{V_f} = \frac{E_c\left(1 - V_p\right)^{-n_E} - V_m E_m}{V_f}$$

Appendix D: Density and mechanical properties

The composite can be investigated relative to the composite density as a function of the fibre weight fraction using the porosity constants for fibres, matrix, strength and stiffness. At first an expression for the composite density is derived:

$$m_f = \left(V_f \rho_f\right) v = \left(\rho_c W_f\right) v$$

$$\Updownarrow$$

$$\rho_c = V_f \frac{\rho_f}{W_f} = \frac{W_f \rho_m}{W_f \rho_m \left(1+\alpha_f\right) + \left(1-W_f\right) \rho_f \left(1+\alpha_m\right)} \times \frac{\rho_f}{W_f}$$

$$\Updownarrow$$

$$\rho_c = \frac{\rho_m \rho_f}{W_f \rho_m \left(1+\alpha_f\right) + \left(1-W_f\right) \rho_f \left(1+\alpha_m\right)}$$

in which v is composite volume. The next point is to get an expression for the composite stiffness E_{cp}:

$$E_{cp} = V_f E_f + V_m E_m$$

$$\Updownarrow$$

$$E_{cp} = \frac{W_f \rho_m E_f}{W_f \rho_m \left(1+\alpha_f\right) + \left(1-W_f\right) \rho_f \left(1+\alpha_m\right)} + \frac{\left(1-W_f\right) \rho_f E_m}{W_f \rho_m \left(1+\alpha_f\right) + \left(1-W_f\right) \rho_f \left(1+\alpha_m\right)}$$

$$\Updownarrow$$

$$E_{cp} = \frac{W_f \rho_m E_f + \left(1-W_f\right) \rho_f E_m}{W_f \rho_m \left(1+\alpha_f\right) + \left(1-W_f\right) \rho_f \left(1+\alpha_m\right)}$$

The next point is to combine the expressions for ρ_c and E_{cp}:

$$\frac{E_{cp}}{\rho_c} = \frac{W_f \rho_m E_f + \left(1-W_f\right) \rho_f E_m}{W_f \rho_m \left(1+\alpha_f\right) + \left(1-W_f\right) \rho_f \left(1+\alpha_m\right)} \times \frac{W_f \rho_m \left(1+\alpha_f\right) + \left(1-W_f\right) \rho_f \left(1+\alpha_m\right)}{\rho_m \rho_f}$$

$$\Updownarrow$$

$$\frac{E_{cp}}{\rho_c} = \frac{W_f \rho_m E_f + \left(1-W_f\right) \rho_f E_m}{\rho_m \rho_f} = \frac{W_f E_f}{\rho_f} + \frac{\left(1-W_f\right) E_m}{\rho_m}$$

by substituting E_{cp} with the real composite stiffness E_c, the following expression is derived:

$$\frac{E_c}{\rho_c} = \left(\frac{W_f E_f}{\rho_f} + \frac{\left(1-W_f\right) E_m}{\rho_m} \right) \left(1-V_p\right)^{n_E}$$

$$\Updownarrow$$

$$\frac{E_c}{\rho_c} = \left(\frac{W_f E_f}{\rho_f} + \frac{\left(1-W_f\right) E_m}{\rho_m} \right) \left(\frac{W_f \rho_m + \left(1-W_f\right) \rho_f}{W_f \rho_m \left(1+\alpha_f\right) + \left(1-W_f\right) \rho_f \left(1+\alpha_m\right)} \right)^{n_E}$$

$$\Updownarrow$$

$$\frac{E_c}{\rho_c} = \left(\frac{W_f E_f}{\rho_f} + \frac{\left(1-W_f\right) E_m}{\rho_m} \right) \times \left(\frac{W_f \left(\rho_m - \rho_f\right) + \rho_f}{W_f \rho_m \left(1+\alpha_f\right) + \left(1-W_f\right) \rho_f \left(1+\alpha_m\right)} \right)^{n_E}$$

The relationship for composite tensile strength can be determined by substituting E_f with σ_f and substituting E_m with $\sigma_m(\varepsilon_u)$.

$$\frac{\sigma_{cu}}{\rho_c} = \left(\frac{W_f \sigma_{fu}}{\rho_f} + \frac{\left(1-W_f\right)\sigma_m\left(\varepsilon_u\right)}{\rho_m} \right)\left(1-V_p\right)^{n_\sigma}$$

$$\Updownarrow$$

$$\frac{\sigma_{cu}}{\rho_c} = \left(\frac{W_f \sigma_{fu}}{\rho_f} + \frac{\left(1-W_f\right)\sigma_m\left(\varepsilon_u\right)}{\rho_m} \right)\left(\frac{W_f \rho_m + \left(1-W_f\right)\rho_f}{W_f \rho_m \left(1+\alpha_f\right) + \left(1-W_f\right)\rho_f \left(1+\alpha_m\right)} \right)^{n_\sigma}$$

$$\Updownarrow$$

$$\frac{\sigma_{cu}}{\rho_c} = \left(\frac{W_f \sigma_{fu}}{\rho_f} + \frac{\left(1-W_f\right)\sigma_m\left(\varepsilon_u\right)}{\rho_m} \right) \times \left(\frac{W_f \left(\rho_m - \rho_f\right) + \rho_f}{W_f \rho_m \left(1+\alpha_f\right) + \left(1-W_f\right)\rho_f \left(1+\alpha_m\right)} \right)^{n_\sigma}$$

Paper I

Changes in chemical composition, degree of crystallisation and polymerisation of cellulose in hemp fibres caused by pre-treatment.

(Proceedings of the 23th Risø International Symposium on Materials Science, Risø National Laboratory, Denmark, pp. 315-323)

Proceedings of the 23rd Risø International Symposium
on Materials Science:
Sustainable Natural and Polymeric Composites – Science and Technology
Editors: H. Lilholt, B. Madsen, H.L. Toftegaard, E. Cendre, M. Megnis,
L.P. Mikkelsen, B.F. Sørensen
Risø National Laboratory, Roskilde, Denmark 2002

CHANGES IN CHEMICAL COMPOSITION, DEGREE OF CRYSTALLISATION AND POLYMERISATION OF CELLULOSE IN HEMP FIBRES CAUSED BY PRE-TREATMENT

A. Thygesen[1,2,3], F. T. Madsen[2], H. Lilholt[1],
C. Felby[2] and A. B. Thomsen[3]

[1]Material Research Department, Risø National Laboratory,
4000 Roskilde, Denmark
[2]The Royal Veterinary and Agricultural University,
1870 Frederiksberg C, Denmark
[3]Plant Research Department, Risø National Laboratory,
4000 Roskilde, Denmark

ABSTRACT

The present work reports on how the chemical composition, the crystallinity and the cellulose chain length in hemp fibres were affected by steam explosion, wet oxidation, and enzymatic defibration, respectively. The degree of crystallization of cellulose in fibre bundles of the manually peeled hemp decreased slightly by the enzymatic defibration but not significantly by the other treatments. The cellulose chain length decreased only significantly by steam explosion. The cellulose fraction was highest in the fibre bundles after wet oxidation.

1. INTRODUCTION

Natural cellulose based fibres are increasingly gaining attention as their application is diversified into engineering end uses such as building materials and structural parts for motor vehicles. Hemp fibre bundles are highly crystalline with a high content of cellulose leading to higher stiffness (Mwaikambo and Ansell, 2002) and were therefore investigated in this study. However one of the drawbacks for industrial use of natural fibres is fibre damage, which occur naturally due to stress during growth and processing of the hemp stalks into fibre bundles and elementary fibres. Pre-treatment of the fibres is required to produce reactive hydroxyl groups and a rough surface for adhesion with polymeric materials (Avella et al., 1998; Kessler and Kohler, 1996).

The crystallinity and degree of polymerisation (DP) of cellulose in the fibre bundles can be used as indicators for changes at the microfibrillar and molecular level, respectively, during pre-treatment. It has been reported that steam explosion resulted in low cellulose loss and wet oxidation resulted in no cellulose loss when hemp fibres were treated (Thomsen et al., 2002). Due to the low losses of mass during wet oxidation and steam explosion, these pre-treatments seemed interesting. However pre-treatment performed at elevated temperature and pressure, might damage the cellulose structure, e.g. crystallinity and DP. Alternatively enzymatic treatment was investigated using different enzyme loadings at ambient temperature. Manually peeled hemp fibres were directly used in steam explosion, wet oxidation and enzymatic treatment, in order to minimise damage prior to the treatments.

2. MATERIALS AND METHODS

2.1 Raw material. Hemp (*Cannabis sativa* L.) variety Felina, which was sown May 7th 2001 with 32 kg seed/ha at a row spacing of 45 cm and harvested October 17th 2001 at Danish Institute of Agricultural Sciences, was used in all experiments. The hemp stalks were picked up manually from the field just after harvest and dried at 30°C for two days. Then the stack of hemp stems was turned around, and the drying process was continued at 25°C for 4 days. The dried stems were cut in a bottom, middle and top section of equal size. Internodes from the middle section were pealed manually and the resulting fibre bundles were cut into 1-3 cm long pieces.

2.2 Steam explosion. Steam explosion was performed at 200°C for 10 min. Hemp fibre bundles (2-3 cm long; 50 g) were placed in a 5 l autoclave. High-pressure water steam (40 bar) was added to the fibre bundles until the temperature of 200°C was reached. The steaming continued for 10 minutes at 200°C and subsequently, pressure was abruptly released (Thomsen et al., 2002). The resulting fibre/water suspension was separated by filtration, washed with water and dried at 60 °C for 50 h.

2.3 Wet oxidation. Wet oxidation was performed in a 2 l loop autoclave designed and constructed at Risø National Laboratory. Water (1 l) and hemp fibre bundles (1.9 g DM (dry matter) of 1 cm long and 16.9 g DM of 3 cm long fibre bundles) were added to the autoclave. The remaining gas volume of 1 l contained oxygen (10 bar) and atmospheric air (1 bar) corresponding to 11 bars. Heating-up and cooling-down times were 0.5 min and 3 min, respectively. The reaction temperature was kept at 170°C for a reaction time of 10 minutes after which the reactor was cooled and the pressure released. The fibre/water suspension was separated by filtration, washed with water and dried at 60 °C for 50 h (Thomsen et al., 2002).

2.4 Enzymatic treatment. Hemp fibre bundles (2-3 cm long) were treated in two runs. In the first run 15 g (14 g DM) fibre bundles were suspended in 1500 ml 50 mM potassium acetate buffer (pH 5.0). Biocide (1.5 g Atamon) and different concentrations of enzyme mixtures (0.015 g, 0.15 g, or 1.5 g Flaxzyme solution) were added. The incubation took place at 40°C for 24 hours with weak magnetic stirring. In the second experiment, 17 g DM hemp fibre bundles were treated in 1800 ml 50 mM potassium acetate buffer (pH 5.0). Biocide (1.8 g Atamon) and Flaxzyme (0.018 g, 0.18 g, or 1.8 g

liquid) were added to the fibre/water solution. The suspension with fibre bundles was incubated at 150 rpm and 40°C for 24 hours. After the treatment the fibre/water suspension was separated by filtration, washed with water and dried at 60°C for 50 h.

2.5 Fibre analysis. The chemical composition of the fibre samples was determined using a gravimetrical method (Browning, 1967). Fibres were initially milled in a Whiley knife mill and passed through a 1 mm sieve. Consecutively degradation and extraction of wax, water-soluble components, pectin, lignin, and hemicellulose in the milled fibres was performed in the chemical analysis. The residual part was almost pure cellulose with a low content of minerals, estimated by ash determination. This purified cellulose was used for determination of the cellulose chain length. The amount of the components remaining after the treatments ($C_{Component}$ (g)) was calculated by Eq. 1, in which $x_{Component}$ is the fraction of component x (g/g) after treatment and $R_{mass,treatment}$ is the total amount of remaining material (g).

$$C_{Component} = x_{Component} \cdot R_{mass,treatment} \tag{1}$$

2.6 Cellulose chain length (DP). Purified cellulose was dried with a dry matter analyser HR73 (Mettler Toledeo) at 105°C. Dried cellulose (0.1 g) was transferred to 25 ml vials with stirring rods. The cellulose was soaked in 15 ml pyridine for 4 h, at 80°C at low stirring rate. Afterward 7 ml phenyl isocyanate was added and the reaction mixture was kept at 80°C for 48 h. Afterwards, the solution was cooled and 80 ml 70% (v/v) methanol was added. The solution was centrifuged (4000 rpm; 5°C; 30 min) and the supernatant was discharged. Cellulose tricarbanilate in the pellet was washed three times with methanol and thereafter 4 times with water. During each washing step the pellet was suspended in the liquid, centrifuged (4000 rpm; 5°C; 10 min) and the supernatant was discharged. The product was dried at 60°C over night (Mallon et al., 2002).

The cellulose tricarbanilate was analysed by size exclusion chromatography (SEC) using two Waters Styragel HT6E columns. Tetrahydrofuran (THF) was used for elution at 1 ml/min at 25°C. Cellulose tricarbonilate (2 mg/ml THF) and Irganox (0.5 mg/ml THF) were dissolved in THF by weak stirring at 30°C for 16 h followed by centrifugation (5°C, 20 min, 3000 rpm). Supernatant (2 ml) was transferred to vials and 200 µl was injected. The refraction index (RI) and the light scattering index (LS) were measured. The cellulose chain length was calculated using Eq. 2 in which $DP_{reference}$ = 7000 has been determined for cellulose in cotton (Saake et al., 1992).

$$DP_{sample} = DP_{reference} \cdot \frac{LS_{sample} \cdot RI_{reference}}{RI_{sample} \cdot LS_{reference}} \tag{2}$$

2.7 Cellulose crystallinity. Defibrated hemp fibre bundles (1 g) were soaked in 100 ml 50 g/l NaOH for 48 h (Mwaikambo and Ansell, 1999). Thereafter the fibres were washed with water and dried at 60°C over night. The dried fibres were milled with a hammer mill (Risø National Laboratory) and pressed to a 1 mm thick tablet using a pressure on 150 MPa. The tablet was analysed reflectometrically (Stoe diffractometer, Cu-radiation (1.54 Å), 40 mA, 25 mv) with a step size of 0.1° for 5 s/step, and analysed in the 2θ-range 5 to 60°.

3. RESULTS AND DISCUSSION

3.1 Chemical composition. None of the treatments resulted in significant loss of cellulose. The highest dry matter loss was obtained by wet oxidation due to removal of lignin, hemicellulose, and non cell wall material, while the enzymatic hydrolysis with low flaxzyme concentration caused the lowest dry matter loss (Table 1). The lignin content was maintained and in some experiments increased slightly during the treatments except for wet oxidation in which lignin was reduced.

Table 1. Changes in chemical composition of the hemp fibre bundles after the pre-treatments. All values are in g after treatment of initial 100 g raw fibres (Eq. 1).

Compo-nent	Raw fibres	Wet oxidation		Steam explosion		0.1% Flaxzyme		1% Flaxzyme		10% Flaxzyme	
wax	3.7	5.1	2.4	1.7	2.5	2.3	3.2	2.1	3.1	2.1	1.3
water extractives	7.7	3.3	2.2	2.7	2.1	2.3	2.0	2.4	2.0	2.6	1.7
pectin	8.6	2.5	2.8	4.8	3.8	5.0	4.5	4.6	3.9	3.9	2.9
lignin	6.0	2.2	1.2	5.1	3.6	4.4	6.3	4.0	7.3	3.3	5.8
hemi-cellulose	14.3	8.3	8.9	11.6	10.2	13.4	11.1	13.1	11.5	12.5	10.9
cellulose	59.7	57.1	58.3	57.1	60.9	59.5	61.8	61.4	60.2	60.4	58.3
total	100.0	79.0	76.0	83.0	83.0	87.0	89.0	88.0	88.0	85.0	81.0

Looking at pectin, lignin and hemicellulose, it is seen that the loss is highest for wet oxidation. Considering enzymatic defibration, higher concentration of flaxzyme lead to slightly higher loss of hemicellulose and pectin.

3.2 Cellulose chain length. The cellulose chain length (DP) in hemp yarn and raw hemp fibres was about 7500 and 6900, respectively. The cellulose chain length did not change significantly by wet oxidation, while it decreased by 15-40% by steam explosion and enzymatic defibration (Table 2). Thus steam explosion induced a physical impact onto the fibres, sufficient to hydrolyse cellulose. By enzymatic defibration, DP decreased by 20-30%. The tendency is that the retention time is only slightly affected by the treatments indicating low decreases in the DP.

Table 2. Degree of polymerisation of cellulose in untreated hemp fibres and hemp fibres subjected to pre-treatment, compared with the retention time measured by size exclusion chromatography.

Sample	DP	Half peak left	Top (ml)	Half peak right	Half peak width
Hemp yarn	7300	11.8	12.4	13.2	1.4
Hemp yarn	7800	11.8	12.4	13.2	1.4
Hemp (raw without nodes)	7000	11.6	12.3	13.4	1.8
Hemp (raw without nodes)	6400	11.6	12.1	13.3	1.7
Hemp (raw without nodes)	7200	11.6	12.1	13.3	1.7
1.WO	6400	11.5	12.1	13.3	1.8
1.WO	6800	11.5	12.2	13.3	1.8
2.WO	7400	11.7	12.2	13.2	1.4
2.WO	7500	11.7	12.3	13.2	1.5
1.STEX	3900	12.0	12.8	14.1	2.1
1.STEX	5700	11.8	12.4	13.5	1.7
2.STEX	5300	11.8	12.4	13.6	1.9
2.STEX	7100	11.7	12.2	13.3	1.6
1% Pectinex	5200	11.7	12.4	13.7	2.0
1% Pectinex	6900	11.8	12.4	13.8	2.0
10% Pectinex	6800	11.8	12.4	13.3	1.5
10% Pectinex	4900	11.8	12.4	13.3	1.5

According to (Wood et al., 1986) there are two major concerns in using cellulose tricarbanilate for SEC analysis. Firstly, it might not be completely formed and secondly, the substituent distribution might not be homogeneous along the cellulose chain. In addition the reaction conditions used for forming cellulose tricarbanilate may cause degradation of the cellulose molecules.

3.3 Cellulose crystallinity. The X-ray diffraction of the hemp fibre bundles measured four significant peaks at the angles $2\theta = 15°$ (101), 16.5° ($10\bar{1}$), 22.3° (002), and 34° (040), respectively (Fig. 1). The peaks for (101), ($10\bar{1}$), and (002) were in agreement with previous findings on native cellulose (Fink and Walenta, 1994) while the peak (040) was also found by analysis of hemp fibres (Mwaikambo and Ansell, 2002). By analysis of various cellulose samples using ^{13}C NMR it has been determined that cellulose I consists of two polymorphs: Iα and Iβ (Atalla and Vanderhart, 1984). Iα cellulose has a triclinic space group and only one repeating cellobiose in the unit cell, thus possessing a parallel structure. Iβ cellulose, is formed by hydrothermal treatment of Iα. In this structure, the chains are also parallel and translated by approximately –1/4b with respect to the origin chain, thus leading to a monoclinic space group. In this study, the authors did not distinguish between Iα and Iβ cellulose, and the entire cellulose content was assumed to be Iβ cellulose.

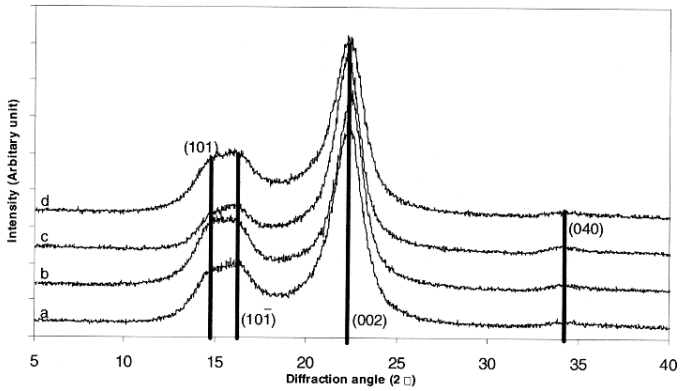

Fig. 1. X-ray diffraction spectra measured using raw (a), wet oxidised (b), steam exploded (c), and enzyme treated hemp fibres.

Several approaches on determination of the cellulose crystallinity have been reported. A frequently used expression is Eq. 3 in which $I_{(002)}$ is the intensity of the (002) peak assumed to represent both crystalline and amorphous material and I_{AM} is the counter reading at a 2θ-angle at 18° representing amorphous material in the cellulose fibres (Mwaikambo and Ansell, 1999).

$$I_C = \frac{I_{(002)} - I_{Am}}{I_{(002)}} \tag{3}$$

The drawback in Eq. 3 is that there was overlapping between the $(10\bar{1})$ peak the (002) peak, which means that the crystallinity is overestimated. In this study, the crystallinity was estimated by assuming that the background intensity represented the amorphous cellulose and that the crystalline cellulose represented the peak area after subtracting the background (Fig. 2). Using this expression the cellulose crystallinity was 62-70% and lowest for steam exploded hemp fibres (Table 3). The crystallite dimension was calculated using the width at the half peak height in the Scherrer equation. The crystal dimension was between 40 and 50 Å (Table 3), determined using the (101), $(10\bar{1})$, and (002) peaks which means that the crystal dimensions are about 6 times larger than the *a* and *c* lengths in the unit cell (Table 3).

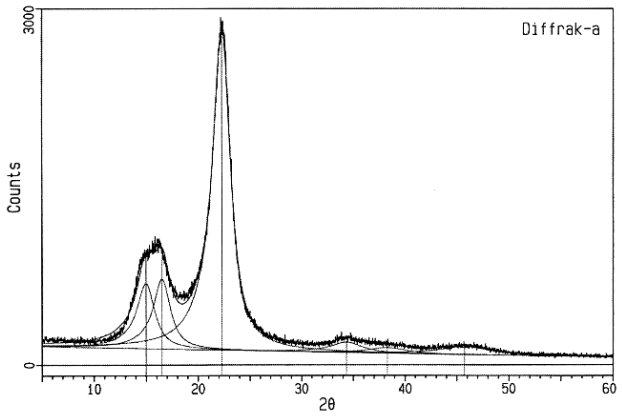

Fig. 2. X-ray diffraction spectrum measured using raw hemp fibres. Polynomial fitting separates the peaks.

Table 3. Peaks, unit cell dimensions assuming a monoclinic space group and crystallite size for the pre-treated hemp fibre bundles.

Defibration	Before defibration	Wet oxidation	Steam explosion	Enzymatic treatment
Significant peak at angle (2θ)				
Peak 101 (°)	14.98	15.05	15.27	15.01
Peak $10\bar{1}$ (°)	16.53	16.49	16.57	16.56
Peak 002 (°)	22.27	22.43	22.24	22.27
Peak 040 (°)	34.34	34.49	34.38	34.39
Monoclinic unit cell parameters				
β (°)	95.60	95.20	94.65	95.59
a (Å)	7.94	7.97	7.76	7.91
b (Å)	10.43	10.39	10.4	10.4
c (Å)	8.01	7.95	8.01	8.01
Crystallite dimension (peak)				
Peak 101 (Å)	44	41	48	45
Peak $10\bar{1}$ (Å)	47	44	51	46
Peak 002 (Å)	45	52	50	44
Peak 040 (Å)	26	31	30	28
Crystallinity (%)	70%	67%	62%	67%

4. CONCLUSIONS

In this study it was found that:

- All treatments resulted in less than 5% mass loss of cellulose.
- Wet oxidation resulted in the most pure cellulose, no decrease in cellulose chain length and a small reduction in crystallinity.
- Steam explosion resulted in moderate increase of cellulose content, decreased cellulose chain length and some reduction in crystallinity.
- Enzymatic defibration resulted in moderate increase of cellulose content, and at higher enzyme concentrations decreased cellulose chain length, and a small reduction in crystallinity.

ACKNOWLEDGEMENT

This work is part of the project "High performance hemp fibres and improved fibre network for composites" supported by the Danish Research Agency of the Ministry of Science. The authors like to thanks to following for guidance and assistance: Poul Flengmark for growing the hemp plants, Sokol Ndoni for size exclusion chromatography, and Kenny Ståhl for X-ray diffraction.

REFERENCES

Atalla, RH, D L Vanderhart, 1984, Native cellulose - A composite of 2 distinct crystalline forms: Science, v. 223, p. 283-285.

Avella,M, L Casale, R Dell'Erba, B Focher, E Martuscelli, A Marzetti, 1998, Broom fibers as reinforcing materials for polypropylene-based composites: Journal of Applied Polymer Science, v. 68, p. 1077-1089.

Browning,BL, 1967, Methods of wood chemistry, New York, Interscience Publishers, A division of John Wiley & Sons, p. 387-427.

Fink,HP, E Walenta, 1994, Röntgenbeugungsuntersuchungen zur übermolekularen struktur von Cellulose im verarbeitungsprozess: Heft, v. 12, p. 739-748.

Kessler,RW, R Kohler, 1996, New strategies for exploiting flax and hemp: Chemtech, v. 26, p. 34-42.

Mallon,S, W B Pedersen, A B Thomsen. A complete method for the determination of cellulose molecular weight distribution in plants and trees. 2002. Ref Type: Unpublished Work

Mwaikambo,LY, M P Ansell, 1999, The effect of chemical treatment on the properties of hemp, sisal, jute and kapok for composite reinforcement: Die Angewandte Makromolekylare Chemie, v. 272, p. 108-116.

Mwaikambo,LY, M P Ansell, 2002, Chemical modification of hemp, sisal, jute, and kapok fibers by alkalization: Journal of Applied Polymer Science, v. 84, p. 2222-2234.

Saake,B, R Patt, J Puls, K J Linow, B Philipp, 1992, Molar-mass distribution of celluloses: Die makromoleculare chemie, v. 61, p. 219-238.

Thomsen,AB, V Bohn, K V Nielsen, B Pallesen, M S Jørgensen, 2002, Effects of chemical-physical pre-treatment processes on hemp fibres: Industrial Crops and Products.

Wood,BF, A H Conner C G Hill, 1986, The effect of precipitation on the molecular-weight distribution of cellulose tricarbanilate: Journal of Applied Polymer Science, v. 32, p. 3703-3712.

Paper II

Hemp fiber microstructure and use of fungal defibration to obtain fibers for composite materials.

Journal of Natural fibers 2(4) pp. 19-37.

Hemp fiber microstructure and use of fungal defibration to obtain fibers for composite materials

Anders Thygesen[*1,2], Geoffrey Daniel[3], Hans Lilholt[1], Anne Belinda Thomsen[4]

[1] Risø National Laboratory, Materials Research Department, P.O. Box 49, DK-4000 Roskilde, Denmark.
[2] The Royal Veterinary and Agricultural University, Danish Centre for Forest, Landscape and Planning, Højbakkegårds Allé 1, DK-2630 Tåstrup, Denmark
[3] Swedish University of Agricultural Sciences, WURC, P.O. Box 7008, SE-75007 Uppsala, Sweden.
[4] Risø National Laboratory, Biosystems Department, P.O. Box 49, DK-4000 Roskilde, Denmark.

***Corresponding Author:** Anders Thygesen: Fax: +45 46775758

Academic degrees, professional titles and e-mail addresses:

M.Sc., Ph.D student Anders Thygesen, E-mail: anders.thygesen@risoe.dk

Dr., Professor Geoffrey Daniel , E-mail: geoff.daniel@trv.slu.se

M.Sc., Ph.D, Senior scientist Hans Lilholt, E-mail: hans.lilholt@risoe.dk

M.Sc., Ph.D, Senior scientist Anne Belinda Thomsen, E-mail: anne.belinda.thomsen@risoe.dk

Journal: Journal of Natural Fibres, In press.

ABSTRACT

Characterization of hemp fibers was carried out to investigate the mild defibration with *Phlebia radiata* Cel 26, a fungus which selectively degraded the epidermis and the lignified middle lamellae. Thin fiber bundles could thereby be produced. The single fiber S2 layer consisted of 1-5 μm thick concentric layers constructed of ca. 100 nm thick lamellae. The microfibril angle showed values of 0-10° for the main part of S2 and 70-90° for S1. The low S2 microfibril angle resulted in fiber bundles with high tensile strength (960 MPa) decreasing to 850 MPa after defibration due to degradation of non cellulosic components.

Key words: *Cannabis sativa* L., bast fibers, cell wall structure, microfibril angle, electron microscopy, histochemistry, *Phlebia radiata* Cel 26.

ACKNOWLEDGEMENTS

This work forms part of the project "High performance hemp fibers and improved fiber network for composites" supported by the Danish Research Agency of the Ministry of Science, the EU COST action E20 and the Wood Ultrastructure Research Center (WURC), Sweden. The support to Ph. D. student Anders Thygesen from WURC is gratefully acknowledged. Senior scientist Poul Flengmark (Danish Institute of Agricultural Sciences) is acknowledged for growing the hemp, Mrs. Ann-Sofie Hansen (WURC) for setting up the fungal cultivations, M. Sc. Frants T. Madsen (The Royal Veterinary and Agricultural University) for instruction in fiber bundle testing and Mr. Henning K. Frederiksen (Risø National Laboratory) for help in composite fabrication. Dr. Claus Felby (The Royal Veterinary and Agricultural University) is acknowledged as supervisor for Anders Thygesen.

INTRODUCTION

This study presents a structural and chemical investigation of hemp fibers (*Cannabis sativa L.*), which have been tested as reinforcement agents in biocomposites in recent years (Madsen & Lilholt, 2003; Mwaikambo & Ansell, 2003). Hemp fibers are advantageous compared to glass fibers with respect to lower density (1.56 g cm^{-3}), similar stiffness (50-70 GPa) and environmental sustainability. Hemp fibers are 1-3 cm long with 60-70 % cellulose whereas wood fibers are 1-3 mm long with 40-50 % cellulose. The part of the hemp plant, which is useful as reinforcement agents in biocomposites, are the primary- and secondary single fibers (bast fibers) present in the bark (cortex) of the plant (Garcia-Jaldon et al., 1998). Parenchyma cells separate bundles of single fibers from one another. Between the single fibers, there are mainly polysaccharides and lignin, which must be selectively removed to obtain fibers for composites. Thus, both improvement of defibration methods and better understanding of single fibers composition are required to develop stronger composites.

Transmission electron microscopy (TEM) has been used previously for observations on mercerized hemp (18 % NaOH) (Purz et al., 1998). However it is difficult to prepare 100 nm thick transverse sections for TEM, so only limited studies have been performed on untreated hemp. The microfibril angle to the fiber axis (MFA) is a major parameter that affects the mechanical properties of plant fibers (Page & Elhosseiny, 1983). The MFA has been determined for hemp fibers as 4° (Fink et al., 1999) and other non woody fibers as 6-25° (Mukherjee & Satyanarayana, 1986) using X-ray diffraction providing an average value across the cell wall.

This study concerns a thorough investigation of hemp fibers. The hemp stems were defibrated by the mutated white rot fungus *Phlebia radiata* Cel 26, which is characteristic due to its lack of cellulases. Histochemical investigations were made to visualize the distribution of lignin, pectin and waxes in the hemp stem – and at the single fiber level. Observations with scanning electron microscopy provided novel and detailed information on the microfibril angle. Cell wall structure and MFA were further characterized by partial decay using the soft rot fungus *Phialophora mutabilis*, which develops cavities orientated along the cellulose microfibrils in plant fibers and wood fibers (Khalili et al., 2000, 2001). Further structural knowledge was obtained by TEM observations of partial cell wall decay patterns of *P. radiata* wild and *P. radiata* Cel 26. Tensile tests of hemp fiber bundles followed by SEM microscopic investigation of the fractured fiber ends revealed details on the microstructure and mechanical properties of the cell wall.

MATERIAL STUDIED

Hemp (*Cannabis sativa* L.) variety *Felina* was sown May 7th 2001 with 32 kg seed ha^{-1} and harvested October 17th 2001. The site is located at 55°20'N, 11°10'E and 0-100 m above sea level. The hemp stems were cut 10 cm above the soil surface and dried at 25-30°C for six days. From the dried stems, the middle section 40-140 cm above the root was investigated. Some stem pieces were treated using the fungi and others were not treated before analysis.

METHODS AND TECHNIQUES

Treatment of hemp stems using fungi

The soft rot fungus *Phialophora mutabilis* 24-E-11 [van Beyma Schol-Schwartz] was inoculated and retained on 20 g l^{-1} malt agar plates at 20°C. Mycelium from one agar plate was homogenized into 100 ml water. From this suspension, 10 ml was added aseptically to a pre-autoclaved (120°C for 30 min) 100 ml Erlenmeyer flask with 50 g wet soil and 5 hemp stem pieces of 3 cm length, placed just below the soil surface (Khalili et al., 2000). Cultures of the white rot fungi *Phlebia radiata* L12-41 (wild) and *Phlebia radiata* Cel 26 (Nyhlen & Nilsson, 1987) and soft rot fungus *P. mutabilis* were set up according to Daniel et al. (1994). Samples were taken after 19 days incubation at 28°C. The stem pieces were removed from the soil, washed carefully in water and either stored at –20°C for light microscopy or fixed and processed for TEM. Due to their weak binding to the xylem, fiber bundles were easily separated from the underlying xylem. These samples were stored in water at 5°C. Cultivations were also performed in liquid medium using 100 g hemp stems as described by Thygesen et al. (unpublished). The liquid medium contained 140 ml of mycelium suspension, made as described above, and 1 l solution of 1.5 g l^{-1} NH_4NO_3, 2.5 g l^{-1} KH_2PO_4, 2 g l^{-1} K_2HPO_4, 1 g l^{-1} $MgSO_4 \cdot 7\ H_2O$ and 2.5 g l^{-1} glucose.

Scanning electron microscopy and delignification

Samples (transverse sections and fiber bundles) were air-dried overnight, and mounted on stubs using double-sided cellotape. Following coating with gold using a Polaron E5000 sputter coater, samples were observed using a Philips XL30 ESEM scanning microscope. Additional hemp fiber bundles (100 mg) were delignified in 10 ml aqueous solution of 50 % v/v acetic acid and 15 % (v/v) H_2O_2. The fiber bundles were incubated at 90°C for 2 hours and washed 5 times with water before preparation for SEM.

Embedding in London resin for transmission electron microscopy

Hemp fiber bundles were fixed in a mixture of 3 % v/v glutaraldehyde (1,5-pentanedialdehyde) and 2 % v/v paraformaldehyde (polyoxymethane) in 0.1 M sodium cacodylate buffer (pH 7.2) (dimethylarsinic acid sodium salt trihydrate dissolved in water). After 3 washes of 15 min in 0.1 M sodium cacodylate buffer, samples were post-fixed overnight at 5°C in 1 % w/v osmium tetroxide in the same buffer. Following 5 washes in water of 15 min, samples were dehydrated in ethanol (20 % to 100 % in steps of 10 % for 10 min) followed by embedding in acrylic London resin [LR White, Basingstoke, U.K.]. During impregnation, samples were subject to vacuum 2 times of 30 min in order to achieve better resin penetration. Samples were placed in gelatin capsules filled with fresh London resin, which was allowed to polymerize at 70°C overnight. Selected material was sectioned using a Reichert Ultracut E and sections were collected on copper grids. Following staining with 50 % ethanolic uranyl acetate for 5 min, sections were viewed using a Philips CM/12 TEM microscope operated at 80 kV.

Fiber dimensions

The width of the fiber lumen was calculated using Image Pro software after light microscopy with 100x magnification. The area of the transverse fiber section including lumen ($A_f \pm \Delta A_f$) was determined by drawing lines around 10 fibers in five transverse

sections ($A_{f,i}$, n = 50) using Image Pro software (Equation 1). The lumen size ($a_{l,i}$) was calculated similarly by drawing a line around the lumen in the fibers. The lumen fraction (L±ΔL) was calculated with Equation 2.

Equation 1 $$A_f = \frac{\sum A_{f,i}}{n}$$

Equation 2 $$L = \frac{\sum a_{l,i}}{\sum A_{f,i}}$$

Tensile testing of hemp fiber bundles

Fiber bundles of 15 mm length (l_{spec}) were strained to fracture at 3 mm span (l_{span}) at a test speed of 0.30 mm min^{-1} using an Instron 5566 with pressley clamps [Type: Stelometer 654 from Zellweger Uster] at 20°C and 66% relative humidity. Following fracture the fiber pieces were weighed (m_{spec}). Some pieces were separated into single fibers and coated with gold and the brash-like fractured ends were examined using SEM. The tensile strength (σ) was calculated based on the force of fracture (F_{max}) and the density of hemp yarn ρ_{spec}=1.56 g ml^{-1}.

Equation 3 $$\sigma = F_{\max} \Big/ \frac{m_{spec}}{l_{spec} \times \rho_{spec}}$$

The elastic modulus (E) was calculated based on linear regression of force versus elongation in the elongation range (Δl) from 0.030 mm to 0.045 mm.

Equation 4 $$E = \left(\frac{dF}{d\Delta l}\right)_{\Delta l = 30-45\,\mu m} \times l_{span} \Big/ \frac{m_{spec}}{l_{spec} \times \rho_{spec}}$$

Histochemical reactions and microfibril angle

Cytochemical reactions were made on transverse hemp stem sections mounted on glass slides in one drop of 50 % (v/v) glycerol in water and a cover slip placed on top. All the experiments were performed in at least triplicates. Light microscopy was performed at 50-630 x magnifications using a Leica DMLS bright field microscope fitted with polarized light filters with images recorded digitally. The following cytochemical reactions were performed:

Lignin - hydroxycinnamyl aldehydes (Wiesner reaction): Sections were stained with two drops of 10 g l^{-1} phloroglucinol in ethanol, followed by addition of 2 drops of 35 % (v/v) HCl (Strivastava, 1966). **Lignin - syringyl** (Mäule reaction): Sections were stained with one drop of 10 g l^{-1} $KMnO_4$ for 5 min followed by three washes in water. Sections were then immersed in 3 % (v/v) HCl for 1 min, washed in water, and immersed in 29 % (v/v) NH_3 for 1 min (Strivastava, 1966; Wu et al., 1992). **Pectin:** Sections were stained with 1 g l^{-1} Ruthenium Red [JMC Speciality Products] (Strivastava, 1966; Jensen, 1962). **Wax:** Sections were immersed in 10 g l^{-1} Sudan IV in 70 % ethanol on a glass slide (Wu et al, 1992).

Microfibril angle: Cell wall cavities formed during *P. mutabilis* colonization and attack before harvest by native colonizing fungi were seen as dark lines using polarized light microscopy. These cavities were orientated parallel with the microfibrils (Khalili et al.,

2000) and their orientation gave thereby an indication of the microfibril orientation. SEM observations of *P. radiata* Cel 26 defibrated and delignified hemp fibers showed slightly darker intermediate lines on the fiber surface parallel with the cellulose microfibrils.

Gravimetric plant fiber analysis

The fibers were milled to pass a 1 mm sieve. From the milled fibers, wax was extracted in chloroform, water-soluble components in water, pectin in EDTA solution, lignin in solution of chlorite and acetic acid and hemicellulose in boric acid and 12 % NaOH solution. The residual part was cellulose with less than 1 % of minerals (Browning, 1967).

RESULTS AND DISCUSSION

The original hemp stems were 1.5-2.5 m tall and 5-15 mm in diameter near the soil surface. The stems contained 35-40 % w/w bast fibers and were organized in layers from the stem pith towards the surface by 1-5 mm xylem, 10-50 μm cambium, 100-300 μm cortex, 20-100 μm epidermis and 2-5 μm cuticle. The definition of stem components are in accordance with Garcia-Jaldon et al. (1998) and aspects of the stems are shown in SEM micrographs (Figure 1) and modeled in Figure 2A.

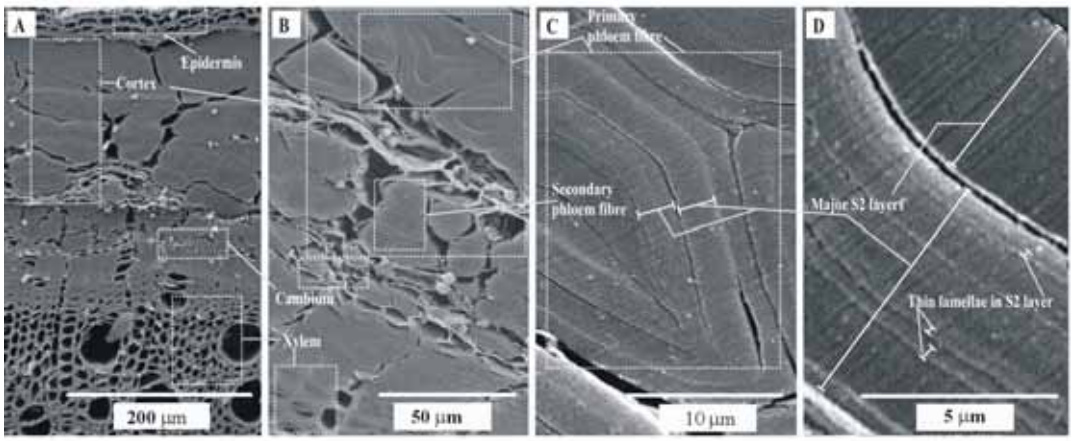

Figure 1. Hemp stem shown at increasing magnification using different transverse sections in SEM: A: Xylem + cambium + cortex + epidermis; B: Primary and secondary single fibers; C: Major layers in primary single fiber; D: Thin lamellae within the S2 layer.

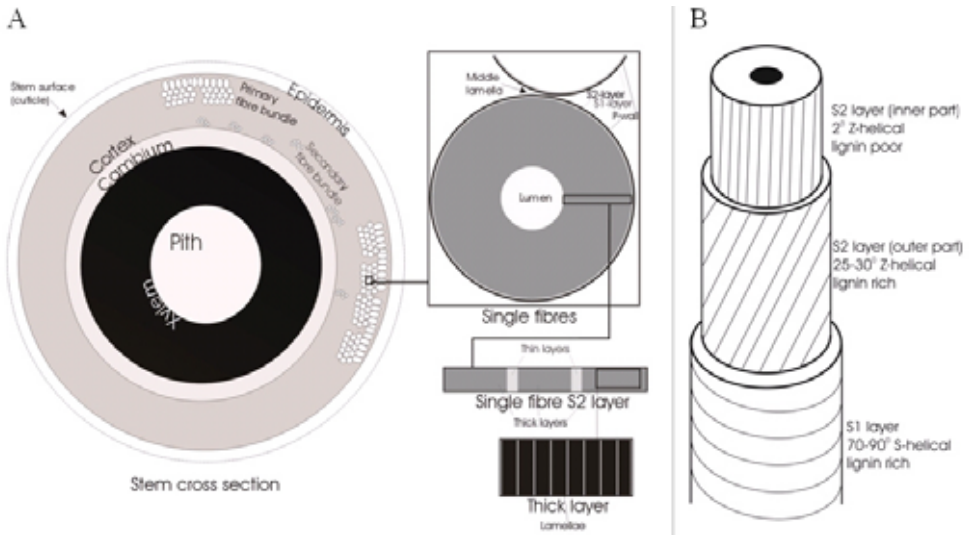

Figure 2. A: Model of transverse stem section zooming to single fibers, secondary cell wall and finally the cell wall lamella structure. B: Model of the microfibril orientation throughout the secondary cell wall.

Architecture of the hemp stem and the single fibers

SEM observations of the cortex showed polygonal-shaped primary and secondary single fibers with 4 to 6 sides (Figure 1A) arranged in fiber bundles of 10-40 fibers. The primary single fibers nearest the stem surface were largest (cell wall thickness = 7-13 μm) and were formed at the early growth stage (Mcdougall et al., 1993). The secondary single fibers near the cambium layer were smaller (cell wall thickness = 3-6 μm) and only present in the thick parts of the stem at the late growth stage (Figure 1B). The area of the transverse fiber section including cell lumen ($A_{f,}$, Equation 1) was 780 $\mu m^2 \pm 300$ μm^2.The single fibers had small lumina (lumen width = 0.5-5 μm) so cell wall synthesis appears to continue until nearly all the cytoplasm space has been used. The lumen fraction in the fibers (L) was 9 % ± 7 %. Therefore the load carrying part of the single fibers is high (1-L = 91 %) presumably resulting in high tensile strength compared to wood fibers with larger lumina.

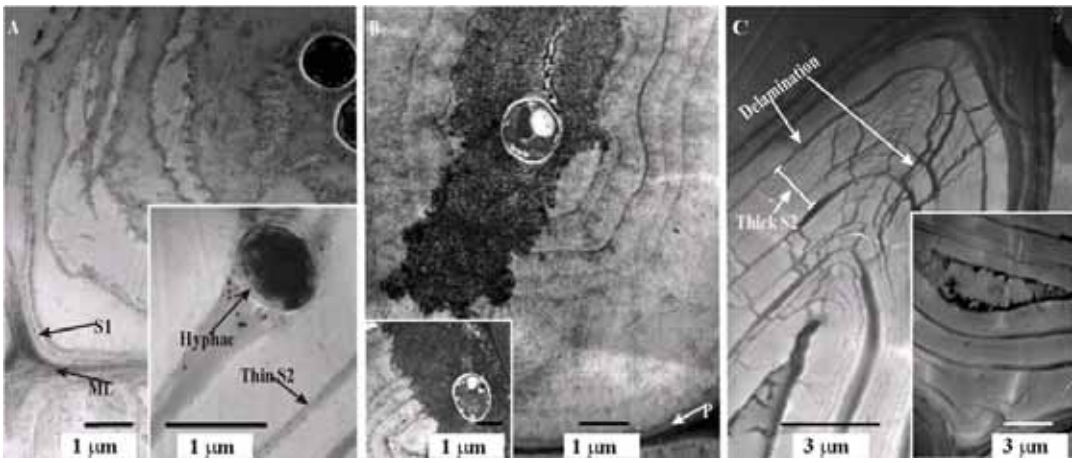

Figure 3. Single fibers partially decayed by fungi (transverse sections). A: P. mutabilis *decay of the thick layers in S2. B:* P. radiata *(wild) decay of the cell wall from the lumen side. C:* P. radiata *Cel 26 decay of the thin layers between the thick concentric S2 layers.*

By TEM microscopy, the single fiber middle lamellae (ML) and primary wall (P) were found to have thickness of 30-50 nm and 70-110 nm, respectively (Figure 3A, B). The secondary cell wall was composed of a 100-130 nm thick S1 layer and a 3-13 μm thick S2 layer. Both SEM and TEM observations showed that the S2 layer had a laminate structure of 1 to 4 major concentric layers of 1-5 μm in thickness. The major layers were constructed of 100 nm thick lamellae (Figure 1C-D, Figure 3C). Thin layers of 200-240 nm in thickness were located between the major concentric layers (Figure 3A). Confirmation for a concentric orientation of the layers was further obtained by SEM observations on the ends of *P. radiata* Cel 26 treated fibers fractured under tension (Figure 4). The major layers separated from each other, further indicating that they were weakly attached to one another.

Microfibril angles of the single fibers

Some single fibers in the H_2O_2 delignified hemp showed evidence of cavities made by naturally occurring fungi before harvest. It was possible to measure the microfibril angle in two adjacent cell wall layers since several parallel cavities crossed each other (Figure 5A). The microfibrils had Z helical orientation with angles in the intervals 0-5° and 25-30°. Superficial attack of other single fibers showed evidence of MFAs in the range of 70-90° with an S helical orientation (Figure 5B), which was confirmed by polarized light microscopy (data not shown). Single fibers from H_2O_2 delignified and *P. radiata* Cel 26 treated hemp stems showed regions where the S1 layer was partly peeled off (Figure 5C). The cellulose aggregates in the S1 and S2 layer beneath were orientated perpendicular and parallel to the fiber axis, respectively. The fracture experiments (Figure 4) showed evidence for a main S2 MFA of 0-10° agreeing with 4° measured previously by X-ray diffraction (Fink et al., 1999). The microfibril model of the single fibers shown in Figure 2B is based on the obtained data.

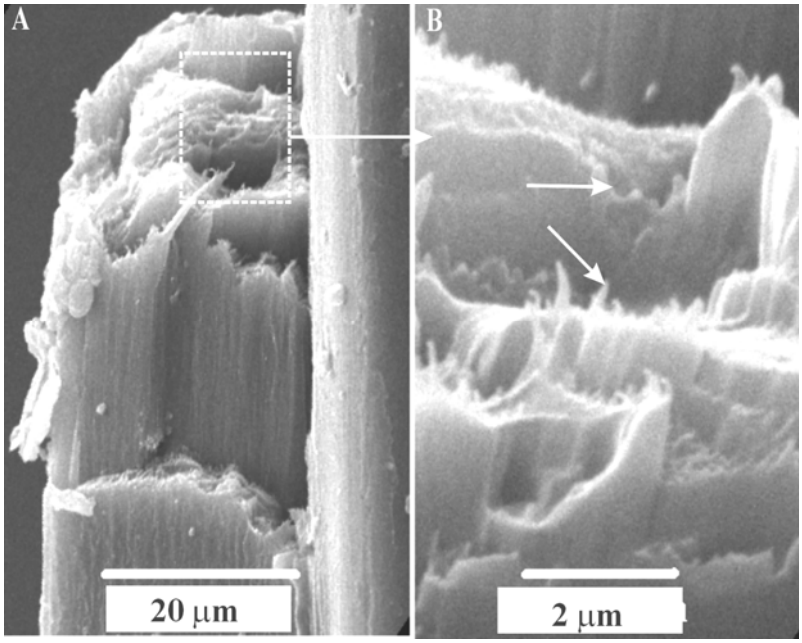

Figure 4. Fractured end of a single fiber showed at increasing magnification. A: Splits developed by radial tension between the major concentric layers due to the weak interface. B: Cellulose aggregates (arrows) apparent at site of fracture.

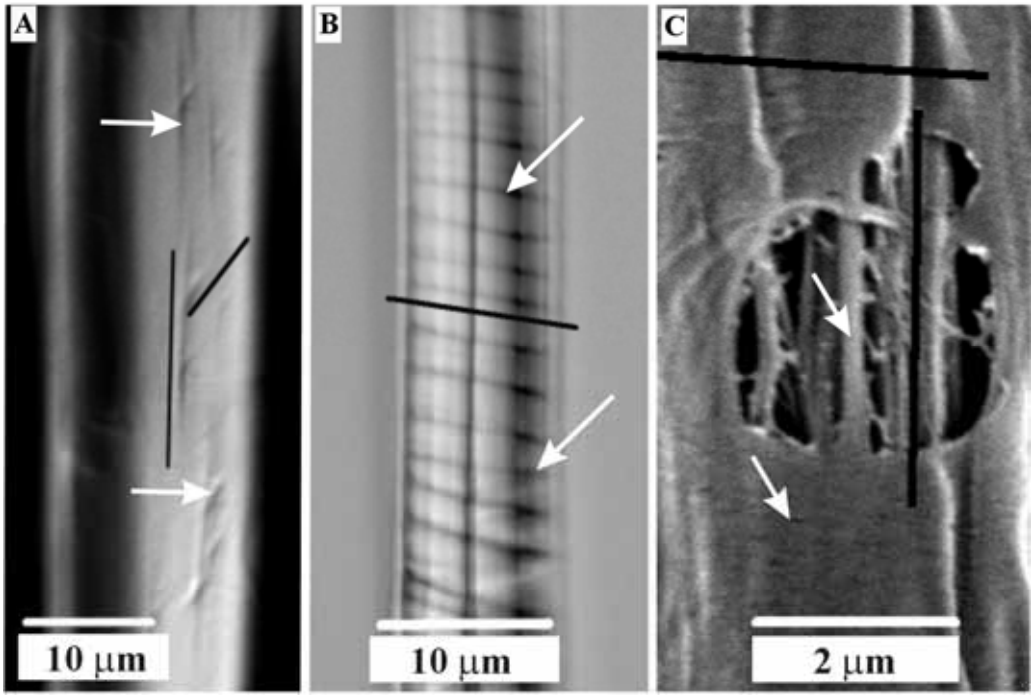

Figure 5. Microfibril angles (MFA) in fungal colonized and delignified single fibers shown with black lines and white arrows: A: Crossing cavities parallel with two different MFA in S2. B: A third MFA identified as dark and winding cavities in S1. C: P. radiata Cel 26 treated fiber with the S1 layer partly stripped off revealing the underlying S2 layer.

Histochemical composition of the structure on hemp stem and single fiber level

Lignin was determined with the Wiesner - and Mäule reactions (Figure 6). The Wiesner reaction stains lignin red by reaction of phloroglucinol with hydroxycinnamyl aldehydes (Strivastava, 1966). The Mäule reaction stains lignin red by oxidation of syringyl lignin with $KMnO_4$-HCl due to the produced 3-methoxy catechol (Wu et al., 1992). The inner part of the single fiber secondary wall was lignin poor as shown by negative Wiesner – and Mäule reactions (Table 1). The outer part of the cell wall was lignified according to positive Wiesner – and Mäule reactions. Lignin was present at highest concentration in the compound middle lamellae. No lignin was present in the cambium while the epidermis contained some lignin (Figure 6). According to the similar intensities found by the Wiesner - and Mäule reactions, the lignin composition appears similar in the xylem and single fibers.

Hemp belongs to the Angiosperm phylum since it has vessel elements. It is eudicotyledon like hardwoods, numerous bushes and herbs, since it has two cotyledons (germinating leaves). Thus it contains hardwood lignin of coniferyl alcohol, sinapyl alcohol and a minor content of *p*-coumaryl alcohol. The first lignification step occurs in the compound middle lamellae, which has the same high lignin content in thick-walled and thin walled fibers (Figure 6). The second lignification step occurs during the synthesis of the outer part of the S2 layer. The lignin synthesis appears reduced in later stages of fiber development due to the low lignin content in the inner part of the S2 layer.

Table 1. Chemical composition of the structure on hemp stem level and single fiber level based on qualitative evaluation (Content: +++ = high, ++ = medium, + = low and 0 = none).

Stem level *Cell part*	Epidermis	Parenchyma cells	Single fibers		
			ML+P	*S1 + outer S2*	*Inner S2*
Cellulose	+	0	+	++	+++
Lignin	0	0	+++	++	+
Pectin	++	+++	++	0	0
Wax	++	0	+	0	0

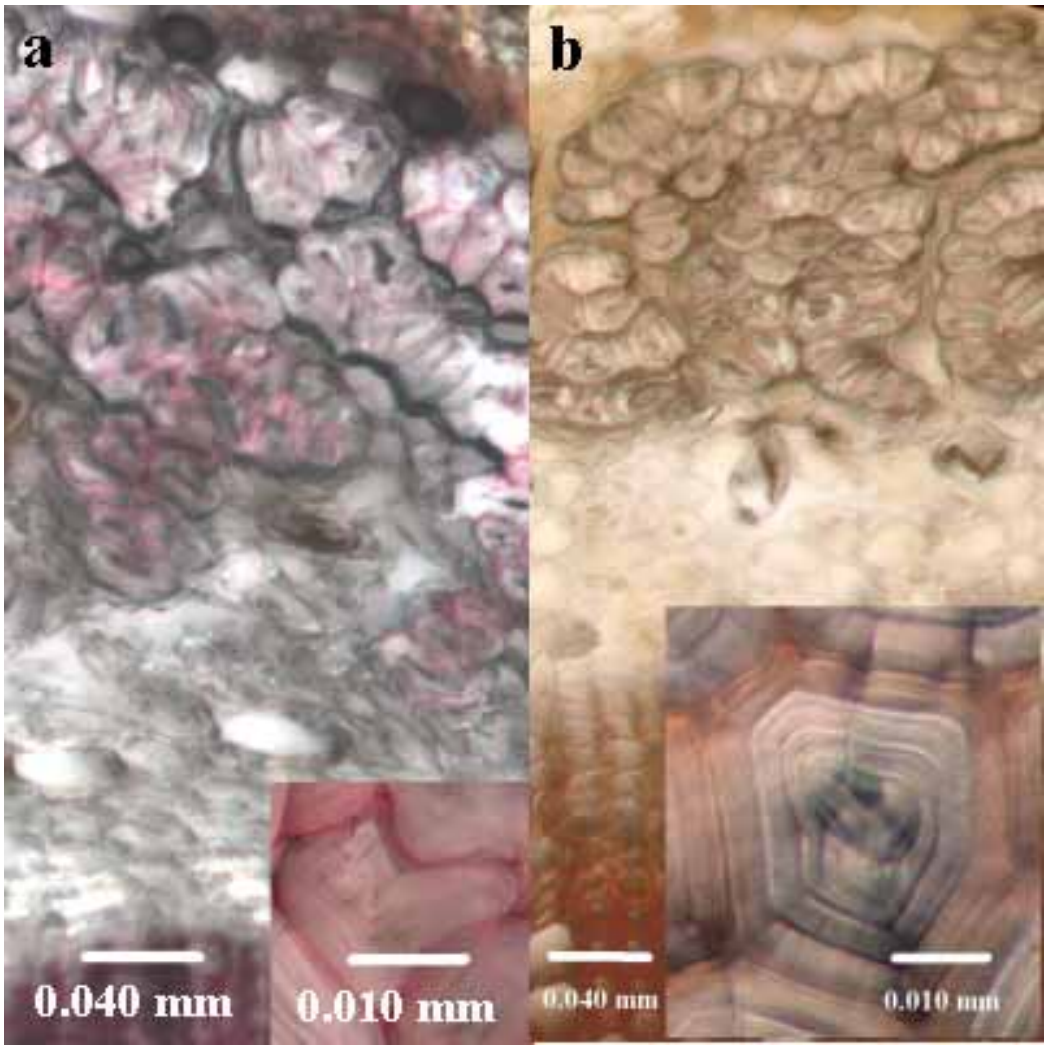

Figure 6. Lignin shown as red colour in transverse sections of hemp stem after the Wiesner reaction (A) and the Mäule reaction (B) (arrows = strongly lignified part of the cell wall).

Pectin was stained with Ruthenium Red by reaction with carboxylic acid side groups (Table 1, Figure 7A). Both the parenchyma cells and the single fiber compound middle lamellae contained pectin, while the secondary wall appeared to lack pectin. Wax was found in the epidermis with highest content in the cuticle layer according to the hydrophobic red staining with Sudan IV (Figure 7B).

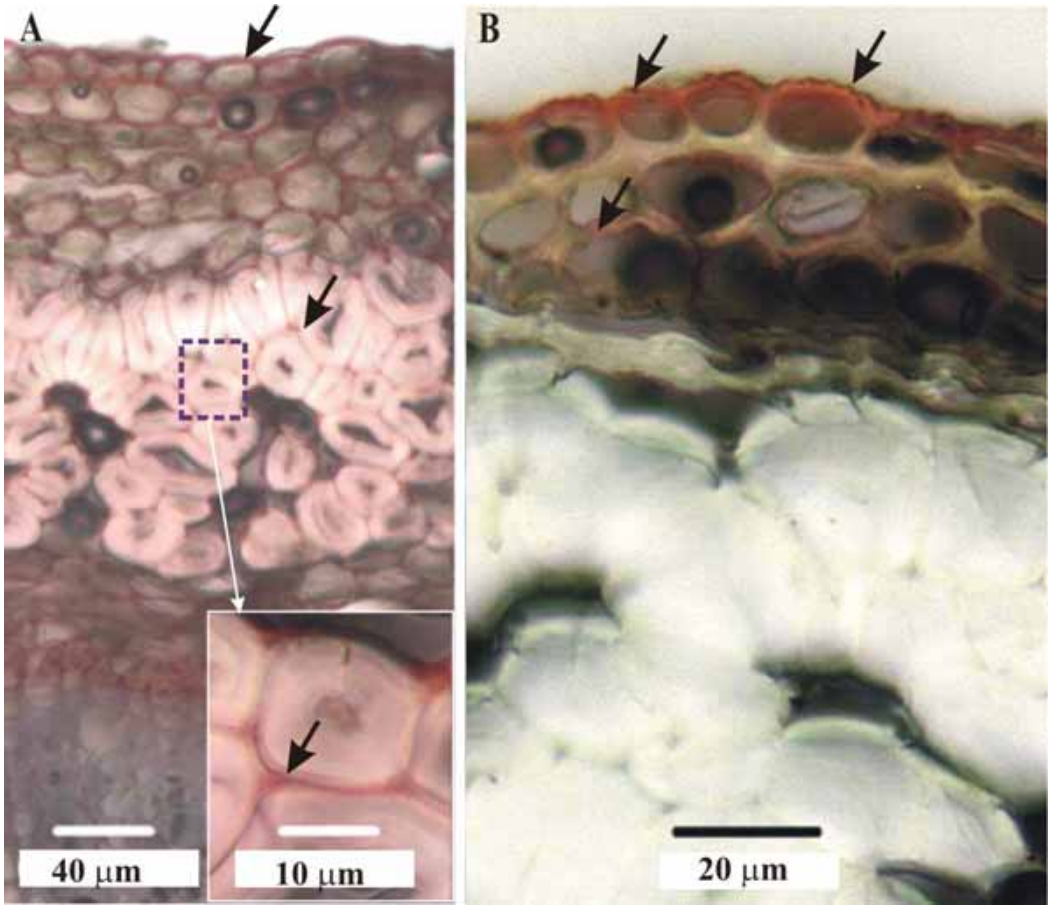

Figure 7. Pectin and wax stained in transverse sections of hemp stem. A: Pectin stained by Ruthenium Red (arrows = pectin rich compound middle lamellae). B: Wax stained by Sudan IV (arrows = wax rich cuticle layer).

Structure of the single fibers determined with fungal defibration and decay

Lignin slows down degradation by soft rot fungi like *P. mutabilis* in wood fibers and the middle lamella and the primary wall normally remain morphologically intact even after severe degradation of the S2 layer (Khalili et al., 2000). In single fibers of hemp, this fungus formed cavities that were restricted to individual layers in the polylaminate S2 layer. The middle lamella and primary wall were degraded slower than S2 due to the higher lignin content (Figure 3A). The partial degradation of middle lamellae was presumably due to its high pectin content. The cavities increased in diameter through cellulose but were inhibited – at least partially – by the thin concentric lamellae acting as a chemical and/or physical barrier. *P. radiata* Cel 26 degraded the middle lamellae between the single fibers and only middle lamellae cell corners remained after advanced stages of decay (Figure 3C). In combination with the chemical analysis (Table 2), this gives evidence for degradation of lignin, which *P. radiata* carries out by oxidation using peroxidases (e. g. Mn- and lignin peroxidases; Hofrichter et al., 2001). The thin layers between the thick concentric layers in S2 appear to lack cellulose since they were selectively removed by *P. radiata* Cel 26 (Figure 3C). Evidence for a different chemical composition in the thin layers was also obtained with *P. radiata* wild, which were more rapidly attacked (Figure 3, inset) in comparison with the thicker concentric layers.

Table 2. Tensile strength (σ) and elastic modulus (E) of hemp fibres tested in bundles and in epoxy-composites (Thygesen et al., unpublished) and the chemical composition of the hemp fibres with or without the P. radiata *Cel 26 defibration.*

Fibre source	Fibre bundle tests		Composite tests		
Mechanical properties	σ (MPa)	E (GPa)	σ (MPa)		E (GPa)
Raw hemp	960±220	23±5	450±120		72±12
Treated hemp, liquid culture	850±240	20±3	590±90		90±17
Chemical composition (% w/w)	Cellulose	Hemicellulose	Lignin	Pectin	Rest
Raw hemp	64	15	4	6	11
Treated hemp, liquid culture	77	15	2	1	5
Treated hemp, soil culture	76	15	2	3	6

The potential of hemp fibers as reinforcing agents in composite materials

The histochemical investigation showed that pectin degradation can provide separation of the fiber bundles from the xylem, but separation of the fiber bundles into single fibers requires lignin degradation (Table 1). Hemicellulose degradation should be avoided to prevent disintegration of the fibers into microfibrils resulting in lower fiber bundle strength (Morvan et al., 1990). Practically no change occurred in the hemicellulose content during the *P. radiata* Cel 26 treatment (Table 2). Epidermis free and cellulose rich (77 % w/w) hemp fiber bundles were produced on the 100 g scale by the *P. radiata* Cel 26 treatment. This could not be done by enzymatic treatment with Flaxzyme (Thygesen et al., 2002) since enzymes presumably cannot penetrate the wax-covered epidermis.

The single fibers were completely penetrated by the low viscosity acrylic resin used as embedding material for TEM microscopy even though the fibers were arranged in bundles. Bundle arrangement of fibers with small lumina has also been reported for jute (Cichocki & Thomason, 2002). Since penetration of the epoxy polymer was complete in composites made with jute fibers, the same should be possible using hemp fibers.

The elastic modulus of 25 GPa has previously been measured in single hemp fibers (Madsen et al., 2003). On fiber bundle level, the *P. radiata* Cel 26 treatment resulted in decreases in stiffness from 23 GPa to 20 GPa and in tensile strength from 960 MPa to 850 MPa caused by extraction of most of the non-cellulosic binding materials (Table 2). Based on the microfibril angle, the cell wall stiffness is lowest in the S1 layer and highest in the inner 70-90 % of the S2 layer (Figure 1B; Davies and Bruce, 1997). Cracks between the concentric layers (Figure 4A, B) observed in the fractured fibers were presumably formed by interlaminar stress.

Composites have been made with hemp fibers from stems treated with *P. radiata* Cel 26. Fiber strength and stiffness of 590 MPa and 90 GPa, respectively, were calculated based on the composition of these composites (Thygesen et al., unpublished; Table 2). The same properties of composites with fibers from untreated hemp were only 450 MPa and 72 GPa due to a poor binding between the hemp bast fibers and the epoxy resin caused by the wax rich cuticle layer. The higher fiber stiffness in composites gives evidence for polymer penetration into the fibers like that reported for flax (Hepworth et al., 2000), which glues the cell wall aggregates together and forms a stiff structure. This compensates for the loss of stiffness and tensile strength induced by degradation of non cellulosic components (Table 2). The obtained fiber stiffness and strength were thereby 25-32 % higher, when the treated fibers were used.

CONCLUSION

- Hemp stems could be defibrated with *P. radiata* Cel 26 on at least the 100 g scale to make fibers, since the pectin and wax rich epidermis was degraded.
- The fibers retained parallel orientation and are thus useful for unidirectional composites.
- Lignin located in the middle lamellae between the single fibers made defibration with pectinase enzymes difficult without simultaneous oxidation of lignin as performed by *P. radiata* Cel 26.
- Fibers defibrated using *P. radiata* Cel 26 were stiffer than untreated fibers in epoxy composites, since the cell wall aggregates were glued together to form a stiff structure.

REFERENCE LIST

Browning, B. L. (1967). *Methods of wood chemistry.* New York: Interscience Publishers, A division of John Wiley & Sons.

Cichocki, F. R., & Thomason, J. L. (2002). Thermoelastic anisotropy of a natural fiber. *Composites Science and Technology*, 62, 669-678.

Daniel, G., & Nilsson, T. (1994). Polylaminate concentric cell wall layering in fibres of *Homalium foetidum* and its effect on degradation by microfungi. In Donaldson LA, Davies, G. C., & Bruce, D. M. (1997). A stress analysis model for composite coaxial cylinders. *Journal of Materials Science*, 32, 5425-5437.

Fink, H. P., Walenta, E., & Kunze, J. (1999). The structure of natural cellulosic fibres - Part 2. The supermolecular structure of bast fibres and their changes by mercerization as revealed by X-ray diffraction and C-13-NMR-spectroscopy. *Papier*, 53, 534-542.

Garcia-Jaldon, C., Dupeyre., D., & Vignon, M. R. (1998). Fibres from semi-retted hemp bundles by steam explosion treatment. *Biomass & Bioenergy*, 14, 251-260.

Hepworth, D. G., Vincent, J. F. V., Jeronimidis, G., & Bruce, D. M. (2000). The penetration of epoxy resin into plant fibre cell walls increases the stiffness of plant fibre composites. *Composites Part A-Applied Science and Manufacturing*, 31, 599-601.

Hofrichter, M., Lundell, T., & Hatakka, A. (2001). Conversion of milled pine wood by manganese peroxidase from *Phlebia radiata*. *Applied Environmental Microbiology*, 67, 4588-4593.

Jensen, W. (1962). *Botanical histochemistry, principles and practice.* San Francisco: WH Freeman and Co.

Khalili, S., Daniel, G., & Nilsson, T. (2000). Use of soft rot fungi for studies on the microstructure of kapok (*Ceiba pentandra* (L.) Gaertn.) fibre cell walls. *Holzforschung*, 54, 229-233.

Khalili, S., Nilsson, T., & Daniel, G. (2001). The use of soft rot fungi for determining the microfibrillar orientation in the S2 layer of pine tracheids. *Holz Als Roh-und Werkstoff*, 58, 439-447.

Madsen, F. T., Burgert, I., Jungnikl, K., Felby, C., & Thomsen, A. B. (2003). Effect of enzyme treatment and steam explosion on tensile properties of single hemp fiber. In 12th International Symposium on Wood and Pulping Chemistry *(ISWPC)* (P80). Madison.

Madsen, B., & Lilholt, H. (2003). Physical and mechanical properties of unidirectional plant fibre composites - an evaluation of the influence of porosity. *Composites Science and Technology*, 63, 1265-1272.

Mcdougall, G. J., Morrison, I. M., Stewart, D., Weyers, J. D. B., & Hillman, J. R. (1993). Plant fibers - botany, chemistry and processing for industrial use. *Journal of the Science of Food and Agriculture*, 62, 1-20.

Morvan, C., Jauneau, A., Flaman, A., Millet, J., & Demarty, M. (1990). Degradation of flax polysaccharides with purified endo-polygalacturonase. *Carbohydrate Polymers*, 13, 149-163.

Mukherjee, P. S., & Satyanarayana, K. G. (1986). An empirical-evaluation of structure property relationships in natural fibers and their fracture-behavior. *Journal of Materials Science*, 21, 4162-4168.

Mwaikambo, L. Y., & Ansell, M. P. (2003). Hemp fibre reinforced cashew nut shell liquid composites. *Composites Science and Technology*, 63, 1297-1305.

Nyhlen, L., & Nilsson, T. (1987). Combined T.E.M. and UV-microscopy on delignification of pine wood by *Phlebia radiata* and four other white rotters. In Odier E, editors. *Proc. of lignin enzymic and microbial degradation symposium.* INRA Publications, p 277-282.

Page, D. H., & Elhosseiny, F. (1983). The mechanical properties of single wood pulp fibers. 6. Fibril angle and the shape of the stress-strain curve. *Pulp & Paper-Canada*, 84, TR99-T100.

Purz, H. J., Fink, H. P., & Graf, H. (1998). Zur Struktur Cellulosischer Naturfasern. *Das Papier*, 6, 315-324.

Strivastava, L. (1966). Histochemical studies on lignin. *Tappi*, 49, 173-183.

Thygesen, A., Lilholt, H., Daniel, G., & Thomsen, A. B. Composites based on fungal retted hemp fibres and epoxy resin. *unpublished*.

Thygesen, A., Madsen, F. T., Lilholt, H., Felby, C., & Thomsen, A. B. (2002). Changes in chemical composition, degree of crystallisation and polymerisation of cellulose in hemp fibres caused by pre-treatment. In Lilholt, H., Madsen, B., Toftegaard, H., Cendre, E., Megnis, M., Mikkelsen, L. P., & Sørensen, B. F., editors. Proceedings of the 23th Risø International Symposium on Materials Science: *Sustainable natural and polymeric composites - science and technology.* Denmark: Risø National Laboratory, p 315-323.

Wu, J., Fukazawa, K., & Ohtani, J. (1992). Distribution of syringyl and guaiacyl lignins in hardwoods in relation to habitat and porosity form in wood. *Holzforschung*, 46, 181-185.

Paper III

On the determination of crystallinity and cellulose content in plant fibres

Cellulose 12 pp. 563-576.

Cellulose (2005) 12:563–576
DOI 10.1007/s10570-005-9001-8

On the determination of crystallinity and cellulose content in plant fibres

Anders Thygesen[1,2,*], Jette Oddershede[3], Hans Lilholt[1], Anne Belinda Thomsen[4] and Kenny Ståhl[3]
[1]*Materials Research Department, Risø National Laboratory, P.O. Box 49, DK-4000, Roskilde, Denmark;* [2]*Danish Centre for Forest, Landscape and Planning, The Royal Veterinary and Agricultural University, Højbakkegård Allé 1, DK-2630, Tåstrup, Denmark;* [3]*Department of Chemistry, Technical University of Denmark, Building 207, DK-2800, Lyngby, Denmark;* [4]*Biosystems Department, Risø National Laboratory, P.O. Box 49, DK-4000, Roskilde, Denmark; *Author for correspondence (e-mail: anders.thygesen@risoe.dk; fax: +45-4677-5758)*

Received 4 January 2005; accepted in revised form 17 June 2005

Key words: Cellulose, Crystallinity, Debye, Plant fibres, Rietveld, X-ray

Abstract

A comparative study of cellulose crystallinity based on the sample crystallinity and the cellulose content in plant fibres was performed for samples of different origin. Strong acid hydrolysis was found superior to agricultural fibre analysis and comprehensive plant fibre analysis for a consistent determination of the cellulose content. Crystallinity determinations were based on X-ray powder diffraction methods using side-loaded samples in reflection (Bragg-Brentano) mode. Rietveld refinements based on the recently published crystal structure of cellulose Iβ followed by integration of the crystalline and amorphous (background) parts were performed. This was shown to be straightforward to use and in many ways advantageous to traditional crystallinity determinations using the Segal or the Ruland–Vonk methods. The determined cellulose crystallinities were 90–100 g/100 g cellulose in plant-based fibres and 60–70 g/100 g cellulose in wood based fibres. These findings are significant in relation to strong fibre composites and bio-ethanol production.

Abbreviations: HPLC – High pressure liquid chromatography; DM – Dry matter

Introduction

Cellulose is technically a very interesting material. Plant fibres, as for instance hemp fibres, have high strength, low density and high sustainability, which can supplement glass fibres in composites (Hepworth et al. 2000; Madsen and Lilholt 2003). It has been shown empirically that the fibre tensile strength and elastic modulus depend on the cellulose content squared (Klinke et al. 2001). Due to the expected correlation between the tensile strength of the fibres and the cellulose crystallinity, it is of interest to find effective and reliable methods to determine the sample crystallinity of cellulose containing materials at different stages of processing. Plant fibre waste materials like corn stover and wheat straw have not proved useful for high performance composite materials due to their low cellulose content and bigger cell lumen resulting in low tensile strength. However, these

materials are useful for bioethanol production after pre-treatment and enzymatic hydrolysis of the cellulose and hemicellulose to monosaccharides (Felby et al. 2003; Varga et al. 2004). The enzymatic hydrolysis for converting cellulose to glucose substrate is mainly performed with exoglucanase for crystalline cellulose and endoglucanase for amorphous cellulose. Hence, it is valuable to know the amount of crystalline cellulose and amorphous cellulose, in the sample to develop enzyme mixtures optimized for the hydrolysis (Teeri and Koivula 1995; Thygesen et al. 2003).

Plant fibres are built essentially of cellulose, hemicellulose, lignin, pectin and minerals. Cellulose consists of both amorphous and crystalline regions. To determine the cellulose crystallinity in plant fibres, accurate determination of the cellulose content is needed, as cellulose is expected to be the only crystalline constituent. Cellulose consists of linear chains of poly[β-1,4-D-anhydroglucopyranose] ($C_{6n}H_{10n+2}O_{5n+1}$ (n = degree of polymerisation of glucose)), which crystallize through hydrogen bonding between the chains and has cellobiose as repeated unit (Figure 1a). The crystal structure of cellulose in higher plants is that of cellulose Iβ (Sarko and Muggli 1974; Nishiyama et al. 2002), which is monoclinic, space group $P2_1$, with the cellulose chains arranged along the unique c-axis (Figure 1b).

X-ray powder diffraction is an obvious method to study the sample crystallinity due to the diffraction peaks from cellulose crystals (Figure 2). However, all materials give rise to X-ray scattering, also the amorphous part of a sample. It is measured that hemicellulose and lignin have diffractograms similar to amorphous cellulose giving wide unspecific peaks (unpublished data). The

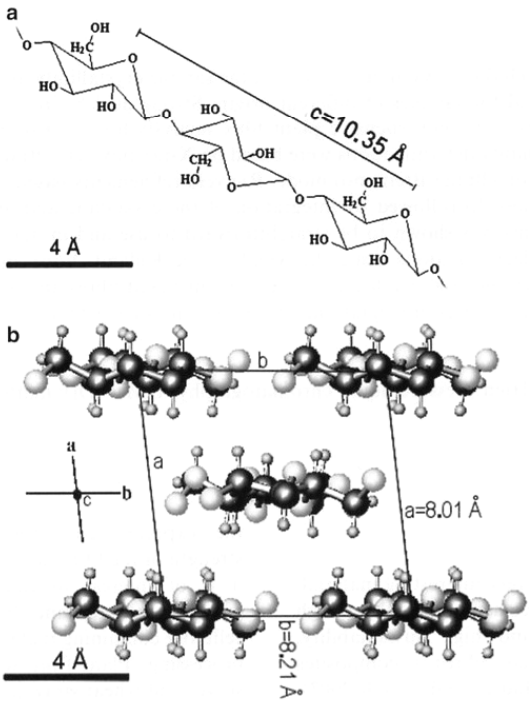

Figure 1. (a) The repeated cellobiose unit in cellulose as compared to the c-axis length. (b) The cellulose Iβ structure viewed along the unique c-axis of the $P2_1$ unit cell with the a- and b-axis in the paper plane (5 molecule chain ends are thereby shown).

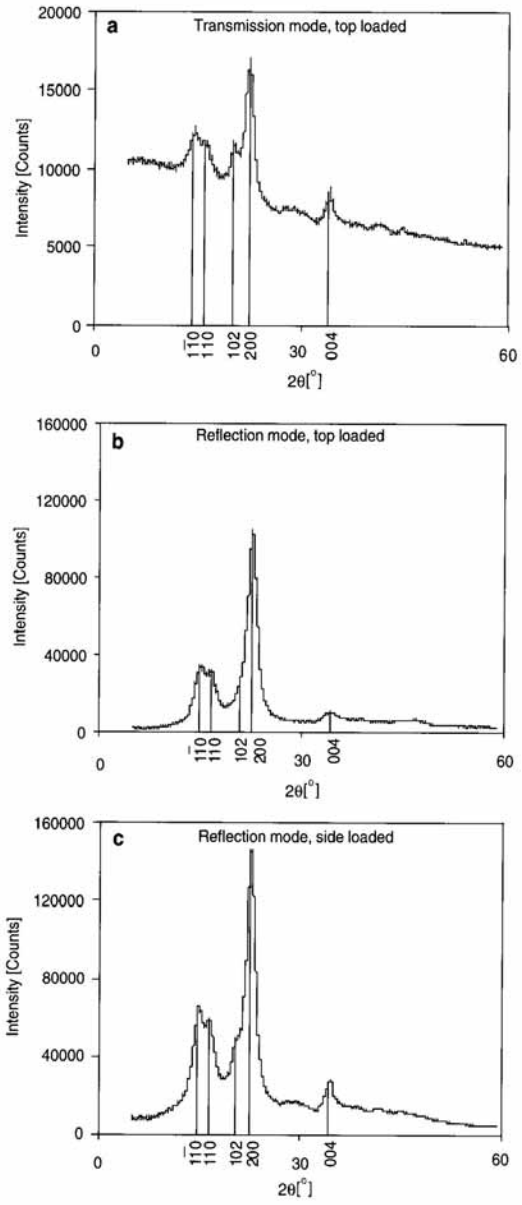

Figure 2. Diffractograms of filter paper measured in transmission mode (a) and reflection mode (b & c) to investigate the effect of diffraction geometry. Both top loaded (b) and side-loaded (c) paper samples are measured to see the effects of sample preparation and preferred orientation.

amorphous scattering will show up as a softly rising and decreasing background. Determination of the sample crystallinity is thus a problem of separating the amorphous from the pure crystalline part of a powder diffraction pattern. With well-crystallized samples, i.e. with large enough crystallites, this is rather simple as such crystallites give sharp diffraction peaks, which can be easily separated from the amorphous background. In the case of cellulose, the crystallites are very small, typically 20–50 Å in diameter, which will cause considerable peak broadening and serious peak overlap. Consequently, the separation of crystalline from amorphous scattering is no longer trivial. The crystallite diameter can be determined with X-ray diffraction based on the width of peaks representing directions perpendicular to the fibre axis (indices: 110, $1\bar{1}0$ and 200), while the crystallite length can be determined based on the width of peaks representing directions parallel with the fibre axis (index: 004) (Figure 2).

The scope of this paper is twofold. Firstly, we want to compare four different methods to assess the crystalline part of a cellulose diffraction pattern in order to determine the sample crystallinity: (1) Segal method, based on the intensity measured at two points in the diffractogram (Segal et al. 1959); (2) Ruland–Vonk method, based on a separate measurement of an amorphous standard scaled to the diffraction pattern (Ruland 1961; Vonk 1973); (3) Rietveld refinement method, based on refinements of the crystal structure, peak parameters and background (Rietveld 1967, 1969); and (4) Debye calculation method, where the crystalline scattering is calculated based on the crystal structure and crystallite size (Debye 1915). Secondly, we want to determine the cellulose content in plant fibres. For this purpose an accurate plant fibre analysis procedure is needed. The three most well known methods were compared: (1) Comprehensive plant fibre analysis (Browning 1967), (2) Agricultural fibre analysis (Goering and Van Soest 1970), and (3) Strong acid hydrolysis (Kaar et al. 1991). The samples used in the present study were purified cellulose (filter paper and Avicel cellulose), hemp fibres, Norway spruce and corn stover, which were chosen to cover a wide range of cellulose contents and biomass types. The samples were used without prior cellulose purification in the X-ray diffraction experiments to avoid modification of the cellulose structure.

Experimental

Materials

Organosolv lignin, (Aldrich 37, 101–7) was used as amorphous reference material. *Filter paper* (Frisenette ApS 165–70) and microcrystalline *Avicel cellulose* (Merck 2351) were used as purified cellulose materials. *Hemp fibres* (*Cannabis sativa* L., *Felina*) were hand peeled from the middle section of hemp stems (Thygesen et al., submitted). *Norway spruce* (*Picae abies*) was obtained from Ølstykke sawmill, Denmark, as a fresh, chipped and bark free material. The wood chips were dried at 20 °C for 7 days and ground with a hammer mill to 5 mm size. *Corn stover* from maize plants (*Zea Mays* L.) grown in Hungary in 2003 was recuperated following threshing in the combine harvester at grain harvest.

Chemical analysis

Before the plant fibre analyses, the samples were milled into particles that could pass a 1 mm sieve. The mineral content was determined by incineration of the raw samples at 550 °C for 3 h. *Comprehensive plant fibre analysis* is a gravimetric method used for fibres from agricultural plants and wood. Wax was extracted in chloroform, water-soluble components in water, pectin in EDTA solution, lignin in chlorite solution and hemicellulose in $NaOH + NaBO_3$ solution with weighing in between each step (Browning 1967). *Agricultural fibre analysis* is a gravimetric method used for analysis of agricultural lignocelluloses (Goering and Van Soest 1970). Non cell wall material (mainly pectin) is extracted in natrium-auryl-sulphate + EDTA + natrium-tetraborate + Na_2HPO_4 + ethylenglukolmonoethylether solution, hemicellulose in 0.5 M H_2SO_4 + cetyltrimethyl-ammonium-bromide solution and lignin in $KMnO_4 + Ag_2SO_4 + Fe(NO_3)_3 + AgNO_3 + KCH_3COO + CH_3COOH$ + butyl alcohol solution followed by filtration and treatment in oxalic acid + 70% ethanol. The amount of remaining solid material was weighed in between each step. *Strong acid hydrolysis* is an HPLC based method, in which the content of sugars in the fibres was measured after sample preparation by swelling in 12 M H_2SO_4 and following hydrolysis at dilute

H_2SO_4 (0.42 M) at 121 °C for 1 h (Kaar et al. 1991). The excess SO_4^{2-} was removed by $Ba(OH)_2$ addition. Shimadzu equipment was used in the HPLC-analysis. The column system used for woody samples consisted of a Rezex RPM column, a deashing cartridge and a security guard (Pb^{2+}) pre-column. The temperature was 80 °C, the eluent was H_2O and the flow rate was 0.6 ml/min. Glucose, xylose, galactose and mannose were detected refractometrically. The column system used for non-woody samples consisted of a Rezex ROA column and a security guard (H^+) pre-column. The temperature was 63 °C, the eluent was 4 mM H_2SO_4 and the flow rate was 0.6 ml/min. Glucose, xylose and arabinose were detected refractometrically.

X-ray powder diffraction

X-ray powder diffraction experiments were performed for sheets of filter paper in both transmission and reflection geometry to determine the best experimental mode. The transmission experiment was performed with a Huber G670 Guinier camera using CuKα_1 radiation. The thin samples were placed at a 45 ° angle to the primary beam and rocked during data accumulation. The data was collected for 30 h and in the 2θ-range 1.4–100 ° with a step size of 0.005°. For the reflection geometry measurements a Philips PW1820/3711 diffractometer with a symmetric θ-2θ Bragg-Brentano scattering geometry, CuKα radiation, a secondary graphite monochromator and an automatic divergence slit was employed. Data were collected in the 2θ-range 5–60° with a step size of 0.02° and a counting time of 20 s per step. The reflection mode intensities were corrected for the effects of the automatic divergence slit. No 2θ-dependent absorption correction is necessary for the symmetric Bragg-Brentano mode with the low-absorbing samples used in this study.

From the resulting diffractogram (Figure 2a) it was clear that the large air scattering contribution to the background of the transmission mode data made it very difficult to estimate the fraction of intensity originating from amorphous components in the sample. This effect was practically absent for the reflection mode diffractograms. Air scattering contributions along with Compton scattering comprise only a few percent of the continuously varying background, so no corrections for these effects were judged necessary. Thermal diffuse scattering (TDS) will contribute both to the continuous background and to the peak intensity and thereby to a large part cancel. However, it should be noted that the presence of uncorrected none-sample contributions to the background to some extent will result in reduced crystallinity values. On the other hand, the reflection mode diffractogram (Figure 2b) was greatly affected by preferred orientation, because the paper sheets consisted mainly of fibres in the lateral plane, giving too weak 00*l* peaks relative to the 110, $1\bar{1}0$ and 200 peaks. When loading fibrous samples into the sample holder from the top and flattening the X-ray illuminated surface, this effect is much enhanced. This effect could be reduced by cutting the sample into small pieces in a knife mill with a 0.5 mm sieve, wetting 0.5 g sample with distilled water, loading it into a sample holder from the side with respect to X-ray illuminated surface, and letting the 2 mm thick fibre sheet air dry overnight before the reflection mode diffractogram (Figure 2c) was recorded. To minimize preferred orientation and air scattering effects, it was therefore decided to perform all X-ray powder diffraction experiments in reflection mode on such side loaded samples. In addition, the number of counts was higher in the reflection diffractograms, which decreased the statistical uncertainty. Each sample was prepared and measured twice. The fibre sheets were dried at 105 °C after the X-ray diffraction experiments in order to determine the sample crystallinity based on the dry matter content.

Determination of the sample crystallinty

The sample crystallinity (g crystalline cellulose/100 g DM) is defined as the ratio of the amount of crystalline cellulose (cellulose Iβ) to the total amount of sample material (dry matter = DM), including crystalline and amorphous cellulose, lignin, hemicellulose, pectin, etc. The cellulose crystallinity is defined as 'g crystalline cellulose/100 g cellulose', and can be calculated as the ratio of the sample crystallinity to the cellulose content of the sample.

$$\text{Cellulose crystallinity} = \frac{\text{g crystalline cellulose}}{\text{g cellulose}} = \frac{\text{g crystalline cellulose/g DM}}{\text{g cellulose/g DM}} \quad (1)$$

Method 1: the Segal method

The sample crystallinity, x_{CR}, has frequently been determined by means of Equation 2 using the height of the 200 peak (I_{200}, $2\theta = 22.7°$) and the minimum between the 200 and 110 peaks (I_{AM}, $2\theta = 18°$) (Figure 3a). I_{200} represents both crystalline and amorphous material while I_{AM} represents amorphous material only.

$$x_{CR} = \frac{I_{200} - I_{AM}}{I_{200}} \quad (2)$$

The expression requires that the amorphous material diffracts with the same intensity at 18° and 22.7°, and that the crystalline cellulose does not contribute to the intensity at 18° (Segal et al. 1959).

Method 2: the Ruland–Vonk method

A way to separate the amorphous and crystalline contributions to the diffracted intensity and estimate the sample crystallinity has been outlined by Ruland (1961) and Vonk (1973). Here, it was assumed that the Bragg peaks are sharp, i.e. the crystallites are large enough for the intensity between the diffraction peaks to be negligible. The amorphous part of the intensity was obtained by measuring the scattering of the compound on amorphous form. This amorphous diffractogram was then scaled by a factor $c(s)$, where $s = 2 \sin\theta/\lambda$, to bring it below the diffractogram of the partly crystalline compound. The scale factor $c(s)$ was allowed to vary continuously throughout the s-interval to meet the requirement that the crystalline diffraction intensity should be zero between some of the diffraction peaks (the diffractograms touch at several points).

In the present work, lignin was chosen as the amorphous standard (c.f. Andersson et al. 2003). Because of the small crystallite sizes, the tails of the diffraction peaks extended far from the peak positions as illustrated in Figure 3a. This had the

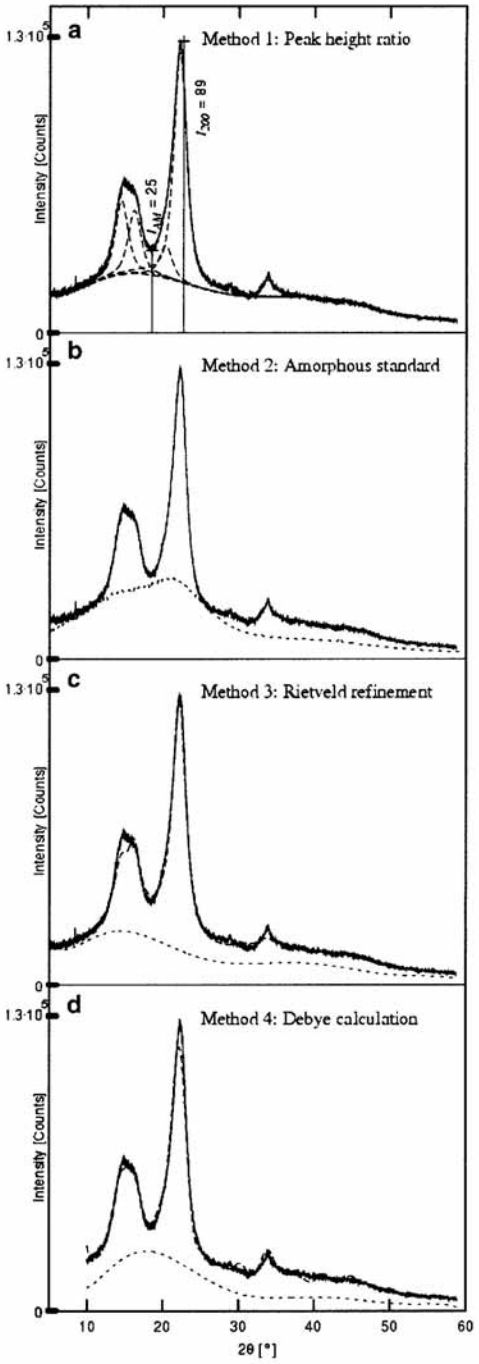

Figure 3. Determination of the crystalline cellulose contents in the hemp fibres measured with the Segal method (a), the Ruland-Vonk method (b), Rietveld refinement (c) and Debye calculation (d). For b, c and d the obtained fits for the amorphous and crystalline diffraction are shown.

effect that the actual background level was well below the diffraction curve of the partly crystalline cellulose sample for practically all scattering angles. The use of a continuously varying scale factor seemed incorrect in the light of Figure 3a, so in this study, it was chosen to use a constant scale factor c to make the background touch the diffractogram in one point/interval only (Figure 3b). Assuming that the intensity $I(s)$ at a given angle is the sum of the crystalline $I_{CR}(s)$ and amorphous $I_{AM}(s)$ contributions, the sample crystallinity was calculated from:

$$x_{CR} = \int_{s_0}^{s_p} I_{CR}(s) \cdot s^2 ds \Big/ \int_{s_0}^{s_p} I(s) \cdot s^2 ds \qquad (3)$$

The integration limits were in this work chosen so only the part of the diffractogram containing visible crystalline intensity was used, i.e. $s_0 = 0.11$ Å^{-1} ($2\theta = 10°$) and $s_p = 0.99$ Å^{-1} ($2\theta = 50°$).

Method 3: Rietveld refinement

The Rietveld method (Rietveld 1967, 1969) uses the full diffraction pattern in a least-squares fitting procedure to simultaneously fit unit cell, crystal structure, peak profile parameters, background, etc. The method requires knowledge of the crystal structure (unit cell, space group and atomic coordinates) as starting parameters. It is today the dominant method for obtaining structural information from powder diffraction data (Young 1993).

Refinements were performed with a modified LHMP1 Rietveld program (Howard and Hill 1986) with the cellulose Iβ crystal structure including thermal parameters from Nishiyama et al. (2002) as input. The best fit for all samples was obtained by refining one scale factor, 10 Chebyshev background parameters, 2 Voigt peak profile parameters, 2 cell dimensions (a and b) and one preferred orientation parameter along the $0k0$-direction (Figure 3c), giving a total of 17 refined parameters for all samples. The full-width half maximum parameters were fixed to values corresponding to those from a LaB_6 standard. The use of a Voigt profile function made it possible to estimate the crystallite dimensions relative to a given direction (here the fibre direction $00l$), but, because of the preferred orientation effects and the minimal size of the crystallites the estimates became quite poor, especially along the fibre direction. Finally the sample crystallinity was calculated using Equation 3 as outlined in Method 2, assuming that the fitted background comprised the amorphous contribution to the diffractogram.

Correct cell parameters of cellulose Iβ are essential to a proper fit. Both the Rietveld refinements of the present study and former studies of the cellulose Iβ crystal structure (Sarko and Muggli 1974; Woodcock and Sarko 1980; Simon et al. 1988; Sugiyama et al. 1991; Koyama et al. 1997; Finkenstadt and Millane 1998; Nishiyama et al. 2002) indicated large variations in the apparent unit cell dimension. It is clear that the true unit cell dimensions of cellulose Iβ are constant at constant temperature. The observed unit cell dimensions, however, are sensitive to the type of radiation (X-rays/neutrons/electrons), method (powder/fibre diffraction) and preparation method. In particular, the recorded 2θ-values depend on the actual penetration depth of the radiation, which directly affect the calculated/refined unit cell dimensions and strongly correlate to the 2θ zero-shift. Due to remaining preferred orientation effects, reflections unique to the c-direction were still severely suppressed. In fact, the cellulose diffraction patterns contained only three strong diffraction peaks, all of which have $l = 0$ (Figure 2). Several combinations of refined parameters were tried with the different samples with the objective to obtain the best possible fit of the crystalline diffraction. The final choice was to refine the a- and b-axis parameters and the preferred orientation parameter. The 2θ zero-shift was fixed to zero, the c-axis parameter to 10.35 Å and the gamma angle to 96.5°, which are average values given in the literature (Figure 1).

Method 4: Debye calculations

The basis of this method is the Debye formula (Debye 1915), which states that the diffracted intensity from a collection of atoms can be calculated as the sum over all interatomic distances r_{ij}:

$$I(s) = \sum_{i,j} f_i(s) f_j(s) \frac{\sin(2\pi s \cdot r_{ij})}{2\pi s \cdot r_{ij}} \qquad (4)$$

where s is defined as before and $f_i(s)$ is the atomic form factor of atom i. Thus, the method

requires a full set of atomic positions for a whole crystal, not just for one unit cell. Consequently, the effects from crystallite size and shape were inherent to the calculated diffractograms. A program was written to calculate the diffractograms for cellulose Iβ crystallites of different shapes and sizes exploiting the structural parameters including thermal parameters of Nishiyama et al. (2002). Both elliptical, cylindrical and box shaped crystallites, each consisting of an assembly of entire unit cells, were tested. The best correspondence to the experimental peak profiles was obtained if the diffractograms were simulated for crystallites of cylindrical shape with the cylinder axis along the fibre direction. To obtain a size distribution, the diffractogram was added to the intensities simulated for cylinders with radii of ± 1 Å. The simulated diffractograms were then fitted to the experimentally obtained patterns by means of a scale factor and a continuously varying background consisting of a 9th order Chebyshev polynomial (Figure 3d).

As with Rietveld refinements it was essential to use correct unit cell dimensions. Therefore, a number of simulations varying *a* and *b* simultaneously in steps of 0.05 Å were carried out. These diffractograms were fitted to the experimentally obtained diffractograms to determine the *a* and *b* parameters that best fitted the given sample. The length of the *c*-axis was fixed to 10.35 Å as argued for the Rietveld refinements (Figure 1). The crystallite size was identified from comparisons to simulated diffractograms with known crystallite dimensions, and the sample crystallinity was determined from the fitted background level using Equation 3 as outlined under Method 2.

Results

Chemical composition

The results of the chemical composition are presented in Table 1. The method that offered the best distinction between cellulose and hemicellulose, and thereby the best determination of these components, was the strong acid hydrolysis. The complex carbohydrates, cellulose and hemicellulose were hydrolysed into monomeric sugars, cellulose to glucose and hemicellulose to xylose, arabinose, galactose and mannose, which were subsequently determined by HPLC. Klason lignin is the insoluble residue after the sample preparation with H_2SO_4. The agricultural fibre analysis gave approximately the same cellulose and hemicellulose results with a lower standard deviation (Table 1), but the method is more laboriously demanding and in some cases unspecific. In comparison, the comprehensive plant fibre analysis gave unrealistically high contents of hemicellulose in the purified cellulose samples (filter paper and Avicel cellulose). Obviously, some cellulose was extracted in the hemicellulose extraction step of the comprehensive plant fibre analysis, a solution of NaOH and boric acid, making this step unspecific for hemicellulose. For Avicel cellulose, the reproducibility in this step was further complicated by the relatively small particle size of the Avicel cellulose, which resulted in extended dissolution, swelling and recrystallization of cellulose I into cellulose II (confirmed by X-ray diffraction). However, the first step in the comprehensive plant fibre analysis is recommended also in the strong

Table 1. Chemical composition of the plant materials measured by the three methods (g/100 g dry matter) and arranged according to: Results from comprehensive plant fibre analysis/agricultural fibre analysis/strong acid hydrolysis. The pooled standard deviations are shown for each method and component. Numbers in bold are results from the strong acid hydrolysis.

Material	Cellulose g/100 g	Hemi-cellulose g/100 g	Lignin g/100 g	Pectin g/100 g	Wax g/100 g	Water extractives g/100 g	Residual[a] g/100 g	Minerals g/100 g
Corn stover	33/32/**33**	33/31/**21**	14/6/**19**	1/–/–	3/–/–	10/–/–	–/24/**20**	**7**
Norway spruce	49/58/**49**	30/18/**20**	17/19/**29**	3/–/–		1/–/–	–/5/**2**	**0**
Hemp fibres	64/68/**63**	14/10/**10**	5/3/**6**	5/–/–	0/–/–	8/–/–	–/14/**17**	**4**
Filter paper	86/93/**84**	10/6/**6**	1/0/**0**	2/–/–	0/–/–	1/–/–	–/1/**8**	**0**
Avicel cellulose	–[b]/95/**87**	–[b]/4/**4**	1/0/**0**	1/–/–		1/–/–	–/0/**10**	**0**
Standard deviation	1.4/0.5/3.1	0.7/0.7/2.1	0.5/0.7/0.5	1.0/–/–	0.1/–/–	1.3/–/–	–/0.5/2.8	0.1

[a]Residual from agricultural fibre analysis and strong acid hydrolysis = pectin + wax + water extractives.[b]The swelling of the relatively small particles resulted in partial extraction of cellulose in the hemicellulose extraction step making the separation of these components impossible.

acid hydrolysis for specific extraction of wax, water-soluble components and pectin by ethanol, which is otherwise included in Klason lignin. The gravimetric extraction steps in the comprehensive plant fibre analysis resulted in consistent contents of 0–1 g/100 g dry matter (DM) for pectin, wax and water extractives in the purified cellulose samples, content levels that were within the uncertainty limits. In the other samples, the content of pectin, wax and water extractives were 1–5 g pectin/100 g DM, 0–3 g wax/100 g DM and 1–10 g water extractives/100 g DM (Table 1).

Crystallinity determinations

The results of the crystallinity and the crystallite dimensions are presented in Tables 2 and 3 and shown graphically in Figure 4.

Method 1: The Segal method

The Segal method (Segal et al. 1959) was very straightforward and fast to use, but the sample crystallinity of 47–83 g/100 g DM (Table 2) were found to be higher than the cellulose contents (Table 1) for both corn stover and hemp fibres (Figure 4). There are several reasons for these unrealistic results. Most importantly the cellulose crystallites are so small that peak overlap is bound to occur in the region around 18° for cellulose Iβ, giving too high values of I_{AM} (Figure 3a). The fact that I_{200} was overestimated due to preferred orientation added another element of uncertainty to the system. When comparing diffractograms for cellulose samples originating from different species there is also the effect that both the apparent cell parameters and the crystallite sizes vary considerably from species to species (Table 3). This results in large variations in the I_{AM} levels, making the Segal method very unreliable when comparing sample crystallinities in general. None of these points have been mentioned in the original work by Segal et al. (1959), where the method was used only for differently purified cellulose samples all originating from cotton. Since it is a simple method, it has been extensively utilized up to this day (Alexander 1969; Buschle-Diller and Zeronian 1992; Mwaikambo and Ansell 1999; De Souza et al. 2002), but the mentioned limitations and assumptions make it unreliable and incorrect.

Table 2. Sample crystallinity (g/100 g dry matter) with pooled standard deviations calculated for each X-ray diffraction method.

Material	Peak height ratio segal g/100 g DM	Amorphous standard (Ruland-Vonk) g/100 g DM	Rietveld refinement g/100 g DM	Debye calculation g/100 g DM
Corn stover	47	39	37	32
Norway spruce	47	56	33	32
Hemp fibres	77	49	60	69
Filter paper	83	72	57	61
Avicel cellulose	62	67	41	39
Standard deviation	1.5	1.4	1.6	2.0

Table 3. Crystallite dimensions of the cellulose in the plant materials calculated by Rietveld refinement and Debye calculation (Å). Numbers in parenthesis = standard deviations.

Material	Rietveld refinement		Debye calculation	
	Length[a] [Å]	Diameter [Å]	Length[a] [Å]	Diameter[b] [Å]
Corn stover	36(4)	30(1)	100	22(2)
Norway spruce	60(6)	30(1)	150	34(2)
Hemp fibres	24(2)	43(1)	50	36(2)
Filter paper	62(2)	60(1)	150	52(2)
Avicel cellulose	64(3)	39(1)	100	38(2)

[a]Along 00*l*. [b]Standard deviations arise from the ±1 Å distribution of the crystallite radii used in the simulations.

Method 2: Ruland–Vonk method

The Ruland–Vonk method as applied in the present study has the great advantage that it is a purely experimental approach to the determination of the sample crystallinity, giving values of 39–72 g/100 g DM (Table 2). However, for all the samples studied the scaled amorphous background touched the diffractogram somewhere in the 2θ-interval between 7 and 13°, thus in the low angle region, where the intensity is most poorly determined due to the fine adjustment of slits and the effects of axial divergence (Figure 3b). Therefore, besides the subjective definition of the scale factor, the Ruland–Vonk method is very sensitive to instrumental inaccuracies. It should be added that the amorphous standard material must be chosen so as to resemble the amorphous components in the samples. In the light of these observations the Ruland–Vonk method is difficult to apply to comparative studies of samples of different origin. Despite the problems mentioned above, the Ruland–Vonk method has been widely accepted as one of the best ways to determine the sample crystallinity in plant fibres during more than a decade (Fink and Walenta 1994; Sao et al. 1994, 1997).

Method 3: Rietveld refinement

During the last 30 years, Rietveld refinement has become the dominant method for refining structural information from powder diffraction when a preliminary structural model is known. Until recently such a model was not available for cellulose. However, with the publication of the cellulose Iβ crystal structure (Nishiyama et al. 2002), Rietveld refinement has become a feasible method for obtaining information about crystallite size and sample crystallinity from diffraction data. As soon as a minimum set of parameters has been found, it is straightforward to carry out refinements for a series of diffraction patterns with any of the Rietveld refinement programs available (Figure 3c).

The decision of which parameters to refine was not trivial for cellulose, since severe peak overlap gave very few resolved peaks (Figure 3a). The limited number of resolved peaks restricted the number of refinable parameters and resulted in large correlations between some of these. As already mentioned, the unit cell dimension in the *c*-direction was intimately linked to the preferred orientation. The unit cell lengths along the *a* and the *b* axis correlated strongly with the 2θ zero shift, and were in average fitted to 8.01 Å and 8.21 Å, respectively (Figure 1). Furthermore, the background level was greatly affected by the choice of peak shape function, since the peak tails extended very differently with different peak shape functions. However, bearing these correlations in mind, it was possible to find a common minimum set of refinement parameters suitable to all of the samples. That made the Rietveld refinement method consistent and straightforward to use, giving values of sample crystallinity in the range 33–60 g/100 g DM (Table 2).

Method 4: Debye calculation

As for the Rietveld refinements, the Debye calculation method requires that the cellulose crystal structure is known. While the entire Rietveld refinement procedure was implemented into one refinement program, the Debye calculation method required two different programs, one to simulate the diffractogram and one to fit the simulated diffractogram to the experimental data and determine the quality of the fit (Figure 3d). Every time a parameter such as the cell dimensions, the crystallite size or shape was changed, a new diffractogram had to be calculated by the simulation program and imported into the fitting program. The simulations are usually computationally heavy, scaling as the number of atoms in the crystallites squared. For crystallites as small as those of cellulose (diameter = 22–52 Å; length = 50–150 Å, Table 3) the simulation time was, however, no more than 1 min per diffractogram on a standard PC, so the bottleneck lies more in finding an appropriate set of parameters, systematically varying them and comparing the resulting diffractograms to the experimental diffraction patterns. Nevertheless, the Debye calculation method has one great advantage over the Rietveld refinement approach: The crystallite dimensions are not fitted by analytical peak profile functions but are included explicitly in the simulations. This fact made the Debye calculation method an excellent reference method for sample crystallinity determinations, giving values in the range 32–69 g/100 g DM (Table 2). It offered the most reliable estimate of the crystalline part of the diffraction pattern, but due to the computing efforts it is less suited as a standard method.

Discussion

Many earlier studies on crystallinity excluded the determination of the chemical fibre composition, so in fact only the sample crystallinity was determined and not the actual cellulose crystallinity. The strong acid hydrolysis was found superior for determination of the cellulose content due to chromatographic differentiation between the monomers in cellulose and hemicellulose (Table 1). The cellulose content in the examined samples was used to determine the cellulose crystallinity (g/100 g cellulose), which was used to evaluate the four investigated methods for crystallinity determination. However, all the three analysis methods seemed reliable when they are used to determine the mass balance over wet oxidation experiments with for example, wheat straw and hemp fibres as raw materials resulting in process recoveries of cellulose in the range 90–110% (Thygesen et al. 2003, 2004; Thomsen et al. 2005). Enzymatic hydrolysis resulted in up to 85% conversion of cellulose into glucose in pre-treated corn stover and pre-treated wheat straw, which seem reasonable. Based on these observations, the chemical analysis methods give reasonable results within an uncertainty interval of 10% of the measured value.

The best experimental mode in the X-ray diffraction experiments was reflection geometry during the measurements to avoid air scattering and obtain higher intensity, since the reflected and not the penetrated X-ray photons were counted (Figure 2). The use of side-loaded samples resulted in close to random orientation of the sample fibres so the ratio between the diffraction peak intensities was similar to the peaks in the diffractogram calculated by the Debye method. Therefore, the use of reflection mode for X-ray powder diffraction and side loading of samples are prerequisites for a reliable and optimal crystallinity determination.

The present comparative study showed that the most consistent and reliable methods for sample crystallinity determinations were the Rietveld and Debye methods. Both methods took full account of the overlapping and widely broadened diffraction peaks of cellulose (Figure 3a). The sample crystallinity determined by the Rietveld refinements and the Debye calculations were consistent and corresponded to realistic cellulose crystallinities below 100 g/100 g cellulose, cf. Figure 4. The Debye method was found an excellent reference method, but required extensive computation, and programs are not generally available. Rietveld refinement on cellulose was after some initial considerations concerning the parameter set, straightforward to carry out and gave consistent results. Combined with the facts that the cellulose Iβ crystal structure has been established (Nishiyama et al. 2002) and that Rietveld refinement

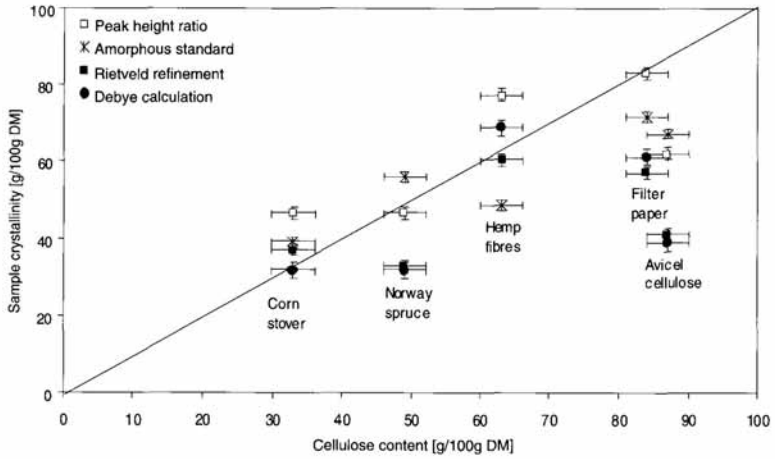

Figure 4. Comparison of the four methods for sample crystallinity determination combined with chemical analysis by the strong acid hydrolysis (g/100 g dry matter). The length of the error bars is one standard deviation.

programs are available, the Rietveld method should be the preferred method for sample crystallinity determinations of plant fibre samples. The Segal and Ruland–Vonk methods do not consider the effect of peak overlap contributing to the apparent background. As a result, the Segal and Ruland–Vonk methods will generally underestimate the sample crystallinity, compared both to the cellulose contents of the samples (Table 1 and Figure 4) and the Debye and Rietveld methods. However, the Ruland–Vonk method is still a robust method and if the peak overlap effect on the apparent background is taken into consideration, it may still be the preferred method when the true amorphous background can be determined experimentally.

Rietveld refinement and Debye calculations gave in addition, an estimate of the crystallite dimensions (Table 3). Reliable determination of the microfibril length was not possible by the Rietveld method due to the weak 004 reflection and peak overlaps. A more reliable determination was obtainable by the Debye method due to the manual fitting of the peaks. Bardage et al. (2004) have by transmission electron microscopy measured the microfibril diameter to 50 Å in Norway spruce pulp fibres, which is on the same level as determined by the Debye method in this study for filter paper (52 Å) and higher than for raw Norway spruce (34 Å) (Table 3). The determined crystallite diameter was thereby comparable or smaller than the microfibril diameter.

The results for cellulose content and crystallinity of the five samples are presented in Table 4 and compared in Figure 5. The corn stover and the hemp fibres are both plant-based and showed a high cellulose crystallinity of 90–100 g/100 g cellulose (full drawn line in Figure 5).

The Norway spruce sample had a cellulose crystallinity of 67 g/100 g cellulose (Table 4), which is comparable to previous findings in fresh Norway spruce (51–71 g/100 g cellulose) by X-ray diffraction (Andersson et al. 2003). The cellulose crystallinity was on the same level in filter paper (65 g/100 g cellulose) and was also comparable to the crystallinity of 68 g/100 g cellulose that has been measured in pine kraft pulp by ^{13}C-NMR by Liitia et al. (2003). The cellulose crystallinity of wood based materials was thereby found to be on

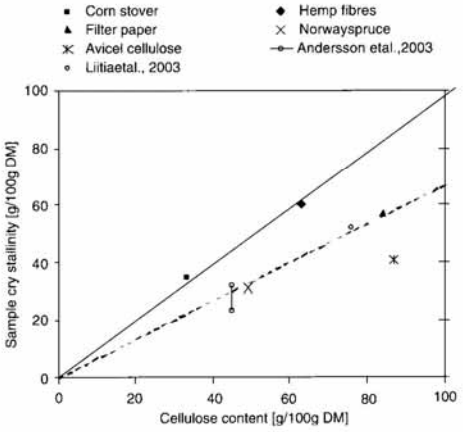

Figure 5. Sample crystallinity determined by Rietveld refinement compared to the cellulose contents measured by strong acid hydrolysis. The relationship for plant based materials (full drawn line) and the relationship for wood based materials (dotted line) are shown.

Table 4. Cellulose crystallinity (g/100 g cellulose) and contents (g/100 g dry matter) of cellulose, crystalline cellulose, amorphous cellulose and residual material, measured by the optimal methods: Strong acid hydrolysis and Rietveld refinement.

Material	Cellulose crystallinity g/100 g cellu.	Cellulose content g/100 g DM	Sample crystallinity g/100 g DM	Amorphous cellulose content g/100 g DM	Residual content
Corn stover	100	33	33	0	67
Norway spruce	67	49	33	16	51
Hemp fibres	96	63	60	3	37
Filter paper	68	84	57	27	16
Avicel cellulose	47	87	41	46	13
Norway spruce[a]	51–71	45	23–32	13–22	55
Pine kraft pulp[b]	68	76	52	24	24

[a]Andersson et al. (2003): Fresh Norway spruce analysed with X-ray powder diffraction and calculated with the Ruland–Vonk method.[b]Liitia et al. (2003): Norway spruce pulp analyzed with ^{13}C-NMR.

the same level, when determined by X-ray diffraction and by ^{13}C-NMR, and the pulping process had only slight effect on the cellulose crystallinity. The present data as well as the literature data are shown in Figure 5 and related by the dotted line, indicating a cellulose crystallinity of 60–70 g/100 g cellulose.

The Avicel cellulose originating from unspecified plant fibres had a low cellulose crystallinity (47 g/100 g cellulose), which shows that the very fine milling and hydrolysis during the cellulose purification decreased the cellulose crystallinity (Figure 5), compared to the plant fibres.

It should be mentioned that the improved methods for determination of cellulose content and cellulose crystallinity are fundamental for further investigations on how the cellulose microstructure affects the fibre strength and the enzymatic hydrolysis of cellulose to glucose. According to this investigation, the cellulose crystallinity is 90–100 g/100 g cellulose in plant-based fibres and 60–70 g/100 g cellulose in wood based fibres (Figure 5). Corn stover is a promising raw material for ethanol production and hemp fibres are interesting for fibre production. The high crystallinity in corn stover indicates that enzymatic hydrolysis for bioethanol production requires a high dosage of exoglucanase enzymes. The high content of cellulose and high crystallinity in hemp fibres indicates a high performance for strong composites.

Conclusions

- Among the investigated techniques, the best experimental mode was reflection geometry for the X-ray diffraction experiments to avoid air scattering, and using side-loaded samples to reduce the effect of preferred orientation.
- The Rietveld method was preferred for sample crystallinity determinations, since it took full account of the overlapping and widely broadened diffraction peaks of cellulose and gave consistent results.
- An accurate method for determination of the cellulose content is needed for determination of the cellulose crystallinity (g/g cellulose) in plant fibres. Strong acid hydrolysis followed by chromatographic measurement of monomers was chosen as the best of the tested methods.
- According to the novel methods, plant based materials have cellulose crystallinity of 90–100 g/100 g cellulose and wood-based materials have 60–70 g/100 g cellulose.
- Reliable methods for the determination of cellulose content and cellulose crystallinity are fundamental for further investigations on how the cellulose microstructure affects the fibre strength and for the development of methods for enzymatic hydrolysis of the cellulose.

Acknowledgements

This work was part of the project 'High performance hemp fibres and improved fibre networks for composites' supported by the Danish Research Agency of the Ministry of Science and of the project EFP Bioethanol part 2 J. nr. 1383/03–0002. Dr. Claus Felby is acknowledged as supervisor for Ph. D. student Anders Thygesen. Mr. Tomas Fernqvist and Mrs. Ingelis Larsen are acknowledged for technical assistance and Dr. Bo Madsen, Dr. Enikö Varga and Dr. Mette Hedegaard Thomsen are acknowledged for discussion and inspiration.

References

Alexander L.E. 1969. X-ray Diffraction Methods in Polymer Science. Wiley-Interscience, New York.

Andersson S., Serimaa R., Paakkari T., Saranpää P. and Pesonen E. 2003. Crystallinity of wood and the size of cellulose crystallites in Norway spruce (*Picea abies*). J. Wood Sci. 49: 531–537.

Bardage S., Donaldson L., Tokoh C. and Daniel G. 2004. Ultrastructure of the cell wall of unbeaten Norway spruce pulp fibre surfaces. Nordic Pulp Paper Res. J. 19(4): 448–452.

Browning B.L. 1967. Methods of Wood Chemistry. Interscience Publishers, A division of John Wiley & Sons, New york.

Buschle-Diller G. and Zeronian S.H. 1992. Enhancing the reactivity and strength of cotton fibres. J. Appl. Polym. Sci. 45(6): 967–979.

Debye P. 1915. Zerstreuung von Röntgenstrahlen. Ann. Phys. 46: 809–823.

De Souza I.J., Bouchard J., Methot M., Berry R. and Argyropoulos D.S. 2002. Carbohydrates in oxygen delignification. Part I: Changes in cellulose crystallinity. J. Pulp Paper Sci. 28(5): 167–170.

Felby C., Klinke H.B., Olsen H.S. and Thomsen A.B. 2003. Ethanol from wheat straw cellulose by wet oxidation pretreatment and simultaneous saccharification and fermentation. ACS Symposium Series 855: 157–174.

Fink H.P. and Walenta E. 1994. Röntgenbeugungsuntersuchungen zur übermolekularen Struktur von Cellulose im Verarbeitungsprozeß. Papier 48(12): 739–748.

Finkenstadt V.L. and Millane R.P. 1998. Crystal structure of Valonia cellulose Iβ. Macromolecules 31(22): 7776–7783.

Goering H.K. and Van Soest P.J. 1970. Forage fiber analyses (apparatus, reagents, procedures and some applications). Agricultural Research Service, USDA, Washington DC.

Hepworth D.G., Bruce D.M., Vincent J.F.V. and Jeronimidis G. 2000. The manufacture and mechanical testing of thermosetting natural fibre composites. J. Mater. Sci. 35(2): 293–298.

Howard C.J. and Hill R.J. 1986. LHMP: a computer program for Rietveld analysis of fixed wavelength X-ray and neutron powder diffraction patterns. AAEC (now ANSTO) Report M112. Lucas Heights Research Laboratory.

Kaar W.E., Cool L.G., Merriman M.M. and Brink D.L. 1991. The complete analysis of wood polysaccharides using HPLC. J. Wood Chem. Technol. 11(4): 447–463.

Klinke H.B., Lilholt H., Toftegaard H., Andersen T.L., Schmidt A.S. and Thomsen A.B. 2001. Wood and plant fibre reinforced polypropylene composites. In 1st world conference on biomass for energy and industry. James & James (Science Publishers), pp. 1082–1085.

Koyama M., Helbert W., Imai T., Sugiyama J. and Henrissat B. 1997. Parallel-up structure evidences the molecular directionality during biosynthesis of bacterial cellulose. Proc. Natl. Acad. Sci. USA 94(17): 9091–9095.

Liitia T., Maunu S.L., Hortling B., Tamminen T., Pekkala O. and Varhimo A. 2003. Cellulose crystallinity and ordering of hemicelluloses in pine and birch pulps as revealed by solid-state NMR spectroscopic methods. Cellulose 10: 307–316.

Madsen B. and Lilholt H. 2003. Physical and mechanical properties of unidirectional plant fibre composites – an evaluation of the influence of porosity. Compos. Sci. Technol. 63(9): 1265–1272.

Mwaikambo L.Y. and Ansell M.P. 1999. The effect of chemical treatment on the properties of hemp, sisal, jute and kapok for composite reinforcement. Angew. Makromol. Chem. 272: 108–116.

Nishiyama Y., Langan P. and Chanzy H. 2002. Crystal structure and hydrogen-bonding system in cellulose Iβ from synchrotron X-ray and neutron fiber diffraction. J. Am. Chem. Society 124(31): 9074–9082.

Rietveld H.M. 1967. Line profiles of neutron powder-diffraction peaks for structure refinement. Acta Crystallogr. 22: 151–152.

Rietveld H.M. 1969. A profile refinement method for nuclear and magnetic structures. J. Appl. Crystallogr. 2: 65–71.

Ruland W. 1961. X-ray determination of crystallinity and diffuse disorder scattering. Acta Crystallogr. 14: 1180–1185.

Sao K.P., Samantaray B.K. and Bhattacherjee S. 1994. X-ray study of crystallinity and disorder in ramie fiber. J. Appl. Polym. Sci. 52: 1687–1694.

Sao K.P., Samantaray B.K. and Bhattacherjee S. 1997. Analysis of lattice distortions in ramie cellulose. J. Appl. Polym. Sci. 66: 2045–2046.

Sarko A. and Muggli R. 1974. Packing analysis of carbohydrates and polysaccharides. 3. *Valonia* cellulose and cellulose-II. Macromolecules 7(4): 486–494.

Segal L., Creely J.J., Martin A.E. and Conrad C.M. 1959. An empirical method for estimating the degree of crystallinity of native cellulose using the X-ray diffractometer. Textile Res. J. 29: 786–794.

Simon I., Glasser L., Scheraga H.A. and Manley R.S. 1988. Structure of cellulose. 2. Low-energy crystalline arrangements. Macromolecules 21(4): 990–998.

Sugiyama J., Vuong R. and Chanzy H. 1991. Electron diffraction study on the two crystalline phases occuring in native cellulose from an algal cell wall. Macromolecules 24(14): 4168–4175.

Teeri T.T. and Koivula A. 1995. Cellulose degradation by native and engineered fungal cellulases. Carbohydr. Eur. 12: 28–33.

Thomsen A.B., Rasmussen S.K., Bohn V., Nielsen K.V. and Thygesen A. 2005. Hemp raw materials: The effect of cultivar, growth conditions and pretreatment on the chemical composition of the fibres. Risø National Laboratory. Report No.: R-1507.

Thygesen A., Thomsen A.B., Schmidt A.S., Jørgensen H., Ahring B.K. and Olsson L. 2003. Production of cellulose and hemicellulose-degrading enzymes by filamentous fungi cultivated on wet-oxidised wheat straw. Enzyme Microb. Technol. 32(5): 606–615.

Thygesen A., Thomsen M.H., Jørgensen H., Christensen B.H. and Thomsen A.B. 2004. Hydrothermal treatment of wheat straw on pilot plant scale, 2nd World Conference and Technology Exhibition on Biomass for Energy, Industry and Climate Protection, Rome, Italy, 10–15th May 2004.

Varga E., Reczey K. and Zacchi G. 2004. Optimization of steam pretreatment of corn stover to enhance enzymatic digestibility. Appl. Biochem. Biotechnol. 113(-16): 509–523.

Vonk C.G. 1973. Computerization of Rulands X-ray method for determination of crystallinity in polymers. J. Appl. Crystallogr. 6: 148–152.

Woodcock C. and Sarko A. 1980. Packing analysis of carbohydrates and polysaccharides. 11. Molecular and crystal-structure of native ramie cellulose. Macromolecules 13(5): 1183–1187.

Young R.A. (ed.) 1993. The Rietveld Method. Oxford University Press.

Paper IV

Comparison of composites made from fungal defibrated hemp with composites of traditional hemp yarn.

In press: Industrial Crops and Products.

Comparison of composites made from fungal defibrated hemp with composites of traditional hemp yarn

Anders Thygesen[1,2,3*], Anne Belinda Thomsen[3], Geoffrey Daniel[4] and Hans Lilholt[1]

[1] Materials Research Department, Risø National Laboratory, P.O. Box 49, DK-4000 Roskilde, Denmark;
[2] Danish Centre for Forest, Landscape and Planning, The Royal Veterinary and Agricultural University, Højbakkegård Allé 1, DK-2630 Tåstrup, Denmark;
[3] Biosystems Department, Risø National Laboratory, P.O. Box 49, DK-4000 Roskilde, Denmark;
[4] Swedish University of Agricultural Sciences, WURC, P.O. Box 7008, SE-75007 Uppsala, Sweden.

***Corresponding Author:**
Anders Thygesen: Fax: +45 46774122; Telephone: +45 46774279;
anders.thygesen@risoe.dk
Correspondence address:
Biosystems Department, Risø National Laboratory,
P.O. Box 49, DK-4000 Roskilde, Denmark

Journal: Industrial Crops and Products, Accepted.

ABSTRACT

Aligned epoxy-matrix composites were made from hemp fibres defibrated with the fungi *Phlebia radiata* Cel 26 and *Ceriporiopsis subvermispora* previously used for bio pulping of wood. The fibres produced by cultivation of *P. radiata* Cel 26 were more cellulose rich (78% w/w) than water-retted hemp due to more degradation of pectin and lignin. Even though the crystalline cellulose content in the fibres remained intact during water retting, the fibre bundle strength decreased, which shows that degradation of other components like pectin reduced the fibre strength. The defibrated hemp fibres had higher fibre stiffness (88-94 GPa) than the hemp yarn (60 GPa), which the fibre twisting in hemp yarn might explain. Even though mild processing was applied, the obtained fibre strength (643 MPa) was similar to the strength of traditionally produced hemp yarn (677 MPa). The fibre strength and stiffness properties are derived from composite data using the rule of mixtures model. The hemp fibre tensile strength increased linearly with cellulose content to 850 MPa for pure cellulose. The fibre stiffness increased also versus the cellulose content and cellulose crystallinity and reached a value of 125 GPa for pure crystalline cellulose.

KEY WORDS

A: *Phlebia radiata* Cel 26, *Ceriporiopsis subvermispora*
B: Fibre composition, cellulose crystallinity
C: Epoxy-matrix composites, mechanical properties

INTRODUCTION

Previous studies have indicated that plant fibres used with aligned fibre arrangement in composite materials have good potential as reinforcement agents due to their low density and high stiffness (Joseph et al., 1996; Hepworth et al., 2000a, 2000b; Hautala et al., 2004). Hemp fibres are an obvious choice among plant fibres due to their high cellulose content, which is expected to result in higher fibre strength (Klinke et al., 2001). Cellulose is of major interest since it is a partly crystalline polymer with potentially high strength (8 GPa; Lilholt & Lawther, 2000). However, the strength of elementary hemp fibres is only 800-2000 MPa (Madsen et al., 2003) and the effective fibre strength is in some cases further reduced when the fibres are used as reinforcement in composite materials (500-700 MPa; Mieck et al., 1996; Madsen & Lilholt, 2003). It is suspected that the fibre damage introduced during processing of hemp for making yarn and finally composite processing decreases fibre strength. It is therefore of interest to determine the potential for hemp fibres in composites using mild processing conditions to reduce fibre damage.

Parenchyma cells rich in pectin and hemicellulose are located between the fibre bundles (Garcia-Jaldon et al., 1998) and bind the hemp bast onto the stem surface. This binding must be degraded by defibration before fibres useful for strong composites can be obtained (Thygesen et al., 2005a). A common defibration method is water retting, in which the hemp is placed under water and attacked by microorganisms originating from the stem surface (Rosember, 1965; Meijer et al., 1995). However bacteria and fungi producing cellulose-degrading enzymes will be present and degrade parts of the fibre cellulosic material. Defibration with pectin-degrading enzymes has also been tested on hemp fibres and found incapable of epidermis degradation. This insufficient and rather irregular defibration process results in very rough fibre bundles (Thygesen et al., 2002). Steam explosion has also been tested resulting in fibres with increased cellulose content of 80 g/100 g dry matter (DM) (Thygesen, 2006). However, very short fibre bundles were obtained, that were difficult to align. In addition the high temperature (185°C) and rapid pressure release during steam explosion caused mechanical and thermal damage to the fibres resulting in lower tensile strength (Madsen et al., 2003). Biological defibration methods have the disadvantage of being slow (5 – 14 days) but an advantage of forming long fibre bundles that are easy to align. Defibration of hemp with defined filamentous fungi has the advantage of producing a specific attack of chemical components in the fibres. Also fungi form hyphae, which can penetrate the epidermis and release enzymes at the sites for desired degradation, resulting in a targeted attack. For example, bio-pulping of wood has been performed using the white rot fungus *Ceriporiopsis subvermispora* (Akhtar et al., 1992) and various fungi have been used for defibration of flax (Henriksson et al., 1997), but the produced fibres have not been tested as reinforcement agents in composite materials.

In this study, aligned hemp fibres were used in composites to investigate the effects of defibration on fibre tensile strength and stiffness. Epoxy was used as matrix material in the composites since it reacts with hydroxyl groups on the plant fibres resulting in covalent fibre-matrix binding (Obrien & Hartman, 1971) although this reaction may be partly hindered by a waxy film on the fibre surface (Bos et al., 2004). When the composites were characterised, the air-filled voids (porosity) were taken into account in

the calculation of volume fractions of matrix and fibres and the determination of fibre strength and stiffness. The hemp fibres were produced by biological defibration procedures since these are expected to be physically and thermally mild compared with steam explosion. The fibres were peeled from the hemp stems by hand to avoid mechanical decortication, which is expected to damage the fibres. Hemp fibres were defibrated by the fungi *Phlebia radiata* Cel 26 and *C. subvermispora* and by water retting and finally compared with raw hemp bast. *P. radiata* is a white rot fungus, which can perform simultaneous degradation of cellulose, hemicellulose, lignin and pectin. In contrast, the mutant *P. radiata* Cel 26 does not appear to degrade cellulose to any significant degree (Nyhlen & Nilsson, 1987; Thygesen et al., 2005a). Fungal incubations were followed by investigation of the fibres with light microscopy and by analysis of the nutrient poor growth medium. Commercial hemp yarn was used as traditionally produced fibres and compared with the mildly defibrated hemp fibres. The chemical composition, crystallinity and tensile strength of the defibrated hemp fibres were measured to correlate the fibre properties with the obtained composite data.

MATERIALS AND METHODS

Raw materials

Hemp (*Cannabis sativa* L., cultivar Felina 34) was grown in Denmark and the middle sections of the stems were used directly for peeling of fibres or defibration (Thygesen et al., 2005a). Hemp yarn with a tex-value of 47 g/km was used [Linificio e Canapificio Nazionale, Italy]. A low viscosity epoxy system (SPX 6872 & SPX 6873; LM-Glasfiber A/S) that incorporates a slow hardener was used as matrix material with a density of 1.136 g/cm^3.

Defibration of hemp and preparation of fibres for composites

Raw hemp bast of 1-4 mm width was peeled by hand from 25 cm long hemp stem pieces. The bast was then wetted in water and aligned before vacuum drying (Hepworth et al., 2000a). Water retting was performed with 20 kg hemp stems in 750 litre water at 35°C for 4 days. Water retted hemp fibres were separated from the stem core, wetted in water and aligned followed by vacuum drying. The fungi *Ceriporiopsis subvermispora* (Akhtar et al., 1992) and *Phlebia radiata* Cel 26 (Nyhlen & Nilsson, 1987), used for fungal defibration, were stored and pre-cultivated on 2 % (w/v) malt agar plates at 20°C. For inoculation, mycelia from one agar plate was homogenised into 100 ml water. Water containing 1.5 g/l NH_4NO_3, 2.5 g/l KH_2PO_4, 2 g/l K_2HPO_4, 1 g/l $MgSO_4 \cdot 7\ H_2O$ and 2.5 g/l glucose was used as growth medium in the cultivation experiments (Thygesen et al., 2005a). The cultivation experiments were performed on small, medium and large scale (Table 1). The growth medium and hemp stem pieces were sterilised in rectangular glass containers at 120°C for 30 min. When the containers were cooled to ambient temperature, the mycelia suspension was added aseptically and the cultivation experiments were conducted at 28°C for 7-31 days. Following fungal defibration, the hemp stem pieces were brushed in water to remove epidermal and fungal material from the stem surface and to separate the fibres from the woody cores of the stems. Fibres from 100 g hemp stems were boiled for 5 minutes in 400 ml neutral detergent containing 3 g/l sodium dodecyl sulphate, 1.86 g/l EDTA ($C_{10}H_{14}N_2Na_2O_8 \cdot 2H_2O$), 0.455 g/l Na_2HPO_4, 0.68 g/l sodium tetraborat ($Na_2B_4O_7 \cdot 10H_2O$) and 1 ml/l ethylenglycolmonoethylether (Goering and van Soest, 1970) to obtain clean fibres and

kill the fungus. The fibres were thereafter washed in water and aligned into a planar sheet followed by vacuum drying. The yield of fibres from the original hemp stems was determined by 2-3 repetitions at the small, medium and large scale.

Table 1. Overview of the experimental conditions used for fungal defibration of hemp and for water retting of hemp

	Hemp g DM[1]	Stem length cm	Mycelium ml	Medium[2]	Time days	Dry matter g/l medium
Fungal defibration						
Small scale	5.4	6	10	75 ml NS	7 – 31	72
Medium scale	45	6	70	625 ml NS	14	72
Large scale	90	25	140	1000 ml NS	14	90
Other methods						
Water retting	20000	25	None	750 l water	4	27

1: DM = Dry matter
2: NS = Nutrient solution as a growth medium

Analysis of the culture broth and the plant fibres

In the fungal culture broth solution, the peroxide content was measured with an analysis stick placed for 1 sec in the solution. The stick was withdrawn from the solution; after 5 sec the content of H_2O_2 was measured on a colour scale [Peroxide 100; Quantofix at Macherey-Nagel in Germany]. The pH-value of the culture broth was measured using a pH-electrode.

Determination of cellulose crystallinity in the plant fibres was done by X-ray diffraction. The raw fibre samples were cut into small pieces in a knife mill with a 0.5 mm sieve. The milled samples (0.5 g) were wetted with distilled water and side loaded into a sample holder to reduce the effect of preferred orientation and thereby get the correct ratio between the diffraction peak areas. The samples of 2 mm thickness were air dried overnight before the diffractograms were recorded. The cellulose crystallinity was measured with X-ray diffraction in reflection mode. A Philips PW1820/3711 diffractometer with Bragg-Brentano scattering geometry, copper K_α-radiation and automatic divergence slits was employed. Data were collected in the 2θ-range 5° – 60° with a step size of 0.02° and a counting time of 20 sec per step. The reflection mode intensities were corrected for the effects of the automatic divergence slit. The diffractograms were divided into crystalline and amorphous contributions by Rietveld refinement. The crystalline diffraction was fitted with the diffraction pattern of Cellulose Iβ and polynomial fitting was used to determine the amount of amorphous diffraction from amorphous cellulose, hemicellulose, lignin, pectin and ashes (Thygesen et al., 2005b).

Before the comprehensive plant fibre analysis, the samples were milled into particles that could pass a 1 mm sieve. This plant fibre analysis method is a gravimetric method for fibres from agricultural plants and wood (Browning, 1967; Thygesen et al., 2005b). Double repetition was used with 4 g fibers passing through the procedure. At first wax was Sohxlet extracted in chloroform for 1 h. Water-soluble components were extracted in 400 ml water for 30 minutes at 25°C. Pectin was extracted in 300 ml 3% EDTA

solution (pH 4) for 4 h at 85°C. Lignin was oxidized and extracted in chlorite solution for 1 h at 75°C (300 ml water+10 g $NaClO_2$+1 ml 100% acetic acid). Hemicellulose was extracted in 100 ml 12% NaOH+2% H_3BO_3 solution for 90 minutes at 25°C. After each step the suspension was filtrated on pre-weighed glass filters and the filter cake washed in water. The contents were determined from the dry matter loss in the extraction steps by drying overnight at 60°C and weighing after each step. The mineral content was determined by incineration of 1 g raw sample at 550°C for 3 h.

Tensile tests on fibre bundles (15 mm long l_f) were done with a 3 mm test span l_{span} at a strain rate of 1.7×10^{-3} s^{-1} using an Instron 5566 with pressley clamps [Type: Stelometer 654 from Zellweger Uster] (Thygesen et al., 2005a). Following fracture the fibre pieces of 15 mm were weighed w_f. The number of repetitions was at least 13 for each sample. The failure stress σ_{fu} was calculated based on the failure force F_{fu} and the fibre density ρ_f:

$$\sigma_{fu} = \frac{F_{fu}}{A_f} = F_{fu} \times \frac{l_f \times \rho_f}{w_f} \qquad \textbf{Equation 1}$$

The fibre density for the investigated hemp fibres and hemp yarn is 1.58 g/cm^3 (Madsen 2004; Thygesen 2006). The maximum density for pure and fully crystalline cellulose is in the range 1.61 to 1.64 g/cm^3, based on crystallographic information (Nishiyama et al., 2002; Thygesen et al., 2005b).

Preparation of composites

The fibre bundles of 6 – 25 cm length were wetted in water and aligned by carting with a comb. In cases of short fibre pieces (6 cm), the aligned fibres were placed on top of each other in three layers with different fibre-end positions to allow stress transfer between the fibres and reduce movement of the fibres in the epoxy flow when the lay-up was being compressed. The hemp yarn composites were made both by hand carting and filament winding (Madsen & Lilholt, 2003). The fibre content in the composites was controlled by the displacement rate during winding. The frame was displaced at a rate that allowed 11 rotations/cm. The epoxy resin (SPX 6872) and hardener (SPX 6873) were mixed in a ratio of 100 g resin to 36 g hardener and poured over the fibres and left for 5 – 10 minutes to allow impregnation. Spacers of 1.5 mm thickness were used to control the laminate thickness. Tape was placed beside the fibres to avoid fibre movement. Finally, a steel plate was placed on the mould and excess resin with air bubbles was squeezed out with clamps. The lay-up was pre-cured at 40°C for 16 hours and thereafter cured at 120°C for 6 hours.

Analysis of the composites

Standard dumb-bell-shaped tensile test specimens (180 × 20 mm with gauge section of 25 × 15 mm) were cut from the laminates. Tensile tests were performed at room temperature on an Instron machine with crosshead speed of 1 mm/min. The strain was measured with two extensometers placed on each side of the test specimens.

Composite structure and fibre bundle size were investigated by SEM-microscopy. Composite pieces were polished on the side perpendicular to the fibre direction using wetted silicon carbide paper [Struers, Denmark] in a series of decreasing roughness

(P#320 for 0.5 min, P#500 for 1 min, P#1000 for 2 min and P#4000 for 4 min). Air-dried pieces were sawed into 4 mm long pieces, mounted on stubs using double-sided cellotape and coated three times with platinum [Agar high resolution sputter coater]. The coated samples were observed using a Philips XL30 ESEM scanning microscope. The fibre bundle transverse section area was determined with Image Pro software.

Calculation of composite composition and mechanical properties

The laminate volumes v_c were calculated based on average values of the thickness t_c measured at 15 points, the length l_c measured at 3 points and the width b_c measured at 3 points, where the subscript *c* denotes composite.

$$v_c = t_c \times b_c \times l_c \qquad \textbf{Equation 5}$$

The fibre weight in the laminates w_f were calculated from the weight of fibres $w_{f,start}$ in the prepared laminate with fibre length $l_{f,start}$. The fibre length was reduced from $l_{f,start}$ to l_c, when the laminates were cut into specimen length (l_c=18 cm). The subscript *f* denotes fibres.

$$w_f = w_{f,start} \times \frac{l_c}{l_{f,start}} \qquad \textbf{Equation 6a}$$

In the composites with wound yarn (filament), w_f was calculated using the number of rotations/cm frame displacement n_r, number of filaments pr. rotation n_s and the filament linear density *Tex*

$$w_f = \left(2n_r \times b_c \times n_s\right) \times \left(Tex \times l_c\right) \qquad \textbf{Equation 3b}$$

The matrix weight w_m was calculated based on w_c and w_f, where the subscript *m* denotes matrix.

$$w_m = w_c - w_f \qquad \textbf{Equation 7}$$

The volume fractions of matrix V_m and fibres V_f were calculated based on the densities of matrix ρ_m and of fibres (ρ_f = 1.58 g/cm^3; Madsen, 2004; Thygesen, 2006).

$$V_f = \frac{w_f}{\rho_f v_c} \qquad \textbf{Equation 5a}$$

$$V_m = \frac{w_m}{\rho_m v_c} \qquad \textbf{Equation 5b}$$

Assuming that on a macroscopic scale a composite material can be divided into three components, fibres, matrix and porosity, the volume fraction of porosity V_p (*p* denotes *porosity*) can be calculated as

$$V_p = 1 - V_m - V_f \qquad \textbf{Equation 6}$$

The composite strain exerted during tensile testing ε was calculated as the average of two extensometer recordings. The tensile strength (ultimate stress) σ_{cu} and stress during testing σ_c were calculated as:

$$\sigma_c = \frac{F}{b_c \times t_c} \qquad \textbf{Equation 7a}$$

The stiffness (E-modulus) of the composites E_c was calculated by linear regression of σ_c versus ε between 0% and 0.1%.

$$E_c = \left(\frac{d\sigma_c}{d\varepsilon} \right)_{\varepsilon=0-0.1\%}$$ **Equation 7b**

Pure epoxy sheets were tested to obtain a stress-strain curve for the matrix material, which was fitted to a second order polynomial, giving E_m=2.93 GPa and k=32.5 GPa (Figure):

$$\sigma_m(\varepsilon) = E_m \times \varepsilon - k \times \varepsilon^2$$ **Equation 8**

The fibre strength σ_{fu} was calculated with the rule of mixtures using the matrix stress σ_m at the strain of composite failure ε_u and the fibre stiffness E_f was calculated using E_m (Hull & Clyne, 1996). With porosity in the composites, σ_{cu} and E_c are reduced to a larger extent than caused by the reduction of V_f and V_m; this is due to the potential stress concentrations originating at the porosities, and is taken into account by the term $(1\text{-}V_p)^n$ (Toftegaard & Lilholt, 2002). Based on detailed investigation of the composites in this study, it was chosen to use n_σ=2.1 and n_E=1 for correction for porosity (Thygesen, 2006). The fibre strength σ_{fu} and the fibre stiffness E_f are thus calculated from Equation 9.

$$\sigma_{cu} = \left(V_f \times \sigma_{fu} + V_m \times \sigma_m(\varepsilon_u)\right)\left(1 - V_p\right)^{n_\sigma} = \sigma_{cup}\left(1 - V_p\right)^{n_\sigma} \Leftrightarrow \sigma_{fu} = \frac{\sigma_{cup} - V_m \times \sigma_m(\varepsilon_u)}{V_f}$$ **Equation 9a**

$$E_c = \left(V_f \times E_f + V_m \times E_m\right)\left(1 - V_p\right)^{n_E} = E_{cp}\left(1 - V_p\right)^{n_E} \Leftrightarrow E_f = \frac{E_{cp} - V_m \times E_m}{V_f}$$ **Equation 9b**

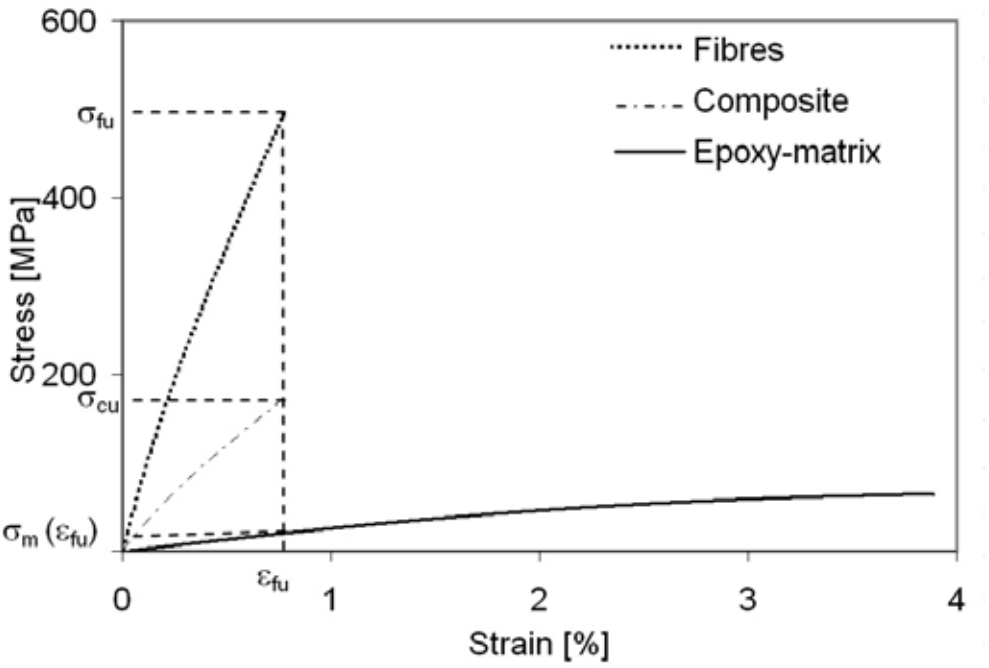

Figure 1. Stress versus strain for epoxy sheets and composites with 33% (v/v) P. radiata defibrated hemp fibres, to show the fracture strain (ε_u) and stress (σ) of matrix (σ_m), composite (σ_{cu}) and fibres (σ_{fu}).

RESULTS

The effect of defibration on hemp fibres

The defibration of hemp by cultivation of *P. radiata* resulted in hemicellulose, pectin and lignin degradation, and the cellulose content in the fibres increased to 78% after 14 days of cultivation (Table 2). The content of crystalline cellulose in the fibres increased from 60 to 66 g/100 g dry matter (DM) due to the increased cellulose content after the fungal cultivation (Table 2). However the cellulose crystallinity decreased from 94 to 84 g/100 g cellulose due to conversion of crystalline cellulose into its amorphous form. The recovery of cellulose was 87% after 14 days using medium scale cultivation (Table 3) so there appeared to be decay of crystalline cellulose. Using small-scale experiments for 31 days there was no further cellulose decay due to the constant fibre yield (Table 3). Previous observations with transmission electron microscopy have also shown the fibre wall to remain intact (Thygesen et al., 2005a). The fibre bundle strength was reduced from 950 MPa in raw hemp bast to 820 MPa after the fungal defibration (Table 2).

The defibration of hemp fibres by cultivation of *C. subvermispora* resulted in cellulose degradation as shown by the cellulose recovery of 87% after 14 days cultivation (Table 3) and by further reduction of the fibre yield after 31 days cultivation (Table 3). The fungus formed a lot of mycelia above the water surface, while hemp stem pieces below the surface were not colonised and the obtained cellulose content was 72% (Table 2). The fungus grew well with low and medium scale cultivation resulting in reduction of pH from 6 to 4.6 (Table 3). The fibre bundle strength was reduced by the cultivation to 780 MPa (Table 2). At large-scale cultivation, sterilisation was insufficient resulting in lower fibre yield after 14 days cultivation (27 g/100 stem) and unchanged pH in the culture broth (Table 3).

Lignin degradation was obtained during the cultivation of *P. radiata* on the hemp due to peroxidase enzymes, as suggested by the presence of H_2O_2 in the cultivation broth (Table 3). Smaller hemp fibre bundles were also obtained by cultivation of *P. radiata* ($3\times10^3 \mu m^2$) than by water retting and by *C. subvermispora* cultivation (Table 2), due to the greater degradation of the lignin rich middle lamellae between the fibres. Water retting was a faster process than fungal defibration (Table 1) due to the lacking of sterilisation and the higher temperature (35°C). However, a more variable quality was obtained due to inhomogeneous colonisation by bacteria and fungi resulting in lower fibre bundle strength (590 MPa, Table 2) and unchanged cellulose crystallinity (Figure 3).

Table 2. Chemical composition, structural properties and strength in fibres from hemp

		Raw hemp bast	Hemp fibres defibrated with:			Hemp yarn
			Water retting	*C. sub.*	*P. rad.*	
Chemical composition						
Cellulose	% w/w	64	74	72	78	83
Hemicellulose	% w/w	15	12	14	13	11
Lignin	% w/w	4	5	5	3	1
Pectin	% w/w	6	3	4	2	1
Water soluble	% w/w	6	3	3	3	1
Wax	% w/w	1	2	1	1	2
Ash	% w/w	4	2	2	1	1
Structure and strength						
Sample crystallinity	% w/w	60	68	63	66	68
Cellulose crystallinity	% w/w	94	92	88	84	82
Fibre bundle transverse section	10^3 μm^2	160	10	50	3	1
Fibre bundle strength	MPa	950 ± 230	590 ± 260	780 ± 170	820 ± 100	660 ± 100

Notes: - 14 days at medium scale (Table 1).
- Comprehensive fibre analysis used for determination of chemical composition.
- $\text{Cellulose crystallinity} = \frac{\text{Sample crystallinity}}{\text{Cellulose content}}$

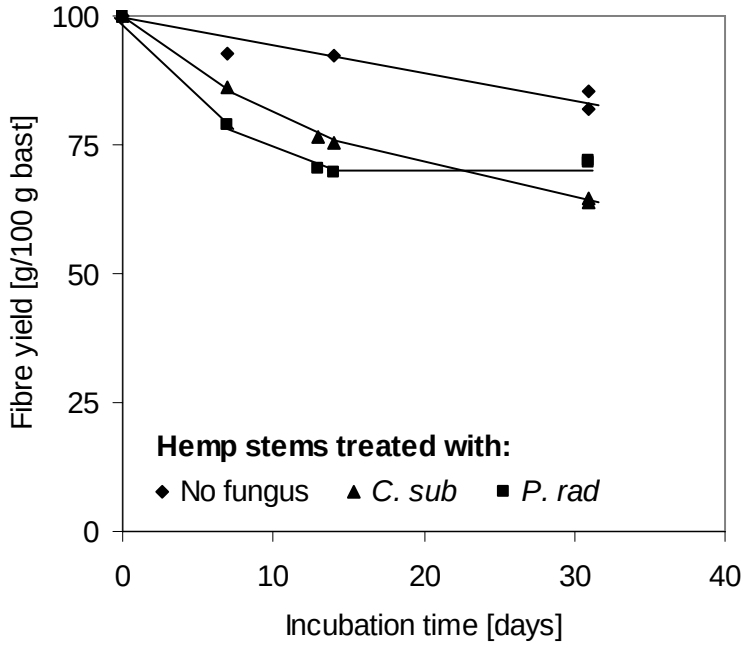

Figure 2. Yield of hemp fibres after small-scale cultivation with P. radiata and C. subvermispora versus time.

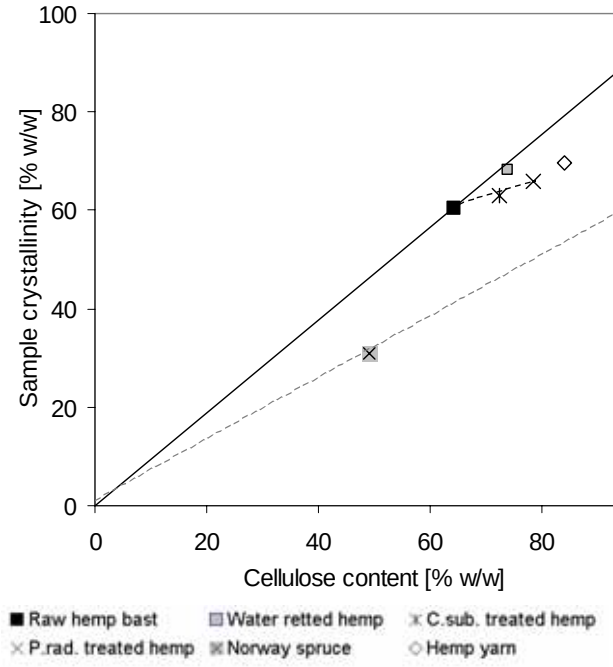

Figure 3. Sample crystallinity determined by Rietveld refinement compared to the cellulose content measured by comprehensive fibre analysis. The relationship for plant based materials (full drawn line) and wood-based fibres (grey dotted line) are shown. The black dotted line shows the tendency for decreasing cellulose crystallinity versus the cellulose content in the fungal defibrated hemp fibres.

Table 3. Process results obtained by fungal defibration of hemp and by water retting of hemp

	Fibre yield[1] g/100 g		Cellulose recov.[2] g/100 g		pH[3]		H_2O_2 mg/l	
Fungal defibration								
	C. sub.	*P. rad.*	*C. sub.*	*P. rad.*	*C. sub.*	*P. rad.*	*C. sub.*	*P. rad.*
Small scale	30/75	27/70	85	85	4.6	5.0	Not analysed	
Medium scale	30/78	28/71	87	87	5.1	5.2	0	1 – 5
Large scale	27/70	23/58	79	71	6.8	4.9	0 – 1	1 – 5
Standard dev.	1.5/3.8	2.1/5.2	4.2	6.4	0.14	0.15		
Other methods								
Water retting	27/68		79		Not analysed		Not analysed	

1: Fibre yield (g fibres/100 g stem)/(g fibres/100 g raw bast)

2: $$\text{Cellulose recovery (g cellulose/100 g cellulose in raw bast)} = \frac{\text{Cellulose content in treated fibres} \times \text{Fibre yield}}{\text{Cellulose content in raw hemp}}$$

3: pH = 6.3±0.3, in the growth medium when the fungal cultivation experiments were started.

4: Standard deviation was calculated as a pooled estimate based on 2-3 repetitions for small, medium and large scale.

Composition of the obtained composites

The obtainable fibre content in the composites decreased versus the fibre bundles transverse section area from 35% v/v with hemp yarn of $1\times10^3\mu m^2$ to 26% v/v with raw hemp bast of $160\times10^3\mu m^2$ (Table 2; Table 4). This was due to the more uniform

transverse section of the small hemp yarn fibres and *P. radiata* defibrated hemp fibres as shown in Figure 4c-d. The larger raw hemp fibres and water retted hemp fibres had a more irregular structure and could therefore not be packed so tightly (Figure 4a-b).

The porosity content in the composites was 2 – 6% v/v with hemp yarn, 2 – 5% v/v with fungal defibrated hemp fibres and 5 – 9% v/v with water retted hemp (Table 4). The data for detailed measurements of V_f and V_p are shown in Figure 5. The porosity content generally increased with increasing fibre content, due to the fibre lumens and to voids at the fibre-matrix interface. Porosity was present to the highest extent in the composites reinforced with raw hemp bast and in the composites with water retted hemp fibres, due to the long distance of epoxy penetration through the epidermis on the fibre bundle surface (Figure 4a-b). This resulted in incomplete impregnation of the fibre bundles resulting in gaps between the matrix and the fibres and within the fibre bundles. Smaller and fewer gaps were found in the composites with hemp yarn and with fungal defibrated hemp fibres for which the epidermis had been removed, as seen by scanning electron microscopy in Figure 4c-d. The epoxy seemed therefore to impregnate these fibres better, resulting in lower porosity content.

Table 4. Physical and mechanical properties of the laminates reinforced with the defibrated hemp fibres and hemp yarn. Consideration of porosity was done with $n_{\square}=2.1$ for the composite tensile strength σ_{cu} and $n_E=1.0$ for the composite stiffness E_c.

Fibre type and defibration		V_f-obt % v/v	V_p-range % v/v	ε_c-average %	σ_m-average MPa	σ_{fu}[3] MPa	E_f[3] GPa
Raw hemp bast	Lay-up	26	6 – 7	0.9	23	**535** ± 117	**78** ± 12
Water retted hemp	Lay-up	31	5 – 9	0.7	19	**586** ± 108	**88** ± 12
C. sub. defibrated hemp	Lay-up short	28	3 – 5	0.7	18	434 ± 63	77 ± 15
	Lay-up[2]					**536**	**88**
P. rad. defibrated hemp	Lay-up short		2 – 4	0.8	22	521 ± 80	82 ± 13
	Lay-up	32	3 – 5	0.9	25	**643** ± 111	**94** ± 15
Hemp yarn	Wound	35	2 – 6	1.8	43	728 ± 44	60 ± 4
	Lay-up		3 – 4	1.6	39	677 ± 92	61 ± 7
Norway spruce[1]	Mature wood	26	74			340	41

1: Mechanical properties for dry Norway spruce (*Picea abies*), with a bulk density of 0.40 g/cm^3 and a cell wall density of 1.50 g/cm^3 after correction of the bulk tensile strength (88 MPa) and stiffness (11 GPa) for porosity (Boutelje & Rydell, 1986; Klinke et al., 2001).

2: Values for "Lay-up short" are multiplied by 1.234 for strength and multiplied by 1.144 for stiffness to consider the effect of short fibre length, see text for details.

3: Standard deviations are determined for the results obtained for the individual test specimens (6 – 8 specimens/laminate) and 3 – 4 laminates/fibre type.

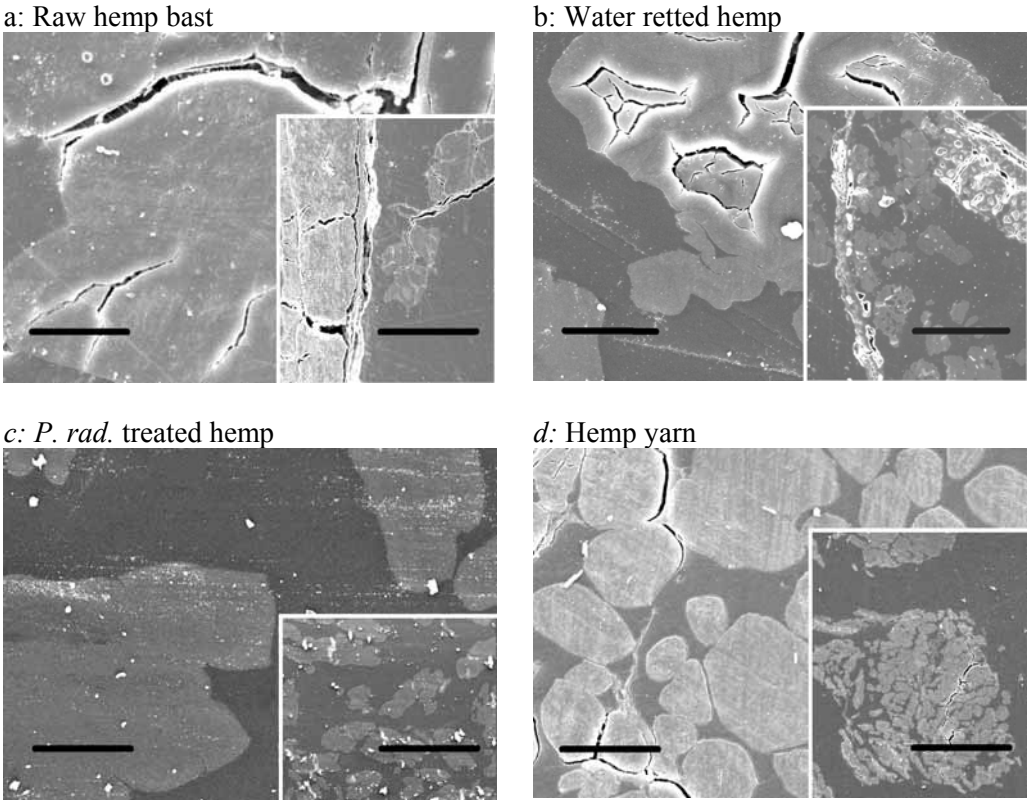

Figure 4. SEM microscopy photos of transverse composite sections recorded at low and high magnification with the defibrated hemp fibres. The small inset pictures have a scale bar length of 200 μm and the background pictures 20 μm.

Composite mechanical properties

The tensile strength and stiffness of the fabricated composites, corrected for porosity are presented in Figure 6 and 7, respectively. The terms σ_{cup} and E_{cp} are calculated from the measured strength and stiffness (σ_{cu} and E_c) using n_σ=2.1 and n_E=1 in Equation 9. Finally, the fibre strength and stiffness determined from σ_{cup} and E_{cp} are calculated from Equation 9 and presented in Table 4.

Filament winding and hand lay-up were used for preparation of fibre sheets for impregnation in epoxy leading to the procedures for composite fabrication. These two fabrication techniques were compared using hemp yarn. The curve for composite tensile strength versus fibre volume fraction showed a slightly higher slope with the wound fibres than with the lay-up of fibres (Figure 6a). The calculated fibre tensile strength with the wound hemp yarn was therefore higher (728 MPa) and also with lower standard deviation (44 MPa) than with the hand lay-up of hemp yarn (677 ± 92 MPa, Table 4). The failure strain of these composites were 1.6 – 1.8% and based on this the failure stress of the epoxy matrix was 39 – 43 MPa (Table 4). For composite stiffness versus the fibre content, the curves for the wound fibres and the lay-up of fibres showed similar slopes (Figure a). The determined fibre stiffness did not therefore appear to be much affected by the preparation method, and the determined fibre stiffness was 60 – 61 GPa (Table 4). For both fibre tensile strength and stiffness, the standard deviation obtained with hand lay-up was twice the standard deviation obtained with filament winding.

Long fibres that pass through the entire test specimen length (18 cm long) were in general used in the fabricated composites except with the hemp fibres defibrated with *C. subvermispora*, which were only obtained as short fibres (6 cm long). The effects of fibre length on composite strength and stiffness were therefore investigated with the fibres produced by cultivation of *P. radiata* obtained at both fibre lengths. The curves for composite strength versus fibre volume fraction were slightly steeper with long fibres than with short fibres (Figure 6a). The effective fibre strength was therefore higher when the long fibres were used than when the overlapping short fibres were used (643 MPa/521 MPa = 1.23, Table 4). This is expected due to the high probability of composite fracture near the fibre-end positions of the short fibres. The curves for composite stiffness versus fibre volume fraction were also slightly steeper with long fibres than with short fibres (Figure 7a). The increase in calculated fibre stiffness when using long fibres as reinforcement instead of short fibres was 94 GPa/82 GPa = 1.14 (Table 4).

The hemp fibres produced in the fungal cultivation experiments were compared based on results obtained with composites reinforced with fibres of short length (6 cm). The curve for composite strength was slightly steeper with the fibres produced by defibration with *P. radiata* than with *C. subvermispora* (Figure 6a). The defibration of hemp by cultivation of *P. radiata* resulted therefore in a higher calculated fibre strength (521 MPa) than the cultivation of *C. subvermispora* (434 MPa) (Table 4). This was in agreement with the measured fibre bundle strength that was also found to be highest for the *P. radiata* defibrated hemp fibres. The curves for composite stiffness versus fibre volume fraction were also slightly steeper with the fibres produced by cultivation of *P. radiata* than *C. subvermispora* (Figure a). The defibration of hemp with *P. radiata* resulted therefore in higher fibre stiffness (82 GPa) than the *C. subvermispora* cultivation (77 GPa) (Table 4).

In order to compare the fungal defibrated hemp fibres with water-retted hemp and raw hemp bast, it was necessary to correct for the effect of short fibre length on the fibre strength and fibre stiffness. This correction was performed with the ratios previously determined for hemp fibres that were defibrated using *P. radiata* (1.23 for fibre tensile strength and 1.14 for fibre stiffness). These corrected values for the hemp fibres defibrated by *C. subvermispora* cultivation are 536 MPa for fibre strength and 88 GPa for fibre stiffness (Table 4).

For raw hemp bast and water-retted hemp (Figure 6b), the curves for composite strength versus V_f were less steep than for the hemp fibres produced by cultivation of *P. radiata* (Figure 6a). The raw hemp bast and the water-retted hemp fibres had therefore lower tensile strength of 535 MPa and 586 MPa, respectively than the *P. radiata* defibrated hemp (643 MPa) (Table 4). The failure strain of hemp fibre composites except the hemp yarn composites was 0.7 – 0.9% and based on this the failure stress of the epoxy matrix was 18 – 25 MPa (Table 4). The highest composite strengths obtained using raw hemp bast, water retted hemp or *P. radiata* defibrated hemp, as reinforcement were 122 MPa, 153 MPa and 174 MPa, respectively without consideration of porosity (σ_{cu}). The composites with hemp fibres produced by cultivation of *P. radiata* were strongest due to the low porosity content, the high fibre strength and the higher obtainable fibre content.

The curves for composite stiffness versus fibre volume fraction were also steeper for the hemp fibres produced by cultivation of *P. radiata* (Figure a) than the curves for raw hemp bast and water retted hemp (Figure b). The raw hemp bast and the water-retted hemp fibres had therefore lower stiffness of 78 GPa and 88 GPa, respectively than the hemp fibres produced by cultivation of *P. radiata* (94 GPa) (Table 4). The highest composite stiffness obtained using raw hemp bast, water retted hemp or *P. radiata* defibrated hemp, as reinforcement were 20 GPa, 26 GPa and 30 GPa, respectively without consideration of porosity (E_c). Cultivation of *P. radiata* for defibration of hemp fibres resulted thereby both in the highest composite strength and highest composite stiffness. Based on obtainable composite strength and stiffness, the best defibration method was cultivation of *P. radiata* followed by water retting and then by cultivation of *C. subvermispora*. It was determined that the hemp fibres tensile strength and stiffness were affected by the defibration methods at 90% probability using analysis of variance (F-test with number of samples = 4 and number of repetitions = 23 for $F_{0.1}$).

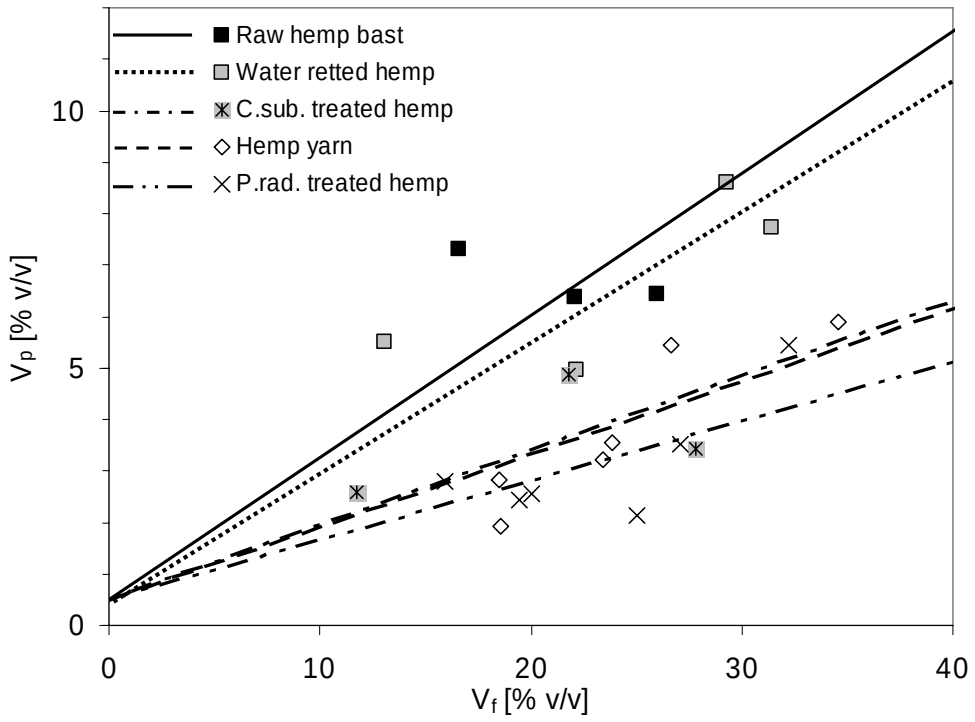

Figure 5. Porosity content in the composites versus fibre volume fraction.

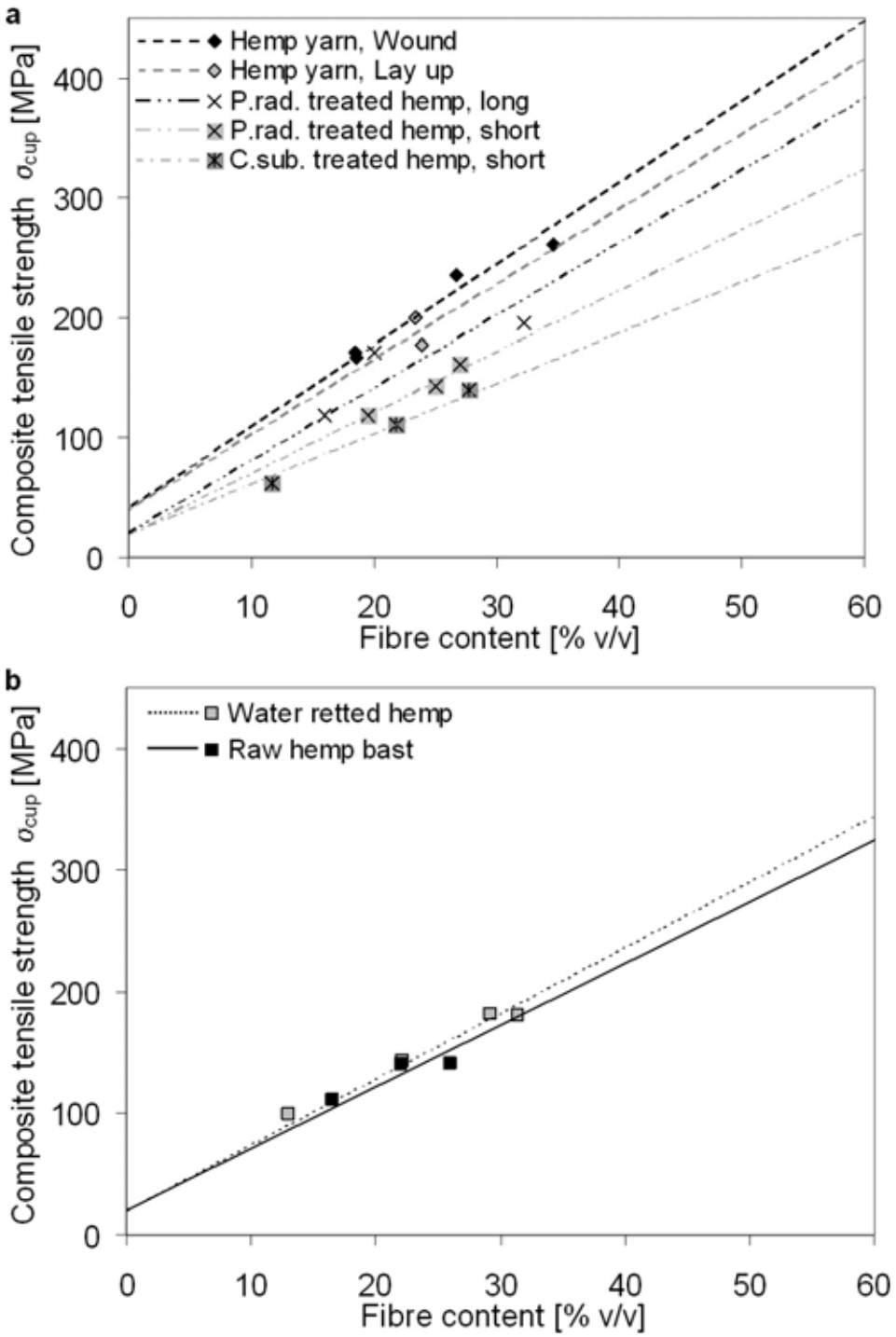

*Figure 6. Effect of composite fabrication (*a*), fibre length (*a*), fungal defibration (*a*) and water retting (*b*) on composite tensile strength after correction for porosity plotted as a function of fibre volume fraction.*

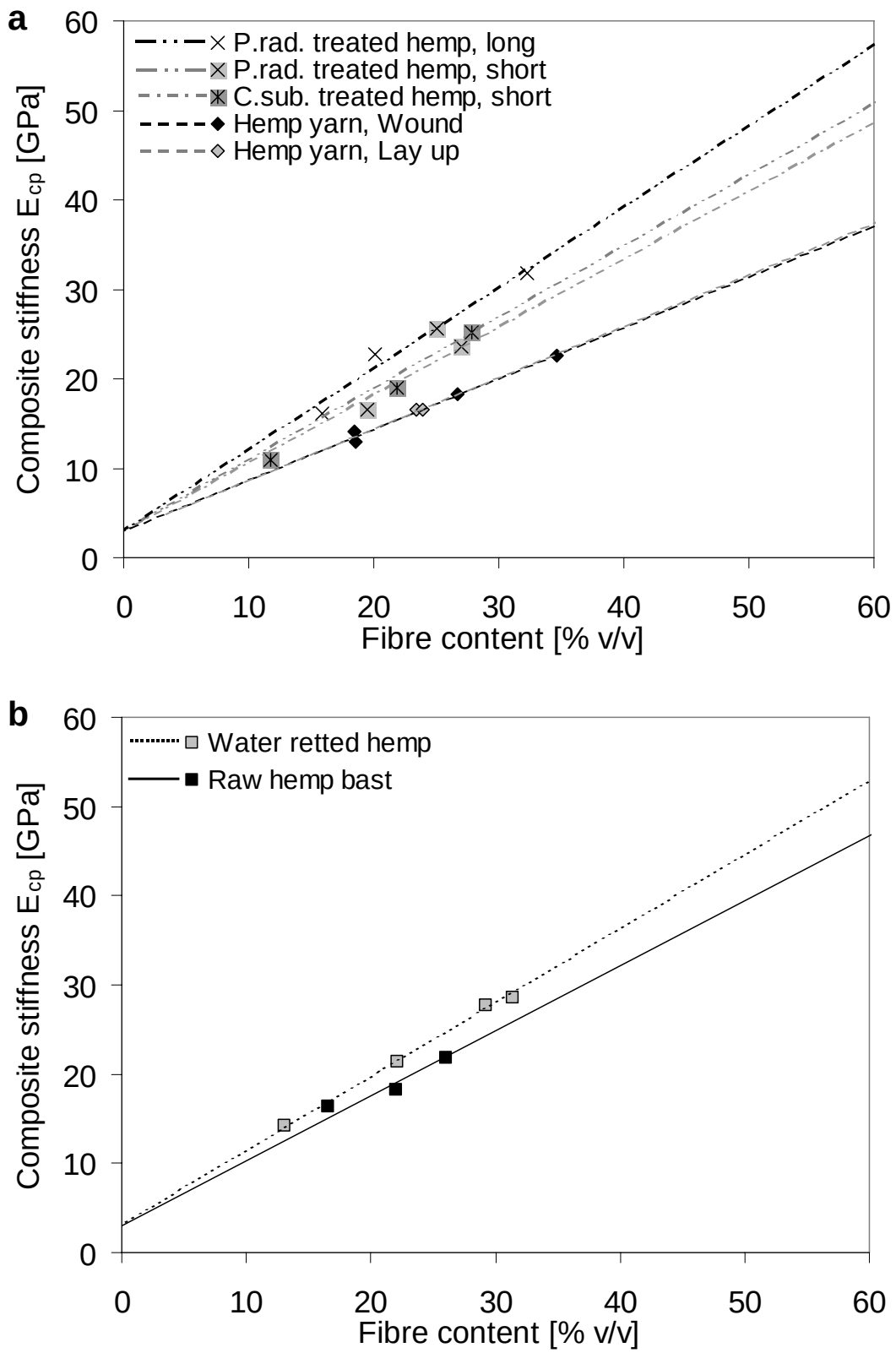

*Figure 7. Effect of composite fabrication (*a*), fibre length (*a*), fungal defibration (*a*) and water retting (*b*) on composite stiffness after correction for porosity plotted as a function of fibre volume fraction.*

DISCUSSION

The defibration of hemp fibres by cultivation of *P. radiata* resulted in fibres with higher cellulose content than water retted hemp and pectinase treated hemp (Thygesen et al., 2002) due to increased degradation of pectin and lignin. The cellulose crystallinity tended to decrease with the cellulose content obtained by the fungal treatments (Figure 3) showing that during processing part of the crystalline cellulose is converted into its amorphous form. A similar chemical composition to *P. radiata* defibrated hemp has been obtained by wet oxidation (Thygesen et al., 2002; Thomsen et al., 2005), which is also an oxidative process resulting in decreased cellulose crystallinity (Thygesen, 2006).

The machine winding and hand lay-up techniques resulted in roughly the same composite strength (Figure 6a), showing that the hand lay-up technique results in the same optimal fibre alignment generally obtained by machine (Madsen & Lilholt, 2003). The fibre length was an important parameter for both calculation of the fibre strength and stiffness due to the high risk of composite failure near the fibre ends, when these are located in the strained specimen section. Therefore, the calculated fibre strength decreased by 1.23 times for composites based on the short fibre length (Figure 6a) and further reduction might occur if the fibre ends are not at random positions.

The fibre strength and stiffness were in general compared based on back calculation from composite data since this involves identical test specimens, accurate measurement of the force and accurate measurement of the strain. However this will cause inaccuracy due to the effect of fibre length and fibre-matrix interface. The advantage with the fibre bundle tensile test is that the fibre strength is measured in a more direct manner. However since the test samples are small and of variable size and geometry it was decided to rely on the composite data.

The composite strength for the laminate with 35% v/v hemp yarn (230 MPa; Figure 6a), was slightly lower than for flax yarn based composites (251 MPa; V_f = 43% v/v) (Madsen & Lilholt, 2003). However the calculated fibre strength was lowest in the flax yarn (575 MPa). The lower strength in composites with *P. radiata* defibrated hemp fibres (174 MPa, Figure 6a) was due to the lower cellulose content, the lower fibre content (32 % v/v) and the lower failure strain of the fibres resulting in lower matrix stress of 25 MPa compared with 39 – 43 MPa (Table 4). Investigations reported by Hepworth et al. (2000b) with raw hemp bast and water retted hemp in epoxy-composites have shown much lower composite strength (80 – 90 MPa) using 20% v/v fibres leading to a fibre strength of 290 – 340 MPa, which can be due to incomplete fibre alignment. The composite stiffness has been found to 27 GPa in composites containing 43 % v/v flax fibres (Madsen & Lilholt, 2003). This corresponds to a fibre stiffness of 58 GPa, which is close to the stiffness for hemp yarn that was calculated in this study (60 GPa).

Even though the hemp fibres were handled with mild methods like hand peeling and fungal defibration, a higher calculated fibre strength than 643 MPa was not obtained, which is similar to the strength of traditionally produced hemp yarn (677 MPa). The similar results are surprising and indicate that the final fibre strength is not very dependent on the defibration method applied (Table 4).

The hemp fibres and the Norway spruce had tensile strength approximately linearly increasing versus the cellulose content showing that pure cellulose has 850 MPa in tensile strength (Figure a). Previous investigations by Klinke et al. (2001) have shown that the strength of pure cellulose is 600 MPa and that the fibre strength increases with cellulose content squared. The different conclusion in this study is due to that aligned fibres were used as reinforcement, which makes it easier to calculate the correct fibre properties than when randomly orientated fibres are used. The determined strength of pure cellulose was about 10% of the theoretical strength reported by Lilholt (2002). Therefore, strength reduction seems to occur from the molecular level to the single fibre level (8000 MPa →1200±400 MPa; Madsen et al., 2003) and from the single fibre level to the fibre assembly level (1200±400 MPa → 643±111 MPa). Single fibres are presumably weakened due to flaws like kinks inside the fibres (Bos et al., 2002), weak interface between the fibre wall concentric lamellae (Thygesen et al., 2005a) and insufficient binding strength between the reinforcing cellulose, hemicellulose, lignin and pectin (Morvan et al., 1990). The fibre damage introduced by the fungal defibration is mainly caused by enzymatic degradation of pectin and lignin. This may lead to degradation of the inter microfibril bonding in the fibres (Thygesen et al., 2005a).

Fibre assemblies are weakened due to variations in single fibre strength as explained by Weibull analysis (Lilholt, 2002) describing the fact that the fibre bundle strength is always lower than the average strength of the same fibres (Coleman, 1958). For flax and cotton fibres, the bundle efficiency has been found as 0.46 – 0.60 indicating that the effective strength of many fibres in for example a composite is roughly half the single fibre strength (Bos et al., 2002; Kompella & Lambros, 2002). It has also been suggested that mild handling and defibration result in high single fibre strength but with larger scatter, counteracting the higher fibre strength in fibre assemblies (bundles) (Bos et al., 2002). These facts explain the similar strength in the composites with traditionally produced hemp yarn and mildly defibrated hemp fibres. This investigation shows thereby that the effective fibre strength is 677 MPa in hemp yarn and 643 MPa in the *P. radiata* defibrated hemp fibres (Table 4) which is within a narrow range, and high compared to literature data on hemp fibres (300-800 MPa) and similar to literature data for flax fibres (500-900 MPa) (Lilholt & Lawther, 2000).

Fibre stiffness increased with the cellulose content in the fibres obtained by the fungal defibration and water retting. A linear dependence on the crystalline cellulose content could be established (Figure 8b). The hemp yarn had lower stiffness than implied from the cellulose content, which may be due to the high twisting angle introduced during the spinning process. It has been stated, that increasing twisting angles decrease fibre stiffness (Page et al., 1977). The wood fibres had lower stiffness, which can be explained by the low cellulose crystallinity (60 – 70%) compared with the hemp fibres (90 – 100%) (Figure 3; Thygesen et al., 2005b). Amorphous cellulose, hemicellulose, lignin and pectin are expected to have lower stiffness than crystalline cellulose, which are linear molecules orientated in the test direction resulting in high stiffness. In contrast, the plant fibre stiffness appeared to increase linearly versus the cellulose content to 125 GPa for pure crystalline cellulose.

This investigation showed that the effective fibre stiffness is 61 GPa in hemp yarn and 94 GPa in the *P. radiata* defibrated hemp fibres (Table 4) which is high compared to literature data on hemp fibres (30-60 GPa), flax fibres (50-70 GPa) and glass fibres (72 GPa) (Lilholt & Lawther, 2000). The high stiffness and low density of the defibrated hemp fibres compared with glass fibres makes hemp a good alternative to glass fibres for material construction.

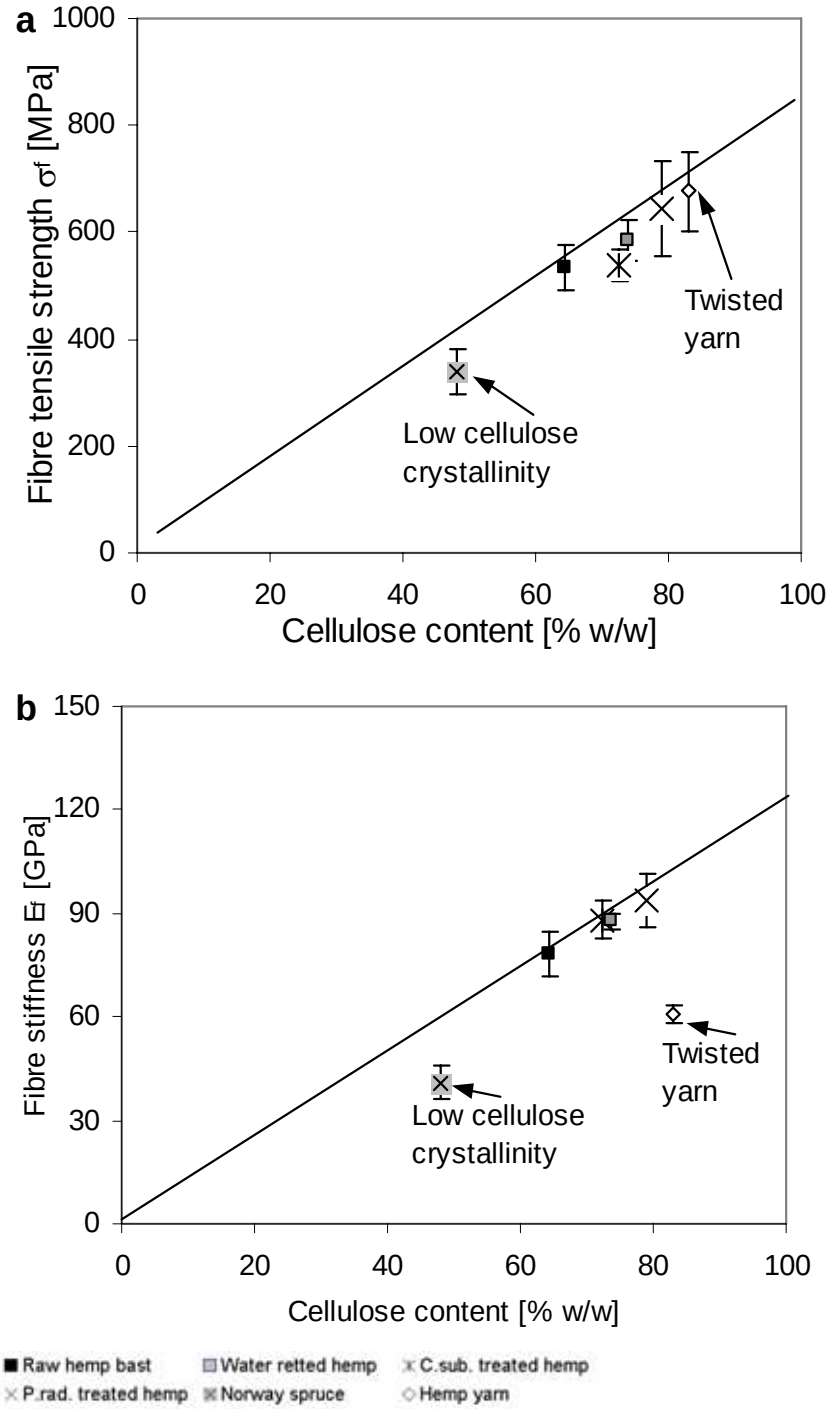

*Figure 8. Fibre tensile strength (*a*) and stiffness (*b*) determined on porosity corrected composite data plotted as a function of cellulose content for defibrated hemp fibres, hemp yarn and Norway spruce. The effects of cellulose crystallinity and twisting angle are indicated.*

CONCLUSIONS

Cultivation of *P. radiata* Cel 26 on hemp stems resulted in fibres with higher cellulose content than water retting of hemp due to more effective degradation of pectin and lignin. The cellulose crystallinity tended to decrease with the cellulose content obtained by the fungal treatments showing that during processing part of the crystalline cellulose is converted into its amorphous form.

Even though the hemp fibres were handled with mild methods like hand peeling and fungal defibration, a fibre strength higher than 643 MPa was not obtained, which is similar to the strength of traditionally produced hemp yarn (677 MPa). The fibre strength and stiffness properties were derived from composite data using the rule of mixtures model.

The effective fibre stiffness was 94 GPa in the *P. radiata* defibrated hemp fibres which is high compared to literature data on flax - (50-70 GPa) and glass fibres (72 GPa). The high stiffness and low density of the defibrated hemp fibres compared with glass fibres makes hemp a good alternative to glass fibres for material construction.

The calculated plant fibre strength appeared to be linearly dependent on cellulose content and independent on cellulose crystallinity and microfibril angle. Pure cellulose had the estimated effective strength 850 MPa that is about 10% of the strength on the molecular level.

The calculated plant fibre stiffness appeared to increase linearly with cellulose content, decrease with microfibril angle and increase with cellulose crystallinity. Pure crystalline cellulose had an estimated stiffness of 125 GPa.

ACKNOWLEDGEMENTS

This work was part of the project “High performance hemp fibres and improved fibre networks for composites” supported by the Danish Research Agency of the Ministry of Science. Dr. Claus Felby (The Royal Veterinary and Agricultural University) is acknowledged as supervisor for Ph.D. student Anders Thygesen. Senior scientist Poul Flengmark (Danish Institute of Agricultural Sciences) is acknowledged for supplying the hemp and Mrs. Ann-Sofie Hansen (WURC) for setting up the fungal cultivation experiments. Mr. Henning K. Frederiksen (Risø National Laboratory) is acknowledged for help in composite fabrication and Mr. Tomas Fernqvist (Risø National Laboratory) for help in the chemical fibre analysis. Dr. Bo Madsen and Engineer Tom L. Andersen (Risø National Laboratory) are acknowledged for discussion and inspiration. Lecturer Kenny Ståhl is gratefully acknowledged for assistance in X-ray measurements and allowing us to use the equipment.

REFERENCES

Akhtar, M., Attridge, M.C., Blanchette, R.A., Myers, G.C., Wall, M.B., Sykes, M.S., Koning, J.W., Burgess, R.R., Wegner, T.H., Kirk, T.K., 1992. The white-rot fungus *Ceriporiopsis subvermispora* saves electrical energy and improves strength properties during biomechanical pulping of wood. In: Kuwahara, M., Shimada, M. (Ed.), Biotechnology in pulp and paper industry, Uni Publishers CO., Tokyo, Japan. 5, pp 3-8.

Bos, H.L., Molenveld, K., Teunissen, W., van Wingerde, A.M., and van Delft, D.R.V., 2004. Compressive behaviour of unidirectional flax fibre reinforced composites. J. Mater. Sci. 39, 2159-2168.

Bos, H.L., Van den Oever, M.J.A., Peters, O.C.J.J., 2002. Tensile and compressive properties of flax fibres for natural fibre reinforced composites. J. Mater. Sci. 37, 1683-1692.

Boutelje, J.B., Rydell, R.R., 1986. Träfakta, 44 träslag i ord och bild. TräteknikCentrum, Stockholm.

Browning, B.L., 1967. Methods of wood chemistry. Interscience Publishers, A division of John Wiley & Sons, New York.

Coleman, B.D., 1958. On strength of classical fibres and fibre bundles. J. Mech. Phys. Solids 7, 60-70.

Garcia-Jaldon, C., Dupeyre, D., Vignon, M.R., 1998. Fibres from semi-retted hemp bundles by steam explosion treatment. Biomass Bioenergy 14, 251-260.

Goering, H.K., Van Soest, P.J., 1970. Forage fiber analyses (apparatus, reagents, procedures and some applications). Agricultural Research Service, USDA, Washington, DC, USA, pp. 1-20.

Hautala, M., Pasila, A., Pirila, J., 2004. Use of hemp and flax in composite manufacture: a search for new production methods. Compos. Part A-Appl. Sci. Manuf. 35, 11-16.

Henriksson, G., Akin, D.E., Hanlin, R.T., Rodriguez, C., Archibald, D.D., Rigsby, L.L., Eriksson, K.E.L., 1997. Identification and retting efficiencies of fungi isolated from dew-retted flax in the United States and Europe. Appl. Environ. Microbiol. 63, 3950-3956.

Hepworth, D.G., Bruce, D.M., Vincent, J.F.V., Jeronimidis, G., 2000a. The manufacture and mechanical testing of thermosetting natural fibre composites. J. Mater. Sci. 35, 293-298.

Hepworth, D.G., Hobson, R.N., Bruce, D.M., Farrent, J.W., 2000b. The use of unretted hemp fibre in composite manufacture. Compos. Part A-Appl. Sci. Manuf. 31, 1279-1283.

Hull, D., Clyne, T.W., 1996. An introduction to composite materials. 2nd edn. Cambridge University Press, United Kingdom.

Joseph, K., Varghese, S., Kalaprasad, G., Thomas, S., Prasannakumari, L., Koshy, P., Pavithran, C., 1996. Influence of interfacial adhesion on the mechanical properties and fracture behaviour of short sisal fibre reinforced polymer composites. Eur. Polym. J. 32, 1243-1250.

Klinke, H.B., Lilholt, H., Toftegaard, H., Andersen, T.L., Schmidt, A.S., Thomsen, A.B., 2001. Wood and plant fibre reinforced polypropylene composites. In: 1st world conference on biomass for energy and industry, James & James (Science Publishers). pp. 1082-1085.

Kompella, M.K., Lambros, J., 2002. Micromechanical characterisation of cellulose fibers. Polym. Test. 21, 523-530.

Lilholt, H., 2002. Strength of cellulose and fibres. In: Lilholt, H., Madsen, B., Toftegaard, H., Cendre, E., Megnis, M., Mikkelsen, L.P., Sørensen, B.F. (Ed.), Sustainable natural and polymeric composites - science and technology. Proceedings of the 23th Risø International Symposium on Materials Science, Risø National Laboratory. Denmark. pp. 225-230.

Lilholt, H., Lawther, J.M., 2000. Natural organic fibres. Elsevier. In: Kelly, A. and Zweben, C. (Ed.), Comprehensive composite materials, vol. 1, pp. 303-325.

Madsen, B., 2004. Properties of plant fibre yarn polymer composites - An experimental study. Ph.D. thesis, BYG-DTU, Technical University of Denmark, ISBN 87-7877-145-5.

Madsen, B., Lilholt, H., 2003. Physical and mechanical properties of unidirectional plant fibre composites - an evaluation of the influence of porosity. Compos. Sci. and Technol. 63, 1265-1272.

Madsen, F.T., Burgert, I., Jungnikl, K., Felby, C., Thomsen, A.B., 2003. Effect of enzyme treatment and steam explosion on tensile properties of single hemp fiber. In: 12th International Symposium on Wood and Pulping Chemistry (ISWPC), Madison, P80.

Meijer, W.J.M., Vertregt, N., Rutgers, B., van de Waart, M., 1995. The pectin content as a measure of the retting and rettability of flax. Ind. Crops Prod. 4, 273-284.

Mieck, K.-P, Lützkendorf, R., Reussmann, T., 1996. Needle-punched hybrid nonwovens of flax and PP fibers -textile semiproducts for manufacturing of fiber composites. Polym. Compos. 17, 873-878.

Morvan, C., Jauneau, A., Flaman, A., Millet, J., Demarty, M., 1990. Degradation of flax polysaccharides with purified endo-polygalacturonase. Carbohydr. Polym. 13, 149-163.

Nishiyama, Y., Langan, P., Chanzy, H. 2002. Crystal structure and hydrogen-bonding system in cellulose Iβ from synchrotron X-ray and neutron fiber diffraction. J. Am. Chem. Soc. 124, 9074-9082.

Nyhlen, L., Nilsson, T., 1987. Combined T.E.M. and UV-microscopy on delignification of pine wood by *Phlebia radiata* and four other white rotters. In: Odier, E. (Ed.), Proc. of Lignin Enzymic and Microbial Degradation Symposium, INRA Publications, pp. 277-282.

Obrien, R.N., Hartman, K., 1971. Air infrared spectroscopy study of epoxy-cellulose interface. J. Polym. Sci. Part C-Polym. Symp. 34, 293.

Page, D.H., El-Hosseiny, F., Winkler, K., and Lancaster, A.P.S., 1977. Elastic modulus of single wood pulp fibers. Tappi 60, 114-117.

Rosember, J.A., 1965. Bacteria responsible for retting of Brazilian flax. Appl. Microbiol. 13, 991-992.

Thomsen, A.B., Rasmussen, S., Bohn, V., Nielsen, K.V., Thygesen, A., 2005. Hemp raw materials: The effect of cultivar, growth conditions and pretreatment on the chemical composition of the fibres. R-1507, Risø National Laboratory, Denmark.

Thygesen, A., 2006. Properties of hemp fibre polymer composites - An optimisation of fibre properties using novel defibration methods and detailed fibre characterisation. Risø-PhD-11(EN), Risø National Laboratory, Denmark.

Thygesen, A., Daniel, G., Lilholt, H., Thomsen, A.B., 2005a. Hemp fiber microstructure and use of fungal defibration to obtain fibers for composite materials. J. Nat. fibres 2, 19-37.

Thygesen, A., Madsen, F.T., Lilholt, H, Felby, C., Thomsen, A.B., 2002. Changes in chemical composition, degree of crystallisation and polymerisation of cellulose in hemp fibres caused by pre-treatment. In: Lilholt, H., Madsen, B., Toftegaard, H., Cendre, E., Megnis, M., Mikkelsen, L.P., Sørensen, B.F. (Ed.), Sustainable natural and polymeric composites - science and technology. Proceedings of the 23th Risø International Symposium on Materials Science, Risø National Laboratory. Denmark, pp. 315-323.

Thygesen, A., Oddershede, J., Lilholt, H., Thomsen, A.B., Ståhl, K., 2005b. On the determination of crystallinity and cellulose content in plant fibres. Cellulose 12, 563-576.

Toftegaard, H. and Lilholt, H., 2002. Effective stiffness and strength of flax fibres derived from short fibre laminates. In: Lilholt, H., Madsen, B., Toftegaard, H., Cendre, E., Megnis, M., Mikkelsen, L.P., Sørensen, B.F. (Ed.), Sustainable natural and polymeric composites - science and technology. Proceedings of the 23th Risø International Symposium on Materials Science, Risø National Laboratory. Denmark, pp. 325-334.

Evaluation of Method for the Determination of Degree of Polymerisation in Cellulose from Hemp

A. Thygesen[1,2], S. Ndoni[1], H. Lilholt[1], F. T. Madsen[2], C. Felby[2] and A.B. Thomsen[1]

[1]Risø National Laboratory, PO Box 49, DK-4000 Roskilde, Denmark
[2]The Royal Veterinary and Agricultural University, DK-1870 Frederiksberg C, Denmark

Abstract

Hemp is a biomass product consisting of cellulose, hemicellulose, lignin and smaller amounts of wax, pectin and protein. For determination of the degree of polymerisation (**DP**) in cellulose from hemp fibres a pure cellulose sample is needed. This was achieved by sequential milling (**m**) and purification (**t**) by extraction of wax, water-soluble components, lignin, and hemicellulose. The purified cellulose was dissolved in pyridine after carbanilation. The carbanilated cellulose was precipitated in methanol and redissolved in tetrahydrofuran (**THF**). DP was measured by size exclusion chromatography (**SEC**) using light scattering (**LS**) and refractive index (**RI**) detection. The effect of the **m** and the **t** procedure were evaluated. Pre-treatment by wet oxidation and steam explosion, two important defibration methods, were examined.

Materials and methods

Purification of cellulose in hemp: Fibres were milled (**m**) followed by consecutive degradation and extraction (**t**) of wax, water-soluble components, pectin, lignin, and hemicellulose. The residual part was almost pure cellulose (Browning, 1967).

Cellulose carbanilation: 100 mg cellulose was swelled in pyridine for 4 hours. Phenyl isocyanate was added and shaken at 80°C for 48 hours. The carbanilated cellulose was first precipitated in methanol (70%). Then it was centrifuged and washed with methanol and water and dried before solubilisation in THF.

Size Exclusion Chromatography: The cellulose tricarbanilate was analysed by SEC using one Waters Styragel HT6E column and one PL MixD column. The eluent was THF at 1 ml/min and 25°C. The sample volume (V_{inj}) 0.200 ml was injected.

Standard: Cotton which was expected to have a degree of polymerisation in the same range as hemp fibres was used as standard. It consisted of cellulose with a weight based average DP (DP_w) of 7000 (Puls, 2002). To test the effect of the **m** and the **t** procedure on DP these treatments were applied on the cotton.

Calculations: The ratio between the signals LS and RI (Fig. 1A) is proportional to the molecular weight (**M**) and $k\,dn/dC$ (Eq. 4), calculated using Eq. 1-3. Since all the SEC measurements were made with the same detector analysing the same material (cellulose tricarbanilate), $k\,dn/dC$ could be assumed as constant. The ratio between the area of the LS peak and the RI peak ($\Sigma LS/\Sigma RI_i$) was found to 19 for cotton. Using Eq. 5, $k\,dn/dC \cdot M_{mon}$ was found to $2.714 \cdot 10^{-3}$, in which M_{mon}=512 g/mol is the monomer molar weight of cellulose tricarbanilate. The LS_i/RI_i ratio was calculated as a function of the retention volume (V_{ri}) (fig. 1B) and fitted using an exponential expression (Eq. 6). This expression seemed useable, with a good fit for all samples, except cotton (mt); Eq. 6 and Eq 4 were used to calculate DP_i based on V_{ri}. DP_w was calculated based on the RI curve and DP_n (Eq. 7). The measured DP_w for hemp fibres (**mt**) was corrected by multiplying with a correction factor calculated from data on cotton cellulose (**f**, Eq. 8).

Equations:

$$LS = k_{ls} \cdot \left(\frac{dn}{dC}\right)^2 \cdot C \cdot M \cdot V_{inj} \quad \text{Eq. 1}$$

$$RI = k_{ri} \cdot \frac{dn}{dC} \cdot C \cdot V_{inj} \quad \text{Eq. 2}$$

$$M = M_{mon} \cdot DP \quad \text{Eq. 3}$$

$$\frac{LS}{V_{inj}} = k \cdot \frac{dn}{dC} \cdot M_{mon} \cdot DP_w \quad \text{Eq. 4}$$

$$\frac{RI}{V_{inj}} = k \cdot \frac{dn}{dC} \cdot M_{mon} \cdot DP_n \quad \text{Eq. 5}$$

$$\frac{LS_i}{RI_i} = b \cdot \exp(a \cdot V_{ri}) \quad \text{Eq. 6}$$

$$DP_n = \frac{\sum RI_i \cdot DP_i}{\sum RI_i} \quad \text{Eq. 7}$$

$$f = \frac{DP_{w,cotton}}{DP_{n,cotton}} = 2.12 \quad \text{Eq. 8}$$

Abbreviations:

C	Concentration
DP	Degree of polymerisation (-)
DP_w	Weight based average DP (-)
LS	Light Scattering (mV)
m	Milled
M	Molar mass (g/mol)
RI	Refractive index (mV)
SEC	Size exclusion chromatography
t	Treated with the cellulose purification procedure
THF	Tetrahydrofuran
V_{inj}	Injection volume (ml)
V_r	Retention volume (ml)

Results

In the cotton, the degree of polymerisation (DP_w) decreased by 19% during the milling step and mostly at high DP values (Fig 1C). When the cotton was milled and treated with the cellulose purification procedure the decrease in DP_w was 54%. For hemp fibres after the same treatment DP_w was 6500 (Table 1).

Assuming roughly that the relative decrease in DP_w for hemp is at least as large as for cotton cellulose we expected a DP_w of at least 13800 for the hemp cellulose before treatment. The wet oxidation did not affect the DP_w while the steam explosion procedure reduced DP_w by 14%.

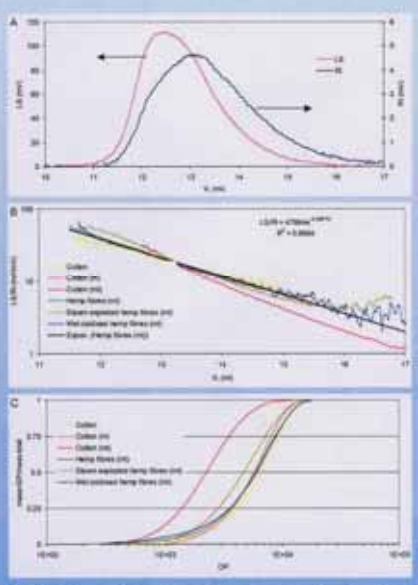

Fig. 1. A: Light scattering and refractive index chromatograms for hemp fibres (mt). B: The LS/RI ratio and exponential regression of LS/RI versus the retention volume. C: Accumulated DP distribution for cotton and hemp fibres.

Table 1. Summary of degree of polymerisation data.

Sample	$DP_{w,raw}$	$DP_{w,corr}$*
Cotton	7000**	
Cotton (m)	5700	
Cotton (mt)	3300	7000
Hemp fibres (m)	6500	13800
Wet oxidized hemp fibres (mt)	6500	13800
Steam exploded hemp fibres (mt)	5600	11900

* Corrected using a correction factor (f = 2.12) calculated from the data on cotton cellulose

** Value from Ref. Puls 2002

Conclusion

- The cellulose purification procedure applied to cotton significantly reduced DP_w in cellulose.
- Steam explosion and wet oxidation can be applied for treatment of hemp fibres with only minor effect on DP_w in cellulose.

Acknowledgement:
This work is part of the project "High performance hemp fibres and super-tex fibre network for composites" supported by the Danish Research Agency of the Ministry of Science.

References:
Browning B.L. 1967, Methods of wood chemistry, New York, Interscience Publishers, A division of John Wiley & Sons, p. 543-617
Puls, J. 2002, Personal communication

CELLULOSE CRYSTALLINITY IN PLANT MATERIALS

Anders Thygesen[1], Jette Oddershede[2], Hans Lilholt[1], Anne Belinda Thomsen[3], Geoffrey Daniel[4] and Kenny Stähl[2]

[1]Materials Research Department, Risø National Laboratory

[2]Department of Chemistry, Technical University of Denmark

[3]Plant Research Department, Risø National Laboratory

[4]Wood Ultrastructure Research Centre, Swedish University of Agricultural Sciences

INTRODUCTION

Plant fibres are getting increasing attention because of their application to the engineering of composite materials. Cellulose is the structural polysaccharide in the partly crystalline plant cell walls, which has a complex not yet completely determined nanostructure. An important step in the characterization of plant fibres is the determination of cellulose crystallinity and crystallite size.

The purpose of this poster is to demonstrate some approaches in the study of plant fibre crystallinity based on X-ray powder diffraction and powder diffraction simulations. The results are based on hemp fibres and regular filter paper as examples of plant material and pure cellulose, respectively

CRYSTAL STRUCTURE OF CELLULOSE-Iβ

CRYSTAL DATA	
FORMULA	$C_{12}H_{20}O_{10}$
Z	2
SPACE GROUP	$P2_1$
a (Å)	7.784(6)
b (Å)	10.38(1)
c (Å)	8.201(8)
β (°)	96.5

Ref.: Nishiyama, Langan & Chanzy. J. Am. Chem. Soc. **124** (2002) 9074.

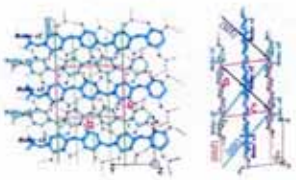

MOLECULAR PACKING IN CELLULOSE-Iβ

PLANT STRUCTURE OF HEMP ON STEM AND PLANT CELL LEVEL

SEM-picture of a transverse section of a hemp stem, showing the xylem, parenchyma cells, fibre bundles, epidermis and cuticle going from the centre of the stem outward.

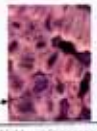

Light microscope image of a fibre bundle stained with Ruthenium red. Pectin is red and located in the middle lamella and in the parenchyma cells.

Light microscope image: Fibre bundle, parenchyma cells and xylem after the Wiesner reaction. Lignin is stained red.

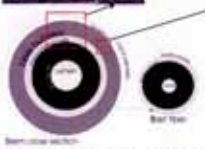

Model of the morphology in hemp stems

FIBRE TREATMENT

Component	Raw hemp fibres (% dwb)	Purified hemp fibres (% dwb)	Filter paper (% dwb)
Cellulose	64.4	77.6	100
Hemicellulose	19.4	19.8	0
Lignin	3.4	1.6	0
Pectin	7.1	1.0	0
Wax	1.0	0.1	0
Water extract	0.4	0.4	0
Ash	4.3	1.0	0
Sum	100.0	101.5	100

Table 1. Chemical composition of the hemp fibres before and after incubation of the white rot fungus *Phebia radiata* Cel 26 on hemp stem pieces in water for 22 days followed by isolation of the fibres. The content of pectin and lignin is reduced by the treatment with 87% and 59%, respectively.

Nominal values for the composition of cellulose filter paper are shown.

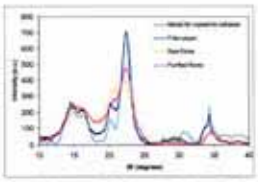

Transmission x-ray diffraction on the three cellulose containing materials stated in table 1. The intensities are corrected for background. As comparison the calculated diffractogram for cellulose I was included.

The filter paper is more crystalline than the hemp fibre samples but not completely crystalline. The purified hemp fibres have a higher content of cellulose I than the raw fibres.

Cellulose crystallinity

Material	Transmission Method 1	Reflection Method 1	Reflection Method 2	Reflection Method 3
Raw hemp fibres	64%	60%	75%	32%
Purified hemp fibres	71%	61%	78%	32%
Filter paper	91%	82%	85%	54%
Crystalline cellulose	97%	97%		100%

Crystallinity determined as weight fraction of the total sample mass.

Crystallinity (Cr) determination methods:

Method 1: I_{200} is the counter reading at a 2θ angle close to 22° and I_{am} is the amorphous counter reading at a 2θ angle of about 18° (Mwaikambo and Ansell, 1999).

Method 2: Crystallinity determined by Rietveld refining of reflection mode data

Method 3: Crystallinity determined by linear combination of the crystalline model and den amorphous background. The curves were normated to have the same average intensity for 2θ angle =[10°-40°].

NB. The cellulose crystallinity must be lower than the content of cellulose in the samples since 20 out of 36 molecules are in the surface of the microfibrils and therefore probably not in complete order.

Method 1: $Cr = \frac{I_{200} - I_{am}}{I_{200}}$

Method 3: $I_{tot} = I_{c,model} \cdot Cr + I_{am} \cdot (1 - Cr)$

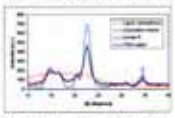

Method 3: Linear fit, demonstrated for filter paper.

PREFERRED ORIENTATION IN FILTER PAPER

- The cellulose fibres prefer to orient themselves with the long fibre axis in the paper plane
- In reflection geometry this gives rise to too weak and too broad 0k0 peaks
- The effect can be reduced by cutting up the paper and side loading the sample holder

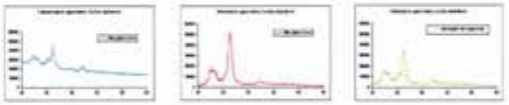

CRYSTALLITE SIZE DETERMINATION

THE DEBYE FORMULA

- $I(q) = \sum_i \sum_j f_i(q)\, f_j(q)\, \sin(q r_{ij}) / q r_{ij}$, where $q = 4\pi\sin(\theta)/\lambda$.
- Explicit calculation of the diffraction pattern from a collection of atoms
- Takes into account particle shape, size and size distribution

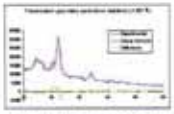

- Cylinders of diameter 5.2(±0.4)nm and length 24(±4)nm along the *b*-axis

THE VOIGT FUNCTION

- Convolution of the Lorentzian and Gaussian functions
- Used in Rietveld refinements
- Can give an estimate of the crystallite dimension in a given direction and perpendicular to this

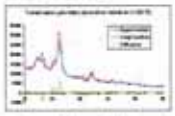

- Needles of thickness 5(0)nm and length 10.8(3)nm along the *b*-axis

CONCLUSIONS

•By linear fittings of the amorphous and crystalline diffractogram the intrinsic crystallinity in cellulose from hemp fibres and filter paper were in the 2θ range [41% (w/w);54% (w/w)].

•By transmission x-ray diffraction higher cellulose crystallinity was determined for the purified hemp fibers than for the raw hemp fibers.

Acknowledgement:

This work is part of the project "High performance hemp fibres and improved fibre network for composites" supported by the Danish Research Agency of the Ministry of Science and EFP Bioethanol production part 2 J. nr. 1383/03-0002.

Microscopical and cytochemical observation on hemp stems with emphasis on fibres

Anders Thygesen[1,2,3], Anne Belinda Thomsen[1], Hans Lilholt[1], Geoffrey Daniel[3]

1: Risø National Laboratory, 4000 Roskilde, Denmark

2: The Royal Veterinary and Agricultural University, 1870 Frederiksberg C, Denmark

3: WURC, Department of Wood Science, SLU, Sweden

Anders.Thygesen@risoe.dk

INTRODUCTION

Hemp fibres are long cellulose rich fibres, strong enough to compete with glass fibres in composite materials. Before the fibres can be useful their isolation from the stem must be improved. To investigate the binding between the fibres, fibre bundles and xylem, the distribution of lignin and pectin in the plant stem was investigated.

MATERIALS & METHODS

- *Hemp (Cannabis sativa* variety *Felina)* grown in Denmark in 2001
- Structure: Scanning electron microscopy
- Lignin: Wiesner reaction and light microscopy
- Pectin: Ruthenium red staining and light microscopy

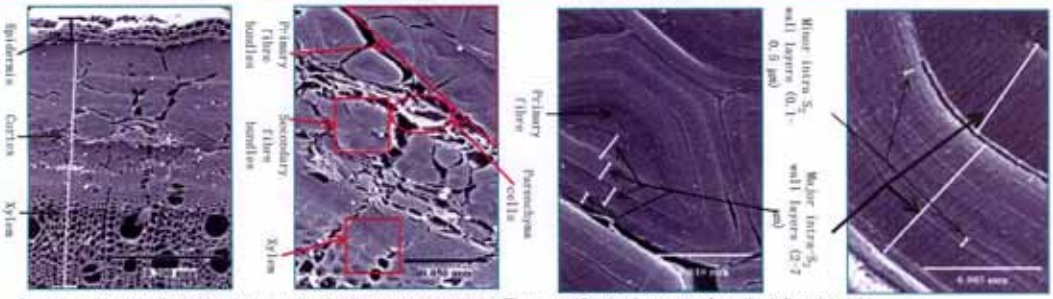

Scanning electron microscopy images showing hemp stem sections. The magnification increases from the left to the right.

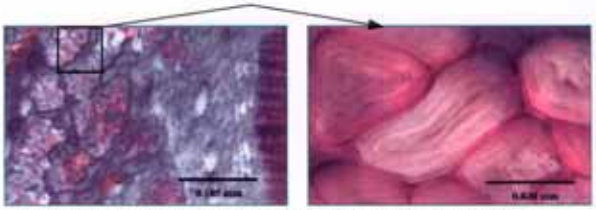

Light microscopy image of Wiesner stained hemp stem section. Lignin is stained dark red.

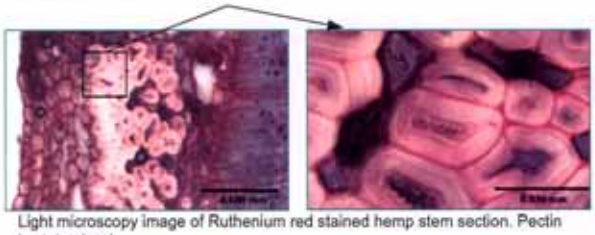

Light microscopy image of Ruthenium red stained hemp stem section. Pectin is stained red.

RESULTS

The fibres:

1. The fibres are arranged in bundles of 4-50 fibres
2. Secondary fibres of 5-10 µm in diameter and primary fibres of 15-50 µm in diameter
3. No visible lumen
4. Compound middle lamellae containing 10-18 % lignin and some pectin
5. The S_2 layer contained only 1-3 % lignin and no pectin
6. The S_2 layer was divided into 1-4 partly separated concentric layers of 2-7 µm in thickness. The partly separated S_2 layer consisted of 100-500 nm thick cellulose lamellae

The parenchyma and epidermal cells:

1. 5-30 µm in diameter
2. 0.5-3 µm thick walls without S_2 layer
3. No lignin in the parenchyma cells but possibly some lignin in the epidermal cells
4. Rich in pectin

The xylem:

1. 15-20 % almost uniformly distributed lignin, determined by chemical analysis
2. Rays with pectin but otherwise no pectin
3. Angiosperm tissue with vessels

CONCLUSIONS

1. Degradation of pectin is required for the release of the fibre bundles from the stem and epidermis
2. Degradation of lignin is required for separation of the individual fibres
3. The delamination within the S_2 layer can affect the stress transfer within the fibres

Calculation of lignin content:

$$\text{Lignin content in tissue} = \text{Lignin content in xylem } (15\text{-}20\ \%) \cdot \frac{\text{Red colour intensity}_{\text{tissue}}}{\text{Red colour intensity}_{\text{xylem}}}$$

Acknowledgement:
This work is part of the project "High performance hemp fibres and improved fibre network for composites" supported by the Danish Research Agency of the Ministry of Science, COST E20 and WURC.

Risø's research is aimed at solving concrete problems in the society.

Research targets are set through continuous dialogue with business, the political system and researchers.

The effects of our research are sustainable energy supply and new technology for the health sector.